



# Applied Gauge/Gravity Duality from Supergravity to Superconductivity

Francesco Aprile

**ADVERTIMENT.** La consulta d'aquesta tesi queda condicionada a l'acceptació de les següents condicions d'ús: La difusió d'aquesta tesi per mitjà del servei TDX ([www.tdx.cat](http://www.tdx.cat)) i a través del Dipòsit Digital de la UB ([diposit.ub.edu](http://diposit.ub.edu)) ha estat autoritzada pels titulars dels drets de propietat intel·lectual únicament per a usos privats emmarcats en activitats d'investigació i docència. No s'autoritza la seva reproducció amb finalitats de lucre ni la seva difusió i posada a disposició des d'un lloc aliè al servei TDX ni al Dipòsit Digital de la UB. No s'autoritza la presentació del seu contingut en una finestra o marc aliè a TDX o al Dipòsit Digital de la UB (framing). Aquesta reserva de drets afecta tant al resum de presentació de la tesi com als seus continguts. En la utilització o cita de parts de la tesi és obligat indicar el nom de la persona autora.

**ADVERTENCIA.** La consulta de esta tesis queda condicionada a la aceptación de las siguientes condiciones de uso: La difusión de esta tesis por medio del servicio TDR ([www.tdx.cat](http://www.tdx.cat)) y a través del Repositorio Digital de la UB ([diposit.ub.edu](http://diposit.ub.edu)) ha sido autorizada por los titulares de los derechos de propiedad intelectual únicamente para usos privados enmarcados en actividades de investigación y docencia. No se autoriza su reproducción con finalidades de lucro ni su difusión y puesta a disposición desde un sitio ajeno al servicio TDR o al Repositorio Digital de la UB. No se autoriza la presentación de su contenido en una ventana o marco ajeno a TDR o al Repositorio Digital de la UB (framing). Esta reserva de derechos afecta tanto al resumen de presentación de la tesis como a sus contenidos. En la utilización o cita de partes de la tesis es obligado indicar el nombre de la persona autora.

**WARNING.** On having consulted this thesis you're accepting the following use conditions: Spreading this thesis by the TDX ([www.tdx.cat](http://www.tdx.cat)) service and by the UB Digital Repository ([diposit.ub.edu](http://diposit.ub.edu)) has been authorized by the titular of the intellectual property rights only for private uses placed in investigation and teaching activities. Reproduction with lucrative aims is not authorized nor its spreading and availability from a site foreign to the TDX service or to the UB Digital Repository. Introducing its content in a window or frame foreign to the TDX service or to the UB Digital Repository is not authorized (framing). Those rights affect to the presentation summary of the thesis as well as to its contents. In the using or citation of parts of the thesis it's obliged to indicate the name of the author.



**Universitat de Barcelona**  
Institut de Ciències del Cosmos  
Departament d'Estructura i Constituents de la Matèria

---

# Applied Gauge/Gravity Duality from Supergravity to Superconductivity

---

**Francesco Aprile**

Director de Tesi: Prof. Jorge G. Russo

Tesi Doctoral  
Any acadèmic 2012/2013  
Programa de doctorat de Física  
Tutor: Prof. Joan Soto



# Preamble

The discovery of the AdS/CFT correspondence is one of the most celebrated results obtained in theoretical physics. The statement of the correspondence is due to Maldacena and it is inferred from the twofold nature of the D-branes, which can be equally described both in terms of open and closed strings. According to the conjecture, the strong coupling dynamics of the  $d$ -dimensional field theory living on the world-volume of the D-branes is described in terms of classical gravity in a the  $d+1$  dimensional AdS space [1]. The change in the dimensionality of the target space time makes the AdS/CFT correspondence a special kind of duality and gives a concrete realization of the idea that gravity is an holographic theory. The geometry of AdS is then interpreted by considering that the dual field theory lives on the boundary of the AdS space and its correlation functions are computed by means of boundary-to-bulk propagators [2, 3]. In this way, a difficult quantum problem in the field theory is reformulated in terms of Einstein's equations with appropriate boundary conditions. The framework that emerges from the holographic principle is the most powerful breakthrough into the dynamics of strongly coupled large  $N$  gauge theories. By providing an alternative intuition with respect to particle physics, it opens up the way to the non perturbative definition of the theory itself. Nowadays, holographic techniques have been successfully applied on a vast number of problems, ranging from the quark-gluon-plasma to the most recent and challenging aspects of condensed matter physics. This thesis is inspired by the so called *interface* between the AdS/CFT correspondence and the physics of Condensed Matter systems.

String theory gives a proper theory of quantum gravity and describes all the different kind of matter that populate the Standard Model. It is certainly a comprehensive theory and for this reason strings may be the most fundamental object that exist in nature. How does it happen that string theory and gauge/gravity duality enter the world of Condensed Matter physics? In order to have a preliminary idea regarding the importance of this approach, let us start from the beginning of the tale.

Local quantum field theories represent the fundamental basis for the description of physical processes at short length scales. At low energies most of the microscopic information is not important and short distances degrees of freedom can be integrated out. Then, according to the Wilsonian renormalization group flow, the resulting theory will be described only by a finite number of relevant and marginal terms [4]. The idea of integrating out microscopic degrees of freedom is geometrically realized in theories with a gravity dual where the bulk radial coordinate represents the resolution scale of the dual field theory. In this case the short distances degrees of freedom of the field theory are associated to near boundary regions of the gravitational background whereas the low energy physics emerges from the shape of the geometry at small radial scales [5].

The call for holography as guiding principle in condensed matter systems, comes from the lack of a field theory explanation for the properties of several many body systems: the high- $T_c$  superconductors. There is a strong experimental evidence indicating that the electronic properties of these materials are remarkably different with respect to those of the conventional materials, which in turn are very well described by the standard Fermi Liquid theory. Therefore, the theory underlying high- $T_c$  superconductors evades the well-established result that the metallic phase of a many-body system of fermions is described by the Fermi liquid theory, independently of the strength of the electron interaction at the lattice scale. Theoretically, the problem can be rephrased by considering that the Fermi liquid theory is an IR free fixed point for the low energy fermionic excitations at the Fermi Surface [6]. In this sense, the relevant question is to understand what happens along the RG flow towards the Fermi Surface in order for the Non Fermi Liquid physics to pop out. The main clue seems to be the emergence of extra gapless degrees of freedom, suggesting the presence of a non trivial conformal fixed point that substitutes the free Fermi Liquid fixed point. This is now a well posed theoretical problem about how to engineer an interesting RG flow dynamics that may resemble the physics of high- $T_c$  superconductors. Holographic theories are very well suited for such purpose and indeed, this is the kind of dynamics that emerges from the bulk of the holographic geometry when finite charge density is introduced in the boundary theory. Thus, high- $T_c$  superconductor may belong to universality classes that admit an holographic description [7, 8]. This thesis discusses and extends in various aspects the theory of the holographic superconductivity introduced in [9].

## Organization of the Thesis

The sequence of chapters can be divided into three blocks.

- The first block contains the introductory chapters. In chapter 1 we illustrate the problem of the high-Tc superconductors making a parallelism between the Fermi Liquid theory, the BCS theory of superconductivity and the theory which is currently supposed to describe electron doped high-Tc superconductors at weak coupling. In chapter 2 we describe the aspects of the AdS/CFT correspondence that will be relevant throughout the reading of the thesis.
- The second block coincides with chapter 3. In this chapter we define the concept of holographic superconductivity and we study phenomenological models of holographic superconductors. These are *bottom-up* models in the sense that they do not come from any particular string theory. This chapter has several important results, among them we mention, the classification of the holographic phase transitions and the characterization of the optical conductivity. Part of this chapter includes the original works presented in [10, 11].
- The third block contains the chapters from 4 to 7. The mainstream is the study of *top-down* models of holographic superconductors that naturally arise as smaller sectors of consistent truncations of type IIB supergravity. In chapter 4 we consider  $\mathcal{N} = 8$  supergravity and we describe the building blocks of  $\mathcal{N} = 2$  supergravity looking for such holographic superconductors. In this setup, the AdS/CFT dictionary is very well understood and we identify the analog of a Cooper pair state. In chapter 5, we discuss holographic superconductivity in the type IIB theory on  $\text{AdS}_5 \times \text{S}^5$  whereas in chapter 6, we consider the more general setting of type IIB theory compactified on Sasaki-Einstein manifolds. Among several examples, we will consider the interesting case of  $\text{AdS}_5 \times \text{T}^{1,1}$ . In chapter 7, we study a four dimensional  $\mathcal{N} = 2$  supergravity which is related to M-theory, we find a novel family of holographic superconductor and we describe in detail the properties of gravitational background providing its interpretation in the dual field theory. The original works which form part of this last block of chapters are presented in [12, 13, 14].

We close the discussion about phenomenological models of holographic superconductivity and supergravity with conclusions and outlook.

Finally, the thesis is equipped with two appendices in which we set up the notation that will be adopted in the various chapters. Both these appendices

are also thought as a quick and practical reminder of known results in the literature about field theory and supergravity.

**Note.** The holographic superconductors that will be discussed in this thesis fall into the category of  $s$ -wave holographic superconductors. Apart from this subject, the author has also contributed to research in  $p$ -wave holographic superconductivity. The original work is presented in [15]. In this work we have studied a sector of the  $\mathcal{N} = 4$   $SU(2) \times U(1)$  gauged supergravity in five dimensions, also known as Romans theory, looking for the condensation of complex 2-form fields dual to a vector order parameter in the field theory. Some of the technology that has been developed to deal with such theory is presented for the  $s$ -wave case in chapter 5.

## Acknowledgements

Foremost, I would like to express my sincere gratitude to my supervisor Prof. Jorge G. Russo, for introducing me to the complex subject of string theory, for his dedication and for his guidance during the period of my PhD. Much of the knowledge I acquired in this field is the result of his constant collaboration and inspiration, activated by his deep curiosity and careful consideration about physics. Especially, I would like to thank him for all the conversations, the works we have done together, for all the scientific support provided for me during this four years and in particular, for the reserved invitation that made me discover Perimeter Institute.

My sincere gratitude also goes to Prof. Matteo Bertolini who first gave me the opportunity of becoming a PhD student in the “late” 2008. With great happiness I remember all the events that led me to where I am now, without his encouragement I would not have made it.

During my PhD I had the pleasure to meet other exceptional people with whom I am in debt for helpful and stimulating discussions. My deepest appreciation goes to Rob Myers, Mukund Rangamani, Diederik Roest, Sebastian Franco, Diego Rodriguez-Gomez and Leonardo Modesto.

I would also like to thank my colleagues for sharing part of their precious time with me. At the edge between physics and all that matters, my thank you goes to Jonathan Toledo, Andrea Borghese, Dani Puigdomènech, Aldo Dector, John Calabrese, Daniele Dorigoni, Tommaso Tufarelli.

More importantly, I express my gratitude to my parents and my sister for being my family and for keeping strong this bond through the distance.

Finally, I hope to meet once again all the wonderful people that crossed and walked along my way during this four years of PhD, without knowing it, they became an important part of my life. I thank all of you!

*Francesco Aprile*

## Financial Support

During the years 2009-2013, the author has been supported by a MEC FPU Grant AP2008-04553 and partially by the Departament d'Estructura i Constituents de la Matèria asesora Espriu. The author is grateful to Perimeter Institute for hospitality. Part of his research was supported by Perimeter Institute for Theoretical Physics. Research at Perimeter Institute is supported by the Government of Canada through Industry Canada and by the Province of Ontario through the Ministry of Economic Development & Innovation.



## Compendi de la Tesi

La seqüència dels capítols es divideix en tres blocs.

- El primer bloc conté els capítols introductoris. Aquests són el capítol 1 i el capítol 2. En el capítol 1 s'il·lustra el problema dels superconductors d'alta temperatura fent un paral·lelisme entre la teoria del líquid de Fermi, la teoria BCS de la superconductivitat i la teoria que ha estat proposada per descriure superconductors d'alta temperatura que estan dopats amb electrons i que es troben en un règim d'acoblament dèbil. En el capítol 2 es descriuen els aspectes de la correspondència AdS/CFT que seran rellevants al llarg de la lectura de la tesi.
- El segon bloc coincideix amb el capítol 3. En aquest capítol es defineix el concepte de la superconductivitat hologràfica i s'estudien els models fenomenològics dels superconductors hologràfics. Aquest capítol té diversos resultats importants, entre ells podem esmentar, la classificació de les transicions de fase en la teoria hologràfica i la caracterització de la conductivitat òptica. Part d'aquest capítol inclou els treballs originals presentats en [10, 11].
- El tercer bloc conté els capítols compresos entre el 4 i el 7. La temàtica principal és l'estudi de models de superconductors hologràfics que deriven de la teoria de cordes i que s'obtenen a partir de truncaments consistents de la supergravetat de tipus IIB. En el capítol 4 considerem la supergravetat  $\mathcal{N} = 8$  en cinc dimensions i descrivim les característiques generals de la supergravetat  $\mathcal{N} = 2$ . Utilitzem aquesta teoria per trobar models de superconductors hologràfics que venen de la teoria de cordes. En aquest cas, el diccionari de la correspondència AdS/CFT resulta precís i ens permet identificar l'anàleg d'un parell de Cooper. En el capítol 5, es discuteix la superconductivitat hologràfica en la teoria de tipus IIB compactificada sobre  $\text{AdS}_5 \times \text{S}^5$ , mentre que en el capítol 6, considerem el context més general de la teoria de tipus IIB compactificada sobre varietats de Sasaki-Einstein. Entre diversos exemples, esmentem el cas interessant de  $\text{AdS}_5 \times \text{T}^{1,1}$ . En el capítol 7, estudiem un model de supergravetat  $\mathcal{N} = 2$  en quatre dimensions que es relaciona amb la teoria M, ens trobem amb una nova família de superconductors hologràfics i descrivim en detall les propietats de l'espai gravitacional, tot seguit, proporcionem la seva interpretació en la teoria dual de camps. Els treballs originals que formen part d'aquest últim bloc de capítols es presenten en [12, 13, 14].

Tanquem la discussió sobre els models fenomenològics de la superconductivitat hologràfica i la supergravetat amb conclusions de caràcter general.

La tesi finalitza amb dos apèndixs, en els quals hem explicat la notació adoptada en els diferents capítols. Aquests apèndixs també constitueixen un recordatori ràpid i pràctic dels resultats coneguts en la literatura sobre la teoria de camps i la supergravetat.

## Resultats obtinguts en aquesta tesi

Recordem al lector la principal dificultat conceptual amb el problema de la superconductivitat d'alta temperatura. La fase normal dels superconductors d'alta temperatura, per damunt del dopatge òptim, es descriu introduint la física no estàndard del líquid de Fermi. En aquesta regió del diagrama de fase, la descripció de les excitacions fermiòniques en termes d'electrons, localitzades a la superfície de Fermi no és aplicable ja que el sistema està interactuant fortament. Per tant, no es pot parlar de “parell de Cooper” per descriure la superconductivitat d'alta temperatura perquè no hi ha electrons per formar un estat lligat. El problema és llavors com descriure el fenomen de la superconductivitat en els materials, o en general en les teories de fort acoblament.

En aquesta tesi s'ha demostrat que la correspondència AdS/CFT proporciona una definició intrínseca de la superconductivitat en teories fortament acoblades amb un dual hologràfic. El pas lògic és reformular el problema de la teoria de camps com un problema de gravetat en un espai asimptòticament AdS. En aquest marc, el condensat de parells de Cooper es descriu en termes d'un espai gravitacional, al qual s'adhereix un camp escalar amb càrrega elèctrica. A partir d'aquí, la teoria entra en una nova fase i la fenomenologia de la corrent superconductora apareix com a conseqüència d'una equació London dual. Aquests espais gravitacionals amb aquestes propietats s'han anomenat superconductors hologràfics. En considerar primer els models fenomenològics de la superconductivitat hologràfica i després teories (fortament acoblades) procedents de la teoria de cordes, hem demostrat que el diagrama de fase d'aquestes teories conté un sector en què el sistema entra espontàniament en la fase superconductora. Per tant, concloem que la superconductivitat hologràfica és un fenomen general en les teories que es descriuen amb un dual gravitacional.

En el capítol 3 analitzem models hologràfics inspirats en la teoria de Landau-Ginzburg. L'anàlisi realitzada en aquest capítol, té com objectiu la classificació de les transicions de fase en aquestes teories. Gran part de les

nostres troballes tenen un anàleg directe en teoria de Landau-Ginzburg, però cal emfatitzar que la naturalesa de la descripció clàssica ha d'atribuir-se a la presència d'un gran nombre de colors en la teoria dual de camps, i no a l'aproximació de camp mitjà. Sorprenentment, en les nostres teories, els exponents crítics en la transició de fase satisfan la identitat de Rushbrooke i les possibles formes de comportament crític es caracteritzen en termes de classes d'universalitat. És interessant observar que aquest resultat, que en la teoria de camps es desprèn dels arguments del grup de renormalització, es reproduïx amb exactitud mitjançant un càlcul de física clàssica en l'espai gravitacional.

Malgrat les similituds amb la teoria de Landau-Ginzburg, hi ha una manera natural per promoure els nostres models fenomenològics en una teoria microscòpica. És possible tenint en compte els models obtinguts de la teoria de cordes en la qual el coneixement precís del diccionari AdS/CFT dona la descripció microscòpica de l'operador que condensa. Hem analitzat un primer exemple en el context de la teoria  $\mathcal{N} = 4$  SYM. En concret, s'han estudiat els camps escalars complexos  $Z_i = \eta_i e^{i\theta_i}$ ,  $i = 1, 2, 3$ , amb una massa  $m^2 L^2 = -4$  i càrrega  $qL = 2$ , que són duals als operadors BPS,

$$O_i = \text{Tr} [\Phi_i^2] , \quad (1)$$

En la secció 6.2 es va estudiar també el camp escalar dual a l'operador bilineal,

$$\tilde{O} \sim \text{Tr} [\lambda\lambda] + \text{h.c.} , \quad (2)$$

on  $\lambda$  és una combinació particular dels fermions  $SU(4)$  de  $\mathcal{N} = 4$  SYM. La nostra anàlisi mostra que els operadors  $O_i$ s competeixen amb  $\tilde{O}$  però aquest últim és el que es condensa. Seria interessant analitzar el diagrama de fase complet de la teoria, però hem limitat la nostra recerca als sectors de la teoria en què la inestabilitat superconductora té un paper prominent.

En el capítol 6, la investigació del model derivant de la teoria de cordes es va basar en la supergravetat  $\mathcal{N} = 2$ . Entre els nostres resultats, hem trobat una possible connexió entre los models  $\gamma$  i l'espectre de la supergravetat de tipus IIB compactificada sobre  $\text{AdS}_5 \times \text{T}^{1,1}$ . La teoria dual representa la teoria de Klebanov-Witten. Suposant que els nostres models viuen en aquesta teoria, hem estudiat els condensats que competeixen i hem trobat un sector de la teoria que exhibeix la superconductivitat hologràfica. Fins i tot en aquest cas, vam arribar a la conclusió que la superconductivitat hologràfica és un fenomen genèric.

Pel que fa als superconductors hologràfics estudiats fins ara, el superconductor construït al capítol 7 revela característiques addicionals. El model té una interessant dinàmica i diversos nous ingredients coexisteixen en el diagrama de

fase. Aquestes són les solucions d'interpolació construïdes a la secció 7.2, les propietats de les solucions de temperatura zero assenyalades en la secció 7.2.1 i la noció de la deformació *double-trace* en AdS / CFT. Cada un d'ells pot estar relacionat amb l'existència de l'espai  $\mathcal{M}_\theta$ , que està completament lligada amb la natura topològica de la varietat escalar  $SU(2,1)/U(2)$ , homeomòrfica a una bola en  $\mathbb{C}^2$ . L'esfera es pot parametritzar en funció de la fibració de Hopf, i al centre de la varietat escalar apareix una degeneració "topològica": és l'espai  $\mathcal{M}_\theta$  que descriu l'aparició de les deformacions marginals de la teoria. Al encendre aquesta deformació marginal, es genera una nova dinàmica que es caracteritza per una transició confinament/deconfinament en l'entropia d'*entanglement* de l'estat fonamental.

La classe de superconductors hologràfics que s'han estudiat són d'ona  $s$ , mentre que el condensat en el *cuprates* té una estructura d'ona  $d$ . En aquest sentit, hem de millorar els nostres models per descriure la superconductivitat d'ona  $d$ . No obstant això, creiem que gran part dels resultats obtinguts en el cas d'ona  $s$ , són vàlids en els models de superconductors hologràfics d'ona  $d$ . Construir models de superconductors hologràfics d'ona  $d$  representa un dels problemes actuals [141].

**Nota.** Els superconductors hologràfics que seran discutits en aquesta tesi pertanyen a la categoria dels superconductors hologràfics d'ona  $s$ . A banda d'aquest tema, l'autor també ha contribuït a la investigació en superconductivitat hologràfica d'ona  $p$ . L'obra original es presenta en [15]. En aquest treball s'ha estudiat un sector de la teoria de supergravetat  $\mathcal{N} = 4$   $SU(2) \times U(1)$  en cinc dimensions, també coneguda com la teoria de Romans, en la qual una 2-forma complexa es condensa. Aquesta 2-forma és dual a un paràmetre d'ordre vectorial en la teoria de camps. Algunes de les tecnologies que s'han desenvolupat per fer front a aquest problema es presenten en el cas de l'ona  $s$  en el capítol 5.

# Contents

|   |            |
|---|------------|
| <b>Preamble</b>   | <b>iii</b> |
| <b>1 High-Tc Superconductors</b>                        | <b>1</b>   |
| 1.1 Ordinary Metals are Fermi Liquid . . . . .          | 2          |
| 1.2 BCS in a nutshell . . . . .                         | 9          |
| 1.3 High-Tc Superconductors . . . . .                   | 15         |
| 1.3.1 Electron doped high-Tc Superconductors . . . . .  | 16         |
| 1.3.2 The Spin-Fermion Model . . . . .                  | 18         |
| 1.3.3 Results and Limitations . . . . .                 | 21         |
| <b>2 Short Introduction to AdS/CFT</b>                  | <b>27</b>  |
| 2.1 Minimal Background of supersymmetry . . . . .       | 27         |
| 2.1.1 Spinors . . . . .                                 | 29         |
| 2.1.2 Extended Supersymmetry . . . . .                  | 31         |
| 2.1.3 R symmetry . . . . .                              | 34         |
| 2.2 Type IIB supergravity . . . . .                     | 36         |
| 2.3 $\mathcal{N} = 4$ Super Yang-Mills . . . . .        | 38         |
| 2.4 The Maldacena Conjecture . . . . .                  | 41         |
| 2.5 Bulk to Boundary Mapping . . . . .                  | 45         |
| 2.5.1 Scalar Field Holography . . . . .                 | 47         |
| 2.5.2 Double Trace Deformations . . . . .               | 51         |
| <b>3 Holographic Superconductors: Phenomenology</b>     | <b>55</b>  |
| 3.1 Setting up the problem . . . . .                    | 55         |
| 3.2 Phenomenological Models . . . . .                   | 57         |
| 3.2.1 Ansatz and Equations of motion . . . . .          | 60         |
| 3.2.2 The shooting method . . . . .                     | 61         |
| 3.2.3 Defining the holographic superconductor . . . . . | 63         |
| 3.3 The uncondensed solution . . . . .                  | 64         |

|          |   |            |
|----------|---|------------|
| 3.4      | The Superconducting Instability . . . . .                   | 66         |
| 3.4.1    | Linearized Analysis . . . . .                               | 68         |
| 3.5      | The Decoupling Limit . . . . .                              | 70         |
| 3.6      | Holographic Phase Transitions . . . . .                     | 72         |
| 3.6.1    | Numerical Results . . . . .                                 | 75         |
| 3.6.2    | Analytical Results for the Condensate . . . . .             | 79         |
| 3.6.3    | Analytical results for the Free Energy . . . . .            | 81         |
| 3.6.4    | Rushbrooke Identity . . . . .                               | 83         |
| 3.7      | Conductivity . . . . .                                      | 84         |
| 3.7.1    | The Schrödinger potential . . . . .                         | 91         |
| 3.8      | Hall Currents: phenomenological approach . . . . .          | 94         |
| 3.8.1    | Asymptotic expansions . . . . .                             | 94         |
| 3.8.2    | Conductivities and Numerical Results . . . . .              | 97         |
| 3.9      | Summary of Results . . . . .                                | 100        |
| <b>4</b> | <b>The Bosonic Sector of Supergravity</b>                   | <b>103</b> |
| 4.1      | $\mathcal{N} = 2$ Supergravity . . . . .                    | 104        |
| 4.1.1    | The Scalar Manifold . . . . .                               | 105        |
| 4.1.2    | The Gauging Procedure . . . . .                             | 108        |
| 4.1.3    | The Action with Matter Couplings . . . . .                  | 111        |
| 4.2      | The Hypermultiplet $SU(2, 1)/U(2)$ . . . . .                | 113        |
| 4.2.1    | Geometrical Properties . . . . .                            | 113        |
| 4.2.2    | One Parameter Family of Theories . . . . .                  | 117        |
| 4.3      | $\mathcal{N} = 8$ Supergravity in $d = 5$ . . . . .         | 119        |
| 4.3.1    | The $U(1)^3$ truncation . . . . .                           | 123        |
| 4.3.2    | The $U(1)^2$ truncation . . . . .                           | 125        |
| 4.3.3    | The minimal gauged $\mathcal{N} = 2$ supergravity . . . . . | 126        |
| 4.4      | The Incomplete Hypermultiplets . . . . .                    | 127        |
| 4.5      | Connecting with $\mathcal{N} = 4$ SYM . . . . .             | 130        |
| <b>5</b> | <b>Hair in 5D <math>\mathcal{N} = 8</math> Supergravity</b> | <b>133</b> |
| 5.1      | Dilatonic Black Holes . . . . .                             | 134        |
| 5.1.1    | Entropy: general features . . . . .                         | 138        |
| 5.2      | Linearized Analysis . . . . .                               | 141        |
| 5.3      | Truncations to a single charge . . . . .                    | 145        |
| 5.4      | The condensed phase . . . . .                               | 148        |
| 5.4.1    | Equations of motion and asymptotic behavior . . . . .       | 149        |
| 5.4.2    | Numerical Results . . . . .                                 | 153        |
| 5.5      | Summary of results . . . . .                                | 158        |

|          |   |            |
|----------|---|------------|
| <b>6</b> | <b>Dynamical Hypermultiplets I</b>                                    | <b>161</b> |
| 6.1      | The $\gamma$ -family of $SU(2,1)/U(2)$ Hypers in 5D . . . . .         | 162        |
| 6.2      | The $\gamma = 1$ Holographic Superconductor . . . . .                 | 166        |
| 6.2.1    | Type IIB Sasaki-Einstein Truncations. . . . .                         | 168        |
| 6.2.2    | The Universal Hypermultiplet. . . . .                                 | 172        |
| 6.3      | The $\gamma = 0$ Holographic Superconductor . . . . .                 | 173        |
| 6.3.1    | Connecting with Type IIB theory on $AdS_5 \times S^5$ . . . . .       | 176        |
| 6.4      | $\gamma = 1/3$ and Hypers of $\mathcal{N} = 8$ supergravity . . . . . | 180        |
| 6.5      | Comments of the Retrograde Condensate . . . . .                       | 181        |
| 6.5.1    | Novel Extremal Solutions from a Superpotential . . . . .              | 181        |
| <b>7</b> | <b>Dynamical Hypermultiplets II</b>                                   | <b>189</b> |
| 7.1      | The 4D $\mathcal{N} = 2$ Supergravity . . . . .                       | 190        |
| 7.1.1    | Geometrical description . . . . .                                     | 191        |
| 7.2      | $\Delta = 1$ Interpolating Solutions . . . . .                        | 197        |
| 7.2.1    | Zero temperature solutions . . . . .                                  | 199        |
| 7.2.2    | Comments on the Extremal Limit . . . . .                              | 203        |
| 7.3      | The Entanglement entropy . . . . .                                    | 204        |
| 7.3.1    | EE at Finite Temperature. . . . .                                     | 207        |
| 7.3.2    | EE at Zero Temperature . . . . .                                      | 207        |
| 7.4      | Optical Conductivity . . . . .  | 211        |
| 7.5      | Dual field theory and marginal deformations . . . . .                 | 213        |
| 7.5.1    | Additional Comments about the dual field theory . . . . .             | 218        |
| <b>8</b> | <b>Conclusions and Outlook</b>  | <b>223</b> |
| <b>A</b> | <b>QFT and Statistical Mechanics: Some Results</b>                    | <b>227</b> |
| <b>B</b> | <b>Menagerie of Special geometry</b>                                  | <b>237</b> |



# Chapter 1

## High-Tc Superconductors

### New Frontiers in Condensed Matter Physics

High-Tc superconductors have shown a variety of remarkable properties. Several experimental observations, indicate that the microscopic structure of these materials preserves a strong amount of quantum correlation even at relatively high temperature. As a result, their phase diagram is characterized by a number of interesting low energy phenomena and exhibits non trivial topology. How this comes about is mostly an open question.

The first example of a high-Tc superconductor dates back to the 1986 [16]. From then, the interest in the subject has been growing and nowadays the literature about unconventional superconductivity and strange metal phase is extremely vast. In this chapter we take a pragmatical point of view and we illustrate some of the main limitations that have been encountered when the problem of high-Tc superconductivity is formulated in a quantum field theory framework. This theoretical problem is hard both conceptually and computationally, probably the solution will require a new way of looking at many body physics in a quantum setting.

This chapter is also a collection of known results in condensed matter physics. In particular, the reader not familiar with statistical quantum field theory will find a useful and very basic introduction to the topic. The history of ordinary metallic phase is our starting point. We review the standard Landau theory of Fermi Liquid and assemble the necessary tools needed to understand the modern take on High-Tc superconductivity. The resulting theory, commonly known as the spin fermion model, correctly captures qualitative features of the phase diagram but unfortunately suffers of strong conceptual limitations.

## 1.1 Ordinary Metals are Fermi Liquid

The aim of this section is to provide evidence for the following statement: the Fermi Liquid (FL) theory describes with success the physics of ordinary metals. First of all, by an ordinary metal we generically mean an element, compound or alloy that is a good conductor of electricity and heat. This experimental definition points out that the microscopic structure of a metal somehow allows a certain fraction of its total electric charge to “freely” move inside the material. On one side, the quantity that specifies how “freely” the electric current flows in the metal, is the electrical resistivity. On the other side, the quantity that roughly indicates the number of degrees of freedom involved in the process is the specific heat. Electric conduction, as well as heat conduction, are two phenomena that occur at room temperature and are quite common. Naively, we could expect that classical physics gives a valuable description of the dynamics which take place in a metal. As we are going to see, this is not the case.

**The classical attempt.** The theory of charge transport assumes that the electrical resistivity is produced by collision events that relax the motion of the electrons. The relaxation time  $\tau$  is then defined as the average time between two consecutive collisions and the Drude Law is a consequence of the Newton’s Law and the definition<sup>1</sup> of the electrical resistivity  $\rho$ . At the classical level the fundamental relation turns out to be,

$$\rho^{-1} = \frac{ne^2\tau}{m} .$$

Here  $n$  is the number of electrons per unit volume that are involved in the transport. The idea that collision events relax the kinetic energy, also leads to the conclusion that the average electronic speed is given by the equipartition theorem:

$$\frac{1}{2}mv_0^2 = \frac{3}{2}k_B T . \tag{1.1}$$

In other words, it is assumed that the speed of the electrons in a metal is determined by the Maxwell-Boltzmann statistics. Therefore, the probability

---

<sup>1</sup>In general, the resistivity is defined to be the proportionality matrix between the electric field  $\vec{E}$  and the induced current density  $\vec{j}$ :  $\vec{E} = \rho\vec{j}$ . The resistivity may depend on the spatial coordinates. In the majority of cases, the current density is vector parallel to the electric field and  $\rho$  is a constant.

of finding electrons with velocities in the range  $(v, v + dv)$  is given by,

$$f_{MB}(v) = n \left[ \frac{m}{2\pi k_B T} \right]^{\frac{3}{2}} e^{-\frac{mv^2}{2k_B T}} . \quad (1.2)$$

This is a natural classical kinetic theory and remarkably the Drude law is a valid and well tested for many fermionic systems. On the other hand if we try to extrapolate low temperature physics from the above classical picture, several inconsistencies pop out. The most evident difficulty comes from the fact that the constant specific heat per electron, predicted by the classical statistics, is not observed in experiments. Furthermore, at low temperature is found that the theoretical estimate of the mean free path,  $l = \tau v_0 \approx 10A$ , is an order  $10^3$  smaller than the experimental value [17].

The clash between this classical theory and the experimental data appeared to be not just a problem of fine tuning of the theory. Indeed, the solution of this puzzle turns out to be one of the most important discoveries of modern physics: a metal is a truly quantum system at low temperature. The Pauli exclusion principle makes clear the main difference with respect to the classical theory: the Maxwell-Boltzmann distribution (1.2) must be replaced by the Fermi-Dirac statistics,

$$f_{FD}(v) = \frac{(m/\hbar)^3}{4\pi^3} \left( e^{(\frac{1}{2}mv^2 - k_B T_0)/k_B T} + 1 \right)^{-1} . \quad (1.3)$$

where  $T_0$  is determined by the normalization  $n = \int dv f_{FD}(v)$ . This conceptual step towards quantum mechanics marks the beginning of the Fermi Liquid theory. More precisely, the Fermi liquid theory is a consistent and solvable quantum theory for a many body problem of fermionic particles.

In the next chapters, we will introduce the Fermi liquid theory by making use of the language of “second quantization”. In the Appendix A we review the basic notation of quantum field theory. Standard references are [18, 19, 20].

**The Fermi Liquid.** The basic setup of our discussion is the microscopic Hamiltonian,

$$\mathcal{H}(\lambda) = \sum_{\mathbf{k}\sigma} (\epsilon_{\mathbf{k}} - \mu) c_{\mathbf{k}\sigma}^\dagger c_{\mathbf{k}\sigma} - \sum_{\mathbf{k}\mathbf{k}'\mathbf{q}\mathbf{q}'} c_{\mathbf{k}}^\dagger c_{\mathbf{q}} \hat{\lambda} c_{\mathbf{k}'}^\dagger c_{\mathbf{q}'} \delta(\mathbf{k} + \mathbf{k}' - \mathbf{q} - \mathbf{q}') , \quad (1.4)$$

where  $\epsilon_{\mathbf{k}} = \mathbf{k}^2/2m$  is the standard kinetic term. In the above formula the spinorial indexes are contracted as follows,

$$c_{\alpha}^\dagger c_{\beta} \hat{\lambda}^{\alpha\beta\gamma\delta} c_{\gamma}^\dagger c_{\delta} . \quad (1.5)$$

The operators  $c_{\mathbf{k}\sigma}$  and  $c_{\mathbf{k}\sigma}^\dagger$  are creation and annihilation operators for a one particle state of momentum  $\mathbf{k}$  and spin  $\sigma$ . They satisfy the anti-commutation relations,

$$\{c_{\mathbf{k}\sigma}, c_{\mathbf{q}\sigma'}^\dagger\} = \delta_{\mathbf{k},\mathbf{q}}\delta_{\sigma\sigma'} . \quad (1.6)$$

For concreteness we consider spin singlet couplings  $\hat{\lambda}$ . In particular, by looking again at the Lorentz structure (1.5) we see that  $\hat{\lambda}$  needs to have the same symmetry properties of  $c_\alpha^\dagger c_\gamma^\dagger c_\beta c_\delta$ . Then, in order to obtain a spin singlet, we fix  $\alpha = \beta$ ,  $\gamma = \delta$  and the result is,

$$\hat{\lambda}^{\alpha\beta\gamma\delta} = \lambda \left( \delta^{\alpha\beta} \delta^{\gamma\delta} - \delta^{\alpha\delta} \delta^{\beta\gamma} \right) , \quad (1.7)$$

where  $\lambda$  can be taken to be a constant or a function of the momenta  $\lambda = \lambda_{\mathbf{k}\mathbf{k}'}$ . A positive (negative)  $\lambda$  corresponds to a repulsive (attractive) interaction.

The free theory corresponds to set  $\hat{\lambda} = 0$  in the Hamiltonian (1.4). Despite its simplicity, the case of free fermions, is enough interesting to capture almost all the relevant ingredients of the Fermi Liquid physics. We briefly sketch what are these ingredients and we will present the Fermi Liquid theory building on these results.

At zero temperature the ground state is obtained by filling all the energy levels  $\epsilon_{\mathbf{k}}$  up to  $\mu$ , according to the Pauli exclusion principle. In momentum space, this ground state is represented by a filled sphere having radius  $k_f = \sqrt{2m\mu}$ . The filled sphere is usually called “Fermi sea”. The term “Fermi Surface” is instead used to indicate the surface having radius  $k_f$ . The Hamiltonian (1.4) can be expressed in terms of the particle number operator  $n_{\mathbf{k}\sigma} = c_{\mathbf{k}\sigma}^\dagger c_{\mathbf{k}\sigma}$ . This operator, when evaluated on the Fermi sea, turns out to be,

$$\langle n_{\mathbf{k}} \rangle = \begin{cases} 1 & \text{if } |\mathbf{k}| < k_f \\ 0 & \text{if } |\mathbf{k}| > k_f \end{cases} . \quad (1.8)$$

The chemical potential  $\mu$  is determined by the relation  $\langle \sum_{\mathbf{k}\sigma} n_{\mathbf{k}\sigma} \rangle = N$ , where  $N$  is the total number of electrons.

The properties of the system will be described by considering the Green’s Function formalism. The Green’s Function is generically defined by the formula

$$G(\mathbf{k}, t) = -i \langle \Psi_0 | T(c_{\mathbf{k}}(t) c_{\mathbf{k}}^\dagger(0)) | \Psi_0 \rangle , \quad (1.9)$$

where  $|\Psi_0\rangle$  is the ground state of the system and  $c_{\mathbf{k}}$  is an operator of the theory. The most interesting result about (1.9) comes from the Lehmann representation. This is a non perturbative formulation which gives informations about the state created by  $c_{\mathbf{p}}^\dagger$  and represented by the wave function  $|\psi\rangle = c_{\mathbf{p}}^\dagger |\Psi_0\rangle$ . In

the Lehmann representation, the Imaginary part of  $G(\mathbf{k}, t)$  plays a central role. Concretely, the only relation that we need to know is the following. Given a complete set of orthogonal eigenstates of the Hamiltonian,

$$\mathcal{H}|\Phi_s\rangle = E_s|\Phi_s\rangle, \quad \sum_s |\Phi_s\rangle\langle\Phi_s| = Id, \quad \langle\Phi_s|\Phi_{s'}\rangle = \delta_{ss'}, \quad (1.10)$$

we define the matrix elements,

$$\psi_{0s} = \langle\Psi_0|c_{\mathbf{p}}|\Phi_s\rangle, \quad (1.11)$$

and we define the spectral function  $A^+(\mathbf{k}, E)$  by the formula,

$$A^+(\mathbf{k}, E)dE = \sum_s |\psi_{0s}|^2 \delta(\mathbf{k} - \mathbf{k}_s), \quad E < \epsilon_s < E + dE. \quad (1.12)$$

The spectral function is a positive measure. As it is common from Fourier analysis,  $A^+(\mathbf{k}, E)dE$  gives informations about the spread of the wave function  $|\psi\rangle$  over the spectrum of eigenstates  $|\Phi_s\rangle$ . Finally, the Lehmann representation implies,

$$A^+(\mathbf{k}, \omega - \mu) = -\frac{1}{\pi} \text{Im} G(\mathbf{k}, \omega), \quad \omega > \mu. \quad (1.13)$$

In the case of the free theory we expect  $|\psi\rangle = c_{\mathbf{p}}^\dagger|\Psi_0\rangle$  to be an eigenstate of the Hamiltonian and therefore we expect the spectral function to be a delta function peaked at the momentum  $\mathbf{p}$ , i.e  $\psi_{0s} = \delta(\mathbf{p} - \mathbf{k}_s)$ .

Straightforward calculations show that the Green's Function for the system of free fermions is

$$G_b(\mathbf{k}, \omega) = \frac{1}{\omega - (\epsilon_{\mathbf{k}} - \mu) + i\delta_{\mathbf{k}}}, \quad \delta_{\mathbf{k}} = \begin{cases} +\delta & \text{if } \epsilon_{\mathbf{k}} - \mu > 0 \\ -\delta & \text{if } \epsilon_{\mathbf{k}} - \mu < 0 \end{cases} \quad (1.14)$$

In the above formula, the infinitesimal quantity  $i\delta_{\mathbf{k}}$  in the denominator prescribes how to go around the pole at  $\omega - (\epsilon_{\mathbf{k}} - \mu)$ . For reference purposes,  $G_b(\mathbf{k}, \omega)$  is the *bare* Green's Function. We can check that our intuition on the spectral function for the free theory is correct. Indeed, by making use of the representation

$$\frac{I(s)}{s + i\delta} = P \left[ \frac{I(s)}{s} \right] - i\pi\delta(s)I(s), \quad (1.15)$$

it is evident that  $A(\mathbf{k}, \omega)$  is a positive delta function peaked at the energy  $\epsilon_{\mathbf{k}} - \mu$ , i.e peaked at the eigenvalues of the free Hamiltonian.

The many body problem of free fermions is the starting point of the theory of Fermi Liquid, developed by Landau in 1957-59. In his original formulation, Landau assumes that there is no phase transition from the free theory

of fermions to a system of interacting fermions when interactions are slowly turned on. Technically, it means that the interactions can be treated in the sense of perturbation theory. As we will see, this assumption is consistent.

Before entering into the details of the diagrammatic expansion, it is instructive to follow the above line of reasoning a step further. Under the assumptions that no phase transitions occurs when the couplings are slowly turned on, the states of the free theory are mapped into states of the interacting system. This map is realized by the adiabatic evolution process. Therefore, by using adiabatic continuity, it is possible to keep labeling the states of the interacting system by the same quantum numbers used in the free theory. These are the particle quantum numbers: the momentum, the spin and the charge. We are therefore lead to the concept of “ quasiparticle ”. Nevertheless, the quasiparticle states are neither exact eigenstates of the interacting Hamiltonian nor real particles. They just represent a good approximation to the Hilbert space of the interacting system in a certain regime. In particular, the validity of the quasiparticle approximation is encoded into the details of the Green’s Function *dressed* by the interaction.

The general form of a dressed Green’s Function is,

$$G(\mathbf{k}, \omega) = \frac{1}{\omega - E_{\mathbf{k}} - \Sigma(\mathbf{k}, \omega) + i\delta_{\mathbf{k}}} , \quad (1.16)$$

where  $E_{\mathbf{k}} = \epsilon_{\mathbf{k}} - \mu$  is the free electron energy measured with respect to the chemical potential and  $\Sigma(\mathbf{k}, \omega)$  is the irreducible self energy calculated in perturbation theory. This self energy is a complex quantity and modifies the bare propagator (1.14) in two different ways. The real part,  $\text{Re}\Sigma(\mathbf{k}, \omega)$ , is a shift of the value of the kinetic energy  $E_{\mathbf{k}}$ . The imaginary part  $\text{Im}\Sigma(\mathbf{k}, \omega)$  introduces a width in the spectral function  $A(\omega, \mathbf{k})$  and it has a more profound meaning: quasiparticles acquire a finite lifetime  $\tau$ . In particular, the spectral function is not a delta function peaked at  $E_{\mathbf{k}} + \text{Re}\Sigma(\mathbf{k}, \omega)$  but assumes the profile of a Lorentian,

$$A^+(\mathbf{k}, \omega) \sim \frac{C}{(\omega - \mathcal{E}_{\mathbf{k}})^2 + 1/\tau^2} , \quad (1.17)$$

where  $C$  and  $\tau$  are determined by  $\text{Re}\Sigma(\mathbf{k}, \omega)$  and  $\text{Im}\Sigma(\mathbf{k}, \omega)$ . We will see how this comes about by explicitly calculating the dressed Green’s Function at leading order in perturbation theory. The first non trivial approximation to the diagrammatic expansion of the self energy comes from the loop diagram shown in Figure 1.1.

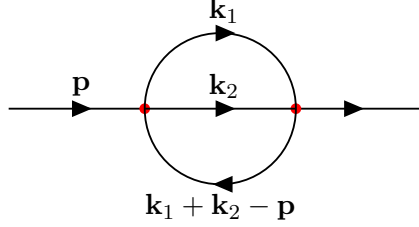


Figure 1.1: *Two loop diagram contributing to the self energy  $\Sigma(\omega, \mathbf{p})$ .*

The details of this calculation can be found in the Appendix A for the case of zero temperature. It is very instructive to follow the computation because it makes evident how the integration over momenta running in the loop is constrained by the presence of the Fermi Surface. As a result, only a shell of energy thickness  $\omega - \mu \ll \mu$  around the Fermi Surface really defines the domain of integration. The imaginary part of the self energy turns out to be,

$$\text{Im}\Sigma(\omega, \mathbf{k}) \propto (\omega - \mu)^\alpha \quad \mathbf{k} \approx \mathbf{k}_F . \quad (1.18)$$

The exponent is  $\alpha = 2$  for dimensions  $D > 2$ . As we will see, the relation (1.18) can be taken to be as the defining property of a Fermi Liquid. We begin by studying the behavior of the dressed Green's Function in the vicinity of the Fermi Surface<sup>2</sup>. The Green's Function can be written in the following form,

$$\begin{aligned} G(\mathbf{k}, \omega) &= \frac{1}{\omega - (E_{\mathbf{k}} + \text{Re}\Sigma(\mathbf{k}, \omega)) - i\text{Im}\Sigma(\mathbf{k}, \omega)} \quad (1.19) \\ &\approx (\omega - \omega \partial_\omega \text{Re}\Sigma - (\mathbf{k} - \mathbf{k}_F) \cdot \partial_{\mathbf{k}}(E_{\mathbf{k}} + \text{Re}\Sigma) - i \text{Im}\Sigma)^{-1} \\ &= (Z^{-1}\omega - (\mathbf{k} - \mathbf{k}_F) \cdot \partial_{\mathbf{k}}(E_{\mathbf{k}} + \text{Re}\Sigma) - i \text{Im}\Sigma)^{-1} \\ &= Z (\omega - \mathcal{E}_{\mathbf{k}} + \frac{i}{\tau})^{-1} , \quad (1.20) \end{aligned}$$

where we have defined,

$$Z^{-1} = 1 - \omega \partial_\omega \text{Re}\Sigma \Big|_{\{\omega=0, \mathbf{k}=\mathbf{k}_F\}} , \quad (1.21)$$

$$\mathcal{E}_{\mathbf{k}} = Z (\mathbf{k} - \mathbf{k}_F) \cdot \partial_{\mathbf{k}}(E_{\mathbf{k}} + \text{Re}\Sigma) \Big|_{\{\omega=0, \mathbf{k}=\mathbf{k}_F\}} , \quad (1.22)$$

$$\tau^{-1} = -Z \text{Im}\Sigma \Big|_{\{\omega=0, \mathbf{k}=\mathbf{k}_F\}} . \quad (1.23)$$

<sup>2</sup>By  $\mathbf{k}_F$  we actually mean  $\mathbf{k}_F \equiv k_F \mathbf{k}/|\mathbf{k}|$ , where  $\mathbf{k}$  is the argument of  $G(\mathbf{k}, \omega)$ .

Then, by considering the relation (1.18), we deduce that the lifetime of the quasiparticle goes to infinity at the Fermi Surface. Thus, the concept of quasiparticle is well defined near the Fermi Surface and the quasiparticle states are long-lived. The case of two dimensions is special and the relation (1.18) changes into  $\text{Im}\Sigma(\omega, \mathbf{p}) \propto (\omega - \mu)^2 \log |\omega - \mu|$ . By the above criteria, the system is still a Fermi Liquid because quasi-particles are long lived. Instead, in the one dimensional case, real and imaginary part of the self energy are of the same order and the Fermi Liquid description is not applicable.

By using the definitions (1.21), the explicit form of the Lorentzian function (1.17) is,

$$A^+(\mathbf{k}, \omega) = \frac{Z/\tau}{(\omega + \mathcal{E}_{\mathbf{k}})^2 + 1/\tau^2} . \quad (1.24)$$

The meaning of  $\text{Im}\Sigma(\omega, \mathbf{p})$  has been clarified in terms of  $\tau$  and now we would like to say something about the amplitude coefficient  $Z$ . The following argument is due to Migdal and Luttinger [21]. The idea is that the expectation value of the particle number operator,  $\langle n_{\mathbf{k}} \rangle$ , is determined by knowledge of the Green's Function through the relation

$$\langle n_{\mathbf{k}} \rangle = -i \lim_{t \rightarrow 0^-} G(\mathbf{k}, t) . \quad (1.25)$$

The Fourier transform of the dressed Green's function (1.20) can be found easily because both (1.20) and the free fermion Green's Function have the same functional form. Then, the final result is,

$$\langle n_{\mathbf{k}} \rangle = Z\theta(\mu - \mathcal{E}_{\mathbf{k}}) , \quad (1.26)$$

where  $\theta(x)$  is the Heaviside step function. Hence, assuming the interaction is such that perturbation theory may be used, the Fermi Surface exists in the interacting system as far as  $Z \neq 0$ . The effective energy  $\mathcal{E}_{\mathbf{k}}$  turns out to be a constant multiplying the linear term ( $|k| - k_F$ ). This constant plays the role of an effective mass  $m^*$  for the quasi-particles and it is defined by,

$$\mathcal{E}_{\mathbf{k}} = (|k| - k_F) \frac{k_F}{m^*}, \quad \frac{k_F}{m^*} = Z \left( \frac{k_F}{m} + \frac{\partial}{\partial |k|} \text{Re}\Sigma \right) \Big|_{|k|=k_F} . \quad (1.27)$$

The success of the Fermi Liquid theory as valuable theory for describing ordinary metals is encoded in the fact that the Fermi Surface survives when the interaction can be treated in perturbation theory. As in the case of free fermions, the low energy physics is mainly determined by the excitation living in a thin shell around the Fermi Surface. Thus, transport phenomena and specific heat in the interacting picture are understood in terms of free theory

arguments adapted to the case of quasi-particles with mass  $m^*$ . In particular, we remind the reader the most common results which are deduced from the Fermi Liquid theory:

- the linear dependence of specific heat  $C_V(T)$  with respect to the temperature,

$$C_V = \frac{1}{V} \frac{\partial U}{\partial T} = 2 \int \frac{d\mathbf{p}}{(2\pi)^3} \mathcal{E}_{\mathbf{p}} \frac{\partial n_{FD}(\mathbf{p})}{\partial T} = \frac{1}{3} m^* k_F T, \quad (1.28)$$

- the quadratic dependence of the resistivity  $r(T)$  with respect to the temperature due to umklapp scattering by an ionic lattice,

$$r(T) \sim T^2. \quad (1.29)$$

## 1.2 BCS in a nutshell

We begin this section by considering another quantum aspect of the Fermi Liquid theory. We are interested in the renormalization of the vertex interaction  $\lambda$ . We can interpret the Feynman diagrams associated with the corresponding perturbative series as quantum contributions to the tree level scattering amplitude of  $2 \rightarrow 2$  quasiparticles. We can sum up a subset of these quantum corrections and as a result obtaining the dressed vertex  $\Gamma$ . The procedure can be stated in terms of the following integral equation<sup>3</sup>,

$$\Gamma(p_1, p_2; p_3, p_4) = \lambda[p_1, p_2; p_3, p_4] + i \int dk \mathcal{I}(k) \quad (1.30)$$

$$\mathcal{I}(k) = \lambda[p_1, p_2; k, q - k] G(k) G(q - k) \Gamma(k, q - k; p_3, p_4). \quad (1.31)$$

We have used the more general form of  $\lambda$  by including the dependence upon the four momenta  $\lambda = \lambda[p_1, p_2; p_3, p_4]$ . However its precise form will not be relevant and we can assume for simplicity that  $\lambda$  is a constant. In (1.31) we have also defined  $q = p_1 + p_2$  and it should be noted that the integration has a cut-off on the energies, which are typically of order the Fermi energy  $\mu$ . At one loop, quantum correction are dominated by the Feynman diagram shown in Figure 1.2 and the result is

$$\Gamma = \lambda \left\{ 1 + N(0) \lambda \left( \frac{1}{2} \log \left| \frac{2\omega_D^2 - w^2}{w^2} \right| + i \frac{\pi}{2} \theta_{2\omega_D + w} \theta_{2\omega_D - w} \right) \right\}^{-1}, \quad (1.32)$$

---

<sup>3</sup>This is a Dyson equation for the dressed vertex  $\Gamma$  and actually gives the  $s$ -channel contribution. However, as it is explained in the Appendix A, other channels are subdominant because of the Fermi surface kinematics.

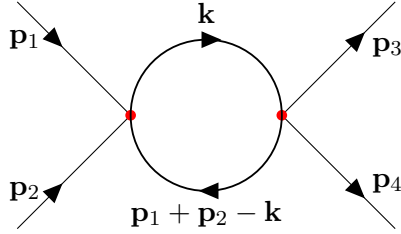


Figure 1.2: *s*-channel or Cooper-channel contribution to the one-loop amplitude in the dressed vertex  $\Gamma(p_1, p_2; p_3, p_4)$ . The integral is given by (1.31).

where  $\omega_D$  is the cut-off that we mentioned. Assuming  $\omega \ll \omega_D$  we find that a pole shows up whenever  $\lambda < 0$ . The position of the pole is

$$\omega_{pole} = +i2\omega_D e^{-\frac{1}{N(0)|\lambda|}} , \quad (1.33)$$

where  $N(0) = mk_F/2\pi^2$  is the density of states at the Fermi surface. The presence of a pole in  $\Gamma$  translates into the presence of a pole in the full Green's function and it is interpreted in terms of two particle excitations. However,  $\omega_{pole}$  is purely imaginary and it is located in the upper half-plane of complex frequency: poles of this type makes the theory unstable. Physically, it means that excitations created at energy  $\omega_{pole}$  will exponentially grow with time destabilizing the ground-state. What is the end point of this instability? The answer to this question came in the 1957 and led to the modern theory of superconductivity. This is the famous Bardeen, Cooper and Schrieffer (BCS) theory which describes the instability (1.33) in terms of interactions between fermions and lattice vibrations [23]. Formulated in the language of the second quantization, this a theory of fermions coupled to phonons.

**The electron-phonon interaction.** The electron-phonon interaction is a sort of ‘‘Yukawa’’ coupling in the language of particle physics. The Hamiltonian governing this interaction has the form,

$$\mathcal{H}_{int} = g \sum_{\mathbf{k}\mathbf{q}} c_{\mathbf{k}+\mathbf{q}}^\dagger c_{\mathbf{k}} (b_{\mathbf{q}} - b_{-\mathbf{q}}^\dagger) , \quad (1.34)$$

where  $b^\dagger(q)$  and  $b(q)$  are respectively creation and annihilation operator for the phonon excitation. In particular, the (real) phonon field is

$$\varphi(x) \propto \sum_q \left( b_{\mathbf{q}} e^{i\mathbf{q}r} + b_{\mathbf{q}}^\dagger e^{-i\mathbf{q}r} \right) . \quad (1.35)$$

The interaction (1.34) arises naturally in solid state physics and comes from the fact that the electrons feel a lattice potential  $W(r - n)$ , where the vector  $n$  indicates the position of the lattice points. Phonon excitations describe the change or shift of the lattice positions and therefore they induce a variation of the potential by the quantity  $\varphi(n)\nabla_n W(r - n)$ . Integration by parts yields the interaction term  $W(r - n)\nabla_n \varphi(n)$  which appears in (1.34). Then, strictly speaking the coupling  $g$  depends on the momentum and just for simplicity we consider it to be constant.

At tree level, the matrix element for the scattering of two electrons mediated by a phonon is given by,

$$\mathcal{A}_{2f \rightarrow 2f} \rightarrow \overbrace{g^2 b_{\mathbf{q}}(t) b_{-\mathbf{q}}^\dagger(0)} c_{\mathbf{k}+\mathbf{q}}^\dagger c_{\mathbf{k}} \Big|_t c_{\mathbf{k}'+\mathbf{q}'}^\dagger c_{\mathbf{k}'} \Big|_0 = \quad (1.36)$$

$$\rightarrow g^2 \mathcal{D}(q) c_{\mathbf{k}+\mathbf{q}}^\dagger c_{\mathbf{k}} \Big|_t c_{\mathbf{k}'-\mathbf{q}}^\dagger c_{\mathbf{k}'} \Big|_0 \quad , \quad (1.37)$$

where the phonon propagator  $\mathcal{D}(q)$  is,

$$\mathcal{D}(\mathbf{q}, \omega) = \frac{\mathcal{U}^2(\mathbf{q})}{\omega^2 - \mathcal{U}^2(\mathbf{q}) + i\delta} \quad , \quad q = (\omega, \mathbf{q}) \quad . \quad (1.38)$$

and  $\mathcal{U}^2(\mathbf{q})$  represents a certain the dispersion relation. Being  $\mathbf{k}' - \mathbf{q} = \mathbf{k}$  we obtain,

$$g^2 \frac{\mathcal{U}^2(\mathbf{k}' - \mathbf{k})}{(\epsilon_{\mathbf{k}'} - \epsilon_{\mathbf{k}})^2 - \mathcal{U}^2(\mathbf{k}' - \mathbf{k}) + i\delta} c_{\mathbf{k}+\mathbf{q}}^\dagger c_{\mathbf{k}} \Big|_t c_{\mathbf{k}}^\dagger c_{\mathbf{k}+\mathbf{q}} \Big|_0 \quad . \quad (1.39)$$

This term can be interpreted as the effective four Fermi coupling  $\lambda$  that appears in the Fermi Liquid theory. It is important to observe that the sign of the expression (1.39) determines whether the interaction is repulsive or attractive. In particular, the condition  $|\epsilon_{\mathbf{k}'} - \epsilon_{\mathbf{k}}| < \mathcal{U}(\mathbf{k}' - \mathbf{k})$  implies that the interaction is attractive. The maximum strength is obtained in the case  $\mathbf{q} = 0$  and  $\mathbf{k}' = -\mathbf{k}$ . From this point of view, the breakdown of the Fermi Liquid theory at  $\lambda < 0$  is understood in terms of this attractive interaction. As a result, the ground state of the system cannot be represented by the Fermi surface.

**The gap equation.** The new ground state of the system is described by the BCS theory. This theory is built on the idea that quasiparticles form a bound state  $\langle c_{\mathbf{k}} c_{-\mathbf{k}} \rangle \neq 0$ . Then, the Fermi surface collapses and the zero temperature ground state is a Bose-Einstein condensate. The bound state is usually referred to as the ‘‘Cooper pair’’. By construction, a Cooper pair transforms in the spin representation  $\mathbf{1}/2 \otimes \mathbf{1}/2 = \mathbf{0} + \mathbf{1}$ . The simplest situation is the spin

singlet case which is also relevant for high-Tc superconductivity. Instead, the dependence with respect to the angular momentum may be non trivial and for example, the most famous high-Tc superconductors, the cuprates, have d-wave angular momentum.

The BCS theory considers the following effective Hamiltonian,

$$\mathcal{H}_{\text{BCS}} = \sum_{\mathbf{k}\sigma} E_{\mathbf{k}} c_{\mathbf{k}\sigma}^{\dagger} c_{\mathbf{k}\sigma} - \sum_{\mathbf{k}, \mathbf{k}'} \lambda_{\mathbf{k}\mathbf{k}'} c_{\mathbf{k}\uparrow}^{\dagger} c_{-\mathbf{k}\downarrow}^{\dagger} c_{-\mathbf{k}'\uparrow} c_{\mathbf{k}'\downarrow} , \quad (1.40)$$

which describes the scattering of quasiparticles in the Cooper channel. Note that  $(c_{-\mathbf{k}\uparrow} c_{\mathbf{k}\downarrow})^{\dagger} = c_{\mathbf{k}\uparrow}^{\dagger} c_{-\mathbf{k}\downarrow}^{\dagger}$  and therefore the above combination is an hermitian operator, as it should be. Note also that  $\lambda_{\mathbf{k}\mathbf{k}'} > 0$  in  $\mathcal{H}_{\text{BCS}}$  corresponds to an attractive interaction. The interaction term satisfies the zero momentum constrain and the sum is taken over  $\mathbf{k}$  and  $\mathbf{k}'$  independently. The ground state of the Hamiltonian (1.40) can be studied by using the Bogoliubov transformation  $\mathcal{B}$ ,

$$\mathcal{B} := \begin{cases} c_{\mathbf{k}\uparrow} = & u_{\mathbf{k}} a_{\mathbf{k}+} + v_{\mathbf{k}} a_{\mathbf{k}-}^{\dagger} \\ c_{-\mathbf{k}\downarrow} = & -v_{\mathbf{k}} a_{\mathbf{k}+}^{\dagger} + u_{\mathbf{k}} a_{\mathbf{k}-} \end{cases} \quad (1.41)$$

The functions  $u_{\mathbf{k}}$  and  $v_{\mathbf{k}}$  are real and even under  $\mathbf{k} \rightarrow -\mathbf{k}$ , i.e  $u_{\mathbf{k}} = u_{-\mathbf{k}}$ ,  $v_{\mathbf{k}} = v_{-\mathbf{k}}$ . A short calculation shows that  $a_{\mathbf{k}}$  and  $a_{\mathbf{k}}^{\dagger}$  satisfies the same anti-commutation relations of the original quasiparticle operators if the following relation holds,

$$u_{\mathbf{k}}^2 + v_{\mathbf{k}}^2 = 1 . \quad (1.42)$$

Finally, the functions  $u_{\mathbf{k}}$  and  $v_{\mathbf{k}}$  will be chosen in order to “optimized” the change of variables in the Hamiltonian. Indeed, in terms of the new operators, (1.40) can be written as the sum of four pieces,

$$\mathcal{H}_{\text{BCS}} = \mathcal{H}^{(0)} + \mathcal{H}^{(D)} + \mathcal{H}^{(ND)} + 4 \text{ Fermi Operators} \quad (1.43)$$

where

$$\begin{aligned} \mathcal{H}^{(0)} &= 2 \sum_{\mathbf{k}} E_{\mathbf{k}} v_{\mathbf{k}}^2 - \sum_{\mathbf{k}\mathbf{k}'} \lambda_{\mathbf{k}\mathbf{k}'} u_{\mathbf{k}'} v_{\mathbf{k}'} u_{\mathbf{k}} v_{\mathbf{k}} \\ \mathcal{H}^{(D)} &= \sum_{\mathbf{k}} \left[ E_{\mathbf{k}} (u_{\mathbf{k}}^2 - v_{\mathbf{k}}^2) + 2u_{\mathbf{k}} v_{\mathbf{k}} \sum_{\mathbf{k}'} \lambda_{\mathbf{k}\mathbf{k}'} u_{\mathbf{k}'} v_{\mathbf{k}'} \right] (a_{\mathbf{k}+}^{\dagger} a_{\mathbf{k}+} + a_{\mathbf{k}-}^{\dagger} a_{\mathbf{k}-}) \\ \mathcal{H}^{(ND)} &= \sum_{\mathbf{k}} \left[ 2E_{\mathbf{k}} u_{\mathbf{k}} v_{\mathbf{k}} - (u_{\mathbf{k}}^2 - v_{\mathbf{k}}^2) \sum_{\mathbf{k}'} \lambda_{\mathbf{k}\mathbf{k}'} u_{\mathbf{k}'} v_{\mathbf{k}'} \right] (a_{\mathbf{k}+}^{\dagger} a_{\mathbf{k}-}^{\dagger} + a_{\mathbf{k}-} a_{\mathbf{k}+}) \end{aligned} \quad (1.44)$$

The first term,  $\mathcal{H}^0$ , is the ground state energy of a Fock space defined by the usual condition  $a_{\mathbf{k}\pm}|0\rangle = 0$ . By applying the standard method of Lagrange

multipliers it easy to see that the minimum of the energy, on the manifold (1.42), is obtained by solving the equation,

$$2E_{\mathbf{k}}u_{\mathbf{k}}v_{\mathbf{k}} = (u_{\mathbf{k}}^2 - v_{\mathbf{k}}^2) \sum_{\mathbf{k}'} \lambda_{\mathbf{k}\mathbf{k}'} u_{\mathbf{k}'}v_{\mathbf{k}'} , \quad (1.45)$$

which on the other hand, coincides with the constraint,  $\mathcal{H}^{(ND)} = 0$ . The notation,

$$\Delta_{\mathbf{k}} = \sum_{\mathbf{k}'} \lambda_{\mathbf{k}\mathbf{k}'} u_{\mathbf{k}'}v_{\mathbf{k}'} \quad (1.46)$$

introduces the gap parameter  $\Delta_{\mathbf{k}}$  as function of  $u_{\mathbf{k}}$  and  $v_{\mathbf{k}}$ . Then, by using (1.42) and (1.45) it is easy to rewrite  $u_{\mathbf{k}}$ ,  $v_{\mathbf{k}}$  and the above equation, only in terms of the gap and the energy  $E_{\mathbf{k}}$ :

$$u_{\mathbf{k}}^2 = \frac{1}{2} \left[ 1 + \frac{E_{\mathbf{k}}}{\sqrt{\Delta_{\mathbf{k}}^2 + E_{\mathbf{k}}^2}} \right] , \quad (1.47)$$

$$v_{\mathbf{k}}^2 = \frac{1}{2} \left[ 1 - \frac{E_{\mathbf{k}}}{\sqrt{\Delta_{\mathbf{k}}^2 + E_{\mathbf{k}}^2}} \right] , \quad (1.48)$$

$$\Delta_{\mathbf{k}} = \frac{1}{2} \sum_{\mathbf{k}'} \frac{\lambda_{\mathbf{k}\mathbf{k}'} \Delta_{\mathbf{k}'}}{\sqrt{\Delta_{\mathbf{k}'}^2 + E_{\mathbf{k}'}^2}} . \quad (1.49)$$

The equation (1.49) is known as the gap equation. As a fruitful exercise we can solve the gap equation for the BCS theory, where  $\lambda_{\mathbf{k}\mathbf{k}'}$  is assumed to be a constant different from zero only if  $\mathbf{k}$  and  $\mathbf{k}'$  lie in a thin shell around the Fermi surface. In this case, the gap has an  $s$ -wave solution  $\Delta_{\mathbf{k}} = \Delta$  and the equation for  $\Delta$  reads,

$$1 = \frac{\lambda}{2} \sum_{\mathbf{k}} \left[ \Delta^2 + E_{\mathbf{k}}^2 \right]^{-1/2} . \quad (1.50)$$

Since we are assuming that only momenta of the order of  $k_F$  contributes to the sum, we may obtain an approximate solution of (1.50) by considering an integral version of it. The measure can be taken to be  $d\mathbf{k} = 4\pi k^2 dk$  and the domain of integration  $[k_F - q, k_F + q]$  for some small  $q$ . The result is,

$$\Delta = 2q \frac{k_F}{m^*} \frac{e^{-v/\lambda}}{1 - e^{-\sigma\lambda}} , \quad v = \frac{2\pi^2}{m^* k_F} . \quad (1.51)$$

and we actually see that  $\Delta$  is non perturbative in  $\lambda$ . The energy of the excitations above the ground state are controlled by  $\mathcal{H}^{(D)}$ . After some algebraic

manipulation involving the gap equation, its eigenvalues are found to be

$$\mathcal{H}^{(D)}(\mathbf{k}) = \frac{1}{2m^*} \sqrt{E_{\mathbf{k}}^2 + \Delta_{\mathbf{k}}^2} (a_{\mathbf{k}+}^\dagger a_{\mathbf{k}+} + a_{\mathbf{k}-}^\dagger a_{\mathbf{k}-}) . \quad (1.52)$$

Thus,  $\Delta$  acquires the meaning of gap and defines the energy gap between the ground state and the first excited state.

**Strength of the Electron-Phonon Mechanism.** In the theory of phonons, it is important to recall the meaning of the Debye momentum. Roughly speaking, the Debye momentum is an upper bound on a generic phonon momentum and it is easily understood as

$$k_D \sim \frac{1}{a} , \quad (1.53)$$

where  $a$  is the interatomic distance. In the range of momenta  $|\mathbf{k}| \in [0, k_D]$  the dispersion relation of acoustic phonons is approximated by

$$\Omega(\mathbf{k}) = \begin{cases} \bar{v} \mathbf{k} & \text{if } |\mathbf{k}| \leq k_D \\ 0 & \text{if } \mathbf{k} > k_D \end{cases} \quad (1.54)$$

being  $\bar{v}$  a mean velocity. Then, we can also define the Debye frequency  $\Omega_D$  to be the maximum frequency associated with  $k_D$ , i.e  $\Omega_D = \bar{v}k_D$ . This remark tells us that the typical cutoff scale in the electron-phonon interaction is  $\Omega_D$  and the four-Fermi coupling in the BCS theory is better described as

$$\theta_{\mathbf{k}} \theta_{\mathbf{k}'} \lambda_{\mathbf{k}\mathbf{k}'} c_{\mathbf{k}\uparrow}^\dagger c_{-\mathbf{k}\downarrow}^\dagger c_{-\mathbf{k}'\uparrow} c_{\mathbf{k}'\downarrow} , \quad (1.55)$$

where

$$\theta_{\mathbf{k}} = \begin{cases} 1 & \text{for } |\epsilon_{\mathbf{k}} - \mu| < \Omega_D \\ 0 & \text{for } |\epsilon_{\mathbf{k}} - \mu| > \Omega_D \end{cases} \quad (1.56)$$

In this sense, the cutoff frequency  $\omega_D$  that appears in the expression of  $\omega_{pole}$  (1.32) can be taken to be the Debye frequency  $\Omega_D$ . From the same expression it is reasonable to estimate that the typical energy scale of the superconducting instability will be

$$E_{crit.} \approx \Omega_D e^{-\frac{1}{N(0)|\lambda|}} . \quad (1.57)$$

This line of reasoning suggests that the Fermi Liquid enters the superconducting phase at a critical temperature of the same order of  $E_{crit.}$ . The finite temperature calculation of  $\Gamma$  shows that the exact result is

$$k_B T_{critic} = \Omega_D e^{-\frac{1}{N(0)|\lambda|}} . \quad (1.58)$$

The electron-phonon mechanism of superconductivity has been successfully applied to explain the pairing in a large variety of materials, among many, we mention Mercury (Hg), Aluminium (Al) and lead (Pb) [24, 25, 26]. The critical temperature in these *conventional* superconductors is of the order of magnitude of  $10K$  and the formula (1.58) agrees with the experimental data. From a theoretical point of view, a superconductor is defined by the interaction that produces the instability and the pairing mechanism. Then, a conventional superconductor is a material such that the pairing instability is mediated by the phonon interactions. It should also be noted that electrons that are bound into a Cooper pair are quite distant in terms of lattice spacing ( $\sim 10^{-4}\text{cm}$ ) and the occupied volume of one Cooper pair contains the center of mass of approximately  $10^6$  different Cooper pairs. In this sense, the Cooper pair is a macroscopic state. Building on this observation it is possible to regard the superconducting instability in terms of an RG flow dynamics in which the four Fermi interaction becomes relevant in the IR [27, 6].

### 1.3 High-Tc Superconductors

With the term *high-Tc superconductors* we mean materials that behave as superconductors at temperature relatively higher than  $\sim 30K$ . The first known high-Tc superconductors were certain compounds of copper and oxygen so called *cuprates*. The order of magnitude of their critical temperature is about  $100K$ , spectacularly higher than the conventional superconductors. Since 2008, another class of high-Tc superconductors is known. These materials are binary compounds of iron and elements from the 5th group and are called iron-based pnictides [28]. Given a high-Tc superconductor, it is possible to engineer a family of high-Tc superconductors doping the parent structure. In particular, doping is divided into electron-doping and hole-doping. The most important novelty is that properties of doped high-Tc superconductors are quite different from that of the parent compound. We will see an example in the next section.

After the discovery of high-Tc superconductivity a natural issue was posed, is it possible to extend the BCS theory so as to explain high-Tc superconductivity? It turns out that electron-phonon interaction is too weak to account for the observed  $T_c$  in these materials, electron-phonon interaction is likely not the glue for high-Tc superconductivity. In particular, experiments rule out the electron-phonon interaction as the one responsible for the high-Tc. The simplest explanation is perhaps the smallness of  $\Omega_D$  in these materials.

Before moving on, it should be noted that the property of having high-Tc is

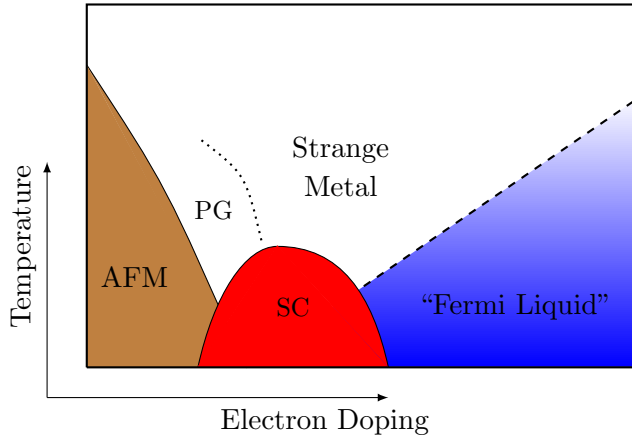


Figure 1.3: *Cartoon of the phase diagram of an electron-doped high- $T_c$  superconductors. The Figure reproduces concretely the case of  $Re_{2-x}Ce_x(CuO_4)$ , but the same topology is found basically in all the known examples.*

certainly important but theoretically does not represent the central feature of the phenomenon of high- $T_c$  superconductivity. We mention the case of  $MgB_2$ , which is an ordinary superconductor with critical temperature ( $\approx 39K$ ) higher than many Fe-pnictides. This example points out that the central question in the problem of high- $T_c$  superconductivity is the study of the pairing mechanism.

### 1.3.1 Electron doped high- $T_c$ Superconductors

The phase diagram of electron doped high- $T_c$  superconductors is described by Figure (1.3). This is not only a useful cartoon but represents, quite realistically, the topology of the phase diagram for various cuprates. The reader interested in experimental pictures, may satisfy his curiosity by having a look at the spectacular results of reference [29]. Quite remarkably, different compounds show the same topology in their phase diagram, perhaps underling that high- $T_c$  superconductivity is related essentially to some universal physics. Hole doped high- $T_c$  superconductors are also very well-known but for the purpose of our presentation we will just consider the case of electron doping<sup>4</sup>.

There are several observations to be made regarding the phase diagram shown in Figure (1.3). First of all, the parent compound of cuprates is a  $2D$

<sup>4</sup>The reason is that electron-doped high- $T_c$  superconductors have a large Fermi Surface.

Heisenberg antiferromagnet and indeed the antiferromagnetic order (AFM) characterizes the region of the phase diagram where the doping is relatively small. On the right hand side of the AFM phase, the superconducting dome has d-wave pairing. Regarding the superconducting dome, it is convenient to define the optimal doping as the doping at which the superconducting temperature reaches its maximum value. Above the superconducting dome the normal state shows “strange” features and the properties of this phase are non Fermi Liquid. We mention the famous linear dependence of the resistivity with the temperature. We also observe that the critical exponent that determines the behavior of the resistivity varies with the doping and gives the linear dependence with the temperature just on top of the superconducting dome. The same happens for other critical exponents. As we move towards the region of high doping, the Fermi Liquid behavior appears again and the critical exponents match with the standard ones. Another peculiar feature of the phase diagram is that, below optimal doping, the gap does not completely disappear at  $T_c$  and the system enters a pseudo-gap phase (PG).

High- $T_c$  superconductors show a phase diagram quite rich and a general analysis seems to be a complicated task. Nevertheless, what really is intriguing is the overlap of the AFM phase with the superconducting dome. As we already said, Figure (1.3) is quite general and therefore this universal overlapping clearly suggests that antiferromagnetism and superconductivity have something to do with each other. We can speculate further on this point by realizing that at zero temperature the system undergoes a quantum phase transition for a finite value of the doping. More precisely, imagining the superconducting dome is absent, we are led to the conclusion that the system quits the AFM phase at a certain value of the doping and flows to right of the phase diagrams towards the Fermi Liquid phase. The phase transition that takes place in between defines a quantum critical point and it is the one we are interested in. Furthermore, because of the AFM phase we expect this quantum critical point to be a magnetic quantum critical point (mQCP). From this point of view, it is natural to think that the anomalous non Fermi liquid behavior is mainly originated by quantum corrections due to fluctuations around the mQCP. In Figure 1.4 we show a cartoon of the phase diagram of electron doped high- $T_c$  superconductors in which the superconducting dome has been removed and the mQCP appears.

Given the above intuition, the Fermi liquid theory still represents the starting point to write down a quantum field theory for the cuprates. Non Fermi Liquid physics is introduced because of the presence of non trivial interactions with the bosonic excitations that describe the AFM phase. In particular, as

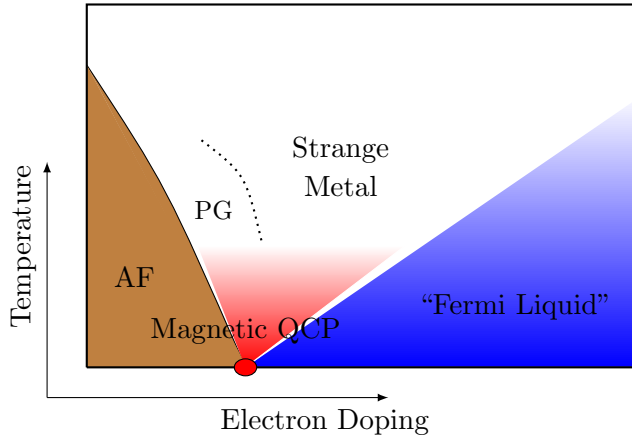


Figure 1.4: Phase diagram as in Figure (1.3). We have removed the superconducting dome in order to clear up our intuition about the magnetic quantum critical point.

we approach the mQCP, these excitations become gapless and we expect IR instabilities to show up in the fermionic correlation functions. Solving for the new theory will lead to the non Fermi Liquid physics. As a first hint that the above intuition is indeed correct, we will show that the  $d$ -wave pairing of the superconducting instability comes for free. In order to do so, we first introduce in more detail the theory and then we show how  $d$ -wave pairing naturally arises.

### 1.3.2 The Spin-Fermion Model

The theory that we consider is called the *spin-fermion model* [30, 31]. The spin-fermion model is a low energy theory and it should be regarded as the RG flow of a more fundamental UV theory. In general, the low energy physics is governed by degrees of freedom which have low energy excitations. For example, one such degree of freedom is the fermion itself since it has an arbitrary low energy near the Fermi surface. We may also consider that typical fermionic momenta are located near the Fermi Surface. Other low energy excitations are bosonic excitations. More precisely, we are mainly interested in the bosonic excitations that describe the AFM phase, i.e. spin density wave (SDW)  $S_{\mathbf{q}}(t)$ . Regarding this statement we need some extra clarification. Indeed, spin density waves are not separate degrees of freedom and they represent collective

modes of fermions. In particular, the spin wave order parameter is,

$$\Delta_{SDW} \sim \sum_k \langle c_{\mathbf{k}\uparrow}^\dagger c_{\mathbf{k}+\mathbf{Q}\downarrow} \rangle \quad (1.59)$$

where  $\mathbf{Q}$  is the ordering vector of the spin wave<sup>5</sup>. It follows that the treatment of spin density wave as separate bosonic degrees of freedom is just a convenient way to separate energy scales. The bare propagator of these collective modes is

$$\chi_b(\mathbf{q}, \Omega) = \frac{\chi_0}{\xi^{-2} + (\mathbf{q} - \mathbf{Q})^2 - (\Omega/v_s)^2} \quad (1.60)$$

where  $\xi$  is the spin correlation length and  $v_s$  is the spin velocity. The correlation length in general depends on the doping  $\xi = \xi(x)$  and the velocity  $v_s$  is of order  $v_F$ , the Fermi velocity. The overall factor  $\chi_0$  is a constant. Strictly speaking,  $\xi^{-1}$  measures the distance from the mQCP. The spin-fermion model is based on the assumption that there exists a single dominant channel for the fermion-fermion interaction which is mediated by the spin collective mode. Then, the effective Lagrangian of this model is

$$\mathcal{L}_{s.f.} = \mathcal{L}_{ferm.} + \mathcal{L}_{spin} + \mathcal{L}_{int.} \quad (1.61)$$

$$\mathcal{L}_{ferm.} = \sum_{\mathbf{k}} c_{\omega,\mathbf{k}}^\dagger G_b^{-1}(\omega, \mathbf{k}) c_{\omega,\mathbf{k}} \quad (1.62)$$

$$\mathcal{L}_{spin} = \frac{1}{2} \chi_b^{-1}(\mathbf{q}, \Omega) S_{\Omega,\mathbf{q}} S_{\Omega,-\mathbf{q}} \quad (1.63)$$

$$\mathcal{L}_{int} = g c_{\omega,\mathbf{k}}^\dagger \vec{\sigma} c_{\omega-\Omega,\mathbf{k}-\mathbf{q}} \vec{S}_{\Omega,\mathbf{q}} + c.c. \quad (1.64)$$

where  $G_b$  is the free fermion propagator  $G_b(\omega, \mathbf{k})^{-1} = \omega - E_{\mathbf{k}}$  and  $\vec{\sigma}$  are the three Pauli matrices ( $\sigma^1, \sigma^2, \sigma^3$ ). In order to understand how the Fermi Surface couples to the spin interaction through the ‘‘Yukawa’’ term (1.64) we consider the concrete example of Figure (1.5). In this case the Fermi Surface is made of lines, more precisely arcs. Even if it is not directly relevant to our discussion, it is important to emphasize that the boundary points of these open lines are identified and therefore the Fermi Surface has the topology of a circle. In the Figure (1.5) we have highlighted eight *hot spots*. These are points on the Fermi Surface that differ by a wave vector  $\mathbf{Q}$ . It is a general experimental fact that the Fermi Surface of the cuprates contains hot spots.

<sup>5</sup>In terms of scattering processes, the propagating particle picks up a momentum  $\mathbf{Q}$  from scattering against the periodic structure of the spiral internal field, and it has its spin changed from  $\sigma'$  to  $\sigma$  by the spin-aligning character of the internal field [19].

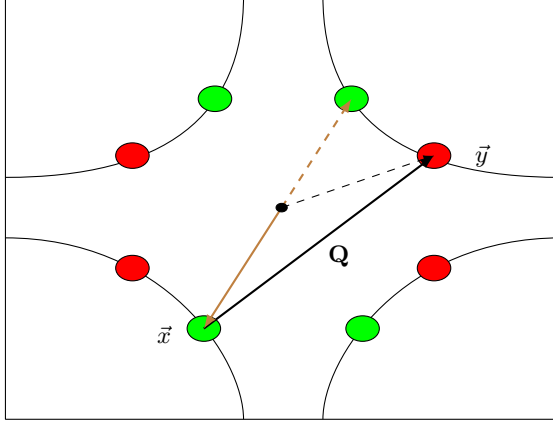


Figure 1.5: *Cartoon of the Fermi Surface for the electron doped cuprates. The scattering process in the spin-fermion model involves a red and a green electron of two opposite arcs. These are the ones such that  $\mathbf{k}_{red} - \mathbf{k}_{green} = \mathbf{Q}$ .*

The presence of the hot spots on the Fermi surface implies that at low energy the tree level spin decay is not kinematically forbidden. Then, the  $\omega^2$  term in the *bare* propagator (1.60) is irrelevant and  $\chi(\mathbf{q}, \Omega)$  can be approximated by its static part.

In analogy with the BCS theory, we can explore what features will have interaction mediated by the spin fluctuations. We assume the general form of the gap equation (1.49) and we only need to specify the coupling function  $\lambda_{\mathbf{k}\mathbf{k}'}$ . The effective “Yukawa” Hamiltonian between the fermions and the spin fluctuation is,

$$\mathcal{H}_{\text{int}} = g \sum_{\mathbf{k}\mathbf{q}} c_{\mathbf{k}+\mathbf{q}\alpha}^\dagger \sigma_{\alpha\beta}^i c_{\mathbf{k}\beta} S_{\mathbf{q}}^i + c.c. . \quad (1.65)$$

By following the same steps that led to (1.39), it easy to see that the Hamiltonian (1.65) generates the following amplitude for the scattering of  $2 \rightarrow 2$  quasiparticles,

$$\mathcal{A}_{2f \rightarrow 2f} \rightarrow g^2 \sigma_{\alpha\beta}^i \sigma_{\gamma\delta}^j \overbrace{S_{\mathbf{q}}^i(t) S_{\mathbf{q}'}^{j\dagger}(0)} c_{\mathbf{k}+\mathbf{q}}^\dagger c_{\mathbf{k}} \Big|_t c_{\mathbf{k}'+\mathbf{q}'}^\dagger c_{\mathbf{k}'} \Big|_0 \quad (1.66)$$

$$\rightarrow \sigma_{\alpha\beta}^i \sigma_{\gamma\delta}^i \frac{\chi_0}{\xi^{-2} + (\mathbf{q} - \mathbf{Q})^2} c_{\mathbf{k}+\mathbf{q}}^\dagger c_{\mathbf{k}} \Big|_t c_{\mathbf{k}'-\mathbf{q}}^\dagger c_{\mathbf{k}'} \Big|_0 . \quad (1.67)$$

Then, the effective four Fermi interaction is,

$$\sigma_{\alpha\beta}^i \sigma_{\gamma\delta}^i \frac{\chi_0}{\xi^{-2} + (\mathbf{q} - \mathbf{Q})^2} \Big|_{\mathbf{q}=\mathbf{k}'-\mathbf{k}} . \quad (1.68)$$

A projection of  $\vec{\sigma}_{\alpha\beta}\vec{\sigma}_{\gamma\delta}$  onto the singlet spin  $\delta_{\alpha\beta}\delta_{\gamma\delta} - \delta_{\alpha\delta}\delta_{\beta\gamma}$  yields a negative  $-3$  factor which enters the gap equation in the following gap equation,

$$\Delta_{\mathbf{k}} = -\frac{3}{2}g^2 \sum_{\mathbf{k}'} \frac{1}{\xi^{-2} + (\mathbf{k}' - \mathbf{k} - \mathbf{Q})^2} \frac{\Delta_{\mathbf{k}'}}{\sqrt{\Delta_{\mathbf{k}'}^2 + E_{\mathbf{k}'}^2}}. \quad (1.69)$$

The main difference with respect to the phonon case is exactly the minus sign due to a summation over spin components. Then, an  $s$ -wave solution is not possible. However, since  $\chi(\mathbf{q})$  is peaked near the antiferromagnetic vector  $\mathbf{Q}$ , the pairing interaction constraints the gap at momenta  $\mathbf{k}$  and  $\mathbf{k} + \mathbf{Q}$ . Then, the overall minus sign cancels provided  $\Delta_{\mathbf{k}} = -\Delta_{\mathbf{k} + \mathbf{Q}}$ . For the cuprates  $\mathbf{Q} = (\pi, \pi)$  and this relation implies  $d_{x^2-y^2}$  symmetry:  $\Delta_{\mathbf{k}} \sim \cos k_x - \cos k_y$ . This is the first good point in favor of the spin fermion model.

### 1.3.3 Results and Limitations

In this section we analyze perturbative quantum corrections to the two bare Green's Functions,  $G_b(\omega, \mathbf{p})$  and  $\chi_b(\Omega, \mathbf{q})$ . The motivation is the same as in the theory of electrons and phonons: we have to check that the attractive interaction is not destroyed when loop diagrams are taken into account. In particular, we have to look at the renormalization of the vertex  $g$  and the self energy  $\Sigma(\omega, \mathbf{k})$  of the electrons. In the phonon case, it can be proven that the perturbative series is stable and the fermionic quasiparticles are always well defined in the vicinity of the Fermi Surface. As we will see, the spin-fermion model behaves differently.

The two leading one-loop Feynman diagrams are shown in Figure (1.6) and (1.7). Our final goal is to understand how quantum corrections modify the Fermi Liquid result (1.18) eventually producing the desired non Fermi Liquid properties. We will proceed by steps and we refer to [30, 31, 32] for a more

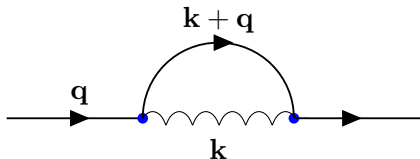


Figure 1.6: One loop diagram contributing to the self energy  $\Sigma(\omega, \mathbf{q})$  in the spin-fermion model. The wavy line is the spin propagator  $\chi_b(\Omega, \mathbf{k})$ .

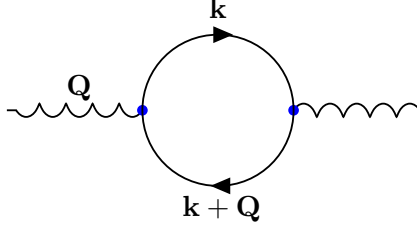


Figure 1.7: One loop diagram contributing to the boson self energy  $\Pi(\mathbf{q}, \omega)$ .

detailed discussion. The integral corresponding to Figure (1.6) is

$$\Sigma(\mathbf{q}, \omega) = -3g^2 \int \frac{d\mathbf{k}}{(2\pi)^3} \frac{d\omega'}{2\pi} G(\mathbf{k} + \mathbf{q}, \omega + \omega') \chi(\mathbf{k}, \omega') \quad (1.70)$$

where  $G$  and  $\chi$  are the exact fermion propagators calculated in perturbation theory. The strategy is to first evaluate the dressed propagator for the spin wave and then we plug the result back into the fermion self energy (1.70) to see what happens.

Quantum corrections to the spin propagator  $\chi(\mathbf{q}, \omega)$  are encoded in the boson self energy  $\Pi(\mathbf{q}, \omega)$  which plays the same role of the fermion self-energy  $\Sigma(\mathbf{q}, \omega)$ . In particular, once  $\Pi(\mathbf{q}, \omega)$  is known, there exists a Dyson equation for the full bosonic *dressed* propagator whose general solution is

$$\chi(\mathbf{q}, \omega)^{-1} = \chi_b(\mathbf{q}, \omega)^{-1} - \frac{\Pi(\mathbf{q}, \omega)}{\chi_0 \xi^2} \quad (1.71)$$

In the above conventions  $\Pi(\mathbf{q}, \omega)$  is dimensionless,

$$\chi(\mathbf{q}, \omega) = \frac{\chi_0 \xi^2}{1 + \xi^2 (\mathbf{q} - \mathbf{Q})^2 - \chi_0^2 (\omega/v_s)^2 - \Pi(\mathbf{q}, \omega)} \quad (1.72)$$

The diagram in Figure (1.7) is a one-loop contribution to  $\Pi(\mathbf{q}, \omega)$  and reads,

$$\Pi(\mathbf{q}, \omega) = 2g^2 \chi_0 \xi^2 \int d\mathbf{k} dw G(\mathbf{k}, w) G(\mathbf{k} + \mathbf{q}, w + \omega) \quad (1.73)$$

Since the bare propagator  $\chi_b(\mathbf{q}, \omega)$  is peaked at the SDW wave vector, it is sufficient to compute the quantum contribution only at  $\mathbf{q} = \mathbf{Q}$ . The result is the following damping term,

$$\Pi(\mathbf{Q}, \omega) = i(g^2 \chi_0 \xi^2) N \frac{\omega}{v^2} = i \frac{\omega}{\omega_{sf}}, \quad (1.74)$$

where  $\omega_{sf} \equiv (g^2 \chi_0 \xi^2 N)^{-1} v^2$  and  $v^2$  depends on the specific form of the dispersion relation  $E_{\mathbf{k}}$ . By dimensional analysis  $v$  is of order  $v_F$ . The factor  $N$  counts the number of hot spots. i.e the number of decaying channels. The one-loop spin propagator  $\chi(\mathbf{q}, \Omega)$  is then,

$$\chi(\mathbf{q}, \Omega) = \frac{\chi_0 \xi^2}{1 + \xi^2 (\mathbf{q} - \mathbf{Q})^2 - i(\Omega/\omega_{sf}) - \chi_0^2 (\Omega/v_s)^2} \quad (1.75)$$

There are two important observations about the expression (1.74). First, the scale  $\omega_{sf}$  sets the reference scale for the loop quantum correction to become relevant. Indeed, for  $\Omega < \omega_{sf}$  the term (1.74) can be neglected and the propagator is essentially the bare propagator. Second, if the scale  $\omega_{sf}$  in part controls the anomalous correction to  $\chi_b(\Omega)$ , the effective coupling constant that we should consider is not just the spin-fermion interaction  $g^2 \chi_0$  but the ratio  $g^2 \chi_0 / \omega_{sf}$ . We formalize this idea in the following way. We consider the two energy scales  $g^2 \chi_0$  and  $\xi/v_F$  and we define the dimensionless coupling  $\lambda$ ,

$$\lambda \equiv g^2 \chi_0 \frac{\xi}{v_F}, \quad (1.76)$$

Then,  $\lambda^2 \propto g^2 \chi_0 / \omega_{sf}^2$  and  $\Pi(\mathbf{Q}, \omega)$  takes the form,

$$\Pi(\mathbf{Q}, \omega) = (\lambda N) \omega \left( \frac{\xi v_F}{v^2} \right). \quad (1.77)$$

The term in parenthesis is by dimensional analysis a typical time scale  $\propto \xi/v_F$ . The physics of the coupling constant is now clear and we will see that  $\lambda$  is the natural coupling that controls the strength of the entire perturbative expansion both for bosons and fermions.

By taking into account  $\Pi(\mathbf{Q}, \omega)$ , we come back to the fermionic self energy (1.70). Substituting the result for the bosonic propagator (1.75) into the self energy integral, we obtain

$$\Sigma(\mathbf{q}, w) = 3g^2 \chi_0 \xi^2 \int \frac{d\mathbf{k}}{(2\pi)^3} \frac{d\omega}{2\pi} \frac{G(\mathbf{k} + \mathbf{q}, \omega + w)}{1 + \xi^2 (\mathbf{k} - \mathbf{Q})^2 - i(\omega/\omega_{sf}) - \chi_0^2 (\omega/v_s)^2} \quad (1.78)$$

We are interested in the case in which the external momentum  $\mathbf{q}$  lies near the hot spot position. We already know that quasiparticles are well defined for momenta in a thin shell around the Fermi surface, therefore we expect most of the non Fermi Liquid behavior to show up in correspondence of the hot spot, where the spin-fermions interaction becomes important. The explicit calculation can be found in the Appendix of [30]. Here we review the result

considering a modified version of the spin-fermion model. This modification is suggested by the following observation: the same dependence of  $N$  in 1.77 arise in a model where the number of hot spots is fixed but there are  $N$  flavors of fermions. In the remaining part of this section we will consider a version of the spin fermion model in which there are  $N$  flavors of fermions and we will assume that a large  $N$  expansion is valid. We will come back on this issue later on, at the moment this is just a convenient simplified setting. Then, the self energy calculation yields,

$$\Sigma(\mathbf{k}_{hs}, w) = 6\lambda \frac{w}{1 + \sqrt{1 - i\frac{|w|}{\omega_{sf}}}} \quad (1.79)$$

and once again  $\lambda$  shows up as the effective coupling constant of the perturbative expansion. We notice that the result does not depend on  $N$  but just on  $\lambda$ . By considering the interesting range of frequencies, namely  $\omega > \omega_{sf}$ , we find that the fermionic self energy (1.79) behaves in non Fermi Liquid fashion,

$$\Sigma(\mathbf{k}_{hs}, w) = \sqrt{4\lambda^2\omega_{sf}} \sqrt{i|w|} \text{sign}(w) . \quad (1.80)$$

Furthermore, the combination of couplings is such that  $\Sigma(\mathbf{k}_{hs}, w)$  does not depend on  $\xi$ , as it should be when a theory is in a quantum critical regime. This result is in agreement with our ideas about the non Fermi liquid physics and the mQCP. The Green's Function at the hot spots becomes

$$G(\mathbf{k}, w) \propto \frac{\sqrt{4\lambda^2\omega_{sf}}\sqrt{i|w|} \text{sign}(w) + E_{\mathbf{k}}}{i|w| - E_{\mathbf{k}}^2/\sqrt{4\lambda^2\omega_{sf}}} . \quad (1.81)$$

This is the most important outcome of the spin-fermion model. By considering (1.81) it is indeed possible to show that properties of the optical conductivity and other observables resembles the ones that are found in the ARPES experiment [33, 34, 35, 36].

With respect to the Fermi Liquid the main difference is the absence of a pole in the propagator at real frequencies. Instead,  $G(\mathbf{k}, w)$  has a pole along the imaginary frequency axis at  $w = E_{\mathbf{k}}^2/\sqrt{4\lambda^2\omega_{sf}}$ . Thus, we are led to the conclusion that quasiparticles are not well defined at the hot spots. In this sense, our intuition about the  $d$ -wave pairing derived from BCS arguments cannot be completely correct. Indeed, the use of the gap equation (1.69) is not justified because quasiparticles at the hot spots loose their integrity. In this case, a possible way out is to say that the pairing mechanism involves electrons with momenta in a small region around the two opposite hot spots. Then, if we calculate the self energy considering not just  $\mathbf{k}_{hs}$  but  $\mathbf{k} \approx \mathbf{k}_{hs} + \mathbf{k}$ , we find

the the Green's Function goes back to the functional form of the Fermi Liquid theory [31]. In other words, the quasiparticle picture breaks down just when  $\mathbf{k} = \mathbf{k}_{hs}$ . Happy with this, we should now reconsider whether the assumptions we have made in the treatment of the spin-fermion model can be trusted.

The first objection is the following. The dimensionless coupling constant that controls the perturbative expansion is in general not a small quantity for real material. In fact, by using photoemission experiments,  $\lambda$  can be estimated to be  $\lambda \sim 2$  near optimal doping. Then, from the theoretical point of view the problem becomes hard because the conventional perturbative expansion breaks down. More precisely, we always expect a flow of the theory to strong coupling because  $\lambda$  diverges like  $\xi$  when the system approach the critical regime  $\xi \rightarrow \infty$ . For this reason, a better motivated setup is to consider the modified version of the spin fermion model and study the large  $N$  limit. However, differently from what happens in matrix theories, the naive counting of powers of  $1/N$  is not correct and the theory is not stable in the large  $N$  limit. In particular, there exists no planar limit [31]. This is due to infrared divergences and it is unavoidable. We conclude that even the large  $N$  expansion is ultimately not under control.

The strong coupling problem is not the only weak point of the spin-fermion dynamics and indeed there is a second objection. The non existence of quasi-particles in the non Fermi Liquid picture poses another theoretical problem: it might be the case that the standard quasi-particle description is not refined enough to describe the physics of the cuprates. Even at weak coupling we have seen an example of this inadequacy. On one hand, the hot spots are precisely the points in which the pairing interaction is the strongest and therefore we expect Cooper pairs to form in agreement with the  $d$ -wave picture. On the other hand, quantum corrections due to the vicinity of the mQCP modify substantially the quasiparticle regime and we have to introduce another scale in the problem which takes into account the distance from the hot spots. This procedure is somehow not natural and there is no experimental evidence that this additional distinction has to be made.

Finally, it should also be said that there is no way we can directly face the strong coupling problem by putting the spin-fermion model on a lattice. The double sign problem has not yet been solved in general and there are only few tricky examples in which it is actually possible to get rid of this problem (see [37] and reference therein).



# Chapter 2

## Short Introduction to AdS/CFT

This chapter is devoted to the AdS/CFT conjecture. This is not an easy subject and requires a certain complicated technology coming from string theory. Our purpose is to produce all the building blocks that are necessary to understand the conjecture. We will make full use of the AdS/CFT machinery in the remaining part of this thesis thus, it is important to have a solid perception of what will be introduced as “the holographic principle”.

Most of the material of this chapter is nowadays standard and very well reviewed in the literature. Our presentation closely follows the main references [38, 39].

### 2.1 Minimal Background of supersymmetry

Historically, supersymmetry has been invoked to overcome the no-go theorem of Coleman and Mandula (CM): a relativistic field theory of massive particles with non trivial scattering, admits a unique symmetry group whose Lie algebra is the direct sum of the Poincaré algebra and a finite-dimensional compact Lie algebra for the internal symmetry [40]. The very definition of the symmetry group is at the base of the field theory description of particle physics. In the first place, fields correspond to representations of the Lorentz group  $SO(1, d)$  and Lagrangians are built out of a set of Lorentz invariants. If the theory has an internal symmetry, fields also transform as representations of the symmetry group and the Lagrangian has to be invariant under this additional transformation. Minimal interactions are obtained by gauging internal symmetries but in principle, any coupling that preserves the structure of the theory may be introduced. From this point of view, the lack of a fundamental principle able to specify uniquely the theory seemed to be hidden in the conclusions of the CM theorem.

It was later realized that new structure could be brought into the theory if fermionic (super)charges were included as part of the algebra:  $\mathcal{N} = 1$  supersymmetry in  $D = 4$  has been the first example of such generalization [41]. The algebra contains the standard Poincarè algebra, generated by  $P_\mu$  and  $M_{[\mu\nu]}$ , and a set of new relations involving a Weyl spinor  $Q_\alpha$ , with  $\alpha = 1, 2$ . This spinor introduces two complex supercharges and the Poincarè algebra is enlarged by the anti-commutation rule,

$$\{Q_\alpha, \bar{Q}_{\bar{\beta}}\} = 2(\sigma^\mu)_{\alpha\bar{\beta}} P_\mu, \quad \bar{Q}_{\bar{\beta}} = (Q_\beta)^* . \quad (2.1)$$

Here,  $\sigma^\mu = (1, -\sigma^i)$  and  $\sigma^i$  are the standard Pauli matrices. The super-algebra closes by imposing,

$$[M_{\mu\nu}, Q_\alpha] = i(\sigma_{\mu\nu})_\alpha{}^\beta Q_\beta, \quad [P_\mu, Q_\alpha] = 0, \quad (2.2)$$

and the analogous relations for  $\bar{Q}_{\bar{\beta}}$ . The  $\sigma_{\mu\nu}$  matrices are usually used to construct the spin 1/2 Lorentz generators in four dimensions and are defined by  $\sigma_{\mu\nu} = -i[\sigma_\mu, \sigma_\nu]/4$ .

The introduction of supersymmetry provides a unification of space-time and internal symmetry and avoids the conclusions of the CM theorem. An important novelty is represented by the interplay between the spin helicity, generated by  $M_{12} \equiv J_3$ , and the supercharges. In particular, from the commutation relations (2.2) we obtain

$$[J_3, Q_1] = \frac{1}{2}Q_1, \quad [J_3, Q_2] = -\frac{1}{2}Q_2, \quad (2.3)$$

and we conclude that  $Q_1$  and  $Q_2$  are effectively rising and lowering operator for the helicity quantum number. Interestingly, the spin component is increased by half unit. In this way supersymmetry establishes a first fundamental connection among bosonic and fermionic degrees of freedom. As a consequence, field theories constructed to be invariant under supersymmetry will show a remarkable structure of couplings. Concretely, given a field theory representation, supersymmetry acts on bosons and fermions in the following schematic form,

$$\begin{aligned} \delta_\epsilon(\text{bosons}) &\rightarrow \bar{\epsilon} \times \text{fermions} \\ \delta_\epsilon(\text{fermions}_\alpha) &\rightarrow \text{bosons } \epsilon_\alpha . \end{aligned} \quad (2.4)$$

The supersymmetry transformation is  $\delta_\epsilon$  and  $\epsilon$  is the infinitesimal parameter is an anti-commuting spinor  $\epsilon_\alpha$  with  $\alpha = 1, 2$ . The “ $\times$ ” operation involves spinorial indexes. Since the Poincarè generators and the supercharges are

joined in the super-algebra, if the theory contains gravity, supersymmetry is promoted to a gauge symmetry and the spinor parameter becomes an arbitrary function of the space-time coordinates,  $\epsilon \rightarrow \epsilon_\alpha(x)$ .

At the classical level, supersymmetry has the appealing property of unifying gravity and matter through non trivial interactions. At the quantum level, supersymmetry leads to surprising results both in the perturbative and in the non-perturbative regime. We refer to the literature for more specific reviews on the subject (for example see [44] and references therein). Our purpose in this chapter is to move as quickly as possible to the statement of the AdS/CFT correspondence.

### 2.1.1 Spinors

Much of the content of supersymmetric field theories is based on spinorial representations of the Lorentz group  $SO(1, d)$ . In this section we give a proper introduction of the topic [45].

The first step is to find a representation of the Clifford Algebra,

$$\{\Gamma^\mu, \Gamma^\nu\} = 2\eta^{\mu\nu}, \quad (2.5)$$

where  $\eta^{\mu\nu} = \text{diag}(-1, +\mathbf{1}_d)$  and  $D = d + 1$  is the space time dimension. Using standard methods of Fock representation we can give an iterative expression of the  $\Gamma$  matrices. Starting from  $D = 2$ , where

$$\Gamma^0 = \begin{pmatrix} 0 & 1 \\ -1 & 0 \end{pmatrix}, \quad \Gamma^1 = \begin{pmatrix} 0 & 1 \\ 1 & 0 \end{pmatrix} \quad (2.6)$$

we define the  $\Gamma$  matrices in even dimensions  $D = 2k + 2$  by the following formulas,

$$\Gamma^\mu = \gamma^\mu \otimes \begin{pmatrix} -1 & 0 \\ 0 & 1 \end{pmatrix}, \quad \mu = 0, 1, \dots, D - 3 \quad (2.7)$$

$$\Gamma^{D-2} = \mathbf{1} \otimes \begin{pmatrix} 0 & 1 \\ 1 & 0 \end{pmatrix}, \quad \Gamma^{D-1} = \mathbf{1} \otimes \begin{pmatrix} 0 & -i \\ i & 0 \end{pmatrix}, \quad (2.8)$$

with  $\gamma^\mu$  the  $2^k \times 2^k$  Dirac matrices in  $D - 2$  dimensions and  $\mathbf{1}$  being the  $2^k \times 2^k$  identity. The tensor products in (2.7) contain  $k + 1$  factors, thus the representation has dimension  $2^{k+1}$ . This is usually called the *Dirac representation*. A Dirac spinor is then a vector with  $2^{k+1}$  complex independent components. We remind the reader that indexes are lowered by means of the  $\eta_{\mu\nu}$  tensor. The generator  $M_{[\mu\nu]}$ , defined as

$$M_{[\mu\nu]} = -\frac{i}{4}[\Gamma_\mu, \Gamma_\nu], \quad (2.9)$$

satisfy the Lorentz algebra,

$$[M_{\mu\nu}, M_{\rho\sigma}] = i(\eta_{\nu\rho}M_{\mu\sigma} - \eta_{\nu\sigma}M_{\mu\rho} - \eta_{\mu\rho}M_{\nu\sigma} + \eta_{\mu\sigma}M_{\nu\rho}) . \quad (2.10)$$

Thus, the Dirac representation turns out to be a representation of the Lorentz algebra as well. However, this is not an irreducible representation. Indeed, the matrix,

$$\Gamma^\bullet = i^{-k} \Gamma^0 \Gamma^1 \dots \Gamma^{d-1} \quad (2.11)$$

has the following properties,

$$(\Gamma^\bullet)^2 = 1 , \quad \{\Gamma^\bullet, \Gamma^\mu\} = 0 , \quad [\Gamma^\bullet, M^{\mu\nu}] = 0 . \quad (2.12)$$

and it is not a multiple of the identity. In particular, the eigenvalues of  $\Gamma^\bullet$  are  $\pm 1$  and  $\text{tr}(\Gamma^\bullet) = 0$ . The explicit construction of the Fock space reveals that a Dirac representation of dimension  $2^{k+1}$  splits into two irreducible representations of dimension  $2^k$  labeled by the eigenvalues of  $\Gamma^\bullet$ . These two irreducible representations are called *Weyl representations* and the eigenvalue of  $\Gamma^\bullet$  is usually called *chirality*. For odd dimensions  $D = 2k + 3$ , the Dirac representation is obtained by adding  $\Gamma^D = \Gamma^\bullet$  or  $\Gamma^D = -\Gamma^\bullet$  to the set of  $\Gamma$  matrices found for  $D = 2k + 2$ . This is now an irreducible representation because  $[\Gamma^D, M_{\mu D}] \neq 0$ , thus for  $D = 2k + 3$  there is a single spinor representation of dimension  $2^{k+1}$ .

Another possible projection of the Dirac representation is a *reality condition*. We begin with even dimensions but we will see that in some cases this type of projection can also be extended to odd dimensions. The matrices  $\pm \Gamma^{\mu\star}$  satisfy the same Clifford algebra as  $\Gamma^\mu$  and they must be related to  $\Gamma^\mu$  by a similarity transformation. These transformations are implemented by defining,

$$B_1 = \Gamma^3 \Gamma^5 \dots \Gamma^{d-1}, \quad B_2 = \Gamma^\bullet B_1. \quad (2.13)$$

We observe that  $\Gamma^3, \Gamma^5, \dots, \Gamma^{D-1}$  are imaginary and the remaining  $\Gamma^\mu$  are real. Then, it is possible to prove that,

$$B_1 \Gamma^\mu B_1^{-1} = (-)^k \Gamma^{\mu\star}, \quad (2.14)$$

$$B_2 \Gamma^\mu B_2^{-1} = (-)^k (-\Gamma^{\mu\star}), \quad (2.15)$$

$$B M^{\mu\nu} B^{-1} = -M^{\mu\nu\star}. \quad (2.16)$$

Thus, the spinors  $\psi$  and  $B^{-1}\psi^\star$ , where  $B$  is either  $B_1$  or  $B_2$ , transform in the same way under Lorentz transformations and we may consider the possibility

| D  | Majorana | Weyl    | Majorana-Weyl | real ind. comp. |
|----|----------|---------|---------------|-----------------|
| 4  | ✓        | complex | -             | <b>4</b>        |
| 5  | -        | -       | -             | <b>8</b>        |
| 10 | ✓        | self    | ✓             | <b>16</b>       |
| 11 | ✓        | -       | -             | <b>32</b>       |

Table 2.1: Smallest spinorial representation in various dimensions. The number of real independent components is obtained by truncating the complex representation of dimension  $2^{k+1}$ . Because of the relations  $B_1\Gamma^\bullet B_1^{-1} = B_2\Gamma^\bullet B_2^{-1} = (-)^k(\Gamma^\bullet)^*$ , for  $k$  even each Weyl representation is its own conjugate whereas for  $k$  odd each Weyl representation is conjugate to the other. This observation becomes relevant in dimensions  $D = 4$  and  $D = 10$ . Adapted from [45].

of imposing a condition between  $\psi$  and  $\psi^*$ . This is the so called *Majorana* condition:  $\psi^* = B\psi$ . Consistency requires,

$$\psi = B^*B \psi \quad \rightarrow \quad B^*B = 1 . \quad (2.17)$$

The cases of  $B_1$  and  $B_2$  are different and give a result which depends on the dimension,

$$B_1^*B_1 = (-)^{k(k+1)/2}, \quad B_2^*B_2 = (-)^{k(k-1)/2} . \quad (2.18)$$

It means that a Majorana condition using  $B_1$  is possible only if  $k = 0$  or  $3 \bmod 4$ , whereas the use of  $B_2$  is allowed only if  $k = 0$  or  $1 \bmod 4$ . If  $k = 0 \bmod 4$  both conditions are equivalent. In odd dimensions  $\Gamma^D = \pm\Gamma^\bullet$  and the relation (2.16) has a definite sign only for  $B = B_1$ . It follows that a Majorana condition is compatible with  $k = 0$  or  $3 \bmod 4$ . We observe that a Majorana condition is possible in  $D = 11$  but not in  $D = 5$ . In table 2.1 we summarize the cases that will be discussed throughout this thesis.

### 2.1.2 Extended Supersymmetry

The algebra of  $\mathcal{N} = 1$  supersymmetry in  $D = 4$  admits a straightforward generalization. We consider  $Q_\alpha^a$ , where  $\alpha$  is a space-time spinor index and  $a = 1, \dots, \mathcal{N}$  labels the distinct supercharges. Then, the minimal extended

super-algebra is

$$\{Q_\alpha^a, \bar{Q}_{\beta b}\} = 2(\sigma^\mu)_{\alpha\bar{\beta}} P_\mu \delta_b^a, \quad \bar{Q}_{\beta b} = (Q_\beta^b)^\star \quad (2.19)$$

We could equally write down this minimal extended super-algebra by considering a four component Majorana spinor. Indeed, in  $D = 4$ , Weyl and Majorana representations turn out to be equivalent and a Majorana spinor  $Q$  can be defined by,

$$Q = \begin{pmatrix} Q_\alpha \\ \bar{Q}^{\bar{\alpha}} \end{pmatrix} \quad \text{with} \quad \bar{Q}^{\bar{\alpha}} \equiv \epsilon^{\bar{\alpha}\bar{\beta}} \bar{Q}_{\bar{\beta}}. \quad (2.20)$$

It is useful to review the collection of massless supermultiplets in the cases of  $D = 4$  extended supersymmetry.

$\mathcal{N} = 2$  : Given the state of greater helicity  $|s\rangle$ , we obtain the other states of the super-multiplet by applying ladder operators of the form  $Q_1^i$  at most two times. The result is,

$$\begin{aligned} \text{hypermultiplet:} & \quad \left(-\frac{1}{2}, 0^2, +\frac{1}{2}\right) \oplus \left(-\frac{1}{2}, 0^2, +\frac{1}{2}\right) \\ \text{vector multiplet:} & \quad \left(-1, -\frac{1^2}{2}, 0\right) \oplus \left(0, +\frac{1^2}{2}, +1\right) \\ \text{graviton multiplet:} & \quad \left(-2, -\frac{3^2}{2}, -1\right) \oplus \left(+1, +\frac{3^2}{2}, +2\right) \end{aligned}$$

The symbol  $\oplus$  stand for the CPT conjugate and the superscript indicates the degeneracy.

$\mathcal{N} = 4$  : Multiplets are larger and are given by

$$\begin{aligned} \text{vector multiplet:} & \quad \left(-1, -\frac{1^4}{2}, 0^6, +\frac{1^4}{2}, +1\right) \\ \text{graviton multiplet:} & \quad \left(-2, -\frac{3^4}{2}, -1^6, -\frac{1^4}{2}, 0\right) \oplus \left(0, +\frac{1^4}{2}, +1^6, +\frac{3^4}{2}, +2\right) \end{aligned}$$

$\mathcal{N} = 8$  : There is only one possible representation:

$$\text{graviton multiplet: } \left( -2, -\frac{3^8}{2}, -1^{28}, -\frac{1^{56}}{2}, 0^{70}, +\frac{1^{56}}{2}, +1^{28}, +\frac{3^8}{2}, +2 \right)$$

Any larger  $N$  algebra would require helicities greater than 2 and therefore  $\mathcal{N} = 8$  coincides with an upper bound. Then, the maximum number of supercharges is  $4 \times 8 = 32$ .

In higher dimensions, supercharges are given by the irreducible representation of the Lorentz group listed in Table 2.1. For the purpose of our discussion, the precise form of these higher dimensional super-algebra is not important and we will only comment on some fundamental features. The first one is that supersymmetry cannot exist in any dimension. Indeed, since we could always reduce to four dimensions by compactifying on tori, the limit of 32 supercharges is always valid. As a consequence,  $D = 11$  is the upper bound and the resulting supersymmetric theory has  $\mathcal{N} = 1$  supersymmetry. The corresponding supermultiplet contains gravity and this  $\mathcal{N} = 1$  theory is more properly described as  $\mathcal{N} = 1$  supergravity<sup>1</sup>.

In ten dimensions the irreducible representation has dimension **16** and maximal supersymmetry corresponds to  $\mathcal{N} = 2$ . An interesting novelty comes out of this case. The Weyl spinor  $\psi$  is reducible and the Majorana condition may be imposed as well. The resulting representations are the **16<sup>+</sup>** and the **16<sup>-</sup>**, where  $\pm$  refers to the chirality. In particular, they are self conjugate because  $\psi$  and  $B^{-1}\psi^*$  have the same chirality. These two irreducible spinors lead to two possible maximal supergravities:

- $D = 10$  type IIA supergravity is obtained by considering

$$Q_\alpha^1 \in \mathbf{16}^+ \quad \text{and} \quad Q_\alpha^2 \in \mathbf{16}^-$$

This theory can also be obtained compactifying the  $D = 11$  theory on a circle. The  $D = 11$  Majorana spinor becomes a  $D = 10$  Majorana spinor which splits into two Majorana-Weyl of opposite chirality.

- $D = 10$  type IIB supergravity is obtained by considering two supercharges of the same chirality, which can be defined to represent the **16**. This theory cannot be obtained by compactifying eleven dimensional supergravity.

---

<sup>1</sup>Generically, we will call supergravity those supersymmetric theories that contains the gravity multiplet.

### 2.1.3 R symmetry

The super-algebra given in (2.1) is invariant under a global phase rotation of the supercharge  $Q_\alpha$ . This group is called  $U(1)_R$  and the label  $R$  stands for  $R$ -symmetry. The main characteristic of this symmetry is that it does not commute with the supercharge. Thus, states that belong to the same supermultiplet have different  $U(1)_R$  charges.

In the case of extended supersymmetry, the abelian  $R$ -symmetry group is usually enhanced to a non abelian group which contains the  $U(1)_R$ . It is not difficult to understand the properties of the full  $R$ -symmetry group [46]. Suppose  $T_A$  are the generators, their action is determined by the matrices  $(U_A)_b^a$  and  $(U_A)^a_b$  as follows

$$[T_A, Q_\alpha^a] = (U_A)^a_b Q_\alpha^b, \quad [T_A, \bar{Q}_{\bar{\alpha}a}] = (U_A)_a^b \bar{Q}_{\bar{\alpha}b}. \quad (2.21)$$

We notice that if  $Q_\alpha$  belongs to the representation  $\square$  of the  $R$ -symmetry group, then  $\bar{Q}_{\bar{\alpha}a}$  belongs to the charge conjugate representation  $\bar{\square}$  and the matrix  $(U_A)_a^b$  is the charge conjugate of  $(U_A)^b_a$ . We distinguish between  $\square$  and  $\bar{\square}$  using an upper and a lower index,  $Q_\alpha^i$  and  $\bar{Q}_{\bar{\alpha}a}$  respectively. This notation has been already implemented in (2.21) and (2.19).

The fundamental relation that determines the nature of the  $R$ -symmetry group is the super-Jacobi identity,

$$0 = [T_A, \{Q^a, \bar{Q}_b\}] = \{[T_A, Q^a], \bar{Q}_b\} + \{[T_A, \bar{Q}_b], Q^a\}. \quad (2.22)$$

The left hand side vanishes because  $[T_A, P_\mu] = 0$  and we obtain  $U^T + U^\star = 0$ . It follows that the  $U$  matrices are anti-hermitian and therefore generate the unitary group  $U(\mathcal{N})$ . In  $D = 4$ , the  $R$ -symmetry group of the  $\mathcal{N}$  extended super-algebra turns out to be  $U(\mathcal{N}) \sim U(1)_R \times SU(\mathcal{N})$ . In particular, the supermultiplets of  $\mathcal{N} = 2$  and  $\mathcal{N} = 4$  supersymmetry do transform under this non abelian  $SU(\mathcal{N})$  group. This is better understood in a field theory language where the states of the supermultiplets are assembled into scalars, spinors, vectors and symmetric spin 2 fields.

- The  $\mathcal{N} = 2$  Graviton multiplet is  $(g_{\mu\nu}, \psi^\mu, \psi_\mu, A^0)$  and contains: two spin 3/2 left Weyl gravitini  $\{\psi^\mu, \psi_\mu\}$  transforming as a doublet under  $SU(2)_R$ ; a single gauge field  $A^0$  usually called graviphoton; a metric tensor  $g_{\mu\nu}$ .
- The  $\mathcal{N} = 2$  Gauge Multiplet is  $\mathcal{A} = (A_\mu, \lambda_{\alpha\pm}, z)$ , where  $\lambda_{\alpha\pm}$  are left Weyl fermions called gauginos and  $z$  is a complex scalar. Under  $SU(2)_R$

symmetry,  $A_\mu$  and  $z$  are singlets, while  $\lambda_+$  and  $\lambda_-$  transform as a doublet.

- The  $\mathcal{N} = 2$  Hypermultiplet is  $\mathcal{H} = (\psi_{\alpha\pm}, H_\pm)$ , where  $\psi_{\alpha\pm}$  are left Weyl fermions called hyperinos and  $H_\pm$  are two complex scalars. Under  $SU(2)_R$  symmetry,  $\psi_\pm$  are singlets, while  $H_+$  and  $H_-$  transform as a doublet.
- The  $\mathcal{N} = 4$  Gauge Multiplet is  $(A_\mu, \lambda_\alpha^a, X^i)$ , where  $\lambda_\alpha^a$  with  $a = 1, \dots, 4$  are left Weyl fermions and  $X^i$  with  $i = 1, \dots, 6$  are real scalars. Under  $SU(4)_R$  symmetry,  $A_\mu$  is a singlet,  $\lambda_\alpha^a$  is a **4** and the scalars  $X^i$  are a rank 2 anti-symmetric **6** or equivalently, they form a vector of  $SO(6)$

The  $R$ -symmetry analysis carried out in four dimensions can be generalized to higher dimensions. We would like to focus on  $D = 11$ ,  $D = 10$  and  $D = 5$ . In the first case, there is no chiral representation and we have to rely on a single Majorana spinor. Consistency of the relation  $\psi^\star = B\psi$ , implies that the matrices  $U$  have to be real. Then, by repeating the calculation (2.22), we find that the  $R$ -symmetry group of a Majorana super-algebra is  $SO(\mathcal{N})$ . Hence, the  $\mathcal{N} = 1$  eleven dimensional supergravity has no  $R$ -symmetry.

In  $D = 10$ , there exist independent left and right Majorana supersymmetry generators. It follows that a rotation  $U$  cannot mix the two independent chirality and therefore, in each chiral sector there can only be an orthogonal  $R$ -symmetry group. The explicit construction of the type II theories reveals that only type IIB theory has a non trivial  $R$ -symmetry group. Indeed, the two supercharges of the  $\mathcal{N} = 2$  theory belong to the same representation and the  $R$ -symmetry turns out to be  $SO(2)$ .

In  $D = 5$  there are no Majorana spinors. However, in the case of extended supersymmetry  $\mathcal{N} = 2k$ , we can define ‘‘symplectic’’ Majorana spinors. These consist of an even number of spinors  $\chi^i$  with  $i = 1, \dots, 2k$ , which satisfy a symplectic generalization of the reality condition, namely

$$\chi^i = \epsilon^{ij} B^{-1} (\chi^j)^\star . \quad (2.23)$$

The consistency check  $\chi^i = (\chi^i)^\star$  works because of the anti-symmetric tensor  $\epsilon^{ij} = -\epsilon^{ji}$ . This tensor is non singular and its normalization is fixed by  $\epsilon^2 = -\mathbf{1}$ , where  $\mathbf{1}_{2k}$  is the  $2k \times 2k$  identity matrix. As in the previous cases, the  $R$ -symmetry is determined by the super-Jacobi identity. This time the super-algebra involves the symplectic structure  $\{Q^i, Q^j\} \sim \epsilon^{ij}$  and the calculation is

slightly modified. The result is  $\varepsilon U^T + U \varepsilon = 0$  which is the definition of the  $\text{Usp}(\mathcal{N})$  algebra. Concluding, in  $D = 5$  the  $R$ -symmetry group exists only for even  $\mathcal{N}$  and it is given by the  $\text{Usp}(\mathcal{N})$  matrices.

## 2.2 Type IIB supergravity

The IIB supergravity is relevant to the AdS/CFT correspondence and we will describe its Lagrangian in more detail [45, 47, 48]. Because of maximal supersymmetry, the only supermultiplet allowed is the massless gravity multiplet in ten dimensions. It is convenient to classify the on-shell degrees of freedom in terms of irreducible representations of the little group  $SO(8)$ ,

$$\text{IIB} : \left[ (\mathbf{1} \oplus \mathbf{28} \oplus \mathbf{35}_E) \oplus (\mathbf{1} \oplus \mathbf{28} \oplus \mathbf{35}_C) \right]_B \oplus \left[ 2 \cdot (\mathbf{8}_S \oplus \mathbf{56}_S) \right]_F \quad (2.24)$$

The subscripts  $B$  and  $F$  refer to bosons and fermions respectively. However, we will be mainly interested in the bosonic sector of the theory. We have splitted the  $SO(8)$  representations in, vielbeins  $E$ , scalars  $\Phi$  and  $C_0$  and a bunch of anti-symmetric forms,  $C_{(2)}$ ,  $C_{(4)}$  and  $B_{(2)}$ . More precisely, these fields correspond to

$$\left\{ \begin{array}{ll} G_{\mu\nu} & \mathbf{35}_E \\ (\Phi, C_0) & \mathbf{1} \oplus \mathbf{1} \\ (B_{\mu\nu}, C_{\mu\nu}) & \mathbf{28} \oplus \mathbf{28} \\ C_{\mu\nu\rho\sigma} & \mathbf{35}_C \end{array} \right. \quad (2.25)$$

The rank 4 anti-symmetric tensor  $C_{(4)}$  has a self-dual field strength. In the context of superstring theory, the fields of type IIB are divided into Neveu–Schwarz (NS) fields and Ramond–Ramond (RR) fields. This notation originates from the world-sheet formalism. We do not have time to review this formalism but it is useful to adopt the same notation. Then, the bosonic

Lagrangian of type IIB supergravity is written as the sum of three pieces,

$$e^{-1}\mathcal{L}_{IIB} = \mathcal{L}_{NS} + \mathcal{L}_{RR} + e^{-1}\mathcal{L}_{CS} , \quad (2.26)$$

$$\mathcal{L}_{NS} = e^{-2\phi} \left( \mathcal{R} + 4\partial_\mu\phi\partial^\mu\phi - \frac{1}{2}|dB_{(2)}|^2 \right) , \quad (2.27)$$

$$\mathcal{L}_{RR} = -\frac{1}{2} \left( |dC_0|^2 - |F_{(3)}|^2 - \frac{1}{2}|F_{(5)}|^2 \right) , \quad (2.28)$$

$$\mathcal{L}_{CS} = -\frac{1}{2}C_{(4)} \wedge dB_{(2)} \wedge dC_{(2)} , \quad (2.29)$$

where

$$F_{(3)} = dC_{(2)} - C_0 \wedge dB_{(2)} , \quad (2.30)$$

$$F_{(5)} = dC_{(4)} - \frac{1}{2}C_{(2)} \wedge dB_{(2)} + \frac{1}{2}B_{(2)} \wedge dC_{(2)} . \quad (2.31)$$

We mentioned that  $F_5$  has to be self dual. There is no covariant action for such condition and we must consider it as an on-shell constraint. Indeed the field equations obtained from  $\mathcal{L}_{IIB}$  are consistent with,

$$\star F_5 = F_5 , \quad (2.32)$$

but they do not imply it.

It turns out that type IIB supergravity has a certain  $SL(2)$  symmetry. This symmetry involves the dilaton field, the zero form  $C_0$  and the 3-forms field strength. It is not manifest in the above formulation and in order to see it we consider the following redefinitions,

$$G_{E\mu\nu} = e^{-\phi/2}G_{\mu\nu}, \quad \tau = C_0 + ie^{-\phi}, \quad F_3^i = \begin{pmatrix} dB_2 \\ F_3 \end{pmatrix} . \quad (2.33)$$

We also define the matrix,

$$S_{ij} = \begin{pmatrix} |\tau|^2 & -\text{Re } \tau \\ -\text{Re } \tau & 1 \end{pmatrix} . \quad (2.34)$$

Then,  $\mathcal{L}_{IIB}$  takes the form

$$\begin{aligned} e^{-1}\mathcal{L}_{IIB} &= \mathcal{R} - \frac{\partial_\mu\bar{\tau}\partial^\mu\tau}{2(\text{Im}\tau)^2} - \frac{1}{2}F_{(3)}^i S_{ij} F_{(3)}^j - \frac{1}{4}|F_{(5)}|^2 \\ &\quad - \frac{\varepsilon_{ij}}{4} e^{-1} C_{(4)} \wedge F_{(3)}^i \wedge F_{(3)}^j . \end{aligned} \quad (2.35)$$

This is the so called Einstein frame where the curvature appears without the dilaton coupling. We note that the action is invariant under the  $SL(2)$  symmetry generated by

$$\tau \rightarrow \frac{a\tau + b}{c\tau + d}, \quad \begin{pmatrix} dB_2 \\ F_3 \end{pmatrix} \rightarrow \begin{pmatrix} d & c \\ b & a \end{pmatrix} \begin{pmatrix} dB_{(2)} \\ dC_{(2)} \end{pmatrix}, \quad (2.36)$$

with  $a, b, c, d$  being four real numbers such that  $ad - bc = 1$ . The  $SL(2)$  invariance of the matrix  $S_{ij}$  is a similarity transformation,  $(\Lambda^{-1})^T S \Lambda^{-1}$ , where  $\Lambda$  is the matrix defined in (2.36). We observe that the 2-form potentials are mixed by this transformation.

### 2.3 $\mathcal{N} = 4$ Super Yang-Mills

In the next section we will discuss the AdS/CFT conjecture. This is a duality between two theories: the first one is type IIB supergravity and the second one is  $\mathcal{N} = 4$  Super Yang Mills (SYM). It is important to have a certain knowledge of both theories so to have a good understanding of the conjecture. Furthermore,  $\mathcal{N} = 4$  SYM is a remarkable theory not just because of the AdS/CFT correspondence. At the quantum level this theory is finite and exactly scale invariant. In particular, the renormalization group  $\beta$ -function vanishes identically. At the non perturbative, a quantum symmetry known as *Montonen-Olive* or *S-duality conjecture* shows up and as a result, weak and strong coupling are exchanged [49, 50].

The Lagrangian of  $\mathcal{N} = 4$  SYM is given by [51],

$$\mathcal{L}_{\mathcal{N}=4} = \text{tr} \left\{ -\frac{1}{2g^2} F_{\mu\nu} F^{\mu\nu} + \frac{\theta_I}{16\pi^2} \epsilon^{\mu\nu\rho\sigma} F_{\mu\nu} F_{\rho\sigma} \right. \quad (2.37)$$

$$\left. - \sum_a i \bar{\lambda}^a \bar{\sigma}^\mu D_\mu \lambda_a - \sum_i D_\mu X^i D^\mu X^i \right. \quad (2.38)$$

$$\left. + \left( g \sum_{a,b,i} C_i^{ab} \lambda_a [X^i, \lambda_b] + cc \right) + \frac{g^2}{2} \sum_{i,j} [X^i, X^j]^2 \right\}. \quad (2.39)$$

The constants  $C_i^{ab}$  and their complex conjugate  $C_{iab}$  are related to the Clifford Dirac matrices for  $SO(6)_R \sim SU(4)_R$ . The Lagrangian can be constructed through dimensional reduction of  $D = 10$  SYM on  $T^6$ . The transformation

laws can be deduced in the same way. They are,

$$\begin{aligned}
\delta X^i &= [Q_\alpha^a, X^i] = C^{iab} \lambda_{\alpha b} , \\
\delta \lambda_b &= \{Q_\alpha^a, \lambda_{\beta b}\} = F_{\mu\nu}^+ (\sigma^{\mu\nu})_\beta^\alpha \delta_b^a + [X^i, X^j] \epsilon_{\alpha\beta} (C_{ij})_b^a , \\
\delta \bar{\lambda}_\beta^b &= \{Q_\alpha^a, \bar{\lambda}_\beta^b\} = C_i^{ab} \bar{\sigma}^\mu_{\alpha\beta} D_\mu X^i , \\
\delta A_\mu &= [Q_\alpha^a, A_\mu] = (\sigma_\mu)_\alpha^{\bar{\beta}} \bar{\lambda}_\beta^a ,
\end{aligned}$$

where  $F_{\mu\nu}^\pm = \frac{1}{2}(F_{\mu\nu} \pm \frac{i}{2}\epsilon^{\mu\nu\rho\sigma} F_{\rho\sigma})$  and  $(C_{ij})_b^a$  are related to bilinears in Clifford Dirac matrices for  $SO(6)_R$ . Classically  $\mathcal{L}_{\mathcal{N}=4}$  is scale invariant. Fields have dimensions

$$[A_\mu] = [X^i] = 1 , \quad [\lambda_a] = \frac{3}{2} , \quad (2.40)$$

and the coupling constants are not spurions, i.e.  $[g] = [\theta_I] = 0$ . All terms in the Lagrangian have dimension four. Remarkably, the full global symmetry group of  $\mathcal{N} = 4$  SYM is the supergroup  $SU(2, 2|4)$  whose constituents are:

- the  $R$ -symmetry group;
- the conformal group  $SO(2, 4) \sim SU(2, 2)$ : generated by translations  $P^\mu$ , Lorentz transformations  $M_{\mu\nu}$ , dilations  $D$  and special conformal transformations  $K^\mu$ ;
- the Poincarè supersymmetries: generated by the supercharges  $Q_\alpha^a$  and their complex conjugates  $\bar{Q}_{\bar{\alpha}a}$  with  $a = 1, \dots, 4$ ;
- the conformal supersymmetries: generated by the supercharges  $S_{\alpha a}$  and their complex conjugates  $\bar{S}_{\bar{\alpha}a}$ . The presence of these extra supercharges results from the fact that the supercharges  $Q_\alpha^a$  and the special conformal transformations  $K^\mu$  do not commute. Since both are symmetries, their commutator must be a symmetry. These are the supercharges  $S_{\alpha a}$ .

The generators of the supergroup have dimensions

$$[D] = [M_{\mu\nu}] = 0 , \quad \begin{cases} [P^\mu] = 1 , & [K^\mu] = -1 , \\ [Q] = 1/2 , & [S] = -1/2 . \end{cases} \quad (2.41)$$

It is our interest to sketch the classification of local gauge invariant operators. These are gauge invariant combinations built out of the fundamental fields of the theory,  $X^i$ ,  $\lambda_a$ ,  $F_{\mu\nu}$ . The use of the covariant derivative  $D_\mu$  is allowed as well. In this case  $[D_\mu] = 1$ .

The starting point of the classification is dimensional analysis. Since the conformal supercharges  $S$  have dimension  $-1/2$ , successive applications of  $S$  to any operator of definite dimension must at some point yield 0. Indeed, it is not possible to have negative dimensions in a unitary representation and actually the only operator with zero dimension turns out to be the identity operator. We define a *superconformal primary operator*  $O$  to be a non vanishing operator such that

$$[S, O] = 0 \quad (\text{bosonic}) , \quad \{S, O\} = 0 \quad (\text{fermionic}) . \quad (2.42)$$

An operator  $O'$  is called a *superconformal descendant* if it can be obtained from another operator  $O$  as

$$\begin{aligned} O' &= [Q, O] && (\text{bosonic}) , \\ O' &= \{Q, O\} && (\text{fermionic}) . \end{aligned} \quad (2.43)$$

An irreducible superconformal representation contains a single superconformal primary operator and a tower of descendants. The dimension of the primary operator is the lowest one in the multiplet, then the dimension of a descendant is obtained by its very definition as  $\Delta_{O'} = \Delta_O + 1/2$ . By analyzing the superalgebra we understand which fields cannot be primary operators, these are fields that are obtained as the commutator with the supercharges. Schematically

$$\begin{aligned} \{Q, \lambda\} &= F^+ + [X, X] , && [Q, X] = \lambda , \\ \{Q, \bar{\lambda}\} &= DX , && [Q, F] = D\lambda . \end{aligned} \quad (2.44)$$

As a result, chiral primary operators can involve neither gauginos  $\lambda$  nor the gauge field strength  $F$ . Thus, they can only be functions of the scalar fields  $X^i$ . The simplest are *single trace operators*, which are of the form

$$\text{tr} \left( X^{\{i_1} X^{i_1} \dots X^{i_n\}} \right) \quad (2.45)$$

where the indexes are symmetrized and belong to the  $\mathbf{6}$  of  $SO(6)_R$ . In general such operators are reducible. Since  $\text{tr} X^i = 0$ , the first non trivial examples are

$$\sum_i \text{tr} X^i X^i \sim \text{Konishi multiplet} , \quad (2.46)$$

$$\text{tr} X^{\{i} X^{j\}} \sim \text{supergravity multiplet} . \quad (2.47)$$

| SYM operator                       | desc       | $\Delta$          | spin                                    | $SU(4)$     |
|------------------------------------|------------|-------------------|---|-------------|
| $\text{tr}X^k$ $k \geq 2$          | -          | $k$               | $(0, 0)$                                | $[0, k, 0]$ |
| $\text{tr}\lambda X^k$ $k \geq 1$  | $Q$        | $k + \frac{3}{2}$ | $\left(\frac{1}{2}, 0\right)$           | $[1, k, 0]$ |
| $\text{tr}\lambda\lambda X^k$      | $Q^2$      | $k + 3$           | $(0, 0)$                                | $[2, k, 0]$ |
| $\text{tr}\lambda\bar{\lambda}X^k$ | $Q\bar{Q}$ | $k + 3$           | $\left(\frac{1}{2}, \frac{1}{2}\right)$ | $[1, k, 1]$ |
| $\text{tr}FX^k$ $k \geq 1$         | $Q^2$      | $k + 2$           | $(1, 0)$                                | $[0, k, 0]$ |

Table 2.2: Example of SYM operators that belong to a definite superconformal multiplet with chiral primary operator  $\text{tr}X^k$   $k \geq 2$ . The range of  $k$  is  $k \geq 0$ , unless otherwise specified. Adapted from [38].

There exist also *multi-trace operators*. These are obtained as product of single trace operators. The unitary representations of the superconformal algebra may be labelled by the quantum numbers of the bosonic subgroup  $SO(1, 3) \times SO(1, 1) \times SU(4)_R$ . The first factor is the Lorentz group which has  $(s_+, s_-) \in SU(2) \times SU(2)$  spin quantum numbers. The second quantum number is the dimension  $\Delta$ . The last one is the  $R$ -symmetry group whose representations are determined by the triplets  $[r_1, r_2, r_3]$  [52]. In particular, the dimension of a given  $SU(4)$  representation is

$$\dim[r_1, r_2, r_3] = \frac{1}{12} \bar{r}_1 \bar{r}_2 \bar{r}_3 (\bar{r}_1 + \bar{r}_2)(\bar{r}_2 + \bar{r}_3)(\bar{r}_1 + \bar{r}_2 + \bar{r}_3), \quad (2.48)$$

where  $\bar{r}_i \equiv r_i + 1$ . The complex conjugation is  $[r_1, r_2, r_3]^* = [r_3, r_2, r_1]$ . So for example,  $[0, 2, 0]$  corresponds to the real representation **20** whereas  $[2, 0, 0]$  is a complex representation and has dimension **10**. It is useful to have in mind a concrete realization of all the things we said. In table 2.2 we consider the chiral primary operator  $\text{tr}(X)^k$ , with  $k \geq 2$  and we show a list of descendants, as exercise, we write down their quantum numbers under  $SO(1, 3) \times SO(1, 1) \times SU(4)_R$ .

## 2.4 The Maldacena Conjecture

The AdS/CFT or Maldacena conjecture [1] is a duality between :

- Type IIB superstring theory on  $\text{AdS}_5 \times \text{S}^5$
- $\mathcal{N} = 4$  SYM in four dimensions with gauge group  $SU(N)$

On the gravity side, the number  $N$  of  $SU(N)$  counts the flux of the self dual 5–form through the five sphere (in the appropriate normalization [53]). Both  $\text{AdS}_5$  and  $\text{S}^5$  have the same radius and the relation between the string coupling  $g_s$  and the Yang-Mills coupling  $g_{YM}$  is

$$\frac{g_{YM}^2}{4\pi} = g_s . \quad (2.49)$$

The  $\mathcal{N} = 4$  SYM theory is supposed to be in the superconformal phase, where  $\langle X \rangle = 0$  and the gauge group is unbroken. This is the strong version of the conjecture and it holds for all values of  $N$  and of  $g_s = g_{YM}^2$ . However, the lack of proper quantum treatment of type IIB superstring in  $\text{AdS}_5 \times \text{S}^5$  makes this strong version of the conjecture hard to test. We will see that a natural limit exists in which the duality is more tractable but still remains non-trivial. This important result led to the foundation of the holographic principle and represents nowadays the most striking insight into the dynamics of strongly coupled theories. It is worth noting that the duality has not been proved yet, nevertheless a number of non trivial consistency check has been provided over the past decades.

In order to understand how the duality comes about we need to introduce a special object: this is the D3-brane. Originally, the 3-brane was found as the solution of type IIB supergravity with maximal rotational symmetry  $SO(1, 3) \times SO(6)$  [54]. In the string frame this solution has a constant dilaton and it is characterized in terms of ansatz,

$$ds^2 = H(\vec{y})^{-1/2} d\vec{x}^2 + H(\vec{y})^{1/2} d\vec{y}^2 , \quad (2.50)$$

$$F_{(5)}^+ = dA + \star dA \quad A = H(\vec{y})^{-1} dx^0 \wedge dx^1 \wedge dx^2 \wedge dx^3 ,$$

where  $\vec{x}$  are the coordinates for the four dimensional Minkowski space-time,  $\vec{y}$  are the coordinates for the transverse six dimensional space and the function  $H$  is parametrized by a single scale factor  $\ell$ ,

$$H(\vec{y}) = 1 + \frac{\ell^4}{y^4}, \quad y = |\vec{y}| . \quad (2.51)$$

In this background the two-form fields vanish,  $B_{(2)} = C_{(2)} = 0$ . On a general ground the D3 brane is a semi-classical gravitational solution that requires a quantum gravity completion at high energy. This completion is provided

by string theory. In particular, type IIB supergravity is understood as the effective theory for the low energy description of a certain superstring dynamics and therefore, the semiclassical D3 brane background is expected to be a solution of the full type IIB string theory modulo stringy corrections. In particular, the understanding of the scale  $\ell$  that appears in the harmonic function  $H(\vec{y})$  follows from the open string description of the 3-brane. In this description the gravitational background is replaced by a  $(3+1)$ -dimensional hypersurface in flat space and the fluctuations of the theory correspond to open strings ending on this hypersurface. The spectrum of the theory is then obtained by quantizing such open strings. The hyperplane is known as D3-brane and the D indicates that vibrating open strings have to satisfy a Dirichlet boundary condition on the brane.

By introducing the dimensionless string coupling constant and the square of the string length scale,  $l_s^2 \sim \alpha'$ , it turns out that the constant  $\ell$ , that appears in (2.51), is fixed to be

$$\ell^4 = 4\pi g_s N \alpha'^2 . \quad (2.52)$$

Here  $N$  is an integer number specifying that the solution (2.50) corresponds to a superposition of  $N$  coincident D3-branes. Historically, this result is due to Polchinski [55] and it is based on string perturbation theory. In this approximation  $g_s \rightarrow 0$  and string theory may be defined in terms of a genus expansion in the string worldsheets. Interactions arise from the joining and splitting of worldsheets and scattering amplitudes are calculated in terms of a weighted sum over topologies. Remarkably, in the limit  $g_s \rightarrow 0$ , the metric (2.50) becomes flat everywhere, excepts on the  $(3+1)$ -dimensional hyperplane at  $\vec{y} = 0$ .

Supergravity is a good approximation to string theory when the extended structure of the strings is not detectable. This means that  $\ell^2 \gg \alpha'$ . Comparing this limit with the formula (2.52) we conclude that this approximation holds whenever  $g_s N \gg 1$ . Then, the condition  $g_s \ll 1$  is simultaneously allowed provided  $N$  is very large. In this case, perturbative string theory is a good approximation. With a number  $N > 1$  of coincident branes, the low energy theory that the open strings describe is  $\mathcal{N} = 4$  SYM in four dimensions with gauge group  $SU(N)$ . It is worth noting that low energy in the present context refers to the particle spectrum of the open strings excitations. The resulting  $SU(N)$  gauge theory is an interacting quantum field theory.

Taking into account all the above reasoning, Maldacena considered the limit

$$\alpha' \rightarrow 0 , \quad U = \frac{y}{\alpha'} \text{ fixed} , \quad g_s N \gg 1 . \quad (2.53)$$

The metric becomes,

$$ds^2 = \alpha' \left[ \frac{U^2}{\sqrt{4\pi g_s N}} d\vec{x}^2 + \sqrt{4\pi g_s N} \frac{dU^2}{U^2} + \sqrt{4\pi g_s N} d\Omega_5^2 \right], \quad (2.54)$$

and describes the five dimensional Anti de Sitter (AdS<sub>5</sub>) times a five-sphere. In units of  $\alpha'$  the metric remains constant and the radius of the five sphere is given by  $L^2/\alpha' = \sqrt{4\pi g_s N}$ . This is the same as the radius of the AdS space as defined in the next section. In the approximation (2.53), there are two equivalent descriptions of the string theory living on the D3 brane, as supergravity on AdS<sub>5</sub>×S<sup>5</sup> and as  $\mathcal{N} = 4$  SYM in four dimensions. By considering the identification  $g'_s \sim g_{YM}^2$  given in (2.49), we see that the limit  $g_s N \gg 1$  implies

$$g_{YM}^2 N \gg 1. \quad (2.55)$$

In the field theory, the limit (2.55) has a precise meaning. We define the 't Hooft coupling,

$$\lambda \equiv g_{YM}^2 N, \quad (2.56)$$

and we consider the *double line* diagrammatic expansion of the partition function. It can be shown that each Feynman diagram, that contributes to this expansion, comes with a factor of,

$$N^{2-2h}(\lambda)^p, \quad (2.57)$$

where both  $h$  and the power  $p$  of  $\lambda$  depend on the specific diagram. The drawing of the diagram in terms of the double line notation is then mapped to a two dimensional surface and  $h$  turns out to be the genus of the corresponding surface. In this way, diagrams are classified as planar diagrams,  $h = 0$ , and non planar diagrams,  $h > 0$ . Since  $h \geq 0$ , in the limit  $N \rightarrow \infty$  only planar diagrams with  $h = 0$  contribute to the partition function and the 't Hooft coupling controls the perturbative expansion of the theory. Then, perturbation theory is valid the regime in which  $\lambda \ll 1$  whereas, according to the Maldacena conjecture, the strong coupling regime,  $\lambda \gg 1$ , admits the dual description in terms of classical gravity on the AdS<sub>5</sub>.

**Mapping Global Symmetries.** The first non trivial test of the duality involves the matching of the global symmetries of the two theories. Global symmetries are physical and therefore we expect a precise correspondence. The bosonic subgroup of  $\mathcal{N} = 4$  SYM is  $SU(2, 2) \times SO(6)_R$ . This is immediately recognized on the AdS side as the isometry group of AdS<sub>5</sub>×S<sup>5</sup>. The completion into the supergroup  $SU(2, 2|4)$  needs some care. Indeed, the D3

brane preserves half of the supersymmetries of type IIB theory, i.e.  $32 \rightarrow 16$  and we conclude that at least we have 16 Poincarè supersymmetries on the AdS background. On the other hand, the superconformal group has 32 supersymmetries but the matching works because in the  $\text{AdS}_5 \times S^5$  background the 16 Poincarè supersymmetries are enhanced to the full superconformal group [56].

## 2.5 Bulk to Boundary Mapping

For the correspondence to be functional, it remains to show how the representations of  $\mathcal{N} = 4$  SYM are mapped into the gravity dual. The spectrum of operators has been explained in section 2.3. On the gravity side, we identify the irreducible representation of the supergroup with the massless and massive supergravity (stringy) degrees of freedom living on  $\text{AdS}_5 \times S^5$ . Concretely, the matching of the single trace operators involves a Kaluza-Klein reduction on the five sphere and a reorganization of the towers in terms of the global symmetry quantum numbers of the field theory. The general idea is simple to explain. We introduce coordinates  $(z, x_\mu)$ ,  $\mu = 0, \dots, 3$  for  $\text{AdS}_5$  and  $y^m$ , with  $m = 1, \dots, 5$  for  $S^5$ . Then, a generic ten dimensional field has the form  $\varphi(z, \vec{x}, \vec{y})$  and can be expanded in spherical harmonics:

$$\varphi(z, \vec{x}, \vec{y}) = \sum_{\Delta=0}^{\infty} \varphi_{\Delta}(z, \vec{x}) Y_{\Delta}(\vec{y}) . \quad (2.58)$$

The field  $\varphi_{\Delta}(z, \vec{x})$  lives on the  $\text{AdS}_5$  space. The functions  $Y_{\Delta}$  form a complete basis of spherical harmonics on  $S^5$  and  $\Delta$  labels the  $SO(6)$  representations. As a result of the compactification, the five dimensional fields  $\varphi_{\Delta}$  receive a contribution to the mass. The most important cases are

$$\begin{array}{ll} \text{scalars} & m^2 L^2 = \Delta(\Delta - 4) , \\ \text{spin } 1/2, 3/2 & |m|L = \Delta - 2 , \\ p - \text{forms} & m^2 L^2 = (\Delta - p)(\Delta + p - 4) , \end{array} \quad (2.59)$$

and we refer to [57, 58] for details. It is worth noting that once type IIB supergravity is compactified on the five sphere, the resulting theory is  $\mathcal{N} = 8$  supergravity in five dimensions. This can be proved by looking at the dimensional reduction of the gravitino degrees of freedom. The more interesting result is that  $\text{AdS}_5$  is a vacuum solution of  $\mathcal{N} = 8$  supergravity. In the following paragraph we introduce some important notions about the general  $\text{AdS}_{d+1}$

space and we will come back on the relation between supergravity and AdS solutions in the next chapters.

**The AdS space.** The  $d + 1$  dimensional anti de Sitter (AdS) space can be obtained from the hyperboloid,

$$-X_{-1}^2 - X_0^2 + X_1^2 + \dots + X_p^2 + X_d^2 = -L^2, \quad (2.60)$$

embedded in a flat  $d + 2$  dimensional space-time. This flat space-time is equipped with the metric  $\eta = \text{diag}(-1, -1, 1, \dots, 1)$  and the symmetry group of the manifold is  $SO(2, d)$ . The constant  $L$  is defined as the *radius* of the AdS space. The metric (2.54) is obtained by considering the change of coordinates,

$$U = (X_{-1} + X_d), \quad x_\mu = L \frac{X_\mu}{U}, \quad V = (X_{-1} - X_d). \quad (2.61)$$

where  $\mu = 0, \dots, d - 1$ . The induced metric is

$$ds^2 = \frac{U^2}{L^2} d\vec{x}^2 + \frac{L^2}{U^2} dU^2 \quad (2.62)$$

and we recognize the similarity with the metric (2.54) obtained in the Maldacena limit. Then, we can also consider the rescaling  $U \rightarrow L^2 U$  and put the metric in the form,

$$ds^2 = L^2 \left( U^2 d\vec{x}^2 + \frac{dU^2}{U^2} \right) \quad (2.63)$$

The Wick rotation  $X_0 \rightarrow iX_0$  yields the euclidean version of the AdS space (EAdS). The, we can map  $EAdS_{d+1}$  onto the upper half space  $\{(z, \vec{x}), z > 0, \vec{x} \in \mathbb{R}^d\}$  with Poincarè metric

$$ds_{AdS}^2 = \frac{L^2}{z^2} (d\vec{x}^2 + dz^2). \quad (2.64)$$

In this case, the coordinates  $U$  and  $z$  are related by the inversion  $z = 1/U$ . It is a simple exercise of differential geometry to see that the AdS space satisfies the Einstein equations with negative cosmological constant. In fact, the Ricci tensor  $R_{\mu\nu}$  calculated from (2.64) is proportional to the AdS metric  $g_{\mu\nu}$  and the constant of proportionality is given by,

$$R_{\mu\nu} = -\frac{d}{R^2} g_{\mu\nu}. \quad (2.65)$$

Then, the action for the above equation is

$$S = \frac{1}{16\pi G_{d+1}} \int \sqrt{g} (\mathcal{R} - \Lambda), \quad \Lambda = -\frac{d(d-1)}{R^2}, \quad (2.66)$$

where  $\sqrt{g}$  is the square root of  $|\det g_{\mu\nu}|$ ,  $\mathcal{R}$  is the scalar curvature and  $G_{d+1}$  the Newton constant in  $d + 1$  dimensions.

There exist two important limits of the metric (2.64). The first one is the limit  $z \rightarrow 0$ . In this case the transverse surface has the topology of  $\mathbb{R}^d$  and the metric is divergent because the scale factor blows up. The other limit is  $z \rightarrow \infty$ . In this case, the metric vanishes and the spacetime is reduced to a single point  $P$ . Then, the boundary of AdS is  $\mathbb{R}^d \cup P$ . It is natural to ask what field theory lives on the boundary of AdS. This question has a unique answer: *a well-defined limit to the boundary of AdS can only exist if the boundary theory is scale invariant* [2]. Thus,  $\mathcal{N} = 4$  SYM is scale invariant and may consistently live at the boundary of AdS. This construction is the building block of the holographic principle and it gives a geometrical description of the dual field theory as seen from the AdS side of the conjecture. However, the Maldacena conjecture implies a lot more about the dual field theory. Indeed, as we have seen in (2.59), irrelevant, marginal and relevant field theory deformations arise from Kaluza-Klein harmonics on  $\text{AdS}_5 \times S^5$  and they are classified according to massive, massless and tachyonic modes in supergravity.

### 2.5.1 Scalar Field Holography

Throughout this thesis we will consider scalar fields. For this reason, it is convenient to work out the details of the AdS/CFT dictionary in some specific cases. We begin with the example of a real scalar field in AdS. We think of it as a perturbation on the  $\text{AdS}_5$  geometry. The equation of motion is

$$(\square + m^2)\varphi = 0 \quad \text{with} \quad m^2 L^2 = \Delta(\Delta - 4) , \quad (2.67)$$

where  $\square$  is the Laplacian operator of  $\text{AdS}_5$ . We can work with Euclidean  $\text{AdS}_5$  setting  $L = 1$  for simplicity. The metric is

$$ds_{AdS}^2 = \frac{1}{z^2}(d\vec{x}^2 + dz^2) . \quad (2.68)$$

Solutions of (2.67) are characterized by the asymptotic behavior as  $z \rightarrow 0$ . Since, the equation of motion is second order there will be two independent fall-off,

$$\varphi(z) = \begin{cases} z^{\Delta_+} & \text{normalizable} \\ z^{4-\Delta_+} & \text{non normalizable} \end{cases} \quad (2.69)$$

Here  $\Delta_+$  is the greatest root of  $m^2 L^2 = \Delta(\Delta - 4)$  and the notion of normalizable and non-normalizable mode depends on the properties of the norm which is defined over the space of solutions [59, 60]. It turns out that there are two

possible ways to define a norm and we will begin by describing the first one. Before, it is useful to point out that the most general solution  $\varphi(z, \vec{x})$  admits a series expansion in the variable  $z$  of the form,

$$\varphi \rightarrow z^{4-\Delta_+} \left( \varphi_0(\vec{x}) + O(z^2) \right) + z^{\Delta_+} \left( A(\vec{x}) + O(z^2) \right). \quad (2.70)$$

In complete generality, we may consider  $d + 1$  dimensions and then specialize the discussion to  $\text{AdS}_5$ . In this case  $m^2 = \Delta(\Delta - d)$  and the two fall-off (2.69) are

$$\Delta_+ = \frac{d}{2} + \sqrt{\frac{d^2}{4} + m^2}, \quad \Delta_- = \frac{d}{2} - \sqrt{\frac{d^2}{4} + m^2} = d - \Delta_+ \quad (2.71)$$

The first natural norm is the Euclidean action. For a real and massive scalar field in  $\text{AdS}_{d+1}$  the Euclidean action reads,

$$S = \frac{1}{2} \int d\vec{x} dz \sqrt{g} \left[ g^{\mu\nu} \partial_\mu \varphi \partial_\nu \varphi + m^2 \varphi^2 \right] \quad (2.72)$$

$$= \frac{1}{2} \int d\vec{x} dz z^{-d+1} \left[ (\partial_z \varphi)^2 + (\partial_i \varphi)^2 + \frac{m^2}{z^2} \varphi^2 \right] \quad (2.73)$$

Assuming  $\varphi \sim z^\Delta$  at the boundary, it is a simple exercise to show that the integral is finite iff  $2\Delta - d > 0$ . Turning to the formula (2.71) we see that,

$$\Delta > \frac{d}{2}, \quad \text{implies that only } \Delta_+ \text{ is allowed.} \quad (2.74)$$

In the cases,  $m^2 > 0$ , the non-normalizable mode is divergent. In the cases,  $-d^2/4 < m^2 < 0$  both modes vanish but only one is normalizable. The inequality  $m^2 \geq -d^2/4$  coincides with the Breitenlohner-Freedman bound and the logarithmic branch that shows up in the case  $m^2 = -d^2/4$  is defined to be a non normalizable solution. The Breitenlohner-Freedman bound is has a physical meaning and the holographic theory is stable if and only if all the scalar fields have masses above the Breitenlohner-Freedman bound. A simple way to understand this statement is to realize that for masses  $m^2 L^2 \leq -d^4/4$  the solutions  $\Delta_+$  and  $\Delta_-$  are complex.

Physically, the normalizable mode corresponds to a bulk excitation. Thus,  $A(x)$  has to be interpreted as a physical fluctuation in the dual field theory. The non normalizable mode  $\varphi_0(\vec{x})$  does not admit this interpretation. Instead, it is better understood as a source for the single trace operator  $\mathcal{O}_\Delta$  dual to bulk scalar field. The precise correspondence is obtained by considering the following statement. There is a one-to-one correspondence between regular

bulk solutions and boundary fields  $\varphi_0(\vec{x})$ . Then, the freedom to specify this boundary field corresponds to the freedom of picking up an arbitrary source in the dual field theory. Once the bulk problem has been solved, the holographic principle defines the generating functional  $\Gamma[\varphi_0]$  for the correlators of the single trace operator  $\mathcal{O}_\Delta$  as the partition function  $Z_S(\varphi_0)$  of the gravitational theory [2, 3]:

$$\exp \left\{ -\Gamma[\varphi_0] \right\} \equiv \left\langle \exp \int d\vec{x} \varphi_0(\vec{x}) \mathcal{O}_\Delta(\vec{x}) \right\rangle = Z_S(\varphi_0) . \quad (2.75)$$

The latter is evaluated on-shell and therefore it is a functional of the source field  $\varphi_0(\vec{x})$  according to the above construction of the bulk solution. The expression of the the generating functional  $\Gamma[\varphi_0]$  is understood as a perturbative expansion in  $\varphi_0$ ,

$$\Gamma[\varphi_0] = \Gamma[0] + \int d\vec{x} \varphi_0(\vec{x}) G_1(\vec{x}) + \frac{1}{2} \int \int d\vec{x}_1 d\vec{x}_2 \varphi_0(\vec{x}_1) \varphi_0(\vec{x}_2) G_2(\vec{x}_1, \vec{x}_2) + \dots ,$$

where

$$\begin{aligned} G_1(\vec{x}) &= \left\langle \mathcal{O}_\Delta(\vec{x}) \right\rangle , \\ G_2(\vec{x}_1, \vec{x}_2) &= \left\langle \mathcal{O}_\Delta(\vec{x}_1) \mathcal{O}_\Delta(\vec{x}_2) \right\rangle_c , \\ G_3(\vec{x}_1, \vec{x}_2, \vec{x}_3) &= \dots . \end{aligned}$$

In the supergravity approximation, the r.h.s of (2.75) is dominated by the classical action and the explicit calculation gives

$$Z_S(\varphi_0) = - \lim_{z \rightarrow 0} z^{d+1-2\Delta} \int d\vec{x} (z^{\Delta-d} \varphi(z, \vec{x})) \partial_z (z^{\Delta-d} \varphi(z, \vec{x})) . \quad (2.76)$$

To be more precise<sup>2</sup>, we can replace

$$z^{\Delta-d} \varphi(z, \vec{x}) \rightarrow \varphi_0(\vec{x}) , \quad (2.77)$$

$$\partial_z (z^{\Delta-d} \varphi(z, \vec{x})) \rightarrow (2\Delta - d) z^{2\Delta-d-1} A(\vec{x}) . \quad (2.78)$$

The result is that  $\langle \mathcal{O}_\Delta(\vec{x}) \rangle$  gets identified with  $A(\vec{x})$ . Summarizing, the AdS/CFT maps a complicated quantum problem such that of finding the generating functional  $\Gamma[\varphi_0]$  of  $\mathcal{N} = 4$  SYM into a problem of classical gravity with boundary

---

<sup>2</sup>On shell the classical action is a total derivative and needs to be properly regularized in order to get rid of unphysical boundary divergences. This is done by adding boundary terms. Clearly, these boundary terms do not enter the equations of motion which remain unvaried. More details can be found in [73] and also in chapter 3

conditions. In particular, the action of type IIB supergravity carries all the informations about the dynamics of the dual field theory.

We point out that another norm, alternative to the Euclidean action, may be considered. This is the integral obtained by (2.72) integrating by part and neglecting the boundary term, namely

$$\frac{1}{2} \int d\vec{x} dz \sqrt{g} \varphi \left( -\nabla^2 + m^2 \right) \varphi . \quad (2.79)$$

By expanding the operator  $\nabla^2$  we find,

$$\frac{1}{2} \int d\vec{x} dz z^{-d+1} \varphi \left[ \left( -\partial_z^2 \varphi + \frac{d-1}{z} \partial_z \varphi - \frac{m^2}{z^2} \varphi \right) - d \partial_i^2 \varphi \right] . \quad (2.80)$$

Then, assuming the behavior  $\varphi \sim z^\Delta F(\vec{x})$ , the first term in parenthesis reduces to the combination  $(\Delta(d-\Delta) + m^2)F(x)$  and vanishes on-shell. Then, the dominant contribution comes from the kinetic energy in the transverse direction and the integral is finite iff  $2\Delta > d-2$ . We conclude that a normalizable mode according to the norm (2.79) satisfies the condition  $\Delta > d/2 - 1$ . Turning to the formula (2.71) we see that,

$$\Delta = \frac{d}{2} - 1, \quad \text{implies that } \Delta_- \text{ is allowed} . \quad (2.81)$$

This condition is weaker than the previous one and is valid in the range of masses  $-d^2/4 < m^2 < -d^2/4 + 1$ . It coincides with the unitarity bound on the dimension of a scalar operator in  $d$  dimensions so we cannot expect to violate this bound. In the range of masses  $-d^2/4 < m^2 < -d^2/4 + 1$  we can either choose  $\Delta_+$  or  $\Delta_-$  as normalizable modes. The first choice is usually referred to as the *standard quantization*, the second choice instead goes under the name of *alternative quantization*. Once the quantization scheme has been chosen, the non normalizable mode is also defined. Then, for the *alternative quantization* the role of the source is played by  $A(\vec{x})$  meaning that the dual operator has dimension  $\Delta_-$ . In this sense, the choice of boundary condition also defines the dual field theory and in general the only knowledge of the mass does not single out the operator  $\mathcal{O}_\Delta$ . Two different AdS theories with a given  $-d^2/4 < m^2 < -d^2/4 + 1$  correspond to two different CFT, one with an operator of dimension  $\Delta_+$  and the other with an operator of dimension  $\Delta_-$ . The explicit calculation of  $\Gamma[A]$  is similar to that of  $\Gamma[\varphi_0]$  carried out in (2.76). In particular, the generator of connected correlators of the  $\Delta_-$  theory is obtained by Legendre transforming the generator of connected correlators of the  $\Delta_+$  theory [60]<sup>3</sup>.

---

<sup>3</sup>Regarding the addition of boundary regulators, we observe that these are different in the two case, standard and alternative quantization.

**Validity of the supergravity approximation.** Since type IIB supergravity is the low energy limit of type IIB string theory, the Newton constant in ten dimensions may be expressed in terms of the dimensionless string coupling  $g_s$  and the string length scale  $l_s^2 = \alpha'$  [45]. The relation is

$$2\kappa_{10}^2 \equiv 16\pi G_{10} = 128\pi^7 g_s^2 \alpha'^4 . \quad (2.82)$$

Then, compactification of type IIB supergravity on the  $S^5$  leads to the definition of the five dimensional Newton constant. To obtain this result we have to remind that the length scale of  $\text{AdS}_5$  and  $S^5$  originates from the D3 brane scale  $L$  given by  $L^4 = 4\pi\alpha'^2 g_s N$  where the integer  $N$  is determined by the flux of the self dual 5-form field strength on  $S^5$ . By construction, the five dimensional Newton constant is,

$$\frac{\kappa_5^2}{8\pi} = G_5 = \frac{G_{10}}{\text{Vol}(S^5)} = \frac{\pi L^3}{2N^2} . \quad (2.83)$$

We deduce that the evaluation of the classical action in (2.75), is justified in the supergravity approximation  $N \gg 1$  because,

$$Z_S[\varphi_0] \approx N^2 S_{IIB}[\varphi_0] + O\left(\frac{1}{N^2}\right) + O\left(\frac{1}{\sqrt{\lambda}}\right) . \quad (2.84)$$

**Back-Reacting Scalars.** All the things we have said about standard and alternative quantization remain valid in the interacting case, where the scalar field sources the Einstein equations and vice-versa. In this case, the problem is to find a five dimensional geometry with the right boundary conditions. Imposing that the gravitational metric has to be asymptotically  $\text{AdS}_5$ , the scalar field is forced to be sub-leading at boundary. However this is not a restriction and as we have seen, there is always a mode whose fall-off goes to zero as  $z \rightarrow 0$ . In the next chapter we will construct explicit examples of asymptotically  $\text{AdS}_{d+1}$  spaces whose bulk geometry is modified by the presence of interacting scalar fields. The dual field theory will have non trivial expectation values for certain single trace operators.

## 2.5.2 Double Trace Deformations

The bulk to boundary mapping outlined in the previous section naturally takes into account single trace operators. This is the result of the Kaluza-Klein reduction on  $\text{AdS}_5 \times S^5$ : given a bulk field, there exists a dual single trace operator defined by the same global symmetry quantum numbers and by the relation (2.59). From this point of view, single trace operators play a

special role and correspond to canonical fields on the AdS side. In the CFT, multi-trace operators may be constructed by using OPE and therefore it is natural to think of them as bound states of the one particle states. However, it is not immediately apparent how to apply the holographic principle to a multi-particle state. Instead, there is relatively simple proposal due to Witten that generalizes the known notion of boundary condition for canonical fields and at the same time produces multi-trace deformations [61].

Let us begin the study of multi-trace boundary conditions by considering the case of a real scalar field of mass  $m^2$  in AdS in the *standard quantization* scheme. Near the boundary at  $z = 0$  the scalar field admits the expansion (2.70), namely

$$\varphi \rightarrow z^{4-\Delta+} \left( \varphi_0(\vec{x}) + O(z^2) \right) + z^{\Delta+} \left( A(\vec{x}) + O(z^2) \right). \quad (2.85)$$

Then, the modes  $A(\vec{x})$  and  $\varphi_0(\vec{x})$ , are interpreted respectively as the expectation value of the dual operator  $\mathcal{O}_\Delta(\vec{x})$  and as the source term in the external coupling  $\varphi_0(\vec{x})\mathcal{O}_\Delta(\vec{x})$ . The main observation is the following. Computing the expectation value,

$$\left\langle \exp \left\{ -N^2 \int d\vec{x} f(x) \mathcal{O}_\Delta \right\} \right\rangle, \quad (2.86)$$

is the same as computing the partition function of the boundary field theory in the presence of a perturbation  $-N^2\mathcal{W}$  added to the Lagrangian where

$$\mathcal{W} = \int d\vec{x} f(x) \mathcal{O}_\Delta. \quad (2.87)$$

In other words, we can equivalently start from an unperturbed Lagrangian and calculate the expectation value of  $\mathcal{W}$  or define the Lagrangian of the theory with  $\mathcal{W}$  built in and calculate the vacuum expectation value. In the first case, the boundary prescription is formally identical to the coupling with the external source through  $\varphi_0(\vec{x})\mathcal{O}_\Delta(\vec{x})$ , where  $\varphi_0(\vec{x}) = f(\vec{x})$ . Since  $A(\vec{x})$  corresponds to the expectation value of  $\mathcal{O}_\Delta$ , this boundary condition can be rewritten as,

$$\varphi_0(\vec{x}) = \frac{\delta\mathcal{W}}{\delta A}(\vec{x}). \quad (2.88)$$

In this language,  $\mathcal{W}$  is interpreted as a functional of  $A(\vec{x})$  obtained by replacing  $\mathcal{O}_\Delta$  everywhere with  $A(\vec{x})$ . Then, multi-trace interactions are associated to a certain choice of  $\mathcal{W}(A)$ .

Double trace deformations are simple to realize. In this case,

$$\varphi_0(\vec{x}) = fA(\vec{x}), \quad \longleftrightarrow \quad \mathcal{W} = \frac{1}{2} \int d\vec{x} fA(\vec{x})^2, \quad (2.89)$$

where  $f$  is now a coupling constant. Unless,  $\Delta_- = \Delta_+$  the coupling will be a dimensionful coupling and the field theory will be deformed by a relevant or by an irrelevant double-trace operator. The case  $\Delta_- = \Delta_+$  is peculiar because it requires a proper treatment of the logarithmic branch. Near the boundary the behavior of the scalar field is,

$$\varphi \rightarrow z^{\Delta_+} \left( \varphi_0(\vec{x}) \log(\mu z) + A(\vec{x}) + O(z^2) \right), \quad (2.90)$$

and a scale  $\mu$  has to be introduced in order to make the argument of the log dimensionless. The coupling  $f$  is marginal by construction. On the other hand  $f$  is not protected by the symmetries and quantum mechanically conformal invariance is violated at order  $f^2$ . The log term reproduces this general analysis and is nicely understood in the dual field theory as the result of a one-loop beta function calculation [61].

We conclude by considering another example. This is suggested by the introduction of the *alternative quantization* scheme. We suppose there exist two scalar fields  $\varphi$  and  $\eta$  with the same mass in the range  $-d^2/4 < m^2 < -d^4/4 + 1$ . We adopt one method of quantization for the scalar  $\varphi$  and the second method of quantization for the scalar  $\eta$  so that  $\varphi$  is dual to an operator  $\mathcal{O}_\varphi$  of dimension  $\Delta_+$  but  $\eta$  is dual to an operator  $\mathcal{O}_\eta$  of dimension of  $\Delta_-$ . Schematically,

$$\varphi(z, \vec{x}) \sim \varphi_0(\vec{x}) z^{\Delta_-} + \mathcal{O}_\varphi(\vec{x}) z^{\Delta_+}, \quad (2.91)$$

$$\eta(z, \vec{x}) \sim \mathcal{O}_\eta(\vec{x}) z^{\Delta_-} + \eta_0(\vec{x}) z^{\Delta_+}, \quad (2.92)$$

The double trace operator we want to consider is the marginal operator

$$\mathcal{W} \sim \int d\vec{x} \mathcal{O}_\eta(\vec{x}) \mathcal{O}_\varphi(\vec{x}).$$

The boundary conditions that implement this deformation are

$$\varphi_0(\vec{x}) = f \mathcal{O}_\eta(\vec{x}), \quad \eta_0(\vec{x}) = f \mathcal{O}_\varphi(\vec{x}), \quad (2.93)$$

where  $f$  is a marginal coupling. The above setup has nice interesting features under renormalization group flow and we refer to [61] for a more detailed discussion. We will find a similar situation by studying gravitational background in the context of four dimensional  $\mathcal{N} = 2$  supergravity coupled to matter fields. As a last remark, we observe that the results obtained in this section admit a straightforward generalization to the case of a complex scalar field.



# Chapter 3

## Holographic Superconductors

In this chapter we define the concept of holographic superconductivity. This is one of the many applications of the AdS/CFT correspondence to the study of concrete physical systems which experience a strongly coupled interaction. For what concerns condensed matter physics, reviews on the subject can be found in the references [62, 63, 64, 65].

Starting from the second section of this chapter, we introduce a family of models which can be considered as *phenomenological* models of holographic superconductivity. These are based on a set of couplings that characterize the physics of the boundary system. In particular, we will see how to reproduce non mean field critical exponents, to engineer a cross-over from a second order to a first order phase transition and also we will see how to tune particular features in the optical conductivity. In the gravitational description, we deal with classical Einstein's equations in a background where an electric gauge field and a charged scalar field are turned on. In the simplest cases, the charged scalar field is minimally coupled to the gauge field. Modifying this setup by adding appropriate couplings, will lead us to the interesting phenomenological properties that we mentioned above.

Before turning into the construction of our holographic models we dedicate the first section of this chapter to a wide introduction about the ideas that are behind the holographic approach to condensed matter applications and the way we will implement such ideas.

### 3.1 Setting up the problem

In the previous chapter we introduced the AdS/CFT correspondence by considering the case of  $N$  coincident D3-branes in type IIB string theory. The

essential point of the Maldacena derivation is a certain *near horizon limit* of the D3 brane solution in supergravity. This procedure is quite general and may be applied to other supergravity backgrounds. In particular, everything we have said regarding the D3-branes carries over for M2-branes and M5-branes [1] and the corresponding supergravity solutions reduce respectively to the product of  $AdS_4 \times S^7$  and  $AdS_7 \times S^4$ . The low energy theory described by  $N$  coincident M2-branes is known in some detail and we refer to [67] for the precise statement of the conjecture. We also mention that examples of gauge/gravity dualities in which the compact space is not a sphere will be discussed in the last chapter of this thesis. They represent a generalization of the Maldacena conjecture and are understood in terms of a certain configuration of D3-branes in ten dimensions.

Since high- $T_c$  superconductors are generally considered to be quasi two-dimensional materials, our gravitational theories are supposed to live either in  $AdS_4$  or in  $AdS_5$ . Therefore, we will be mainly interested in those field theories that are obtained from D3-branes or M2-branes. At this point, our holographic approach to the problem of high- $T_c$  superconductivity needs some clarification. The discussion of section 1.3.3 points out that the solution to the problem of high- $T_c$  superconductivity is beyond perturbative quantum field theory. Most likely, the quasiparticle picture is totally inadequate to describe properties of the phase diagram in the cuprates and a more fundamental reformulation of the low energy degrees of freedom is necessary. From this point of view, the AdS/CFT correspondence may be used to map a difficult quantum problem, that involves strong coupling physics, into a classical problem of gravity in AdS. The price we pay is that the dual field theory is an  $SU(N)$  gauge theory taken in the large  $N$  limit. In this sense, field theories with known holographic duals cannot be “simply” reproduced in the laboratory neither their microscopic Lagrangian be compared to the spin-fermion model. Nevertheless, we would like to probe these field theories in a typical condensed matter setup and in particular, we would like to engineer an holographic state characterized by a certain thermodynamical ensemble and a certain ‘electric’  $U(1)$  global symmetry. Eventually, heat up the system by considering finite temperature. Then, we will focus on the following question, do large  $N$  field theory exhibit the phenomena of (high- $T_c$ ) superconductivity? We will answer this question building an holographic superconductor. The latter will be a genuine strongly coupled state which can be studied quite easily thanks to the AdS/CFT correspondence. It is important to mention that very non trivial results based on this kind of construction suggest that high- $T_c$  superconductors and strange metals may belong to universality classes that admit an holographic description [7, 8]. For this reason, the study of holographic su-

perconductivity may be used as a complementary tool to determine the class of universality of certain strongly coupled condensed matter systems.

Let us indicate our general strategy. The study of holographic superconductivity in a field theory with a known holographic dual begins by considering a certain set of operators which have an analog in condensed matter physics. For example, we may consider the analog of the Cooper-pair operator in  $\mathcal{N} = 4$  SYM. On the gravity side, this set of operators will be described by a certain truncation of the full supergravity theory which identifies the AdS/CFT correspondence. Then, our task is to find the desired *consistent* truncation in the full supergravity theory. This is not as simple as it seems and therefore we first would like to have a controlled phenomenological model to play with. In this way, the search for holographic superconductivity in string theory or in M-theory will be guided by a better understanding of the set up. In particular, instead of looking at all the truncations of the full supergravity theory, we will restrict our attention to those truncations which correctly generalizes nice properties of the phenomenological models.

Motivated by the above line of reasoning, we study a class of phenomenological models which contain the minimal ingredients required to build a holographic superconductor. The advantage of our models is that string theory and M-theory models are particular cases corresponding to a specific choice of the phenomenological couplings. Therefore, even without knowing the exact supergravity truncation, an educated guess will probably lead us to describe the same physics of the more fundamental theories originating from D3-branes or M2-branes. On the other hand, by tuning the phenomenological couplings we will have access to a wide range of properties and as a result, we will be able to show how the AdS/CFT correspondence naturally generalizes at strong coupling the Landau-Ginzburg (mean field) theory and the Widom scalings theory [66].

## 3.2 Phenomenological Models

The Landau-Ginzburg theory is the bridge between the microscopic BCS theory and a field theory description of the superconductivity. We recall that the Landau-Ginzburg theory is the effective field theory description of a superconductor near the superconducting phase transition. Its microscopic derivation is based on the general formalism of the Hubbard-Stratonovich transformations applied to the BCS theory. As a result, the path integral of the BCS

theory can be written in the form,

$$\mathcal{Z} = \int \mathcal{D}[\varphi, \bar{\varphi}, c, \bar{c}] e^{-S}, \quad (3.1)$$

$$S = \int_0^\beta d\tau \left( \sum_{\mathbf{k}} \bar{c}_{\mathbf{k}} G_b^{-1}(\mathbf{k}, \tau) c_{\mathbf{k}} + \bar{\varphi} \Delta + \bar{\Delta} \varphi + \frac{\varphi \bar{\varphi}}{\lambda} \right), \quad (3.2)$$

$$\Delta = \sum_{\mathbf{k}} c_{-\mathbf{k}\uparrow} c_{\mathbf{k}\downarrow}, \quad (3.3)$$

where we have introduced the gaussian field  $\varphi$ . By integrating out  $\varphi$ , we recover the standard form of the BCS Hamiltonian whereas, by integrating out the fermionic field we obtain an effective action for  $\varphi$ . This is the effective action which defines the Landau-Ginzburg theory [68]. At the lowest order in  $\varphi$ , we find,

$$S_{eff} \cong \frac{K}{2} |\partial\varphi|^2 - \frac{t}{2} |\varphi|^2 - u |\varphi|^4. \quad (3.4)$$

This action is invariant under a global  $U(1)$  symmetry and the parameters  $t$ ,  $u$  and  $K$  are determined by the diagrammatic expansion of the microscopic theory (in the weak coupling regime). The coefficient  $u$  is positive definite, i.e.  $u > 0$ . The importance of (3.4) is the following:  $\varphi$  is an order parameter for the superconducting phase transition. For  $t < 0$  the minimum of the potential is  $\langle \varphi \rangle = \sqrt{(-t)/(4u)}$  and the  $U(1)$  symmetry is spontaneously broken, for  $t > 0$  the minimum sits at the origin and  $\langle \varphi \rangle = 0$ . In the microscopic theory the phase corresponding to  $\langle \varphi \rangle \neq 0$  describes the superconducting phase whereas the phase corresponding to  $\langle \varphi \rangle = 0$  describes the normal phase.

Normally the superfluid phase is the one which is associated with spontaneous symmetry breaking while the superconducting phase is associated with the Higgs mechanism of the  $U(1)$  electromagnetic gauge field. Both are related to  $\langle \varphi \rangle \neq 0$ , the difference is the presence of a dynamical photon. This photon is introduced in the action (3.4) by gauging the  $U(1)$  global symmetry,

$$S_{eff} \cong \frac{1}{4} F_{\mu\nu} F^{\mu\nu} + \frac{K}{2} |(\partial_\mu - 2ieA_\mu)\varphi|^2 - \frac{t}{2} |\varphi|^2 - u |\varphi|^4. \quad (3.5)$$

Here  $A_\mu$  is the  $U(1)$  gauge field and  $F_{\mu\nu}$  is the corresponding field strength. As a result, when  $\langle \varphi \rangle \neq 0$  the photon acquires a mass and the system enters the Higgs phase. In this phase, the London equations can be derived from the Maxwell equations by considering a gauge in which the field  $\varphi$  is real. In this sense, the magnetic properties of the superconductors are a consequence of the Higgs mechanism. We will argue that for the kind of questions that will be

relevant to us, the difference between a superfluid and a superconducting phase transition in field theory is not important, and eventually we can pretend that the global symmetry group is weakly gauged.

Summarizing, before looking at the microscopic operators of a given holographic field theory, an holographic superconductor is defined by a symmetry breaking pattern in which a global  $U(1)$  symmetry is spontaneously broken. This is quite a general definition and will be our starting point for the construction of gravitational theories supporting holographic superconductivity. The basic ingredients are found in AdS/CFT dictionary. They are: a  $U(1)$  gauge field in AdS which is dual to a global  $U(1)$  current in the boundary; a charged bulk scalar field which plays the role of the order parameter [69, 70].

The simplest gravitational action we may consider with such ingredients is the following,

$$\mathcal{S} = \frac{1}{16\pi G_5} \int d^{d+1}x \sqrt{g} \mathcal{L} , \quad (3.6)$$

$$\mathcal{L} = \mathcal{R} - \frac{1}{4} F^{\mu\nu} F_{\mu\nu} + \frac{d(d-1)}{L^2} U(|\psi|) - \overline{D_\mu \psi} D^\mu \psi . \quad (3.7)$$

This is the Einstein-Hilbert action coupled to a gauge field  $A_\mu$  and a complex scalar field  $\psi$ . In particular,  $\mathcal{R}$  is the scalar curvature,  $F_{\mu\nu}$  is the field strength of the gauge field defined by  $F_{\mu\nu} \equiv \partial_{[\mu} A_{\nu]}$  and  $D_\mu \psi$  is the covariant derivative,

$$D_\mu \psi = \partial_\mu \psi - iq A_\mu \psi . \quad (3.8)$$

The complex scalar has charge  $q$  and it is minimally coupled to the gauge field. The function  $U(|\psi|)$  is a generic scalar potential normalized so that  $U(0) = 1$ . Then, the cosmological constant is that of  $AdS_{d+1}$  and the theory has an AdS solution

$$\eta = 0 , \quad A_\mu = 0 , \quad ds^2 = \frac{r^2}{L^2} (-dt^2 + d\vec{x}_{d-1}^2) + L^2 \frac{dr^2}{r^2} . \quad (3.9)$$

By considering the redefinition  $\psi = \eta e^{i\theta} / \sqrt{2}$  we may write the above Lagrangian in terms of a real scalar field  $\eta$  and a Stückelberg field  $\theta$ . The result is,

$$\mathcal{L} = \mathcal{R} - \frac{1}{4} F^{\mu\nu} F_{\mu\nu} + \frac{d(d-1)}{L^2} U(|\psi|) - \frac{1}{2} (\partial\eta)^2 - \frac{1}{2} q^2 \eta^2 (\partial_\mu \theta - A_\mu)^2 . \quad (3.10)$$

Given the above structure, the most general Lagrangian will contain arbitrary functions of the scalar field  $\eta$ . These functions represent the phenomenological

couplings of the theory. The most general model is parametrized by three of them [10, 71], namely

$$\mathcal{L} = \mathcal{R} - \frac{1}{4}G(\eta) F^{\mu\nu}F_{\mu\nu} + \frac{d(d-1)}{L^2}U(\eta) - \frac{1}{2}(\partial\eta)^2 - \frac{1}{2}J(\eta) (\partial_\mu\theta - A_\mu)^2. \quad (3.11)$$

In principle, we may also consider a coupling of the form  $K(\eta)\mathcal{R}$  and a non linear kinetic term for the scalar field  $\eta$ . We can get rid of both these terms by a suitable Weyl rescaling and a field redefinition, respectively. For reference purposes, it is useful to define two particular class of models specified by the behavior of the couplings at small  $\eta$ . Models in the class A have the following structure:

$$G(\eta) \cong 1 + \kappa \eta^2 + O(\eta^4), \quad (3.12)$$

$$U(\eta) \cong 1 - \frac{m^2}{2d(d-1)} \eta^2 + O(\eta^4), \quad (3.13)$$

$$J(\eta) \cong q^2\eta^2 + O(\eta^4). \quad (3.14)$$

This class of couplings is also defined to be invariant under the  $\mathbf{Z}_2$  symmetry  $\eta \rightarrow -\eta$ . The first model of holographic superconductors (henceforth, the HHH model) has been constructed and studied by the authors of [9]. This is recovered upon setting  $\kappa = 0$ , with  $U = 1 + \frac{1}{6} \eta^2$  and  $J = q^2\eta^2$ . A slight generalization of the couplings  $U(\eta)$ ,  $J(\eta)$  and  $G(\eta)$  is to allow odd powers of  $\eta$ . Therefore, we define the second class of models, called class B, considering more general exponents in the small  $\eta$  expansion:

$$G(\eta) \cong 1 + \kappa \eta^2 + g_0\eta^a, \quad (3.15)$$

$$U(\eta) \cong 1 - \frac{m^2}{2d(d-1)} \eta^2 + u_0\eta^b, \quad (3.16)$$

$$J(\eta) \cong q^2\eta^2 + j_0\eta^c, \quad (3.17)$$

Here  $a, b, c$  are assumed to be real, positive numbers, with  $a, b, c > 2$ . The function  $G(\eta)$  and  $J(\eta)$  must be positive definite for unitarity. For generic values of  $a, b, c$ , this model contains also non-analytic interactions in  $\eta$  which are well defined only when  $\eta \geq 0$ .

In the next section we study classical solution of the Lagrangian (3.11) and we describe how to construct an holographic superconductor.

### 3.2.1 Ansatz and Equations of motion

We set  $d = 1 + 2$  for concreteness and we fix the gauge  $\theta = 0$ . The choice of the two spatial dimensions is also dictated by the fact that high-Tc superconduc-

tors are quasi two-dimensional systems. However, analytical and numerical results, valid for  $d = 3$ , admits a straightforward generalization to higher dimension. In particular, the case of  $d = 1 + 3$  is also relevant to the description of high-Tc superconductivity. The Lagrangian (3.11) takes the form

$$\mathcal{L} = R - \frac{1}{4}G(\eta) F^{\mu\nu}F_{\mu\nu} + \frac{6}{L^2}U(\eta) - \frac{1}{2}(\partial\eta)^2 - \frac{1}{2}J(\eta)A_\mu A^\mu . \quad (3.18)$$

We consider the following static ansatz

$$ds^2 = -g(r)e^{-\chi(r)}dt^2 + r^2(dx^2 + dy^2) + \frac{dr^2}{g(r)} , \quad (3.19)$$

$$A = \Phi(r)dt , \quad \eta = \eta(r) . \quad (3.20)$$

Then, the effective Lagrangian takes the form

$$\sqrt{g}\mathcal{L} = -2e^{-\frac{\chi}{2}}(rg)' + \frac{r^2}{2}G(\eta)e^{\frac{\chi}{2}}\Phi'^2 + \frac{6r^2}{L^2}e^{-\frac{\chi}{2}}U(\eta) - \frac{r^2}{2}e^{-\frac{\chi}{2}}g\eta'^2 + \frac{r^2}{2g}e^{\frac{\chi}{2}}J(\eta)\Phi^2 . \quad (3.21)$$

The equations of motion reduce to,

$$\chi' + \frac{r}{2}\eta'^2 + \frac{r}{2g^2}e^\chi J(\eta)\Phi^2 = 0 , \quad (3.22)$$

$$\frac{1}{4}\eta'^2 + \frac{G(\eta)}{4g}e^\chi\Phi'(r)^2 + \frac{g'}{rg} + \frac{1}{r^2} - \frac{3}{L^2g}U(\eta) + \frac{1}{4g^2}e^\chi J(\eta)\Phi^2 = 0 , \quad (3.23)$$

$$\Phi'' + \Phi' \left( \frac{2}{r} + \frac{\chi'}{2} + \frac{\partial_\eta G \eta'}{G} \right) - \frac{J(\eta)}{gG(\eta)}\Phi = 0 , \quad (3.24)$$

$$\eta'' + \eta' \left( \frac{2}{r} - \frac{\chi'}{2} + \frac{g'}{g} \right) + \frac{1}{2g}e^\chi \partial_\eta G \Phi'^2 + \frac{6}{L^2g} \partial_\eta U + \frac{1}{2g^2}e^\chi \partial_\eta J \Phi^2 = 0 . \quad (3.25)$$

### 3.2.2 The shooting method

To our knowledge, the basic strategy to solve these equations has been described for the first time in [9] and technically, it makes use of an adapted version of the numerical shooting method. In this section we go through all the basics steps that are needed in order to built such solution. The first step is the introduction of a finite temperature.

We introduce a finite temperature  $T$  in the dual field theory by considering black holes in the bulk. The temperature  $T$  is then the Hawking temperature of the black hole. This is calculated by examining the behavior of the metric

(3.19) in the Euclidean regime in the vicinity of the horizon at  $r = r_h$ . By definition  $r_h$  is the greatest simple root of  $g(r)$ . Setting  $t = i\tau$  and  $z^2 = (r - r_h)$ , the metric can be written in the form,

$$ds^2 \propto dz^2 + \left[ \frac{g'(r_h)e^{-\chi(r_h)/2}}{2} \right]^2 z^2 d\tau^2 + \dots \quad (3.26)$$

The conical singularity at the horizon (now  $z = 0$ ) is avoided if  $\tau$  is assigned the period  $2\pi\beta$  where  $1/\beta^2$  is the coefficient of the term  $z^2 d\tau^2$  in (3.26). The inverse of this periodicity in imaginary time is the Hawking temperature,

$$T = \frac{g'e^{-\chi/2}}{4\pi} \Big|_{r=r_h} . \quad (3.27)$$

We construct black hole solutions by postulating the existence of an horizon at  $r = r_h$  and integrating the equations of motion up to  $r \rightarrow \infty$ . In particular, we require the black hole to be asymptotically AdS so to apply the standard AdS/CFT correspondence. The limit  $r \rightarrow \infty$  is commonly indicated as the ultraviolet limit (UV) of the gravitational background whereas the extremal bulk region is regarded as the infra-red limit (IR).

Naively, the equations (3.22)-(3.25) are singular at the horizon because of the terms  $1/g$  and  $1/g^2$  that appear in (3.24) and (3.25). Thus, we need to work out a series expansion for the fields  $\Phi$  and  $\eta$  in order to have a well posed Cauchy problem. It turns out that the most general expansion,

$$g(r) \approx g'(r_h)(r - r_h) + O((r - r_h)^2) , \quad (3.28)$$

$$\chi(r) \approx \chi_h + \chi'(r_h)(r - r_h) + O((r - r_h)^2) , \quad (3.29)$$

$$\Phi(r) \approx \Phi(r_h) + \Phi'(r_h)(r - r_h) + O((r - r_h)^2) , \quad (3.30)$$

$$\eta(r) \approx \eta_h + \eta'(r_h)(r - r_h) + O((r - r_h)^2) , \quad (3.31)$$

is fixed by three independent parameters

$$\eta_h , \quad \Phi'(r_h) \equiv E_h , \quad \chi_h . \quad (3.32)$$

At the lowest order we find

$$g'(r_h) = r_h \left( 3U(\eta_h) - \frac{G(\eta_h)}{4} e^{\chi_h} \Phi'(r_h)^2 \right) , \quad (3.33)$$

$$\Phi(r_h) = 0 , \quad (3.34)$$

$$\eta'(r_h) = -\frac{1}{g'(r_h)} \left( \frac{e^{\chi_h}}{2} \partial_\eta G(\eta_h) \Phi'(r_h)^2 + 6\partial_\eta U(\eta_h) \right) . \quad (3.35)$$

All the other coefficients in the series expansion are determined in terms of the three parameters (3.32). The total number of parameters we have to specify in order to find the black hole solution is then  $3 + 1$  where the latter is the value of the horizon radius. However, two scaling symmetry that can be used to reduce the number of the numerical inputs. By considering,

$$r \rightarrow ar, \quad (t, \vec{x}) \rightarrow a^{-1}(t, \vec{x}), \quad g \rightarrow a^2g, \quad \Phi \rightarrow a\Phi, \quad (3.36)$$

we may set  $r_h = 1$ . By considering, and

$$e^\chi \rightarrow a^2e^\chi, \quad t \rightarrow at, \quad \Phi \rightarrow a\Phi. \quad (3.37)$$

we may set  $\chi_h = 1$ . As a result, the horizon expansion and therefore a generic solution to the equations of motion is determined only by  $\eta_h$  and  $E_h$ . For any given value of these two parameters, it is possible to integrate the equations of motion up to the boundary finding a numerical solution.

### 3.2.3 Defining the holographic superconductor

The analysis of the numerical solution follows by studying its large  $r$  behavior. First of all, we should guarantee that the black hole is asymptotically AdS. To this aim, we remind the reader that  $\eta(r)$  is characterized by two independent modes with different boundary asymptotics,

$$\lim_{r \rightarrow \infty} \eta(r) \approx \frac{\eta^{(1)}}{r^{3-\Delta_2}} + \frac{\eta^{(2)}}{r^{\Delta_2}}. \quad (3.38)$$

In particular,  $\Delta_2$  is the greatest root of the equation  $\Delta(\Delta - 4) = m^2L^2$ . Since the AdS solution in our phenomenological models (3.9) corresponds to  $\eta = 0$ , a necessary condition for the black hole to be asymptotically AdS is that  $\eta \rightarrow 0$  as  $r \rightarrow \infty$ . For generic values of  $m^2$ , one of the two boundary modes (3.38) blows up and thus we need to impose a relation between  $\eta_h$  and  $E_h$  such that the coefficient of this blowing up mode is set to zero. This choice is consistent with the general asymptotic expansion of the functions  $\Phi(r)$ ,  $g(r)$  and  $\chi(r)$  and in particular no other conditions are needed to be imposed in order for the black hole to be asymptotically AdS. For every choice of mass  $m^2$ , we generalize the above prescription and we set to zero the coefficient of the non-normalizable mode. As a consequence, we are left with a one-parameter family of solutions. This family of solutions defines our holographic superconductor.

At this point, it is useful to work out an example. We compute the asymptotic expansion of the functions  $g(r)$ ,  $\chi(r)$ ,  $\Phi(r)$  in the case of  $m^2L^2 = -2$ .

For convenience, we also consider an the off-shell configuration in which both  $\eta^{(1)}$  and  $\eta^{(2)}$  are non zero, even if by construction the non-normalizable mode is set to zero. We find,

$$\eta(r) = \frac{\eta^{(1)}}{r} + \frac{\eta^{(2)}}{r^2} + \dots \quad (3.39)$$

$$\Phi(r) = \mu - \frac{\rho}{r} + \dots \quad (3.40)$$

$$e^{-\chi(r)}g(r) = r^2 - \frac{1}{r} \left( M + \frac{2}{3}\eta^{(1)}\eta^{(2)} \right) + \dots \quad (3.41)$$

In the last expression we have used the inverse scaling (3.37) to set to zero the asymptotic value of  $\chi(r)$ . Similarly to the horizon expansion, the asymptotic expansion is fixed by the knowledge of certain parameters. These are,

$$\mu, \quad \rho, \quad \eta^{(1)}, \quad \eta^{(2)}, \quad M. \quad (3.42)$$

It should be clear that they are not independent because we know that the number of independent parameter is reduced to one. The notation we will use is the following. We define  $\mu$  as the chemical potential,  $\rho$  as the charge density and  $M$  as the mass of the black hole. All these parameters have a physical interpretation in the dual field theory. In the next chapter we comment on the meaning of  $\mu$  and  $\rho$ . We will come back on the meaning of  $M$  in section 3.6.

**Alternative Quantization.** In the cases in which  $d^2/4 < m^2 < d^2/4 + 1$ , both  $\Delta_1$  and  $\Delta_2$  correspond to a vanishing solution at the boundary and we are allowed to modify our prescription. In principle we can either set  $\eta^{(1)}$  or  $\eta^{(2)}$  to zero. This ambiguity corresponds to the choice of quantization scheme discussed in section 2.5.1. The first choice,  $\eta^{(1)} = 0$ , corresponds to the standard quantization scheme whereas the second choice,  $\eta^{(2)} = 0$ , corresponds to the alternative quantization scheme. We remind the reader that  $m^2 = d^2/4 = m_{BF}^2$  is the Breitenlohner-Freedman bound on the masses.

### 3.3 The uncondensed solution

The uncondensed solution is by definition a gravitational solution where  $\eta(r)$  is identically vanishing. In AdS<sub>4</sub>, this is described by the Reissner-Nördstrom

black hole,

$$\chi = \eta = 0, \quad \Phi(r) = \rho \left( \frac{1}{r_h} - \frac{1}{r} \right), \quad (3.43)$$

$$g(r) = r^2 - \frac{1}{r} \left( r_h^3 + \frac{\rho}{4r_h} \right) + \frac{\rho^2}{4r^2}. \quad (3.44)$$

With respect to the general construction (3.40) and (3.41), the values of  $\mu$  and  $M$  have been fixed by the requirement that  $\Phi(r_h) = 0$  and  $g(r_h) = 0$ . Without loss of generality we may restore an arbitrary chemical potential by considering the off-shell solution,

$$\Phi(r) = \mu - \frac{\rho}{r}. \quad (3.45)$$

According to the AdS/CFT dictionary,  $\mu$  is the non-normalizable mode of the time component of the bulk gauge field  $A_\mu$ . In the boundary, this mode sources the time component of a  $U(1)$  current  $\mathcal{J}_\mu$  which is dual to  $A_\mu$ . The value of  $\rho$  is then proportional to the expectation value of  $\mathcal{J}_t$  and therefore it describes a finite charge density in the dual field theory. In this sense, we can say that the Reissner-Nördstrom solution represents a state in the dual field theory with finite charge density. It is therefore reasonable to fix the value of the charge density of the system and take the temperature as the only parameter that specifies the Reissner-Nördstrom solution. We fix the value of the charge density to unity for convenience. In complete generality, this is done by considering the scaling (3.36) which introduces the radial coordinate  $\tilde{r} = r/\sqrt{\rho}$ . In this new coordinate system we find,

$$\tilde{\Phi} = \frac{\mu}{\sqrt{\rho}} - \frac{1}{\tilde{r}}, \quad \tilde{T} = \frac{T}{\sqrt{\rho}}. \quad (3.46)$$

It is easy to check that the same results are trivially obtained upon setting  $\rho = 1$  in the two expressions (3.43) and (3.44). However, in the superconducting case, we do not have analytic control on the full solution and therefore we will always consider the dimensionless temperature  $T/\sqrt{\rho}$ , where  $T$  is deduced from (3.27) by using the expression (3.33).

In the field theory, considering the black hole solution at fixed charge density corresponds to a precise choice of thermodynamical ensemble, i.e. the canonical ensemble. Instead, considering a fixed chemical potential corresponds to working in the grand canonical ensemble. It should be clear, from the above analysis, that in the bulk geometry, fixing  $\mu$  or  $\rho$ , is a matter of scaling symmetry.

It is a simple exercise to generalize the Reissner-Nördstrom solution to arbitrary dimensions. The ansatz for the metric and the gauge field is the same as in (3.19) and the result is

$$g(r) = r^2 - \frac{1}{r^{d-2}} \left( r_h^d + \frac{Q^2}{r_h^{d-2}} \right) + \frac{d-2}{d-1} \frac{\rho^2}{2r^{2d-4}}, \quad (3.47)$$

$$\Phi(r) = \rho \left( \frac{1}{r_h^{d-2}} - \frac{1}{r^{d-2}} \right), \quad Q^2 = \frac{d-2}{2(d-1)} \rho^2, \quad (3.48)$$

where we also have  $\chi = \eta = 0$ . By using the scaling (3.36), we are allowed to express the temperature  $T$  in terms of the dimensionless ratio  $T/\rho^{1/(d-1)}$ . The same observation is valid for any superconducting solution.

**A last remark.** The superconducting black hole is defined as an electric black hole with a charged hair turned on. The non trivial profile of  $\eta(r)$  is such that  $\eta^{(i)} \equiv O^{(i)} \neq 0$  with  $i = 1, 2$  according to the quantization scheme. Applying the AdS/CFT dictionary,  $O^{(i)} \neq 0$  corresponds to having a non trivial expectation value for the operator dual to scalar field. Since, this operator is charged under a global  $U(1)$  symmetry in the field theory, the  $U(1)$  is spontaneously broken. This mechanism is similar to that of the Landau Ginzburg theory: if  $\eta(r) = 0$  the  $U(1)$  symmetry is preserved, if  $\eta(r) \neq 0$  the symmetry is spontaneously broken. In this sense, it is interesting to note that the holographic dual of this spontaneous symmetry breaking is the Higgs mechanism in the bulk.

Before moving on, it is important to have a clear picture about the physical meaning of the black hole solutions we have described. Technically, what we have shown is the following. First, we have constructed a generic electric black hole which is asymptotically AdS and has a background charged scalar field turned on. Second, we have mapped this solution to a state in the field theory through the AdS/CFT correspondence. At this point, we emphasize that we still have to work hard in order to claim that such solution describes holographic superconductivity. We will give the complete proof of this statement in the sections 3.6 and 3.7.

### 3.4 The Superconducting Instability

It should be said that finding a numerical solution to the equations of motion (3.22)-(3.25) is not a simple task. Therefore, we would like to have a clue

indicating us the existence of such solutions. The argument goes as follows [9, 72].

In the Fermi Liquid theory the superconducting instability shows up by calculating the scattering amplitude in the Cooper channel. We cannot reproduce this calculation in the holographic setup nevertheless, we may consider a similar line of reasoning: we study the zero temperature limit of the Reissner-Nördstrom black, which is supposed to describe a finite charge density state analogous to the Fermi Liquid, and we look whether the linearized perturbation in the charged scalar field “channel” destabilizes the background geometry. Then, if the extremal<sup>1</sup> Reissner-Nördstrom black hole is found to be unstable under this perturbation we deduce that the full back-reacting solution will resolve this instability by turning on bulk charged scalar field. This mechanism is the holographic dual of the Cooper pair instability.

Using the scaling symmetry (3.36) to set the horizon radius  $r_h$  to one, the temperature of the Reissner-Nördstrom black hole is

$$T = \frac{12 - \rho^2}{16\pi} \quad (3.49)$$

and the extremal solution corresponds to  $\rho = 2\sqrt{3}$ . The key point is that the near horizon limit of this solution is  $AdS_2 \times \mathbb{R}^2$ ,

$$ds^2 = -6(r-1)^2 dt^2 + \frac{dr^2}{6(r-1)^2} + dx^2 + dy^2, \quad \Phi = 2\sqrt{3}(r-1). \quad (3.50)$$

Then, by plugging the metric (3.50) into the scalar wave equation (3.25) and changing variable so that  $\tilde{r} = r - 1$ , we find that the scalar perturbation at leading order satisfies the following wave equation in  $AdS_2$ ,

$$\eta'' + \frac{2}{\tilde{r}}\eta - \frac{m_{eff}^2}{\tilde{r}^2}\eta = 0, \quad m_{eff}^2 = \frac{m^2 - 2q^2}{6}. \quad (3.51)$$

We observe that in the extremal limit, the mass of the scalar field receives an additional negative contribution which comes from the minimal coupling with the gauge field. The result is that the effective mass  $m_{eff}^2$  depends on the combination  $m^2 - 2q^2$  and can be tuned by modifying the value of charge  $q$ .

The AdS/CFT correspondence provides a simple way to probe the stability of the  $AdS_{d+1}$  background under linearized perturbations. For the case of a scalar field the condition is that the mass of the scalar must be above the

---

<sup>1</sup>Sometimes we may refer to the zero temperature limit of a certain family of black holes as the extremal limit.

Breitenlohner-Freedman bound. For  $AdS_2$  the Breitenlohner-Freedman bound is  $m_{BF}^2 = -1/4$ . Thus, the instability arises if

$$m^2 - 2q^2 < -\frac{3}{2} \quad (3.52)$$

Of course the mass  $m$  must be above the Breitenlohner-Freedman bound for  $AdS_4$ . Given that  $m^2 > -9/4$ , we interpret the inequality (3.52) as a condition on the charge and we deduce that for high enough values of the charge  $q$  the Reissner-Nördstrom black hole is unstable. We expect this instability to be resolved by a superconducting black hole.

### 3.4.1 Linearized Analysis

Before looking at the backreacting superconducting solutions, there exists a second piece of evidence that we may consider. This is inspired by the following observation. For a second order phase transition, the condensate goes to zero at the critical temperature and we expect the bulk scalar field to be a small perturbation of the black hole geometry. In this limit, the black hole geometry is well approximated by the Reissner-Nördstrom black hole and we may restrict the search for a superconducting solution to the study of a single linearized equation. This is the equation of the charged scalar field  $\eta(r)$  in the Reissner-Nördstrom background.

Since  $\eta$  is supposed to be a small perturbation, the couplings  $J(\eta)$ ,  $G(\eta)$  and  $U(\eta)$ , that appear in (3.25), are well approximated by their expansions around  $\eta = 0$ . In this sense, the model of class B reduce to the models of the class A because higher order terms are irrelevant at the linearized level. Then, we end up with the following exact expressions

$$J(\eta) = q^2 \eta^2, \quad (3.53)$$

$$G(\eta) = 1 + \kappa \eta^2, \quad (3.54)$$

$$U(\eta) = 1 + \frac{m^2}{12} \eta^2. \quad (3.55)$$

The equation we want to solve is,

$$\eta''(r) + F_1[r, r_h, \rho] \eta'(r) + F_2[r, r_h, \rho, \kappa, q, m] \eta(r) = 0, \quad (3.56)$$

$$F_1[r, r_h, \rho] = \frac{g'}{g} + \frac{2}{r}, \quad (3.57)$$

$$F_2[r, r_h, \rho, m^2, q^2] = \frac{1}{g} \left( \kappa \Phi'(r)^2 + m^2 \right) + \frac{q^2 \Phi^2}{g^2} q^2 \Phi^2. \quad (3.58)$$

where the function  $g(r)$  and  $\Phi(r)$  are given in (3.43)-(3.44). We observe that the function  $F_2$  depends explicitly on the choice of the phenomenological parameters,  $\kappa$ ,  $q$  and  $m$ .

The behavior of  $\eta(r)$  at the horizon follows from the general analysis of section 3.2.1 but the Cauchy problem is slightly different and we now explain how to set up the numerics. In the present case, the expansion (3.31) is determined by the parameter  $\eta_h \equiv \eta(r_h)$  and by the background values of  $\rho$  and  $r_h$ ,

$$\eta(r) \approx \eta_h + \eta'(r_h)(r - r_h) + \frac{1}{2}\eta''(r_h)(r - r_h)^2 + \dots \quad (3.59)$$

$$\begin{aligned} \eta'(r_h) &= -\eta_h \left( \kappa \frac{\rho^2}{r_h^4} + m^2 \right) \frac{4r_h^3}{12r_h^4 - 1} \\ \eta''(r_h) &= \dots \end{aligned} \quad (3.60)$$

The relation between  $\eta'(r_h)$  and  $\eta_h$  ensures that the differential equation (3.56) is non singular at the horizon. Furthermore, since this equation is linear in  $\eta$ , the parameter  $\eta_h \equiv \eta(r_h)$  can be fixed to an arbitrary value without loss of generality. We can also fix the normalization of the charge density at  $\rho = 1$ . Then, we are left with one free parameter, the horizon radius  $r_h$ . The boundary condition is  $\eta^{(i)} = 0$ , where  $i = 1$  for the standard quantization scheme and  $i = 2$  for the alternative quantization scheme. The strategy is to vary the value of  $r_h$  until the desired boundary condition is matched. Since the temperature is related to  $r_h$  through the relation

$$T = \left. \frac{g'e^{-\chi/2}}{4\pi} \right|_{r=r_h} = \frac{1}{16\pi} \left( 12r_h - \frac{1}{r_h^3} \right) \quad (3.61)$$

a scan of all possible values of  $r_h$  is physically a scan of all possible temperatures. Therefore, if the condition  $\eta^{(i)} = 0$  has a solution, there will be a corresponding temperature  $\mathcal{T}$  such that a superconducting solution with a small condensate exists. We may reintroduce the dependence upon the charge density  $\rho$  by considering the dimensionless quantity  $\mathcal{T}/\rho^{1/2}$ . Put it in this way, it should be clear that the numerical problem can be equally solved by setting  $r_h = 1$  and letting vary  $\rho$  until the boundary condition  $\eta^{(i)} = 0$  is matched.

In Figure 3.1 we show a plot of the temperature  $\mathcal{T}$  as function of the charge  $q$  in the case  $m^2L^2 = -2$  and  $\kappa = 0$ . We have considered the standard quantization scheme in which  $O^{(1)} = 0$ . In the cases in which both quantization schemes are allowed, like the present one, the temperature  $\mathcal{T}$  is scheme-dependent. However, in both schemes we find the same qualitative

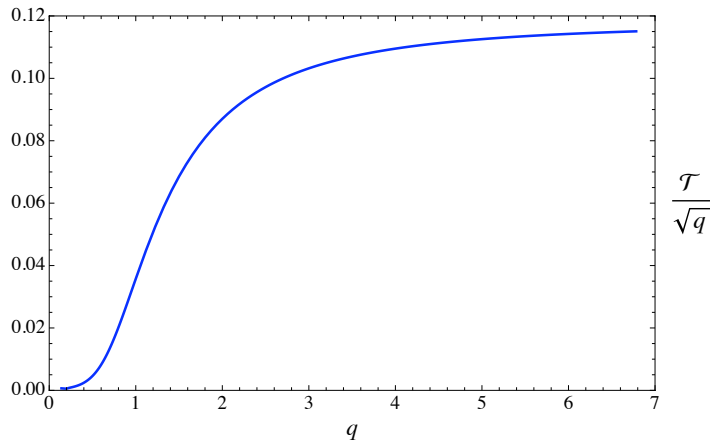


Figure 3.1: Critical Temperature  $\mathcal{T}$  as function of the charge parameter  $q$ , obtained from the linearized analysis in the HHH model in  $\text{AdS}_4$ . The mass is  $m^2 L^2 = -2$  and the charge density  $\rho = 1$ .

behavior. We have also studied the behavior of the temperature  $\mathcal{T}$  as function of the parameter  $\kappa$  fixing  $q$  and  $m^2 L^2$ . The result is that for  $\kappa > 0$  the critical temperature increases whereas for  $\kappa < 0$  it decreases. We will comment more on the role of the parameter  $\kappa$  in the section 3.6.1. In particular, we will give an analytic argument which explains the dependence of  $\mathcal{T}$  as function of the phenomenological parameters  $q, m, \kappa$ .

### 3.5 The Decoupling Limit

The discussion about the superconducting instability and the critical temperature  $\mathcal{T}$ , pointed out that when the charged scalar can be taken to be small, backreaction can be neglected. Then, the bulk black hole is well approximated by the uncondensed black. We would like to generalize this idea by considering a limit in which not only the charged scalar field, but also the the Maxwell field, does not backreact on the black hole [70]. In order to make our argument more explicit, we look at the equations of motion for the metric fields  $g(r)$  and  $\chi(r)$  in a sample case:  $J(\eta) = q^2 \eta^2$ ,  $G(\eta) = 1$  and  $U(\eta) = 1 - m^2 \eta^2 / 12$ . The

equations of motion (3.22)-(3.23) become,

$$\chi' + \frac{r}{2}\eta'^2 + \frac{r}{2g^2}e^\chi q^2 \eta^2 \Phi^2 = 0 , \quad (3.62)$$

$$\frac{1}{4}\eta'^2 + \frac{1}{4g}e^\chi \Phi'(r)^2 + \frac{g'}{rg} + \frac{1}{r^2} - \frac{3}{L^2 g} + \frac{m^2}{4}\eta^2 + \frac{1}{4g^2}e^\chi q^2 \eta^2 \Phi^2 = 0 . \quad (3.63)$$

The probe limit we are seeking is  $q \rightarrow \infty$  with  $q\eta$  and  $q\Phi$  held fixed. In this limit the matter fields drops out of the Einstein's equations and the metric is solved by the Schwarzschild black hole. In  $d + 1$  dimensions, this solution is described by

$$g(r) = r^2 - \frac{r_h^d}{r^{d-2}} , \quad \chi(r) = 0 . \quad (3.64)$$

In the same limit, the Maxwell equation and scalar equation, (3.24) and (3.25), remain unchanged and scale like  $1/q$ . In this sense, matter fields can be treated as  $1/q$  perturbation of the Schwarzschild black hole. It is also important to observe that once the probe limit has been taken,  $q$  does not appear in the equations of motion. Formally this is the same as considering  $q = 1$  in the Schwarzschild black hole background. However, the critical temperature  $\mathcal{T}_{probe}$  obtained by studying the superconducting solution in the probe limit has to be compared with the limit  $\mathcal{T}/\sqrt{q}$  as  $q \rightarrow \infty$  in the backreacting case. We can check this statement by looking at Figure (3.1) where it is evident that the  $\mathcal{T}/\sqrt{q}$  approaches a limiting value as  $q \rightarrow \infty$ .

The probe limit in models of the class B is more complicated. We prefer to skip the formal analysis of this more general situation and we define their ‘‘probe’’ limit with the matter Lagrangian,

$$\mathcal{L}_{matter} = -\frac{1}{4}G(\eta) F^{\mu\nu} F_{\mu\nu} + \frac{d(d-1)}{L^2}U(\eta) - \frac{1}{2}(\partial\eta)^2 - \frac{1}{2}J(\eta) (\partial_\mu\theta - A_\mu)^2 . \quad (3.65)$$

As we will see in the next section, there are cases in which backreaction is not really important and the probe limit (3.65) essentially describes the same physics. Then, the numerical problem is relatively easier to treat.

Summarizing, the probe limit reduces the full numerical problem to the study of (3.24) and (3.25) where  $\chi = 0$  and  $g(r)$  is given by (3.64), namely

$$\Phi'' + \Phi' \left( \frac{2}{r} + \frac{\partial_\eta G \eta'}{G} \right) - \frac{J(\eta)}{gG(\eta)} \Phi = 0 , \quad (3.66)$$

$$\eta'' + \eta' \left( \frac{2}{r} + \frac{g'}{g} \right) + \frac{1}{2g} \partial_\eta G \Phi'(r)^2 + \frac{6}{g} \partial_\eta U + \frac{1}{2g^2} \partial_\eta J \Phi^2 = 0 . \quad (3.67)$$

The procedure to integrate these equations closely follows the one described in section 3.2.2. We fix the value of the horizon and we obtain a one parameter family of solution  $\eta(r)$ ,  $\Phi(r)$ , by imposing the boundary constraint  $O^{(1)} = 0$  or  $O^{(2)} = 0$ . Then, we can parametrize the superconducting solution with the dimensionless temperature  $T/\sqrt{\rho}$  where  $T = 3/4\pi$ .

### 3.6 Holographic Phase Transitions

In the previous sections we prepared the numerical machinery required to build a full backreacting holographic superconductor. We have also provided evidence that holographic superconductors do exist and, as a result of the linearized analysis, we have calculated the critical temperature  $\mathcal{T}$ . This is an important point because a priori we do not know how the phase space of solutions will look like. In principle there could exist more than one family of holographic superconductors which are not continuously connected to the one whose condensate becomes small as the temperature  $\mathcal{T}$  is approached. Therefore, the knowledge of  $\mathcal{T}$  is a good starting point for the numerical procedure.

In this section we show our numerical results obtained for several phenomenological models. It is convenient to consider a reference model and the HHH model is the candidate. More general couplings  $G(\eta)$ ,  $J(\eta)$  and  $U(\eta)$  can be thought of as deformations of the HHH model and as we will see, couplings belonging to the class B will determine a rich and interesting phase diagram.

It is important to keep in mind what are the physical observables that characterize the superconducting phase and eventually the transition from the uncondensed to the superconducting phase. The latter is not only specified by the behavior of the condensate as a function of the temperature but in order to claim that a phase transition takes place, we have to check that the difference of free energy between the uncondensed and the superconducting phase, favors the superconductor. This is not completely automatic and in fact phase transitions are usually distinguished in first order, second order or higher order. Strictly speaking, the presence of a condensate is not a sufficient condition for superconductivity to actually exist.

**Computation of the Free Energy from Holography.** Since our analysis strongly depends on the knowledge of the free energy, we now show how to calculate this quantity from the bulk. In the presence of a finite charge density or a finite chemical potential, the grand-canonical potential is defined to be

$$\Omega \equiv F - \mu_{ft}\rho_{ft} = -T \log Z . \tag{3.68}$$

where  $F$  is the free energy,  $\mu_{ft}$  and  $\rho_{ft}$  are the chemical potential and the charge density of the field theory,  $Z$  is the thermal partition function of the system. In a quantum field theory, the thermal partition function  $Z$  is defined by a path integral in the euclidean time,

$$Z = \int \mathcal{D}\psi e^{-S_E[\psi, A]} \quad (3.69)$$

where the action  $S_E$  is the effective action that describes the system. In the Landau-Ginzburg theory, for example, we consider the effective action of a complex scalar field and we introduce a chemical potential  $\mu$ , by gauging the  $U(1)$  global symmetry and coupling the system to a non-dynamical gauge field  $A$ . The result is formally written in (3.69).

The AdS/CFT prescription allows to compute  $Z$  in terms of the the gravitational action evaluated on the solution. The grand canonical potential which corresponds to the uncondensed phase is calculated analytically from the Reissner-Nördstrom black hole. The grand canonical potential corresponding to the superconducting phase will be instead obtained from our numerical solutions. In section 2.5.1 we discussed some general properties of  $Z$ . Here, we adapt those arguments to the specific case of the holographic superconductors. As we will see, the procedure to obtain  $Z$  requires an *holographic renormalization* [9, 73].

First of all, we show that the Euclidean action is a total derivative. Indeed, Einstein's equations imply that,

$$G_{\mu\nu} \equiv R_{\mu\nu} - \frac{1}{2}\mathcal{R} g_{\mu\nu} = \frac{1}{2}r^2(\mathcal{L} - \mathcal{R}) \quad (3.70)$$

where  $R_{\mu\nu}$  is the Ricci tensor. Since  $G_{\mu\nu}g^{\mu\nu} = -\mathcal{R}$  we finally obtain

$$\mathcal{L} = -G^t_t - G^r_r = \frac{1}{r^2} [ (rg)' + (rge^{-\chi})'e^\chi ] , \quad (3.71)$$

$$S_E = \frac{1}{2\kappa_4^2} \int d^3x \int_{r_h}^{r_\infty} dr [ 2rg(r)e^{-\chi/2} ]' = \frac{1}{2\kappa_4^2} \int d^3x 2rge^{-\chi/2} \Big|_{r \rightarrow \infty} \quad (3.72)$$

Plugging the asymptotic expansion (3.39) into (3.72) we find a divergent quantity:

$$\left( 2rg(r)e^{-\chi(r)/2} \right) \Big|_{r \rightarrow \infty} = 2r^3 + O^{(1)}O^{(1)} r - 2M + \frac{8}{3}O^{(1)}O^{(2)} . \quad (3.73)$$

In the above formula, the divergent terms are classified according to powers of  $r$ . The  $r^3$  term originates from the integration over the  $AdS$  space and

it is regulated by the Gibbons-Hawking term plus a boundary cosmological constant,

$$S_{GH} = \frac{1}{2\kappa_4^2} \int d^3x \sqrt{-g_B} \left( 2K + \frac{4}{L} \right) . \quad (3.74)$$

The metric  $g_B$  is the induced metric at the boundary and  $K$  is the trace of the extrinsic curvature defined by

$$K^{\mu\nu} = -\frac{1}{2} (\nabla^\mu n^\nu + \nabla^\nu n^\mu) , \quad (3.75)$$

with  $n^\mu$  outward pointing unit vector, normal to the boundary.

The term which is linearly divergent in  $r$  comes from the integration over the radial profile of the scalar fields. It is removed by considering a boundary action for the scalar. This is not uniquely specified unless the quantization scheme has been fixed. Indeed, we can have boundary terms built out of  $\eta$  and  $n^\mu \partial_\mu \eta$  or a linear combination of them. It turns out that the counterterm in the standard quantization scheme, where  $O^{(1)}$  is held fixed, it is given by

$$S_2 = \frac{1}{2\kappa_4^2} \int d^3x \sqrt{-g_B} 2 z_2^2 / L , \quad (3.76)$$

whereas the counterterm in the alternative quantization scheme, where  $O^{(2)}$  is held fixed, it is given by

$$S_1 = -\frac{1}{2\kappa_4^2} \int d^3x \sqrt{-g_B} ( 4 z_1 n^\mu \partial_\mu z_1 + 2 z_1^2 / L ) . \quad (3.77)$$

Then, the renormalized euclidean action is finite and it is given by,

$$\mathcal{S}_{ren} = S_E + S_{GH} + S_i . \quad (3.78)$$

with  $i = 1, 2$  depending of the quantization scheme. Taking into account both choices, the final result is,

$$\mathcal{S}_{ren} = \frac{1}{\kappa_4^2} \int d^3x \left( -\frac{M}{2} + \gamma O^{(1)} O^{(2)} \right) , \quad (3.79)$$

where  $\gamma = 2/3$  in the first case and  $\gamma = -4/3$  in the second case. In our superconducting solutions, regardless of the quantization scheme, the product  $O^{(1)} O^{(2)} = 0$  and  $\Omega$  turns out to be proportional to the mass of the black hole. Formally, this is the same result we obtain by considering just the uncondensed phase with  $\eta$  set to zero from the beginning. Therefore, we conclude

that the superconducting solution is thermodynamically favored if the uncondensed black hole releases part of its energy by turning on the charged scalar. More precisely, the thermodynamical quantity we need to compute from our numerical data is

$$F = (\Omega + \mu\rho_{ft}) = -\frac{M}{2\kappa_4^2} + \mu_{ft}\rho_{ft} , \quad (3.80)$$

$$\Delta(F) = F_{supercond.} - F_{normalphase} . \quad (3.81)$$

$\Delta(F) < 0$  implies that the superconducting phase dominates the thermodynamics. In the above formula the chemical potential of the field theory is given by the coefficient  $\mu$  of the asymptotic expansion of the field  $\Phi(r)$ , i.e  $\mu_{ft} = \mu$ . Instead, the charge density  $\rho_{ft}$  is defined by

$$\rho_{ft} = \frac{\delta W[A]}{\delta A_t} , \quad e^{W[A]} = \int \mathcal{D}\psi e^{-S_E[\psi, A]} . \quad (3.82)$$

In the holographic calculation the relevant part of the action is the Maxwell action and  $A_t$  is the source according to the AdS/CFT dictionary, i.e. the chemical potential  $\mu$ . Then, by evaluating the Maxwell equation it turns out that the exact value of  $\rho_{ft}$ , in terms the asymptotic value  $\rho$ , depends on the space-time dimensions:  $\rho_{ft} = (d/2 - 1)\rho/\kappa_{d+1}^2$ . We can check this statement by considering the canonical ensemble and the following identity,

$$F = \Omega + \mu\rho_{ft} = \mathcal{E} - sT . \quad (3.83)$$

The temperature is the Hawking temperature, the entropy is defined as  $s = A/(4G_4)$  where  $A$  is the area of the horizon and the energy  $\mathcal{E}$  is the ADM energy [74]. Then, the calculation of these two quantities is independent from that of  $\Omega$  and verifying the identity (3.83) it is actually a good numerical check.

### 3.6.1 Numerical Results

In this section we study the full set of equations (3.22)-(3.25) and we construct numerical holographic superconductors. Our first example considers the following phenomenological couplings,

$$G(\eta) = \frac{1}{1 + \kappa\eta^2} , \quad U(\eta) = 1 + \frac{\eta^2}{6} , \quad J(\eta) = q^2\eta^2 . \quad (3.84)$$

In Figure 3.2 we show a plot of the condensate  $O^{(2)}$  as function of the temperature for  $qL = 3$  and  $\kappa = 0.5, 3, 5, 9$ . For  $\kappa = 0$  we recover the HHH

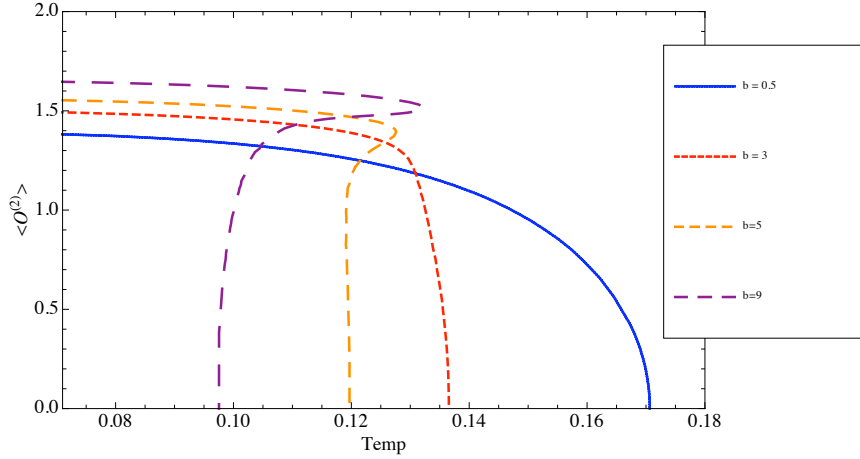


Figure 3.2: Condensate as function of the temperature for the models with  $G(\eta) = (1 + \kappa\eta^2)^{-1}$  for  $\kappa = 0.5, 3, 5, 9$  at  $\rho = 1$ . On the left hand side of the Figure and from bottom to top, the  $\kappa = 0.5$  is the case described by the undermost curve at  $T = 0$ . Adapted from [10].

model. In this case, the critical temperature is  $\mathcal{T} \approx 0.18$  (see for example Fig. 3.1) and the curve behaves identically to the curve obtained for  $\kappa = 0.5$ . The only qualitative difference between the case  $\kappa = 0$  and  $\kappa = 0.5$  is the value of the critical temperature. By looking at other values of  $\kappa$ , it is clear that  $\mathcal{T}$  decreases as long as  $\kappa$  increases. Quite interestingly, above some critical value  $b_{cr} \sim 3$  more than one superconducting solutions appears and the condensate has two branches: a lower branch that emerges at the temperature  $\mathcal{T}$  and an upper branch whose condensate is approximately constant all the way down to zero temperature. In order to understand how to interpret these two branches we look at the free energy plotted in Figure 3.3.

The relevant cases are  $\kappa = 5$  and  $\kappa = 9$  and the Figure 3.3 shows a plot of  $\Delta(F)$ . The superconducting solution is thermodynamically preferred only if  $\Delta(F) < 0$ . This condition defines the critical temperature  $T_c$  for the phase transition: for  $T > T_c$  the system is found in the uncondensed phase whereas for  $T < T_c$  the system enters the superconducting phase. Now it is clear that  $\mathcal{T}$  can be different from  $T_c$  and that both temperatures coincide only if the phase transition is second order. In this case, the condensate goes to zero at  $T_c$ . On the other hand, for  $\kappa = 5$  and  $\kappa = 9$  the phase transition is first order and the condensate jumps discontinuously. The free energy is continuous but

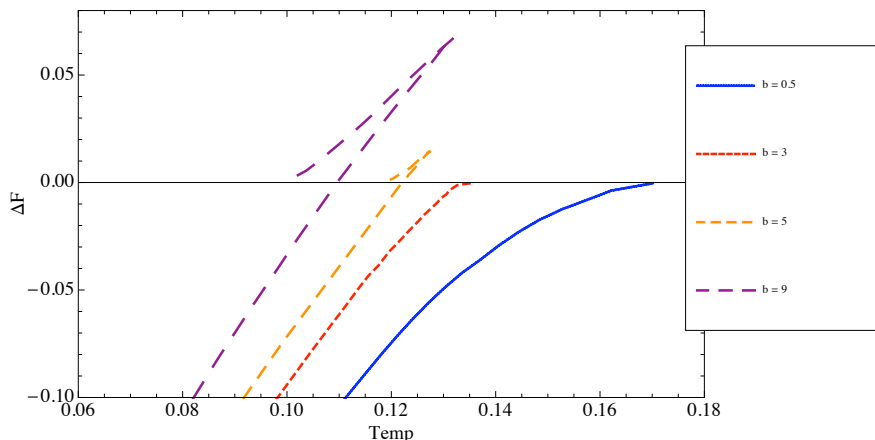


Figure 3.3: Normalized free energy for the models with  $G(\eta) = (1 + \kappa\eta^2)^{-1}$  for  $\kappa = 0.5, 3, 5, 9$ . From right to left, the  $\kappa = 0.5$  is the case described by the rightmost curve. Adapted from [10].

not differentiable.

For small values of  $\kappa$  the phase transition is second order and we can study the critical exponents that characterize the process. One of such critical exponents is defined by  $O^{(2)} \sim (T_c - T)^\alpha$ . We find that  $\alpha = 1/2$  for all  $b \leq b_{cr}$ . This is the mean field value that also characterizes the phase transition in the Landau-Ginzburg theory. It may be naively surprising that our strongly coupled theory shows a mean field behavior. We understand this result as a consequence of the large  $N$  limit. Non-mean field behavior is expected to be controlled by  $1/N$  corrections and cannot be captured in the supergravity approximation.

Our second example considers the following phenomenological couplings,

$$G(\eta) = \frac{1}{(1 + g_0\eta^a)}, \quad U(\eta) = 1 + \frac{\eta^2}{6}, \quad J(\eta) = q^2\eta^2. \quad (3.85)$$

with  $\eta > 0$  and  $a = 3.75, 3.5, 3.25$ . We are introducing by hand non integer powers of  $\eta$  and we would like to see how the mean field behavior is modified. We do not expect such couplings to arise from string/M-theory compactification. Nevertheless, our approach is purely phenomenological and it is justified as long as we can describe interesting physical properties.

In Figure 3.4 we show a plot of the condensate  $O^{(2)}$  for the different models.

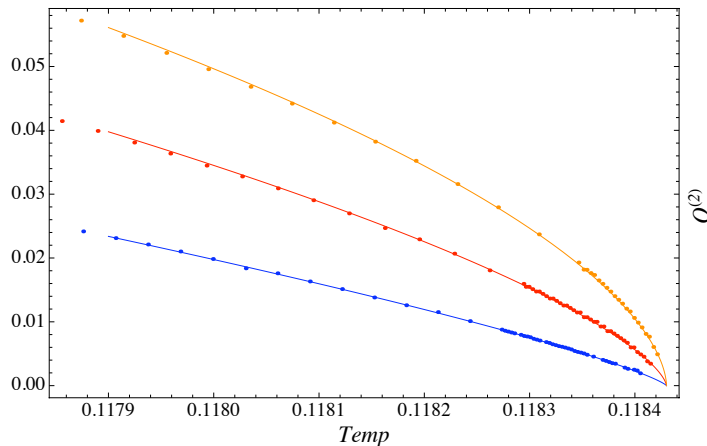


Figure 3.4:  $\langle O^{(2)} \rangle$  as function of the temperature for the models with  $G(\eta) = (1 + g_0 \eta^a)^{-1}$  for  $a = 3.75$  (orange), 3.5 (red), 3.25 (blue). Behavior of the condensate in the vicinity of the critical temperature. Adapted from [10].

The most salient feature is the following. Even if the critical temperature does not depend on  $a$  the critical exponent  $\alpha$  does. In particular, our numerical data are well approximated by the law,

$$\alpha \cong (a - 2)^{-1}. \quad (3.86)$$

In Figure 3.5 we use a log-log plot to zoom in a small region around  $T_c - T$  and we explicitly check that  $\alpha$  reproduces the law (3.86). We have also studied the case  $a = 3$  which gives  $\alpha = 1$ .

Our third example consider couplings of the form

$$G(\eta) = 1, \quad U(\eta) = 1 + \frac{\eta^2}{6}, \quad J(\eta) = q^2 \eta^2 + j_0 \eta^c \quad (3.87)$$

with  $\eta > 0$  and non integer powers  $c$ . In all these cases we recover the same features that are present for the models in the class (3.85). We are able to generalize the law (3.86) to include the case  $j_0 \neq 0$  [75]. This is found to be,

$$\alpha \cong (\min\{a, c\} - 2)^{-1}. \quad (3.88)$$

The main results we have obtained in this section are:

- The critical temperature is controlled by the parameters  $m$ ,  $q$  and  $\kappa$ . In particular it is independent from the higher order terms proportional to

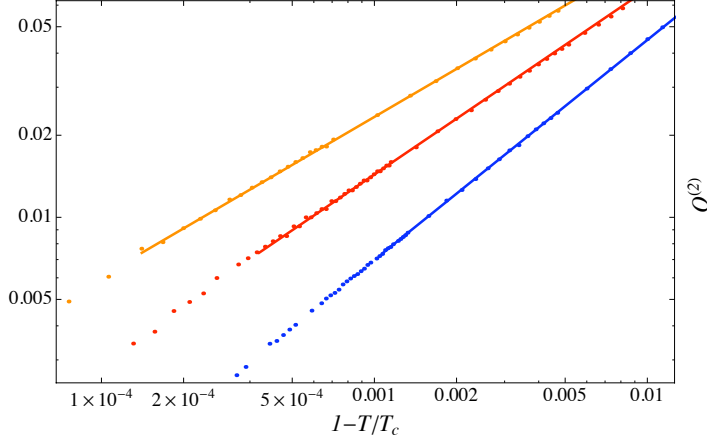


Figure 3.5:  $\langle O^{(2)} \rangle$  vs  $(1 - T/T_c)$  for the models with  $G(\eta) = (1 + g_0\eta^a)$  for  $a = 3.75$  (orange), 3.5 (red), 3.25 (blue). The slopes of the curve identify the different critical exponents. Adapted from [10].

$g_0$  and  $j_0$ . Given a model which exhibits a second order phase transition, we are able to engineer a first order phase transition by tuning the value of  $\kappa$  in the coupling  $G(\eta)$ .

- The critical exponent  $\alpha$ , defined as  $O \sim (T_c - T)^\alpha$ , is controlled by the exponent  $a$  and  $c$  through the relation (3.88).

The Widow scaling theory can be defined from the free energy (3.4) by adding appropriate deformations [66]. Since critical exponents are found to depend on the type of field theory deformations, our holographic models are very much in the same spirit as the Widow scaling theory. For this reason, we would like to have a better analytical control of the problem and see how far we can put forward the analogy with the Landau-Ginzburg theory. A general problem of interest is to determine whether real materials can be approximated by general holographic models to some extent. If so, the results in this chapter can be used to determine the best holographic fit, within our class of models, for a given material.

### 3.6.2 Analytical Results for the Condensate

Critical exponents are obtained by considering the behavior of the system in the vicinity of the critical temperature where backreaction is weak. Thus, the

probe limit is a convenient approximation. In particular our results are valid also for a generic backreacting solution as far as we are closed to the critical temperature.

A useful approach for studying the equations of motion (3.66) and (3.67) is to use a series expansion of  $\eta$  and  $\Phi$  near the horizon [11]. By using the scaling symmetry we set  $r_h = 1$ . In terms of the variable  $z = 1/r$  the expansion reads,

$$\begin{aligned}\eta^{(K)}(z) &= \eta_h + \eta_1(1-z) + \eta_2(1-z)^2 + \dots + \eta_N(1-z)^K, \\ \Phi^{(K)}(z) &= \Phi_1(1-z) + \Phi_2(1-z)^2 + \dots + \Phi_N(1-z)^K,\end{aligned}\quad (3.89)$$

We work with a finite number of terms and therefore the series is truncated at some order  $K$ .

The coefficients  $\eta_j$  and  $\Phi_j$  can be solved in terms of  $\eta_h$  and  $\Phi_1$  using the equations of motion for every  $j > 1$ . The series (3.89) converges to the solutions  $\eta(z)$  and  $\Phi(z)$  as  $K \rightarrow \infty$ . Then, we match these expansions with the asymptotic behavior at the boundary, (3.40) and (3.41). We find,

$$\left\{ \begin{array}{l} \eta^{(K)}(0) = \eta_\infty(0) \\ \partial_z \eta^{(K)}(0) = \partial_z \eta_\infty(0) \end{array} \right. \quad \left\{ \begin{array}{l} \Phi^{(N)}(0) = \Phi_\infty(0) \\ \partial_z \Phi^{(N)}(0) = \partial_z \Phi_\infty(0) \end{array} \right. \quad (3.90)$$

We consider models in the class B parametrized by:  $\kappa, q, g_0, u_0, j_0, a, b$  and  $c$ . As we will see, these models capture all the terms that are important when the system is close to the phase transition. For concreteness, we focus on the  $\langle O^{(2)} \rangle = 0$  scheme. There are five parameters  $\eta_h, \Phi_1$  (from the horizon side) and  $\eta^{(1)}, \mu, \rho$  (from the boundary side). These conditions can be solved for four parameters in terms of either  $\rho$  or  $\mu$ .<sup>2</sup> Furthermore, close to the critical temperature,  $O^{(1)} = \eta^{(1)}$  is linear in  $\eta_h$ .

Expressing  $r_h$  in terms of  $T$  by using  $r_h = 4\pi T/3$ , we find the following generic structure,

$$1 - \frac{T}{T_c^{(K)}(\kappa, q^2)} = A_K(\kappa, q^2) \langle O^{(1)} \rangle^2 + g_0 B_K(a) \langle O^{(1)} \rangle^{a-2} + u_0 C_K(b) \langle O^{(1)} \rangle^{b-2} + j_0 D_K(c) \langle O^{(1)} \rangle^{c-2} + \dots \quad (3.91)$$

where “...” denotes terms that are of higher order in  $\eta_h$ . Here,  $T_c^{(K)}$  is the critical temperature obtained by truncating the series at order  $K$ . As  $K \rightarrow \infty$

---

<sup>2</sup>Another possibility is to implement the matching at some intermediate point  $z_m$ , with  $0 < z_m < 1$ , as done in [76]. While having variable  $z_m$  allows one to obtain better solutions at fixed order  $K$  in the expansion, it introduces complicated algebraic equations that prevent the application of this method at large  $K$ .

we should recover the numerical critical temperature  $T_c$ . The key point is that the structure of (3.91) remains the same at each successive order in  $K$ . The different functions (including  $T_c^{(K)}$ ) get corrections, but the general form of the equation already reveals interesting information about the phase transition. In particular, it gives the explicit functional dependence of the order parameter on the temperature and it gives the explicit analytic expression for the critical exponent  $\alpha$ . For  $a, b, c \geq 4$ , the leading term in (3.91) is  $\eta^2$ . In this case we find

$$\langle O^{(1)} \rangle \cong \text{const.} \left( 1 - \frac{T}{T_c} \right)^{\frac{1}{2}}, \quad \text{for } T \cong T_c, \quad (3.92)$$

as in mean field theory. When either  $a, b$  or  $c$  is less than 4, then the leading term is  $\eta^{a_0-2}$ , where  $a_0 \equiv \min\{a, b, c\}$ . In this case, we find

$$\langle O^{(1)} \rangle \cong \text{const.} \left( 1 - \frac{T}{T_c} \right)^\alpha, \quad \alpha = \frac{1}{a_0 - 2}, \quad a_0 = \min\{a, b, c\}. \quad (3.93)$$

Because of the presence of the term  $A_K(\kappa, q^2)\langle O^{(1)} \rangle^2$ , generically one has the bound  $\alpha \geq 1/2$ . This value is in perfect agreement with the numeric results. Remarkably, the correct value of exponents can be determined from the expansion at lowest order, in contrast to quantities such as the critical temperature which needs a numerical analysis.

In principle, it is possible that  $A_{K \rightarrow \infty}(\kappa, q^2)$  vanishes for some real value of  $\kappa/q^2$ . However, numerical study suggests that before this occurs the transition changes into a first order phase transition. Finally, let us mention that an equation with the same structure as (3.91) is obtained in the  $\eta^{(1)} = 0$  scheme where  $\langle O^{(2)} \rangle$  takes an expectation value, so the same considerations apply in this case.

We also note that the critical temperature  $T_c$  appearing in (3.91) depends only on  $\kappa$  and  $q$ , i.e. on the quadratic terms in the expansion of  $G(\eta)$ ,  $U(\eta)$  and  $J(\eta)$ . By introducing a general mass  $m^2$  parameter in  $U$ ,  $T_c$  is more generally a function of  $\kappa$ ,  $m$ , and  $q$ . This observation agrees with our statement regarding the linearized analysis.

### 3.6.3 Analytical results for the Free Energy

Let us now turn to the study of the free energy for our general models (3.65). As standard, the free energy is given by the gravity on-shell action. This quantity is divergent, and thus needs to be regularized before further physical interpretation. Regularizing the action with a radial cut-off  $r_B$ , it is not difficult to show that the structure of such action is

$$S^{(1,\mu)} = \frac{\mu \rho}{2} + \frac{r_B (\eta^{(1)})^2}{2L} + \dots, \quad (3.94)$$

where the dots stand for finite terms irrelevant at this stage. In addition, we keep the superscripts to remind that we will focus on the case with fixed chemical potential and the  $\langle O_2 \rangle = 0$  scheme. Since this action is divergent, we need the appropriate counterterms to renormalize it. In the probe limit this is,

$$\Delta S_B = -\frac{1}{2} \int_B [\sqrt{g_B} \eta^2] \quad (3.95)$$

being  $g_B$  the induced metric on the boundary  $B$ . Then, the free energy for the general models (3.65) takes the form

$$F = -\frac{\mu \rho}{2} - \frac{O^{(1)} O^{(2)}}{2} + \frac{r_H^3}{2} \int dz \left[ \frac{\eta}{2} \partial_\eta G(\eta) (\partial_z \Phi)^2 + \right. \quad (3.96) \\ \left. + \eta \partial_\eta J \frac{\Phi^2}{2z^2(1-z^3)} + \frac{1}{z^4} (\eta \partial_\eta U(\eta) - 2U(\eta)) \right],$$

Near the critical point, where  $\eta$  is small, we can use the expansion for the models of the class B and write

$$F = -\frac{\mu \rho}{2} - \frac{O^{(1)} O^{(2)}}{2} + \frac{r_H^3}{2} \int dz \left[ \frac{a g_0}{2} z^a \chi^a (\partial_z \Phi)^2 + \right. \quad (3.97) \\ \left. + \left( q^2 \chi^2 + \frac{m j_0}{2} z^{m-2} \chi^m \right) \frac{\Phi^2}{(1-z^3)} + \frac{u_0 (b-2)}{z^{4-b}} \chi^b \right]$$

where we have introduced  $\chi = z^{-1} \eta$  and dropped the superscript. We have also set  $\kappa = 0$  to maintain the same critical temperature.

In order to further proceed, we can use the series solution to the equations of motion as in (3.89). Inserting the resulting expressions in (3.97) we obtain

$$F^{(K)} - F_0^{(K)}(\kappa, q^2) = \mathcal{A}_{(K)}(\kappa, q^2) \langle O^{(1)} \rangle^2 + g_0 \mathcal{B}_{(K)}(a) \langle O^{(1)} \rangle^a \quad (3.98) \\ + u_0 \mathcal{C}_{(K)}(c) \langle O^{(1)} \rangle^b + j_0 \mathcal{D}_{(K)}(b) \langle O^{(1)} \rangle^c + \dots$$

This equation generically depends on the temperature  $T$  whereas  $\mathcal{B}_{(K)}$ ,  $\mathcal{C}_{(K)}$ ,  $\mathcal{D}_{(K)}$  also depend on  $(\kappa, q^2)$ . The “...” denotes terms with higher powers of  $\eta_h$ . The general structure of (3.97) is independent of  $K$  and we have also verified that the expansion in (3.99) approximates the exact (numerical) free energy close to the phase transition.

The critical temperature at order  $K$  corresponds to the value at which  $\mathcal{A}_{(K)}$  changes its sign

$$\mathcal{A}_{(K)} \sim (T - T_c^{(K)}(\kappa, q^2)) + \dots \quad (3.99)$$

As discussed previously, the holographic free energy functional (3.97) can be thought of as a sort of generalized version of the Landau-Ginzburg free energy. For integer values of the exponents  $a$ ,  $b$  and  $c$ , we can think that the extra couplings in  $G(\eta)$ ,  $U(\eta)$  and  $J(\eta)$  correspond to the effect of higher dimensional operators in the bulk effective field theory.

### 3.6.4 Rushbrooke Identity

The free energy (3.97) contains all the relevant information about the system close to the phase transition [11]. By minimizing it with respect of  $O^{(1)}$  we can obtain the physical VEV of the condensate as a function of the temperature. In particular, we can consistently check that the critical exponent  $\alpha$  obtained in this way coincides with the one we got numerically. Substituting such value into the free energy (3.99), we can determine the behavior of the specific heat close to the critical temperature. We obtain

$$\Delta c_v = -T \frac{d^2 F}{dT^2} \equiv \text{const.} (T_c - T)^{-\beta}, \quad \beta = -\frac{4 - a_0}{a_0 - 2}. \quad (3.100)$$

where  $a_0 = \text{Min}\{a, b, c\}$  appeared earlier in (3.93). Note in particular that we automatically get  $\beta + 2\alpha = 1$ . In [77], it was shown that holographic superconductors have a universal value  $\gamma = 1$  for the critical exponent associated with the thermodynamic susceptibility,  $\chi_T \propto (T_c - T)^{-\gamma}$ . The same analysis leads to  $\gamma = 1$  also in the present more general models. Putting these values together, we find that the critical exponents in the models of the class B verify the Rushbrooke identity:

$$\beta + 2\alpha + \gamma = 2. \quad (3.101)$$

Since  $2 < a_0 \leq 4$ , we find that  $\alpha \geq 1/2$  and  $\beta \leq 0$ . For  $\beta < 0$  (or  $2 < a_0 < 4$ ) the specific heat is continuous across the transition. This means that the transition is at least of third order (using the Ehrenfest convention that the order of the phase transition is the lowest one at which the derivative of the free energy is discontinuous). More generally, the phase transition is of order  $n$  for

$$n - 1 \geq 2\alpha > n - 2. \quad (3.102)$$

In other words, for these models the order of the phase transition is given by

$$n = \lceil 2\alpha + 1 \rceil = \lceil \frac{a_0}{a_0 - 2} \rceil, \quad (3.103)$$

where  $[x]$  denotes the smallest integer greater or equal than  $x$ . The transition will be of higher order than 3 if  $a_0 < 3$ . However, in this case,  $\beta > 1$  and the critical curve becomes concave near  $T_c$ . These cases are of some theoretical interest because there is a temperature  $T_1 < T_c$  where  $d^2\langle O_i \rangle/dT^2$  changes sign. The change in the sign of  $d^2\langle O_i \rangle/dT^2$  could be an indicator of another phase transition, though we will not further inquire on this point. It should be mentioned that *there are examples of real superconductors with third order phase transitions* (see e.g. [78]).

### 3.7 Conductivity

So far we have studied properties of our superconducting solutions in the vicinity of the second order phase transition. In particular, we have shown that critical exponents are controlled only by the lowest order terms in the small condensate expansion of the functions  $G(\eta)$ ,  $U(\eta)$  and  $J(\eta)$ . In this section we move on by analyzing dynamical properties of the holographic superconductors. Our purpose is to characterize the optical conductivity  $\sigma(\omega)$  in terms of the functions  $G(\eta)$ ,  $U(\eta)$  and  $J(\eta)$  and see how the holographic result differs from the standard results obtained in the weak coupling BCS theory. For this reason, we first review some basic aspect of the transport phenomenon in superconducting phase.

It is well known that in ordinary and high-Tc superconductors, the resistivity vanishes identically when the system enters the superconducting phase. Theoretically this statement can be inferred from the behavior of the optical conductivity as the frequency goes to zero. Indeed, by using the Kramers-Kronig relation,

$$\text{Im}[\sigma(\omega)] = -\frac{1}{\pi}P \int_{-\infty}^{\infty} \frac{\text{Re}[\sigma(\omega')]d\omega'}{\omega' - \omega} \quad (3.104)$$

we can see that the real part of the conductivity contains a delta function,  $\text{Re}[\sigma(\omega)] = \pi\delta(\omega)$ , if and only if the imaginary part has a pole  $\text{Im}[\sigma(\omega)] = 1/\omega$ . In the BCS theory, this calculation shows that

$$\sigma(\omega) = \pi \frac{n_s 2e^2}{m_e} \delta(\omega) \quad \text{as} \quad \omega \rightarrow 0, \quad (3.105)$$

where  $n_s$  is the density of electrons that are bounded into a Cooper pair state. Physically, the vanishing of the resistivity is a consequence of a gap in the spectrum of the superconductor: the Cooper pairs superconduct because at low energies there are no dissipative states accessible [20]. This gap can be seen from the real part of the optical conductivity which is suppressed in a certain

range of frequencies  $0 < \omega < \omega_g$ . Then,  $\omega_g$  is understood as the energy required to break apart the Cooper pair and by general reasoning it is expected to be some integer multiple of the energy of its constitutive electrons. In the weak coupling limit this is given by  $\omega_g = 2\Delta$ . We expect our holographic solutions to describe strongly coupled physics and throughout this section we will make reference to the BCS picture in order to highlight the main differences.

Let us first briefly recall how to calculate the conductivity in the holographic setting. The relation between an induced electric current  $\vec{J}$  in a given material and the presence of an external electric field  $\vec{E}$  is,

$$J_a = \sigma_{ab} E_b \quad (3.106)$$

This is a linear response analysis which defines the conductivity matrix  $\sigma_{ab}$  and involves as external source the electric field  $\vec{E}$ . In the language of the AdS/CFT correspondence, the  $U(1)$  current is dual to the bulk gauge field and the prescription to compute  $\sigma_{ab}$  is the following. We study a gauge boson perturbation of the superconducting background with fixed source term at the boundary and we read from the bulk solution the asymptotic value of  $\vec{J}$ . From its very definition we calculate  $\sigma_{ab}$ <sup>3</sup>. In the probe limit we just need to consider the Maxwell equations whereas in the backreacting case, the gauge boson perturbation couples to a perturbation of the metric. Since the probe limit is a particular case, we will first proceed by discussing the general backreacting case. We consider  $d = 3$  and we will briefly comment on the AdS<sub>5</sub> case.

The ansatz (3.19) is isotropic in the spacial directions and therefore we expect  $\sigma_{ab}$  to be proportional to identity. Following [69, 9], we consider time-dependent perturbations of the form  $A_x = a_x(r) e^{-i\omega t}$  and  $g_{tx} = f(r) e^{-i\omega t}$ . These fluctuations satisfy the equations

$$a_x'' + \left( \frac{g'}{g} - \frac{\chi'}{2} + \frac{\partial_\eta G \eta'}{G} \right) a_x' + \left( \frac{\omega^2}{g^2} e^\chi - \frac{J}{gG} \right) a_x = \frac{\Phi'}{g} e^\chi \left( -f' + \frac{2}{r} f \right),$$

$$f' - \frac{2}{r} f + G \phi' a_x = 0.$$

Substituting the second equation into the first one, we find

$$a_x'' + \left( \frac{g'}{g} - \frac{\chi'}{2} + \frac{\partial_\eta G \eta'}{G} \right) a_x' + \left( \frac{\omega^2}{g^2} e^\chi - \frac{G\Phi'^2}{g} e^\chi - \frac{J}{gG} \right) a_x = 0. \quad (3.107)$$

---

<sup>3</sup>There is a technical assumption in the derivation of the Kramers-Kronig relation (3.104) and we actually need to check the following:  $\sigma(\omega)$  is analytic in the upper half-plane of complex  $\omega$  and vanishes as  $|\omega| \rightarrow \infty$ . In general,  $\sigma(\omega)$  is proportional to a retarded Green's function and therefore the analyticity condition is satisfied. It remains to be seen whether the boundary condition as  $|\omega| \rightarrow \infty$  can be fulfilled.

This is the equation governing the gauge boson perturbation in the backreacting case. The probe limit is easily deduced: we set  $\chi = 0$  from the beginning and we observe that the r.h.s of the equation (3.107) is absent. Then, we are left with the equation

$$a_x'' + \left( \frac{g'}{g} + \frac{\partial_\eta G \eta'}{G} \right) a_x' + \left( \frac{\omega^2}{g^2} - \frac{J}{gG} \right) a_x = 0 . \quad (3.108)$$

The black hole background has a finite temperature thus there will be two sources of singularities at the horizon due to the terms  $1/g^2$  and  $1/g$ . The solution describing gauge boson falling into the horizon at  $(r - r_h)$  has the form

$$a_x(r) \approx a_x^{(0)} (r - r_h)^{-i\beta\omega} \left( 1 + a_x^{(1)}(r - r_h) + \dots \right) . \quad (3.109)$$

The coefficient  $\beta$  is fixed in order to regularize the  $1/g^2$  divergence at the horizon. The term proportional to  $1/g$  instead is regularized by a choice of  $a_x^{(1)}$ . We remind the reader that the gauge boson equation, (3.107) or (3.108), is linear and therefore the coefficient  $a_x^{(0)}$  is arbitrary and can be fixed to one without loss of generality. Once we integrate the gauge boson equation from the horizon, the asymptotic behavior of the perturbations is found to be

$$a_x = A_x^{(0)} + \frac{A_x^{(1)}}{r} + \dots , \quad ( A = e^{-i\omega t} a_x(r) ) \quad (3.110)$$

The conductivity can then be obtained from the formula (3.106) and the relation  $E_i = -\partial_t A_i$ ,  $i = 1, 2$ ,

$$\sigma = \frac{J_x}{E_x} = -\frac{iA_x^{(1)}}{\omega A_x^{(0)}} , \quad (3.111)$$

where in the second equality we have used the AdS/CFT dictionary.

As a warm up exercise we can calculate the conductivity in the uncondensed phase  $\eta = 0$ . It turns out that in the probe limit, which corresponds to the  $AdS_4$  Schwarzschild black hole, the solution is analytic and reads [79],

$$a_x(r) = \exp \left[ -i \frac{\omega}{6r_h} \left( \log \frac{(r - r_h)^2}{r^2 + rr_h + r_h^2} + 2\sqrt{3} \arctan \frac{2r + r_h}{\sqrt{3}r_h} \right) \right] \quad (3.112)$$

expanding at large  $r$  yields the normal phase conductivity,

$$\sigma_{n.p.}(\omega) = 1 . \quad (3.113)$$

Quite remarkably, the conductivity in the Schwarzschild background is a constant independent of the frequency. At finite charge density, the uncondensed phase is represented by the Reissner-Nördstrom black hole. Then, the  $\omega$  dependence is restored and the solution needs a numerical analysis [80]. In particular,  $\text{Re}\sigma(\omega) \leq 1$  and it has a minimum at  $\omega = 0$ ,  $\text{Im}\sigma(\omega)$  has a pole at  $\omega = 0$  and by means of the Kramers-Kronig relation, we deduce that  $\sigma(\omega)$  has a delta function at  $\omega = 0$ . This result is naively surprising because it implies an infinite DC conductivity in the uncondensed phase. However, this infinite conductivity is not superconductivity but follows from translation invariance. This observation is important and help us to understand a property of the holographic superconductors: the vanishing of the resistivity must arise from the holographic dual of the London equation. We will see how this comes about in the next paragraphs.

As a last remark, we notice that regardless of the couplings  $G(\eta)$  and  $J(\eta)$ , the equation (3.108) in limit  $\omega \gg 1$  is dominated only by the  $\omega^2$  term. Thus we expect the limit  $\omega \gg 1$  to be a universal limit. We have checked this statement for the Reissner-Nördstrom black hole and we will see explicitly that our holographic superconductors reproduce the behavior  $\sigma(\omega) \rightarrow 1$  when  $\omega \gg 1$ . For convenience, we will work in the probe limit where the numerical effort is drastically reduced.

The study of the conductivity in our class of phenomenological holographic superconductors begins with a first example. We choose the model:

$$G = 1, \quad U = 1 + \frac{\eta^2}{6}, \quad J = \eta^2 + j_0\eta^4, \quad (3.114)$$

with  $j_0 \geq 0$ . This choice provides a one-parameter family of deformations with respect to the basic HHH model where  $J$  remains positive for all  $\eta$ . Figure 3.6 shows the conductivity for  $j_0 = 0.6$  in the  $\langle O_1 \rangle = 0$  scheme. The most salient feature of this plot is the presence of a “gap” at low temperature and the appearance of resonance peaks. These peaks increase in number and become narrower and higher as the temperature is gradually lowered. The lowest temperature curve in Figure 3.7 is at  $T = 0.24$ . Here the first peak in  $\text{Re} \sigma(\omega)$  cannot be seen numerically because it has become narrower than the numerical grid. However, its presence can be inferred from the  $1/(\omega - \omega')$  behavior of  $\text{Im} \sigma(\omega)$ , shown in Figure 3.7, through the Kramers-Kronig relation. In the limit  $j_0 \rightarrow 0$  the peaks disappear but the presence of the gap persists.

For temperatures  $T < T_c$ , i.e. when the system enters the superconducting phase, we expect to find an infinite DC conductivity. This properties is true

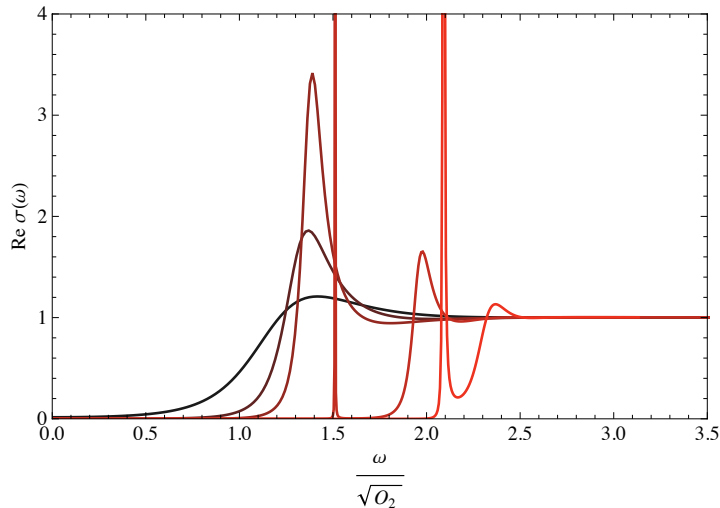


Figure 3.6: Real part of the conductivity as a function of frequency for  $J = \eta^2 + j_0\eta^4$  with  $j_0 = 0.6$  in the  $\langle O_1 \rangle = 0$  scheme. The curves correspond to different values of  $T/T_c$  equal to 0.24, 0.29, 0.50, 0.61, 0.81 (the curves with lower temperatures are those that go to zero more rapidly as  $\omega \rightarrow 0$ ). Adapted from [11]

in general regardless of the specific couplings  $J(\eta)$ ,  $G(\eta)$ . In particular, we can check from Figure 3.7 that  $\text{Re } \sigma(\omega) \sim \delta(\omega)$ . We would like to understand the origin of this infinite DC conductivity in terms of an holographic London equation. This is a tricky point and we now explain why [9]. It should be clear from the discussion about the uncondensed phase that translation invariance implies an infinite DC conductivity. This same observation holds for the superconducting black hole and we have to conclude that the infinite DC that appears in Figure 3.7 is in part due to the translational invariance. Thus, in order to distinguish between the normal and the superconducting phase we have to refine our analysis. The London equation

$$J_i(\omega, k) = -n_s A_i(\omega, k) \quad (3.115)$$

was proposed to explain both the infinite conductivity and the Meissner effect of superconductors. In the limit  $k = 0$  and  $\omega \rightarrow 0$ , we can take a time derivative of both sides of the London equation and find

$$J_i(\omega, 0) = \frac{in_s}{\omega} E_i(\omega, 0) . \quad (3.116)$$

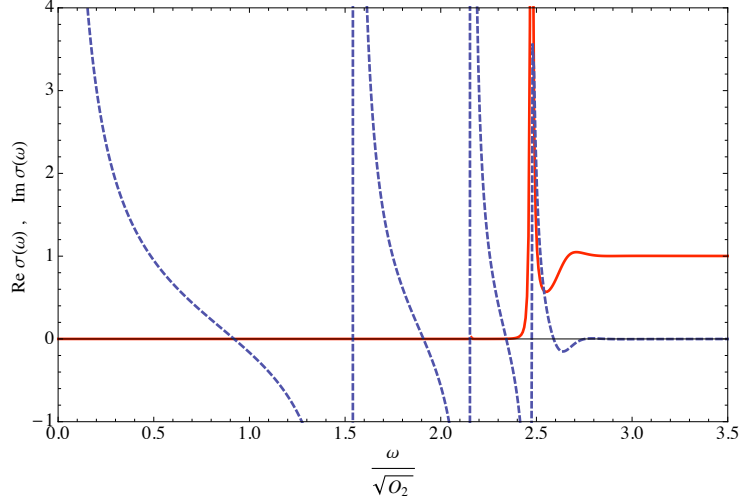


Figure 3.7: Real and imaginary part of the conductivity as a function of frequency for  $J = \eta^2 + j_0\eta^4$  with  $j_0 = 0.6$  in the  $\langle O_1 \rangle = 0$  scheme. The curve corresponds to the values of  $T/T_c$  equal to 0.24. Adapted from [11]

This relation explains the infinite DC conductivity. On the other hand, by considering the curl of the London equation and the limit  $\omega = 0$  and  $k \rightarrow 0$  we obtain,

$$i\epsilon_{ijk}k^j J^l(0, k) = -n_s B_i . \quad (3.117)$$

This relation together with the Maxwell's equation implies that magnetic lines are excluded from the superconductor. It is important that both the superconductivity and the Meissner effect follow from the London equation. In particular, a perfect conductor would also have an infinite DC conductivity but there would be no vortex excitations to indicate the existence of Cooper pairs. Indeed, the original physical principle behind this phenomenon is the symmetry breaking mechanism. With this reasoning in mind, we observe that (in the simplest case of  $G(\eta) = 1$  and  $J(\eta) = q^2\eta^2$ ) the differential equation for the gauge boson perturbation reads,

$$\left(\frac{w^2}{g} - \frac{k}{r^2}\right) a_x + (ga'_x)' = q^2\eta^2 a_x , \quad (3.118)$$

where  $'$  denotes differentiation with respect to  $r$ . Ignoring the radial dependence, this equation describes a vector field with mass proportional to  $q^2\eta^2$ . This mass, should give rise to the usual effects of superconductivity and the equation should be thought of as the holographic dual of the London equation.

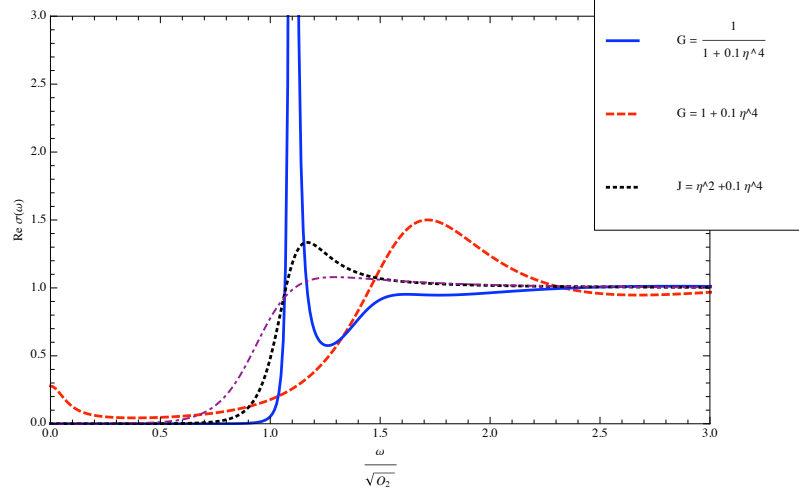


Figure 3.8: Conductivity as a function of frequency for HHH (dashed-dotted line) and for the different deformations of the model. These are given by the (3.114), (3.121) and (3.122). The quantization scheme is  $\langle O_1 \rangle = 0$  and the plot is taken at  $T = 0.415 T_c$ . Adapted from [11]

We point out that another indication in favor of the above interpretation comes from the numerical value of

$$\text{Im } \sigma(\omega) \approx \frac{A}{\omega}, \quad \text{at } \omega \approx 0 \quad (3.119)$$

In the uncondensed phase we know from [80] that

$$\text{Im } \sigma_{m.p.}(\omega) \approx \frac{4\rho^2}{3(4r_h^4 + \rho^2)} \frac{r_h}{\omega} + O(1) \quad (3.120)$$

but as we lower the temperature so that  $T \leq T_c$ , we expect to see a different value of the residue. This is what happens when we turn on the bulk scalar field and actually signals the onset of superconductivity.

Having understood general properties of the conductivity we now consider two different deformations of the basic HHH model:

$$G = 1 + g_0 \eta^4, \quad U = 1 + \frac{\eta^2}{6}, \quad J = \eta^2, \quad (3.121)$$

or

$$G = \frac{1}{1 + g_0 \eta^4}, \quad U = 1 + \frac{\eta^2}{6}, \quad J = \eta^2, \quad (3.122)$$

with  $g_0 \geq 0$ . These two models together with (3.114) belong to the same universality class, since they have the same critical temperature and the same critical exponents. Our purpose is to compare the conductivity in these models for a given temperature  $T < T_c$ . Indeed, a natural question is to what extent transport properties are sensitive to the choice of deformations. Figure 3.8 shows the result. There is a fourth curve in the Figure representing the HHH model. It is clear that the conductivity undergoes significant changes which strongly depend on the specific deformation. The model (3.122) exhibits sharp peaks while the models (3.114), (3.121) have a smoother behavior. It is interesting to observe that similar peaks have been found in real high-Tc superconductors in relation to Raman scattering measurements (see e.g. [81, 82]). In the real materials, they originate from phonons of energy  $\omega > \omega_g$  which acquire a finite lifetime due to collisions with electronic excitations (not suppressed above the gap). In the holographic context it is not clear what is the origin of the peaks and we can only say that they appear as consequence of a vector perturbation of the superconducting background. It would be interesting to further investigate this analogy. We leave this problem for the future.

### 3.7.1 The Schrödinger potential

In the previous section we explored several interesting features of the optical conductivity. In particular, the presence of an infinite DC conductivity and the presence of a gap  $\omega_g$ , seemed to be a universal feature of every holographic superconductors. As far as we can understand from the numerical data, it is possible to extrapolate that

$$\lim_{\omega \rightarrow 0} \text{Re}[\sigma(\omega)] \sim e^{\Delta_i/T} \quad (3.123)$$

where  $\Delta$  is proportional to  $\omega_g$ . The coefficient of proportionality is in general a rational number whose exact value can be found from the numerics. In this section, we reformulate the calculation of the conductivity in terms of a one dimensional Schrödinger problem. This approach will provide a simple and intuitive understanding of all the qualitative features of the conductivity that we have already described. Furthermore, it allows us to make a precise statements about the existence of a gap  $\omega_g$ . As we will see, there are cases in which the numerical extrapolation cannot be trusted and the relation (3.123) is not correct.

The equation for the gauge boson perturbation reads,

$$a_x'' + \left( \frac{g'}{g} - \frac{\chi'}{2} + \frac{\partial_\eta G \eta'}{G} \right) a_x' + \left( \frac{\omega^2}{g^2} e^\chi - \frac{G \Phi'^2}{g} e^\chi - \frac{J}{gG} \right) a_x = 0 . \quad (3.124)$$

We introduce the new variables,

$$dz = \frac{e^{\chi/2}}{g} dr , \quad \Psi = \sqrt{G} a_x . \quad (3.125)$$

At large  $r$ ,  $dz = dr/r^2$  and we can choose the integration constant so that  $z = -1/r$ . In this description the UV coincides with the limit  $z \rightarrow 0^-$ . Since  $g$  vanishes at least linearly at the horizon and  $\chi$  is monotonically decreasing,  $dz \sim dr/(r - r_h)$  at the horizon. Then,  $r_h$  is mapped to  $z \rightarrow -\infty$  and the bulk coordinate runs over the interval  $(-\infty, 0^-]$ . In terms of  $z$  and  $\Psi$ , (3.124) takes the form of a standard Schrödinger equation:

$$-\frac{d^2 \Psi}{dz^2} + V(z) \Psi = \omega^2 \Psi \quad (3.126)$$

where

$$V \equiv g(G \Phi'^2 + \frac{J}{G} e^{-\chi}) + g^2 e^{-\chi} \left( \frac{G''}{2G} - \frac{G'^2}{4G^2} + \frac{G'}{2G} \left( \frac{g'}{g} - \frac{\chi'}{2} \right) \right) , \quad (3.127)$$

and the prime derivative is respect to  $r$ . In the probe approximation  $\chi = 0$  and the term proportional to  $\Phi'(r)^2$  can be dropped. Near  $z = 0$ , we may consider  $J(\eta) \cong q^2 \eta^2$  without loss of generality. Then,  $V(z) = \rho^2 z^2 + q^2 (O^{(1)} z^{\Delta-1})^2$ . So the potential vanishes if  $\Delta > 1$ ,  $V(0)$  is a constant for  $\Delta = 1$  and  $V(z)$  diverges if  $1/2 < \Delta < 1$ . In all these case, it is convenient to extend the definition of  $V(z)$  so that  $V(z) = 0$  for  $z > 0$ .

An in-falling gauge boson can be thought of as an incoming wave from the right. This wave will be partially transmitted and partially reflected by the potential barrier. The transmitted wave satisfies incoming boundary condition at the horizon. Writing the solution for  $z > 0$  as  $a_x(z) = e^{-i\omega z} + R e^{i\omega z}$ , we find

$$a_x(0) = 1 + R , \quad \partial_z a_x(0) = -i\omega(1 - R) . \quad (3.128)$$

Then, the conductivity turns out to be

$$\sigma(w) = -\frac{i}{w} \frac{a_x^{(1)}}{a_x^{(0)}} = \frac{1 - R}{1 + R} . \quad (3.129)$$

This result provides a great insight into the qualitative features of the conductivity. Let us assume for concreteness that  $V$  is bounded. At frequencies below the height of the barrier, the probability of transmission will be small and  $R$  will be closed to one. We conclude that  $\sigma(\omega)$  at low frequencies will be suppressed. It is also clear that at frequency above the height of the barrier  $R$  will be small and  $\sigma(\omega) \approx 1$ . It follows that the typical size of the gap is set by the height of the barrier,  $\omega_g \sim \sqrt{V_{max}}$ . However, the key point about  $\omega_g$  is that  $\text{Re}\sigma(\omega)$  is never strictly zero unless  $V > 0$  in the limit  $\zeta \rightarrow -\infty$ , i.e.  $V$  remains positive and does not vanish at the horizon. In particular, we notice that in the non extremal case, since  $\eta(r_h)$  finite and  $g(r_h) = 0$  by construction,  $V(z) = 0$  at the horizon and there is no gap at finite temperature even if the numerical analysis suggests that the conductivity is suppressed. The question is then, what happens in the zero temperature limit. Does  $V(z)$  remain zero at the horizon? To answer this question we need to find the extremal backreacting solution and we cannot rely on the probe approximation.

We mention that for the HHH model this extremal solution has been found in [83] and it has been proven that  $V(z)$  remains zero at the horizon. Therefore there is no “hard gap” and the relation (3.123) turns out to be wrong:  $\sigma(\omega)$  stays finite. In the more general case, in which  $G(\eta)$  or  $J(\eta)$  deform the HHH model, it is quite complicated to figure out how the extremal solution looks like. In this sense we cannot make a precise statement about the existence of a well defined  $w_g$ . Since the deformed models differs substantially from the HHH model in the limit  $\eta \gg 1$ , we believe that turning on  $J(\eta)$  and  $G(\eta)$  induces important changes in the IR physics and perhaps leads to an “hard gap” phenomenology.

As a last remark, we observe that the Schrödinger potential approach also explains the spikes in the conductivity that we have found for example in Figure 3.6. By using standard WKB matching formula, spikes will occur when there exists  $\omega$  satisfying

$$\int_{-z_0}^0 dz \sqrt{\omega^2 - V(z)} + \frac{\pi}{4} = n\pi \quad (3.130)$$

for some integer  $n$ , where  $V(-z_0) = \omega^2$ . It is important to stress that these spikes do not correspond to quasinormal modes because they do not vanish at infinity. In other words, they are not bound states.

### 3.8 Hall Currents: phenomenological approach

We shall now incorporate a new term in the phenomenological Lagrangian (3.11). This is given by

$$\delta S = \int d^{3+1}x \frac{1}{4} \Theta(\eta) \epsilon^{\mu\nu\rho\sigma} F_{\mu\nu} F_{\rho\sigma} . \quad (3.131)$$

For generic  $\Theta(\eta)$ , this term violates parity and time-reversal symmetry [11].

Even though a priori it contributes to the equations of motion as soon as  $\partial_\eta \Theta \neq 0$ , it is easy to see that for the particular ansatz (3.19) it actually gives a vanishing contribution. Therefore we find exactly the same uncondensed and condensed black hole solutions irrespective of the coupling  $\Theta(\eta)$ . Nonetheless, this coupling will affect the conductivities in an important way. The equation of motion for  $A_y$  shows that this new interaction leads to the interesting effect that an electric field in the  $x$  direction turns on an electric field in the direction  $y$ , in very much the same fashion as in the Hall effect, this time without the presence of a magnetic field. The basic idea behind this effect was first raised in [84] in the context of a model having a constant  $\Theta$ . The advantage of a coupling  $\Theta(\eta)$  with  $\partial_\eta \Theta \neq 0$  is that it can incorporate non-trivial temperature and frequency dependence on the Hall conductivity. Moreover, we may choose  $\Theta$  such that  $\Theta(0) = 0$ , meaning that  $\Theta$  is turned on only in the condensed phase.

#### 3.8.1 Asymptotic expansions

Let us consider the most general model with non-trivial  $\Theta(\eta)$ . The relevant part of the action is:

$$S = \int d^4x \left( \sqrt{-\hat{g}} \left( -\frac{1}{4} G(\eta) F^{\mu\nu} F_{\mu\nu} - \frac{1}{2} J(\eta) A_\mu A^\mu \right) + \frac{1}{4} \Theta(\eta) \epsilon^{\mu\nu\rho\sigma} F_{\mu\nu} F_{\rho\sigma} \right) . \quad (3.132)$$

The variation with respect to  $A_\sigma$  leads to a generalized version of the London equation

$$\partial_\mu \sqrt{-\hat{g}} G(\eta) F^{\mu\sigma} - \sqrt{-\hat{g}} J(\eta) A^\sigma - \epsilon^{\mu\nu\rho\sigma} F_{\mu\nu} \partial_\rho \Theta(\eta) = 0 . \quad (3.133)$$

Using the ansatz (3.19) we find that the equation (3.24) for the potential  $\Phi$  remains unchanged. In order to calculate the conductivity we consider a perturbation  $A_\mu = A_\mu(t, r)$  to the background. We will ignore backreaction and consider as usual the linear order. The effect produced by the new  $\Theta$

term in (3.133) is to couple (at first order) the bulk perturbations  $A_x$  and  $A_y$ . Indeed the equations of motion are ( $\epsilon^{txy} = 1$ )

$$\partial_r^2 A_x + \left( \frac{\partial_r g}{g} + \frac{\partial_r G}{G} \right) \partial_r A_x - \frac{1}{g^2} \partial_t^2 A_x - \frac{J}{gG} A_x - \frac{2}{gG(\eta)} \partial_t A_y \partial_r \Theta = 0, \quad (3.134)$$

$$\partial_r^2 A_y + \left( \frac{\partial_r g}{g} + \frac{\partial_r G}{G} \right) \partial_r A_y - \frac{1}{g^2} \partial_t^2 A_y - \frac{J}{gG} A_y + \frac{2}{gG(\eta)} \partial_t A_x \partial_r \Theta = 0. \quad (3.135)$$

We observe that the equations (3.141) do not depend on the value of  $\Theta(0)$ . Expanding in Fourier modes

$$A_x = \int d\omega e^{-i\omega t} a_x(r; \omega), \quad (3.136)$$

$$A_y = \int d\omega e^{-i\omega t} a_y(r; \omega), \quad (3.137)$$

the equations for the modes  $a_x(r; \omega)$ ,  $a_y(r; \omega)$  become

$$a_x'' + \left( \frac{g'}{g} + \frac{G'}{G} \right) a_x' + \left( \frac{\omega^2}{g^2} - \frac{J}{gG} \right) a_x + 2i\omega \frac{\Theta'}{gG(\eta)} a_y = 0, \quad (3.138)$$

$$a_y'' + \left( \frac{g'}{g} + \frac{G'}{G} \right) a_y' + \left( \frac{\omega^2}{g^2} - \frac{J}{gG} \right) a_y - 2i\omega \frac{\Theta'}{gG(\eta)} a_x = 0, \quad (3.139)$$

where prime indicates differentiation with respect to  $r$  (so that  $G' = \partial_\eta G \eta'$ ,  $\Theta' = \partial_\eta \Theta \eta'$ ). The system (3.138)-(3.139) can be decoupled introducing complex coordinates,  $z = x + iy$ , so that

$$A_z = \frac{1}{2}(a_x - ia_y), \quad A_{\bar{z}} = \frac{1}{2}(a_x + ia_y).$$

Using the notation,

$$\hat{P} = \partial_r^2 + \left( \frac{g'}{g} + \frac{G'}{G} \right) \partial_r + \left( \frac{\omega^2}{g^2} - \frac{J}{gG} \right), \quad \hat{Q} = 2\omega \frac{\Theta'}{gG(\eta)}, \quad (3.140)$$

the equations take the form

$$\hat{P}A_z - \hat{Q}A_z = 0, \quad \hat{P}A_{\bar{z}} + \hat{Q}A_{\bar{z}} = 0. \quad (3.141)$$

Note that the asymptotic behavior of (3.141) is not modified by the new term; indeed for  $r \rightarrow \infty$  we have

$$A_z'' + \frac{2}{r} A_z' - 2\omega \frac{\partial_\eta \Theta}{r^2} \eta' A_z = 0, \quad (3.142)$$

$$A_{\bar{z}}'' + \frac{2}{r} A_{\bar{z}}' + 2\omega \frac{\partial_\eta \Theta}{r^2} \eta' A_{\bar{z}} = 0. \quad (3.143)$$

Since  $\eta'$  is  $O(1/r^2)$  or  $O(1/r^3)$ , the  $\Theta$  term can be neglected at large  $r$ . Then the asymptotic solutions are the same as in the  $\Theta = 0$  case,

$$A_z = A_z^{(0)} + \frac{A_z^{(1)}}{r}, \quad (3.144)$$

$$A_{\bar{z}} = A_{\bar{z}}^{(0)} + \frac{A_{\bar{z}}^{(1)}}{r}. \quad (3.145)$$

To compute causal behavior, we solve for the fluctuations with ingoing-wave boundary conditions at the horizon. This requires

$$A_z \sim C_z \left(1 - \frac{r}{r_h}\right)^{-i\omega/3} a_z(r), \quad (3.146)$$

$$A_{\bar{z}} \sim C_{\bar{z}} \left(1 - \frac{r}{r_h}\right)^{-i\omega/3} a_{\bar{z}}(r), \quad (3.147)$$

with  $a_z(r) = 1 + a_z^{(1)}(1 - r/r_h) + \dots$  and similarly for  $a_{\bar{z}}$ . Because (3.141) are linear and homogeneous equations we can first set  $C_z = C_{\bar{z}} = 1$  and find the solutions  $\mathcal{A}_z, \mathcal{A}_{\bar{z}}$ . Then, the most general solutions are obtained as

$$A_z = C_z \mathcal{A}_z, \quad A_{\bar{z}} = C_{\bar{z}} \mathcal{A}_{\bar{z}}. \quad (3.148)$$

From the above expressions we find,

$$a_x = C_{\bar{z}} \mathcal{A}_{\bar{z}} + C_z \mathcal{A}_z, \quad a_y = -i(C_{\bar{z}} \mathcal{A}_{\bar{z}} - C_z \mathcal{A}_z). \quad (3.149)$$

To uncover the physical meaning of  $C_z$  and  $C_{\bar{z}}$ , we consider the asymptotic behavior (3.145) and find

$$\begin{cases} a_x(\omega) = a_x^{(0)} + \frac{a_x^{(1)}}{r} \\ a_x^{(0)} = C_{\bar{z}} \mathcal{A}_{\bar{z}}^{(0)} + C_z \mathcal{A}_z^{(0)} \\ a_y^{(0)} = -i(C_{\bar{z}} \mathcal{A}_{\bar{z}}^{(0)} - C_z \mathcal{A}_z^{(0)}) \end{cases} \quad \begin{cases} a_y(\omega) = a_y^{(0)} + \frac{a_y^{(1)}}{r} \\ a_x^{(1)} = C_{\bar{z}} \mathcal{A}_{\bar{z}}^{(1)} + C_z \mathcal{A}_z^{(1)}, \\ a_y^{(1)} = -i(C_{\bar{z}} \mathcal{A}_{\bar{z}}^{(1)} - C_z \mathcal{A}_z^{(1)}) \end{cases} \quad (3.150)$$

As usual, the leading term in the asymptotic expansion of the fields is related to the source in the dual theory; therefore, from the definition  $E_i = -\partial_t A_i$ ,  $i = x, y$ , we obtain the system,

$$\begin{cases} E_x = i\omega a_x^{(0)} = C_{\bar{z}} i\omega \mathcal{A}_{\bar{z}}^{(0)} + C_z i\omega \mathcal{A}_z^{(0)} \\ iE_y = i^2 \omega a_y^{(0)} = C_{\bar{z}} i\omega \mathcal{A}_{\bar{z}}^{(0)} - C_z i\omega \mathcal{A}_z^{(0)} \end{cases} \quad (3.151)$$

In this way, the integration constants  $C_z$  and  $C_{\bar{z}}$  get related to the physical sources  $E_x$  and  $E_y$ . Solving for  $C_z$  and  $C_{\bar{z}}$  we find the expressions

$$C_{\bar{z}} = \frac{E_x + iE_y}{2i\omega\mathcal{A}_{\bar{z}}^{(0)}}, \quad C_z = \frac{E_x - iE_y}{2i\omega\mathcal{A}_z^{(0)}}. \quad (3.152)$$

The asymptotic coefficients  $a_x^{(1)}$  and  $a_y^{(1)}$  in the expansion (3.150) can now be written in terms of the electric field components as

$$a_x^{(1)} = +\frac{1}{i\omega} \left( \frac{\mathcal{A}_{\bar{z}}^{(1)}}{\mathcal{A}_{\bar{z}}^{(0)}} + \frac{\mathcal{A}_z^{(1)}}{\mathcal{A}_z^{(0)}} \right) \frac{E_x}{2} + \frac{1}{\omega} \left( \frac{\mathcal{A}_{\bar{z}}^{(1)}}{\mathcal{A}_{\bar{z}}^{(0)}} - \frac{\mathcal{A}_z^{(1)}}{\mathcal{A}_z^{(0)}} \right) \frac{E_y}{2}, \quad (3.153)$$

$$a_y^{(1)} = -\frac{1}{\omega} \left( \frac{\mathcal{A}_{\bar{z}}^{(1)}}{\mathcal{A}_{\bar{z}}^{(0)}} - \frac{\mathcal{A}_z^{(1)}}{\mathcal{A}_z^{(0)}} \right) \frac{E_x}{2} + \frac{1}{i\omega} \left( \frac{\mathcal{A}_{\bar{z}}^{(1)}}{\mathcal{A}_{\bar{z}}^{(0)}} + \frac{\mathcal{A}_z^{(1)}}{\mathcal{A}_z^{(0)}} \right) \frac{E_y}{2}. \quad (3.154)$$

This expression will be the starting point for the discussion about the conductivity.

### 3.8.2 Conductivities and Numerical Results

It is convenient to rewrite the Lagrangian appearing (3.132) in the form

$$\mathcal{L} = \left( \sqrt{-\hat{g}} \left( -\frac{1}{2} G(\eta) F^{\mu\nu} \partial_\mu A_\nu - \frac{1}{2} J(\eta) A_\mu A^\mu \right) + \frac{1}{2} \Theta(\eta) \epsilon^{\mu\nu\rho\sigma} F_{\mu\nu} \partial_\rho A_\sigma \right). \quad (3.155)$$

From the equation (3.133) we find the relation

$$-\frac{1}{2} \sqrt{-\hat{g}} J(\eta) A^\mu A_\mu = -\frac{1}{2} \partial_\mu (\sqrt{-\hat{g}} G(\eta) F^{\mu\nu}) A_\nu + \frac{1}{2} \epsilon^{\mu\nu\rho\sigma} F_{\mu\nu} \partial_\rho \Theta A_\sigma = 0. \quad (3.156)$$

Substituting (3.156) into (3.155) and using the results of the previous section we obtain the following form for the on-shell action

$$S_{o.s.} = \frac{1}{2} \int d^2x \int d\omega \left[ a_x^{(0)}(\omega) a_x^{(1)}(-\omega) + a_y^{(0)}(\omega) a_y^{(1)}(-\omega) \right. \quad (3.157)$$

$$\left. + i\omega \Theta(0) \epsilon^{ij} a_i^{(0)}(\omega) a_j^{(0)}(-\omega) \right], \quad (3.158)$$

where  $i, j = x, y$  and we use the convention  $\epsilon^{xy} = 1$ .

The leading term in the asymptotic expansion of the fields determines a source in the dual theory, while the “normalizable” term will give the expectation value of the dual current. Therefore, from (3.150) and the definition

$E_i = -\partial_t A_i$ , we get,

$$J_x = \frac{\delta S_{o.s.}}{\delta a_x^{(0)}} = a_x^{(1)}(\omega) - i\omega\Theta(0)a_y^{(0)}(\omega) = a_x^{(1)}(\omega) - \Theta(0)E_y, \quad (3.159)$$

$$J_y = \frac{\delta S_{o.s.}}{\delta a_y^{(0)}} = a_y^{(1)}(\omega) + i\omega\Theta(0)a_x^{(0)}(\omega) = a_y^{(1)}(\omega) + \Theta(0)E_x. \quad (3.160)$$

Using the expressions (3.153)-(3.154) we derive the components of the conductivity matrix, defined by  $J_i = \sigma_{ij}E_j$ ,

$$\begin{aligned} \sigma_{xx} &= \frac{1}{2}(\sigma_{zz} + \sigma_{\bar{z}\bar{z}}) = \sigma_{yy}, \\ \sigma_{xy} &= \frac{1}{2i}(\sigma_{zz} - \sigma_{\bar{z}\bar{z}}) = -\sigma_{yx}, \end{aligned} \quad (3.161)$$

where  $\sigma_{zz}$ ,  $\sigma_{\bar{z}\bar{z}}$  represent the conductivities for left-oriented and right-oriented circular polarizations of the electric field,

$$\sigma_{zz} = \frac{1}{i\omega} \frac{\mathcal{A}_z^{(1)}}{\mathcal{A}_z^{(0)}}, \quad \sigma_{\bar{z}\bar{z}} = \frac{1}{i\omega} \frac{\mathcal{A}_{\bar{z}}^{(1)}}{\mathcal{A}_{\bar{z}}^{(0)}}, \quad \sigma_{z\bar{z}} = 0. \quad (3.162)$$

The relations  $\sigma_{xx} = \sigma_{yy}$  and  $\sigma_{xy} = -\sigma_{yx}$  are a consequence of isotropy. In a parity-preserving theory,  $\sigma_{zz}$  and  $\sigma_{\bar{z}\bar{z}}$  are equal to each other, and the Hall conductivity  $\sigma_{xy}$  (proportional to the difference) vanishes. On the contrary, in a parity-violating theory, they differ, giving rise to a non-trivial Hall effect: turning on an external electric field in the  $x$  direction implies that the system must automatically produce an electric field in the  $y$  direction and a non-trivial  $J_y$  current (and viceversa). For a generic  $\Theta(\eta)$ , parity symmetry is explicitly broken in the present model and we indeed obtain a non-trivial Hall conductivity  $\sigma_{xy}$ , even if  $\Theta(0) = 0$ . In the uncondensed phase,  $\eta \equiv 0$ , and the parity-violating interaction is not turned on. The system has vanishing Hall conductivity as expected.

Here we shall consider as an example the HHH model with the addition of the term (3.131), where  $\Theta = \eta^n$ . For the numerics we consider  $q = 1$ . The  $n = 1$  case is of interest, being the simplest case. The  $n = 2$  case is also of interest, since this case is easily incorporated in the context of HHH model with a complex scalar field  $\psi$  by adding to the HHH model the interaction  $\psi^*\psi F \wedge F$ .

Our aim is to compute  $\sigma_{xx}$  and  $\sigma_{xy}$  using (3.161) and (3.162), by numerically solving the differential equations (3.141), which for this particular choice

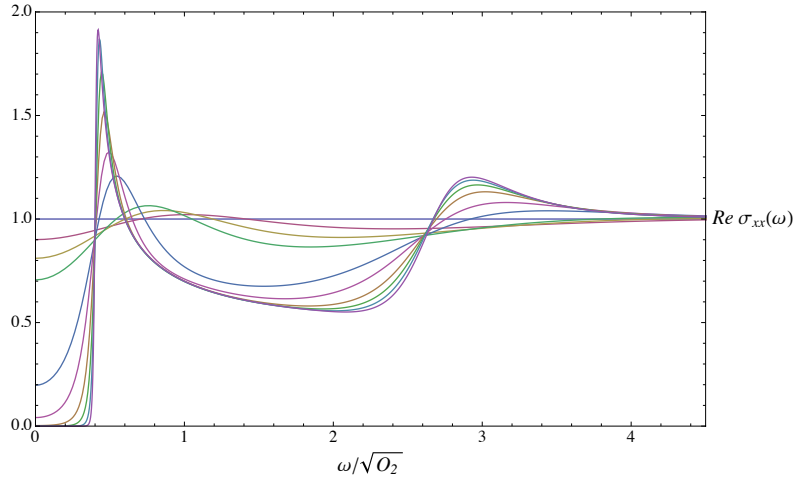


Figure 3.9:  $\text{Re}(\sigma_{xx})$  vs.  $\omega$  for the HHH model deformed by  $\Theta = \eta^n$  with  $n = 1$  at various temperatures, in the scheme where  $\langle O_2 \rangle$  is non-zero. Lower temperatures corresponds to curves with lower intercepts at  $\omega = 0$ . Adapted from [11].

of couplings read

$$\begin{aligned}
 A_z'' + \frac{g'}{g} A_z' + \left( \frac{\omega^2}{g^2} - \frac{\eta^2}{g} - 2n\omega\eta^{n-1} \frac{\eta'}{g} \right) A_z &= 0, \\
 A_{\bar{z}}'' + \frac{g'}{g} A_{\bar{z}}' + \left( \frac{\omega^2}{g^2} - \frac{\eta^2}{g} + 2n\omega\eta^{n-1} \frac{\eta'}{g} \right) A_{\bar{z}} &= 0.
 \end{aligned} \tag{3.163}$$

with  $g$  given by the HHH model.

Solving these equations numerically with the boundary conditions as described in the previous section, we compute the conductivities (3.161) and (3.162) at different temperatures. The result for the model with  $n = 1$ , obtained in the scheme where  $\langle O_1 \rangle = 0$ , are shown in Figures 3.9 ( $\text{Re}\sigma_{xx}$ ) and Figure 3.10 ( $\text{Re}\sigma_{xy}$ ). The model with  $n = 2$  reproduces qualitatively similar features but with many more peaks.

We have verified the following important feature. While the conductivity  $\text{Re}\sigma_{xx}$  has the expected delta function singularity at  $\omega = 0$ , the Hall conductivity  $\text{Re}\sigma_{xy}$  has a finite value in the DC ( $\omega = 0$ ) case. This is seen more clearly from the behavior of  $\text{Im}\sigma_{xx}$  and  $\text{Im}\sigma_{xy}$  near  $\omega = 0$ . The numerical analysis shows that  $\text{Im}\sigma_{xx} \sim 1/\omega$  while  $\text{Im}\sigma_{xy} \sim \omega^0$  as  $\omega \rightarrow 0$ .

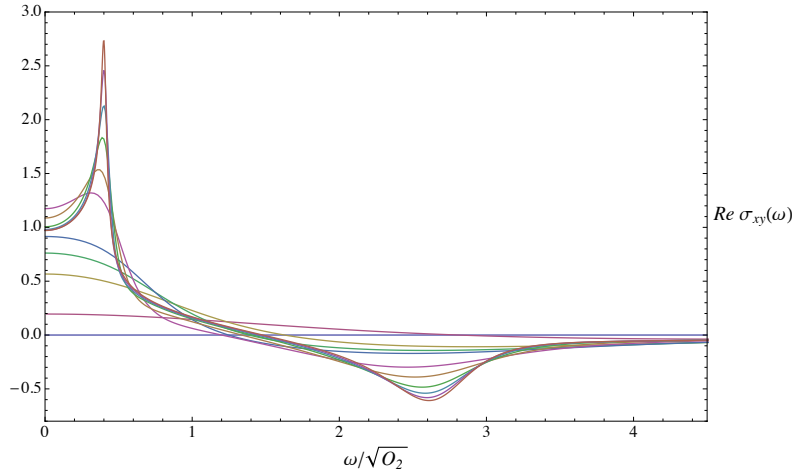


Figure 3.10:  $\text{Re}(\sigma_{xy})$  vs.  $\omega$  for the HHH model deformed by  $\Theta = \eta^n$  with  $n = 1$  at various temperatures, in the scheme where  $\langle O_2 \rangle$  is non-zero. Here the curves with lower temperatures are those which have higher value of  $\text{Re}(\sigma_{xy})$  at the frequency of the peak. Adapted from [11].

### 3.9 Summary of Results

In this chapter we have studied the so called *phenomenological* models of holographic superconductivity. These are gravitational models with a Maxwell gauge field and a charged scalar field, built out of three generalized couplings:  $G(\eta)$ ,  $J(\eta)$  and the potential  $U(\eta)$ . The simplest model of this family is the HHH model.

We have shown that the gravity dual of a state with finite charge density has a superconducting instability which favors the black hole to develop a charged hair. In the HHH model the system enters a superconducting phase at some critical temperature. The phase transition is second order and the critical exponents at the phase transition are mean field. This is a consequence of the large  $N$  limit and it is also quite a remarkable result. Indeed, we would like to emphasize the analogy between the holographic approach and the standard Landau-Ginzburg theory. However, we should remind that the systems we studied are actually in a regime of strong coupling and, as we have shown in section 3.6.1, once we turn on the phenomenological couplings, the dynamics of the phase transition is substantially different from that of the HHH model. This is an encouraging result and the most surprising aspect is the possibility of engineering non mean field critical exponents at the phase transition. As

it happens for the Widom scaling theory, not all the critical exponents are independent, instead they are related to each other by the Rushbrooke identity. In our strongly interacting theory this result follows by a simple calculation in the holographic dual.

The study of the conductivity has been our second test concerning holographic superconductivity. Vector perturbations of the background determine the optical conductivity and these are found to be controlled by a London type equation. Thus, we expect all the kind of phenomenology that can be derived from this equation. In particular, we have found that the infinite DC conductivity is a universal features and does not depend on the choice of the couplings. The problem of the existence of an energy gap is instead related to a more specific aspect of the gravitational solution which may be model dependent. Indeed, by considering W-shaped potentials we can induce in the superconductor an RG flow towards an IR conformal fixed point which is represented by the minimum of the potential. Then, we expect certain scaling relations to show up and as a consequence we should find  $\sigma(\omega) \sim \omega^\gamma$  at low frequency.

Finally, we have studied the effect of parity violating terms in the action. These are found to generate Hall currents even in the absence of an external magnetic field. It is interesting to note how the parity breaking mechanism in the bulk translates into a parity violation in the boundary.

It is important to note that we have not discussed examples of condensation driven by a non trivial scalar potential, away from the critical temperature. We will cover this issue in chapter 6 by introducing the class of zero temperature solutions called *charged domain walls*. We anticipate that the potential turns out to be a relevant ingredient for the construction of these zero temperature solutions. In particular, non HHH potentials lead to important changes in the physics of the superconducting phase, in some cases similar to the presence of a non trivial  $G(\eta)$ , in some other cases, completely counterintuitive.



# Chapter 4

## The Bosonic Sector of Supergravity

In this chapter we construct models of holographic superconductors in the context of string theory. We will consider the framework of supergravity because low energy physics of string theory and M-theory is well described by supergravity in ten and eleven dimensions.

This study is mainly motivated by two complementary observations. First, string theory comes with a huge landscape of models and holographic superconductivity may play a role in the phase diagram of some of these theories. In particular, universal properties of holographic superconductivity could be intimately related to a certain class of internal manifold chosen in the KK compactification. Second, from the point of view of condensed matter applications, it is important to have a microscopic description of the holographic superconductors. In other words, the details of the microscopic operator which condenses are relevant to make contact with realistic condensed matter systems. By considering examples in which the AdS/CFT dictionary is well understood it is actually possible to address this issue.

The best known example of AdS/CFT duality has been given in the context of open strings attached to D3 branes. In this case the field theory is unique, it is  $\mathcal{N} = 4$  SYM in four dimensions with gauge group  $SU(N)$ . At large 't Hooft coupling the gravity dual is given by  $\mathcal{N} = 8$  supergravity in five dimensions. In this case it is possible to fully identify the bulk fields in terms of dual operators in  $\mathcal{N} = 4$  SYM. We will describe examples of this exact matching throughout this chapter. It is worth saying that,  $\mathcal{N} = 8$  maximal supergravity is a wonderfully complicated theory even if our interest will be concentrated only in its bosonic sector. There are 42 scalars to deal with and the topology of the scalar potential is far from being classified.

The strategy we are going to use is essentially adapted from holographic RG-flow techniques. The basic idea is to provide consistent truncations of

$\mathcal{N} = 8$  supergravity to smaller and tractable sectors which contain gauge fields and charged scalars. Various interesting truncations will lead to  $\mathcal{N} = 2$  supergravity theories and for this reason  $\mathcal{N} = 2$  supergravity is our preferred starting point.

## 4.1 $\mathcal{N} = 2$ Supergravity

We consider the bosonic sector of the  $\mathcal{N} = 2$  supergravity and we describe the general form the Lagrangian for space-time dimensions  $d = 5$  and  $d = 4$ . We recall the types of multiplets that will play a relevant role in our discussion <sup>1</sup>,

- The graviton multiplet. It contains the metric and a single gauge field which is usually called graviphoton.
- The gauge multiplet  $\mathcal{A}$ . The bosonic content of this multiplet depends on the number of dimensions  $d$ . In five dimensions, a gauge multiplet contains a vector field  $A_\mu$  and a real scalar  $\phi$ . In four dimensions, by a simple KK argument, the gauge multiplet contains a vector field  $A_\mu$  and a complex scalar field  $z$ .
- The hypermultiplet  $\mathcal{H}$ . It contains two complex scalars equivalently described by four real scalars  $q^u$  with  $u = 1, \dots, 4$ . The properties of the hypermultiplets do not depend on the dimension  $d$ .

These supermultiplets contain fermions as well but we will not describe the fermionic action. We just point out that in four dimensions it is equivalent to consider Majorana or Weyl fermions (with definite chirality), whereas in five dimensions, being the supergravity  $\mathcal{N} = 2$ , spinors are chosen to be symplectic Majorana.

In this chapter we are mainly interested in a collection of supermultiplets. Concretely, we consider

$n_V$  gauge multiplets  $\mathcal{A}_I$  labeled by  $I = 1, \dots, n_V$ ,

$n_H$  hypermultiplets  $\mathcal{H}_X$  labeled by  $X = 1, \dots, n_H$ .

Regarding the gauge multiplets, we refer to the real scalar fields in  $d = 5$  with  $\phi^x$  where  $x = 1, \dots, n_V$ , and to the complex scalars in  $d = 4$  with  $\{z^\alpha, \bar{z}^{\bar{\alpha}}\}$  where  $\alpha = 1, \dots, n_V$ . The real hyperscalars are generically indicated by  $q^u$

---

<sup>1</sup>In five dimensions it is possible to consider also tensor multiplets, but for the purpose of our presentation they are not relevant. The inclusion of tensor multiplets in the  $\mathcal{N} = 2$  supergravity can be found in [86] and references therein.

with  $u = 1, \dots, 4n_H$ . The whole set of scalars, without making a distinction between  $\mathcal{A}$  and  $\mathcal{H}$ , will be denoted either by the vector  $\vec{v}$  or by the components  $v^i$ , with  $i = 1, \dots, n_V + n_H$ . Taking into account the graviphoton, the total number of vector fields in the theory is  $n_V + 1$ . Then, the graviphoton is usually included in the list of gauge fields by considering the notation  $A_\mu^I$  with  $I = 0, \dots, n_V$ .

Pure  $\mathcal{N} = 2$  supergravity contains only the graviton multiplet. The Lagrangian is uniquely determined and its bosonic part corresponds to Einstein-Maxwell theory with negative cosmological constant [85]. Matter fields are introduced by means of gauge multiplets and hypermultiplets. The structure of the couplings among matter fields and pure  $\mathcal{N} = 2$  supergravity is constrained by requiring that the whole Lagrangian is invariant under local  $\mathcal{N} = 2$  transformations. The Lagrangian and the transformation rules are quite involved and we refer to the literature for their explicit construction [86, 87, 88]. Nevertheless, three geometrical data are enough to determine this Lagrangian.

#### 4.1.1 The Scalar Manifold

The first two building blocks of the  $\mathcal{N} = 2$  supergravity are encoded in the geometry that describes the scalar manifold. Indeed, the structure of  $\mathcal{N} = 2$  supergravity is closely tied to the geometry of special Kähler manifolds. In order to introduce this family of special geometries, it is convenient to begin by defining the class of Kähler manifolds. A Kähler manifold is a Riemannian manifold  $M$  of real dimension  $2n$ , endowed with the almost complex structure  $J$  and the hermitian metric  $g$ , such that  $J$  is covariantly constant with respect to the Levi-Civita connection. Considering a local chart of  $2n$  real coordinates  $\vec{\varphi}$ , an almost complex structure is a real valued tensor  $J_i^j(\vec{\varphi})$  on the tangent space of the manifold, defined by the property  $J^2 = -1$ . Then, the hermitian metric  $g$  satisfy the relation  $JgJ^T = g$ . As a consequence of the definition,  $M$  is also a complex manifold and therefore can be equally covered by local holomorphic charts with  $n$  complex coordinates  $\{z^\alpha, \bar{z}^{\bar{\alpha}}\}$ . In particular, the transition functions between these complex charts are holomorphic functions. In these complex coordinates the metric  $g$  has only indexes  $g_{\alpha\bar{\beta}}$ . An important result about the class of Kähler manifolds is that the Kähler 2-form, defined on the real basis  $d\phi^i \wedge d\phi^j$  with components  $J_{ij} = J_i^m g_{mj}$ , is a closed 2-form.

$\mathcal{N} = 2$  supergravity requires the scalar manifold  $\mathcal{M}$  to be defined by the following geometries:

- The scalars of the hypermultiplets are coordinates for a quaternionic

Kähler manifold  $\mathcal{Q}$  and the choice of  $\mathcal{Q}$  fixes the self-interactions of the hypermultiplets.

- The scalars of the vector multiplets are coordinates for a very special real manifold  $\mathcal{V}$  and a special Kähler geometry  $\mathcal{S}$ , respectively in  $d = 5$  and  $d = 4$ . The choice of the manifold fixes the self-interactions of the scalars and the couplings of these scalars with the gauge vectors.

The scalar manifold  $\mathcal{M}$  is the product space  $\mathcal{S} \otimes \mathcal{Q}$  in  $d = 4$  and  $\mathcal{V} \otimes \mathcal{Q}$  in  $d = 5$ . In both cases this manifold is equipped with a smooth Euclidean signature metric  $g_{ij}$ , which defines the non linear  $\sigma$ -model for the scalars  $\vec{v}$ ,

$$\mathcal{L}_{\mathcal{N}=2} \supset g_{ij} \partial_\mu v^i \partial^\mu v^j . \quad (4.1)$$

The metric  $g_{ij}$  is block diagonal on the product spaces:

$$(d = 5) \quad g_{ij} = \begin{pmatrix} G_{xy} & 0 \\ 0 & H_{uv} \end{pmatrix} , \quad (4.2)$$

$$(d = 4) \quad g_{ij} = \begin{pmatrix} G_{\alpha\bar{\beta}} & 0 \\ 0 & H_{uv} \end{pmatrix} . \quad (4.3)$$

As already stated, the manifolds  $\mathcal{Q}$  and  $\mathcal{S}$  belong to the class of special geometries. This means that special Kähler geometry and the quaternionic Kähler geometry are Kähler manifolds with additional properties. In particular, we emphasize that in supergravity, what becomes “special”, is the role of the  $R$ -symmetry group in relation to the manifolds  $\mathcal{Q}$  and  $\mathcal{S}$ .

Let us remind the reader that, the  $R$ -symmetry group in  $d = 5$  is  $SU(2)$ , whereas the  $R$ -symmetry group in  $d = 4$  is  $Usp(2) \sim SU(2) \times U(1)$ . The  $U(1)$  factor is peculiar of four dimensions and it is associated with a specific geometric structure inherent in  $\mathcal{S}$ . A similar specific structure, associated with the  $SU(2)$  group, defines  $\mathcal{Q}$  as quaternionic Kähler manifold. This  $SU(2)$  structure is the same both in  $d = 5$  and  $d = 4$ . The relation between the  $R$ -symmetry group and the geometric properties of  $\mathcal{M}$  can be formulated in pure mathematical terms.

Both in  $d = 4$  and  $d = 5$ , local supersymmetry requires the existence of a principal  $SU(2)$ -bundle over  $\mathcal{Q}$ . The connection on this  $SU(2)$ -bundle is such that the Kähler 2-form over  $\mathcal{Q}$  can be identified with the curvature 2-form on the bundle. In  $d = 4$ , local supersymmetry requires the existence of a principal  $U(1)$ -bundle over  $\mathcal{S}$  such that the first Chern-class equals the cohomology class of the Kähler 2-form on  $\mathcal{S}$ .

The invariance under  $\mathcal{N} = 2$  supersymmetry also constrains the non linear  $\sigma$ -model for the field strengths  $F^I = dA^I$ . Indeed  $\mathcal{N} = 2$  supersymmetry implies the existence of a kinetic matrix  $N_{IJ}$  which couples the field strengths with the scalars of the vector multiplets. In particular:  $N_{IJ} = N_{IJ}(\phi^x)$  in  $d = 5$  and  $N_{IJ} = N_{IJ}(z^\alpha, \bar{z}^{\bar{\alpha}})$  in  $d = 4$ . In both cases the index  $I$  runs over  $0, \dots, n_V$  and therefore it includes the graviphoton. The form of the kinetic matrix is fixed by the geometrical structure associated with the scalar manifolds. The details about the metric  $g_{ij}$ , the kinetic matrix  $N_{IJ}$  and the properties of the special manifolds are summarized in the Appendix B. These details are necessary to fully understand the form of the bosonic Lagrangian but can be skipped in a first reading.

By considering just the input of the scalar manifold  $\mathcal{M}$ , the bosonic Lagrangian of  $\mathcal{N} = 2$  supergravity coupled to matter field is schematically represented by a “kinetic” theory of the type

$$\mathcal{R} + g_{ij} \partial_\mu v^i \partial^\mu v^j + N_{IJ} F_{\mu\nu}^I F^{\mu\nu J} . \quad (4.4)$$

It is worth saying that the connections of the  $U(1)$ -bundle and  $SU(2)$ -bundle, which form part of the geometry of  $\mathcal{M}$ , shows up only at the level of the covariant derivative acting on the fermions. These are the gravitini and the partner of the scalars, gaugini and hyperini. Because the variation under supersymmetry of these fields involves directly the scalars of the associated multiplets, the bosonic Lagrangian of  $\mathcal{N} = 2$  supergravity knows about the connections of the  $U(1)$ -bundle and  $SU(2)$ -bundle. This important point will be clarified in relation to the gauging procedure that we present in the next section.

It is a general fact that, whatever non linear  $\sigma$ -model is considered, the fermion fields are represented by a class of sections on the geometry of the scalar manifold. Then, the covariant derivatives acting on these fields are defined by introducing a set of connections. In order to distinguish between the space-time Lorentz connections and the connections living on the scalar manifold, we refer to the latter as composite connections. In this sense, the connections of the  $U(1)$ -bundle and  $SU(2)$ -bundle are composite connections. They are not the only ones. The complete list of composite connections is given in the Appendix B. In particular, we introduce the  $\Gamma_i^j$  connection for the gaugini living in the vector multiplets and the  $\Delta_\alpha^\beta$  connection for the hyperini of the hypermultiplets. These two already exist in the rigid  $\mathcal{N} = 2$  theory, whereas the  $U(1)$ -bundle and  $SU(2)$ -bundle connections represent a supergravity effect and are absent in rigid supersymmetry. Let us remind the reader that in  $d = 5$  the  $U(1)$ -bundle connection is absent and the  $R$ -symmetry group only acts on the hyperscalars.

We conclude this section by introducing some notation. In relation to quaternionic manifold and the  $SU(2)$ -bundle, there is an extra  $SU(2)$  index  $x = 1, 2, 3$ , that labels the complex structures  $J^x$  and the connections  $\omega^x$ . In particular, the triplet of connections  $\omega^x$  has components  $\omega^x = \omega_u^x dq^u$  and the resulting 2-form curvatures are  $\Omega(\omega)^x = \Omega_{uv}^x dq^u \wedge dq^v$ . Regarding the scalar manifold  $\mathcal{S}$  and the connection on the  $U(1)$ -bundle, this will be indicated by  $Q = Q_\alpha dz^\alpha + \bar{Q}_{\bar{\beta}} d\bar{z}^\beta$ .

### 4.1.2 The Gauging Procedure

Three geometrical data are necessary in order to specify the Lagrangian of  $\mathcal{N} = 2$  supergravity coupled to matter fields and we have described the first two. From the point of view of the kinetic theory (4.4), it is also evident that part of the dynamics is lacking. For example, there is no potential. The third ingredient in the construction of the complete theory is the introduction of a gauge group. As a consequence of the gauging procedure, the kinetic theory gets modified by the replacement of ordinary derivatives with covariant derivatives and by the appearance of new terms:

- ▶ fermion–fermion bilinears with scalar field dependent coefficients
- ▶ a scalar potential  $V(\mathcal{M})$

We are mainly interested in the gauging itself and the associated scalar potential. In order to understand how the gauging works we need to introduce some background.

It has been already said that the kinetic theory of matter fields is defined by a non linear sigma model on the target space  $\mathcal{M}$ . By definition,  $\mathcal{M}$  is equipped with a metric  $g_{ij}$ . The metric  $g_{ij}$  is in general a non trivial function of the scalar fields  $\vec{v}$ . Very explicitly, we want to write  $g_{ij} = g_{ij}(\vec{v})$ . An isometry of the metric is a field reparametrization,  $\vec{v} \rightarrow F(\vec{v})$ , which leaves the functional form of  $g_{ij}$  unchanged. A Killing vector is defined as the infinitesimal generator of this isometry. In particular, the Killing symmetry associated with the Killing vector is a special case of an infinitesimal (internal) symmetry  $\delta_\theta$ , where  $\theta$  is the infinitesimal parameter of the transformations [46, 90]. In terms of these infinitesimal transformations, the Killing vectors  $K_\Lambda^i(\vec{v})$  are defined by the relation,

$$\delta_\theta v^i = \theta^\Lambda K_\Lambda^i(\vec{v}), \quad \text{such that} \quad \delta_\theta g_{ij}(\vec{v}) = 0. \quad (4.5)$$

The index  $\Lambda$  that appears in (4.5) counts the number of isometries.

In many cases of interest, the manifolds  $\mathcal{S}$  and  $\mathcal{Q}$  are “homogeneous spaces”. By definition, a given manifold  $\mathcal{M}$  is said to be a homogeneous space for a group  $\mathcal{G}$ , if the map  $\mathcal{G} \times \mathcal{M} \ni (\mathfrak{a}, x) \rightarrow \mathfrak{a} \cdot x \in \mathcal{M}$  is a diffeomorphism and it acts transitively on  $\mathcal{M}$ . The dot operation formally define the action of  $\mathcal{G}$  on  $\mathcal{M}$ . The isotropy group  $\mathcal{I}_x$  of  $x \in \mathcal{M}$  is the set of the elements in the group  $\mathcal{G}$  that leaves  $x$  unvaried. It can be proved that there exist a one-to-one mapping between the manifold  $\mathcal{M}$  and the coset space  $\mathcal{G}/\mathcal{I}$  [91]. The result that we want to stress is the following,

Considering scalar manifolds  $\mathcal{S}$  or  $\mathcal{Q}$  which are homogeneous spaces of the type  $\mathcal{G}/\mathcal{I}$ , with  $\mathcal{G}$  non compact and  $\mathcal{I}$  its maximal compact subgroup, then, the  $R$ -symmetry group is embedded (partially or totally) in the isotropy group  $\mathcal{I}$ .

The homogeneous spaces that will be considered later in this chapter are

$$SU(1, 1)/U(1), \quad SU(2, 1)/U(2) . \quad (4.6)$$

The gauging of matter coupled to  $\mathcal{N} = 2$  supergravity is achieved by realizing the Yang-Mills gauge group  $G$  as a subgroup of the isometries of the scalar manifold  $\mathcal{M}$ . The dimension of  $G$  is bounded by the number of vectors, that means  $\dim G \leq n_V + 1$ . Two cases need to be distinguished, the gauge group  $G$  is the abelian group  $U(1)^{n_V+1}$  and the gauge group  $G$  is non abelian. In this last case the Lie algebra of the gauge group and in particular the structure constants  $f_{\Lambda\Sigma}^Z$ , are obtained by working out the Lie bracket relations of the Killing vectors,

$$K_{\Lambda}^j \partial_j K_{\Sigma}^i - K_{\Sigma}^j \partial_j K_{\Lambda}^i = f_{\Lambda\Sigma}^Z K_Z^i . \quad (4.7)$$

It is extremely important to keep in mind that:

for non abelian vector multiplets, the scalars parametrizing  $\mathcal{S}$  in  $d = 4$  or  $\mathcal{V}$  in  $d = 5$  transform in the adjoint representation<sup>2</sup>. In the abelian case, the manifolds  $\mathcal{S}$  and  $\mathcal{V}$  are not required to have any isometry and if the hyperscalars are charged with respect to some  $U(1)$ , then  $\mathcal{Q}$  should at list have  $n_v + 1$  abelian isometry.

---

<sup>2</sup>In general, the adjoint representation is given in terms of the structure constants of the algebra,  $f_{IJ}^K$  where  $I, J, K = 1, \dots, \#$  of generators. By definition  $f_{IJ}^K = -f_{JI}^K$ .

Once the above observation has been taken into account, the gauging proceeds by introducing at most  $n_V + 1$  Killing vectors generically acting on  $\mathcal{M}$ ,

$$v^i \longrightarrow \begin{cases} \begin{cases} \phi^x + \theta^\Lambda K_\Lambda^x(\phi) & \text{in } d = 5, \\ z^\alpha + \theta^\Lambda K_\Lambda^\alpha(z) & \text{in } d = 4, \end{cases} \\ q^u + \theta^\Lambda K_\Lambda^u(q). \end{cases} \quad (4.8)$$

Then, there are two steps to follow: i) gauge the covariant derivatives, ii) gauge the composite connections. This is a well-established procedure, introduced for the first time by the authors of [92]. Explicit formulas for the gauging can be found in [86, 87]. By considering the bosons of the theory, the first step is quite immediate. For the hyperscalars we have,

$$\partial_\mu q^u \rightarrow D_\mu q^u = \partial_\mu q^u - c_{\text{YM}} A_\mu^\Lambda K_\Lambda^u(q). \quad (4.9)$$

For the scalars in the vector multiplets we have,

$$\begin{cases} \partial_\mu \phi^x \rightarrow D_\mu \phi^x = \partial_\mu \phi^x - c_{\text{YM}} A_\mu^\Lambda K_\Lambda^x(\phi) & d = 5, \\ \partial_\mu z^\alpha \rightarrow D_\mu z^\alpha = \partial_\mu z^\alpha - c_{\text{YM}} A_\mu^\Lambda K_\Lambda^\alpha(z) & d = 4, \end{cases} \quad (4.10)$$

Finally, for the gauge fields we have,

$$F_{\mu\nu} = \partial_\mu A_\nu^\Lambda - \partial_\nu A_\mu^\Lambda + c_{\text{YM}} f_{MN}^\Lambda A_\mu^M A_\nu^N \quad (4.11)$$

Regarding the second step, we point out that the gauging of the composite connections  $Q$  and  $\omega$  involves the introduction of “prepotentials”. These are important because the scalar potential  $V$  will be expressed mostly in terms of the prepotentials. We briefly review how prepotentials are related to the Killing vectors.

The structure of special Kähler and quaternionic Kähler manifolds implies that the Killing equations are solved by *real* prepotentials,

$$K_\Lambda^\alpha = -i G^{\alpha\bar{\beta}} \partial_{\bar{\beta}} \mathcal{P}_\Lambda^0, \quad (4.12)$$

$$K_\Lambda^u J_{uv}^i = \partial_v \mathcal{P}_\Lambda^i + 2\epsilon^{ijk} \omega_v^j \mathcal{P}_\Lambda^k. \quad (4.13)$$

In  $d = 5$  there is no  $\mathcal{P}^{(0)}$ : as we already emphasized the  $R$ -symmetry group is just  $SU(2)$ . It is possible to obtain explicit formulas for the prepotentials. For example, in the case of the quaternionic manifold, the triplet of prepotentials

is expressed in terms of the killing vector and the complex structures by the relation,

$$2n_H \vec{\mathcal{P}}_\Lambda = -\vec{J}_u^v \nabla_v K_\Lambda^u . \quad (4.14)$$

Formula (4.14) will be relevant in the discussion of section 4.2.

In the case of a non abelian gauge group with structure constants  $f_{\Lambda\Sigma}^\Gamma$ , the Killing vectors need to satisfy the following ‘‘equivariance’’ relations imposed by supersymmetry. We will not make use these relations and we report them just for sake of completeness. They are,

$$G_{\alpha\bar{\beta}}(K_\Lambda^\alpha K_\Sigma^{\bar{\beta}} - K_\Sigma^\alpha K_\Lambda^{\bar{\beta}}) = -i f_{\Lambda\Sigma}^\Gamma \mathcal{P}_\Gamma^0 , \quad (4.15)$$

$$J_{uv}^i K_\Lambda^u K_\Sigma^v + \epsilon^{ijk} \mathcal{P}_\Lambda^j \mathcal{P}_\Sigma^k = f_{\Lambda\Sigma}^\Gamma \mathcal{P}^i . \quad (4.16)$$

Although basic and incomplete with respect to the huge literature about  $\mathcal{N} = 2$  supergravity, the background that we have described so far, contains the fundamental tools that allow the reader to fully understand the Lagrangians described in the next paragraphs, as well as the subsequent calculations.

### 4.1.3 The Action with Matter Couplings

We present here the Lagrangian for bosonic  $\mathcal{N} = 2$  supergravity coupled to matter field in  $d = 5$  and  $d = 4$ . It is useful to describe both cases so to appreciate the differences, especially for what concerns the potential. We refer to the Appendix B when some special notation is introduced.

**Five Dimensions** The bosonic part of the  $\mathcal{N} = 2$  supergravity action coupled to matter field has been worked out in [86]. The result is,

$$e^{-1} \mathcal{L}_{\mathcal{N}=2}^{(5)} = \mathcal{R} + \mathcal{L}_{vectors}^{(5)} + \mathcal{L}_{scalars}^{(5)} + e^{-1} \mathcal{L}_{CS}^{(5)} . \quad (4.17)$$

where the three  $\mathcal{L}^{(5)}$ -pieces correspond to,

$$\begin{aligned} \mathcal{L}_{vectors}^{(5)} &= -\frac{1}{2} a_{IJ} F_{\mu\nu}^I F^{\mu\nu J} , \\ \mathcal{L}_{scalar}^{(5)} &= -G_{xy} D_\mu \phi^x D^\mu \phi^y - H_{uv} D_\mu q^u D^\mu q^v - V(q, \phi) , \end{aligned} \quad (4.18)$$

$$\mathcal{L}_{CS}^{(5)} = \frac{1}{3\sqrt{6}} C_{IJK} \epsilon^{\mu\nu\rho\sigma\tau} F_{\mu\nu}^I F_{\rho\sigma}^J A_\tau^K . \quad (4.19)$$

The kinetic matrix for the self interactions in the vector multiplets has been redefined with the symbol  $a_{IJ} = a_{IJ}(\phi)$ . The latin indexes  $I, J$  run over  $0, \dots, n_V$ , therefore they include the graviphoton. The potential  $V(q^u, \phi^x)$  is<sup>3</sup>

$$V(q, \phi) = -2c_R^2 P^r P^r + c_R^2 P_x^r P_y^r G^{xy} + \frac{3}{2} c_{YM}^2 K^u K^v H_{uv}, \quad (4.20)$$

where the following notation has been introduced,

$$P^r \equiv h^I(\phi) \mathcal{P}_I^r(q), \quad P_x^r \equiv -\sqrt{\frac{3}{2}} \partial_x P^r, \quad K^u = K_I^u h^I(\phi). \quad (4.21)$$

In Appendix B we define the functions  $h^I(\phi)$  and we give the explicit form of the matrix  $a_{IJ}(\phi)$ . Both these quantities are related to the special real geometry of the manifold  $\mathcal{V}$ .

**Four Dimensions** The bosonic part of the  $\mathcal{N} = 2$  supergravity action coupled to matter fields is given in [46, 87]. The result is,

$$e^{-1} \mathcal{L}_{\mathcal{N}=2}^{(4)} = \mathcal{R} + \mathcal{L}_{vectors}^{(4)} + \mathcal{L}_{scalars}^{(4)} + e^{-1} \mathcal{L}_{CS}^{(4)}. \quad (4.22)$$

Similarly to the five dimensional case, the  $\mathcal{L}^{(4)}$ -pieces correspond to,

$$\mathcal{L}_{vectors}^{(4)} = +\frac{1}{2} (\text{Im} \mathcal{N}_{IJ}) F_{\mu\nu}^I F^{\mu\nu J} - \frac{1}{4} (\text{Re} \mathcal{N}_{IJ}) \epsilon^{\mu\nu\rho\sigma} F_{\mu\nu}^I F_{\rho\sigma}^J, \quad (4.23)$$

$$\mathcal{L}_{scalar}^{(4)} = -2G_{\alpha\bar{\beta}} D_\mu z^\alpha D^\mu \bar{z}^{\bar{\beta}} - H_{uv} D_\mu q^u D^\mu q^v - 2V(q^u, z^\alpha, \bar{z}^{\bar{\alpha}}), \quad (4.24)$$

$$\mathcal{L}_{CS}^{(4)} = \frac{4}{3} C_{IJK} \epsilon^{\mu\nu\rho\sigma} A_\mu^I A_\nu^J \left( \partial_\rho A_\sigma^K + \frac{3}{8} f_{LM}^K A_\rho^L A_\sigma^M \right). \quad (4.25)$$

The kinetic matrix in  $d = 4$  is  $\mathcal{N}_{IJ} = \mathcal{N}_{IJ}(z^\alpha, \bar{z}^{\bar{\alpha}})$ . Also in this case the latin indexes take into account the graviphoton. The kinetic matrix is complex and its real part fixes the structure of the  $\epsilon^{\mu\nu\rho\sigma} F_{\mu\nu}^I F^{\mu\nu J}$  kinetic term (which obviously does not exist in  $d = 5$ ). The potential  $V(q^u, z^\alpha, \bar{z}^{\bar{\alpha}})$  is,

$$\begin{aligned} V(q^u, z^\alpha, \bar{z}^{\bar{\alpha}}) &= -2 \left( \frac{1}{2} (\text{Im} \mathcal{N})^{-1|IJ} + 4 \bar{X}^I X^J \right) \vec{P}_I \cdot \vec{P}_J \\ &\quad + 2 \bar{X}^I X^J \left( 2K_I^u K_J^v H_{uv} + K_I^\alpha K_J^{\bar{\beta}} G_{\alpha\bar{\beta}} \right). \end{aligned} \quad (4.26)$$

where the functions  $X^I(z^\alpha)$  and  $\bar{X}^{\bar{I}}(\bar{z}^{\bar{\alpha}})$  are defined in the Appendix B.

<sup>3</sup>With respect to the notation of [86], we have a slightly different normalization. There is a global factor  $1/2$  multiplying the Lagrangian and  $\mathcal{P}_{here}^r = 2\mathcal{P}_{there}^r$ .

## 4.2 The Hypermultiplet $SU(2, 1)/U(2)$

The coset space  $\mathcal{H} = SU(2, 1)/U(2)$  is a quaternionic manifold of real dimension four. It represents the first element of a bigger tower of quaternionic homogeneous manifolds called Wolf spaces  $X(m)$  [93],

$$X(m) = \frac{SU(2, m)}{SU(m) \times SU(2) \times U(1)} . \quad (4.27)$$

The choice  $m = 1$  corresponds to  $SU(2, 1)/U(2)$ . In five dimension, this coset space, is historically known as the “ universal hypermultiplet” [94]. Even in four dimensions, we may refer to it as the universal hypermultiplet.

### 4.2.1 Geometrical Properties

The manifold  $\mathcal{H}$  belongs to the class of special geometries. For the quaternionic case, it means that  $\mathcal{H}$  has an  $SU(2)$ -bundle whose connection has non zero curvature. The coset space that we are considering has a relatively simple structure and some of the details related to the special geometry can be worked out without difficulties. To start with, we consider two complex coordinates  $\zeta_1$  and  $\zeta_2$ . In this coordinates the metric on  $\mathcal{H}$  is,

$$\frac{ds^2}{2} = \frac{d\zeta_1 \bar{d}\bar{\zeta}_1 + d\zeta_2 \bar{d}\bar{\zeta}_2}{(1 - |\zeta_1|^2 - |\zeta_2|^2)} + \frac{(\bar{\zeta}_1 d\zeta_1 + \bar{\zeta}_2 d\zeta_2)(\zeta_1 \bar{d}\bar{\zeta}_1 + \zeta_2 \bar{d}\bar{\zeta}_2)}{(1 - |\zeta_1|^2 - |\zeta_2|^2)^2} , \quad (4.28)$$

where  $\zeta_1 \bar{\zeta}_1 + \zeta_2 \bar{\zeta}_2 < 1$ . The boundary of  $\mathcal{H}$  is the three-sphere in  $\mathbb{C}^2$  and the quaternionic manifold itself is topologically the open ball in  $\mathbb{C}^2$  [95]. This topological property is manifest when the following change of coordinates is considered,

$$\zeta_1 = \tau \cos \frac{\theta}{2} e^{i(\varphi+\psi)/2} , \quad \zeta_2 = \tau \sin \frac{\theta}{2} e^{-i(\varphi-\psi)/2} . \quad (4.29)$$

Then, the metric takes the form,

$$\frac{ds^2}{2} = \frac{d\tau^2}{(1 - \tau^2)^2} + \frac{\tau^2}{4(1 - \tau^2)} (\sigma_1^2 + \sigma_2^2) + \frac{\tau^2}{4(1 - \tau^2)^2} \sigma_3^2 , \quad (4.30)$$

where  $\hat{\sigma}_i$  are the standard left invariant one-forms,

$$\begin{aligned} \hat{\sigma}_1 &= \cos \psi \, d\theta + \sin \psi \sin \theta \, d\varphi , \\ \hat{\sigma}_2 &= -\sin \psi \, d\theta + \cos \psi \sin \theta \, d\varphi , \\ \hat{\sigma}_3 &= d\psi + \cos \theta \, d\varphi . \end{aligned}$$

The definition of these new variables is restricted to,  $r \in [0, 1)$ ,  $\theta \in [0, \pi)$ ,  $\varphi \in [0, 2\pi)$  and  $\psi \in [0, 4\pi)$ . In the complex coordinates  $\{\zeta_1, \zeta_2\}$ , the metric (4.28) is a Kähler metric whose Kähler potential is

$$K = -\log(1 - \zeta_1 \bar{\zeta}_1 - \zeta_2 \bar{\zeta}_2) . \quad (4.31)$$

The isotropy group of  $\mathcal{H}$  is  $U(2) = SU(2)_R \times U(1)$  and the gauging procedure requires the knowledge of the Killing vectors associated with these 4 isometries. We expect to find linear Killing vectors and therefore the analysis simplifies.

It is clear, from the Kähler potential that the combination  $|\zeta_1|^2 + |\zeta_2|^2$  is  $U(2)$  invariant. Two  $U(1)$  symmetries are given by

$$\zeta_1 \rightarrow e^{i\theta_1} \zeta_1, \quad \zeta_2 \rightarrow e^{i\theta_2} \zeta_2 . \quad (4.32)$$

The first one is an  $SO(2)$  rotation in the complex plane  $\zeta_1$ , the second one instead, is a rotation in the  $\zeta_2$  plane. The remaining part of the isotropy group rotates the coordinates  $\{\zeta_1, \zeta_2\}$ , thought as a doublet of  $SU(2)$ . This is intuitive when we look at the invariant combination

$$|\zeta_1|^2 + |\zeta_2|^2 . \quad (4.33)$$

It is also instructive to examine the metric (4.28): we recognize that the combinations

$$d\zeta_1 \bar{d}\zeta_1 + d\zeta_2 \bar{d}\zeta_2, \quad \bar{\zeta}_1 d\zeta_1 + \bar{\zeta}_2 d\zeta_2, \quad \zeta_1 \bar{d}\zeta_1 + \zeta_2 \bar{d}\zeta_2, \quad (4.34)$$

work exactly as the invariant  $|\zeta_1|^2 + |\zeta_2|^2$ . Several  $SU(2)$  doublets could be equally considered, for example instead of  $\{\zeta_1, \zeta_2\}$  we could take  $\{\zeta_1, \bar{\zeta}_2\}$  or the complex conjugates of these two doublets. They all lead to the invariant combination (4.33) when the scalar product with their complex conjugate has been taken. It turns out that a convenient choice is the isometry given by

$$\begin{pmatrix} \zeta_1 \\ \zeta_2 \end{pmatrix} \rightarrow \mathcal{R}_\theta \begin{pmatrix} \zeta_1 \\ \zeta_2 \end{pmatrix} \quad \mathcal{R}_\theta \equiv \begin{pmatrix} \cos \theta & \sin \theta \\ -\sin \theta & \cos \theta \end{pmatrix} . \quad (4.35)$$

The last isometry of the  $U(2)$  group is the complex conjugate of this third one, which is of course independent in  $\mathbb{C}^2$ .

The four isometries described so far are generated by the following Killing vectors,

$$H_1 = \zeta_1 \partial_{\zeta_1} - \bar{\zeta}_1 \bar{\partial}_{\zeta_1} \quad H_2 = \zeta_2 \partial_{\zeta_2} - \bar{\zeta}_2 \bar{\partial}_{\zeta_2} \quad (4.36)$$

$$L_1 = \zeta_2 \partial_{\zeta_1} - \bar{\zeta}_1 \bar{\partial}_{\zeta_2} \quad \bar{L}_1 = \bar{\zeta}_2 \bar{\partial}_{\zeta_1} - \zeta_1 \partial_{\zeta_2} . \quad (4.37)$$

In particular, the algebra of this  $U(2)$  group splits into the two sub-algebras of  $SU(2)$  and  $U(1)$ :

$$SU(2) \times U(1) = \begin{cases} F_1 = \frac{1}{2}(L_1 - \bar{L}_1) , \\ F_2 = \frac{1}{2i}(L_1 + \bar{L}_1) , \\ F_3 = \frac{1}{2}(H_2 - H_1) , \\ F_8 = \frac{\sqrt{3}}{2}(H_1 + H_2) , \end{cases} \quad (4.38)$$

The  $SU(2)$  algebra, associated with  $(F_1, F_2, F_3)$ , satisfies the standard commutation relations  $[F_i, F_j] = i\epsilon_{ijk}F_k$ , where the indexes run over  $\{1, 2, 3\}$ . The  $U(1)$  generator  $F_8$  is orthogonal to this  $SU(2)$  algebra, i.e  $[F_i, F_8] = 0$  with  $i = 1, 2, 3$ . The coset space  $SU(2, 1)$  is completely generated by Killing vectors. In addition to (4.38) there exist non linear and non compact Killing vectors given by,

$$L_2 = \partial_{\zeta_1} - \bar{\zeta}_1 \bar{\zeta}_2 \bar{\partial}_{\zeta_2} - \bar{\zeta}_1^2 \bar{\partial}_{\zeta_1} , \quad \bar{L}_2 = \bar{\partial}_{\zeta_1} - \zeta_1 \zeta_2 \partial_{\zeta_2} - \zeta_1^2 \partial_{\zeta_1} , \quad (4.39)$$

$$L_3 = \bar{\partial}_{\zeta_2} - \zeta_1 \zeta_2 \partial_{\zeta_1} - \zeta_2^2 \partial_{\zeta_2} , \quad \bar{L}_3 = \partial_{\zeta_2} - \bar{\zeta}_1 \bar{\zeta}_2 \bar{\partial}_{\zeta_1} - \bar{\zeta}_2^2 \bar{\partial}_{\zeta_2} . \quad (4.40)$$

The set of  $F_i$ , where the index  $i = 1, \dots, 8$  and we have defined

$$F_4 = -\frac{1}{2}(L_2 + \bar{L}_2) , \quad F_5 = \frac{i}{2}(L_2 - \bar{L}_2) , \quad (4.41)$$

$$F_6 = \frac{1}{2}(L_3 + \bar{L}_3) , \quad F_7 = -\frac{i}{2}(L_3 - \bar{L}_3) . \quad (4.42)$$

closes the algebra of  $SU(3)$  [95, 96].

The quaternionic manifold  $\mathcal{H}$  can be described by several systems of coordinates. We define two different systems of coordinates that are known in the literature [97, 98]. The first one is given by the complex coordinates  $\{S, C\}$ , which obey the relation

$$\zeta_1 = \frac{1 - S}{1 + S} , \quad \zeta_2 = \frac{2C}{1 + S} . \quad (4.43)$$

With respect to  $S$  and  $C$  the Kähler potential, modulo a Kähler transformation, takes the form

$$K = -\log(S + \bar{S} - 2|C|^2) . \quad (4.44)$$

The second set of coordinates are the real quaternionic coordinates  $q^u = \{V, \sigma, \theta, \tau\}$  defined by

$$S = V + i\sigma + \theta^2 + \tau^2 , \quad C = \theta + i\tau , \quad (4.45)$$

In these variables the metric becomes

$$ds^2 = \frac{dV^2}{2V^2} + \frac{1}{2V^2}(d\sigma + 2\theta d\tau - 2\tau d\theta)^2 + \frac{2}{V}(d\tau^2 + d\theta^2) . \quad (4.46)$$

An easy calculation relates the  $q^u$  to the original  $\zeta_1$  and  $\zeta_2$ <sup>4</sup>. In both cases,  $\{S, C\}$  and  $\{V, \sigma, \theta, \tau\}$ , the domain of validity is diffeomorphic to  $\zeta_1 \bar{\zeta}_1 + \zeta_2 \bar{\zeta}_2 < 1$ . The quaternionic vielbeins  $f^{iA}$  are particularly nice in this last set of coordinates:  $f^{iA} = f_u^{iA} dq^u$ . By introducing the one-forms

$$u = \frac{d\theta + id\tau}{\sqrt{V}} , \quad v = \frac{1}{2V} (dV + id\sigma + 2i(\theta d\tau - \tau d\theta)) , \quad (4.47)$$

we find

$$f^{iA} = \begin{pmatrix} u & -v \\ \bar{v} & \bar{u} \end{pmatrix} , \quad ds^2 = f^{iA} f^{jB} \varepsilon_{ij} C_{AB} . \quad (4.48)$$

It is a matter of coordinate transformations to express the vielbeins as functions of  $\{\zeta_1, \zeta_2\}$  or  $\{S, C\}$ . In all these cases the triplet of complex structures is built out of the vielbeins by means of the relation,

$$\vec{J}_u^v = -i f_u^{iA} (\vec{\sigma})_i^j f_{jA}^v , \quad (4.49)$$

where  $f_{jA}^v$  are the inverse vielbeins and  $\sigma_i^j$  are the Pauli matrixes. The special geometry is then encoded in the  $SU(2)$  connections  $\omega^x = \omega_m^x dq^m$  defined by the relation,

$$\nabla_m (J^x)_n^v + 2\epsilon^{xyz} \omega_m^y (J^z)_n^v = 0 , \quad (4.50)$$

The derivative  $\nabla_m (J^x)_n^v$  is the covariant derivative of a tensor (with one upper and one lower index) with respect to the Levi-Civita connection on  $\mathcal{H}$ . The solution of (4.50) is,

$$\omega^1 = -\frac{d\tau}{\sqrt{V}} , \quad \omega^2 = \frac{d\theta}{\sqrt{V}} , \quad \omega^3 = -\frac{1}{4V}(d\sigma - 2\tau d\theta + 2\theta d\tau) . \quad (4.51)$$

The curvature  $\Omega^x(\omega)$  is non zero and it is given by,

$$\Omega^1 = -\frac{1}{2V^{3/2}} (-d\tau \wedge dV + d\sigma \wedge d\theta + 2\theta d\tau \wedge d\theta) , \quad (4.52)$$

$$\Omega^2 = -\frac{1}{2V^{3/2}} (+d\theta \wedge dV + d\sigma \wedge d\tau - 2\tau d\theta \wedge d\tau) , \quad (4.53)$$

$$\Omega^3 = -\frac{1}{V} d\theta \wedge d\tau + \frac{1}{4V^2} (d\sigma \wedge dV - 2\tau d\theta \wedge dV + 2\theta d\tau \wedge dV) . \quad (4.54)$$

---

<sup>4</sup>In CY compactifications, the coordinate  $V$  acquires the meaning of the volume of the CY manifold [97, 99].

An easy calculation makes manifest the fundamental relation of quaternion geometry: the curvature form  $\Omega(\omega)$  is proportional to the Kähler form,

$$\Omega_{uv}^x = -\frac{1}{2}H_{uv}(J^x)^w_v . \quad (4.55)$$

### 4.2.2 One Parameter Family of Theories

The final purpose of our analysis is the construction of a  $\mathcal{N} = 2$  gauged supergravity coupled to the universal hypermultiplet. We consider an abelian gauge group and therefore no other vectors but the graviphoton are present. The gauging is straightforward thanks to the knowledge of the Killing vectors identified in (4.38). The procedure requires the abelian gauge group to be embedded into the isotropy group of the scalar manifolds. We emphasize that this embedding is not unique and can be parametrized by the following Killing vector [96],

$$K(\zeta_1, \zeta_2) = -i \mathfrak{f}_d \left( \alpha_3 F_3 + \frac{\beta}{\sqrt{3}} F_8 \right) . \quad (4.56)$$

The ratio of  $\beta/\alpha_3$  specifies the direction of  $K(\zeta_1, \zeta_2)$  inside the  $U(2)$  isotropy group (and  $\mathfrak{f}_d$  is an overall normalization). We define  $\gamma$  as the ratio  $\beta/\alpha_3$ . This parameter gives a family of abelian  $\mathcal{N} = 2$  supergravity coupled to  $\mathcal{H}$ . The construction of this family of theories in dimensions  $d = 5$  and  $d = 4$  is the main result of this section.

The general Lagrangian of gauged  $\mathcal{N} = 2$  supergravity with matter couplings contains various contributions. These were given in (4.17) and (4.22). With respect to the  $SU(2, 1)/U(2)$  model that we aim to construct, we are able to reduce the Lagrangians  $\mathcal{L}_{\mathcal{N}=2}^{(5)}$  and  $\mathcal{L}_{\mathcal{N}=2}^{(4)}$  to the standard form,

$$e^{-1}\mathcal{L}_{\mathcal{H}} = \mathcal{R} - \frac{1}{4}F^{\mu\nu}F_{\mu\nu} - 2h_{i\bar{j}}D^\mu\zeta_i\overline{D_\mu\zeta_j} - P^{(d)}(\zeta_1, \zeta_2) . \quad (4.57)$$

We now explain in detail how this result follows from (4.17) and (4.22). The kinetic matrix for the gauge fields is one dimensional. It corresponds to the trivial case in which there is the graviphoton but there are no vector multiplets. In particular  $\mathcal{N}_{IJ} = \mathcal{N}_{00}$  in  $d = 4$  and  $a_{IJ} = a_{00}$ . These two matrix elements are fixed by  $\mathcal{N} = 2$  supersymmetry and are understood in terms of the geometrical data given in the Appendix B. The result is,

$$\text{Im}\mathcal{N}_{00} = -\frac{1}{2} , \quad a_{00} = 1 . \quad (4.58)$$

In five dimensions the standard kinetic term for the gauge boson is obtained after the rescaling  $A^0 \rightarrow A^0/\sqrt{2}$ . The tensor  $h_{i\bar{j}}$  is the metric on the coset

space  $\mathcal{H}$ , already introduced in (4.28),

$$h_{i\bar{j}}d\zeta_i d\bar{\zeta}_{\bar{j}} = \frac{d\zeta_1 d\bar{\zeta}_1 + d\zeta_2 d\bar{\zeta}_2}{(1 - |\zeta_1|^2 - |\zeta_2|^2)} + \frac{(\bar{\zeta}_1 d\zeta_1 + \bar{\zeta}_2 d\zeta_2)(\zeta_1 d\bar{\zeta}_1 + \zeta_2 d\bar{\zeta}_2)}{(1 - |\zeta_1|^2 - |\zeta_2|^2)^2}. \quad (4.59)$$

In the complex coordinates  $\zeta_1$  and  $\zeta_2$  it is natural to express the metric as a tensor with one holomorphic index and one anti-holomorphic index, according to the standard formulation of Kähler geometry. The covariant derivatives are defined by the general formula (4.10). With the following choice of normalization,  $f_4 = 2$  in  $d = 4$  and  $f_5 = 2\sqrt{2}$  in  $d = 5$ , we find,

$$\begin{cases} D_\mu \zeta_1 \equiv \partial_\mu \zeta_1 - iA_\mu \alpha_3 (\gamma + 1) \zeta_1 \\ D_\mu \zeta_2 \equiv \partial_\mu \zeta_2 - iA_\mu \alpha_3 (\gamma - 1) \zeta_2 \end{cases} \quad \gamma \equiv \frac{\beta}{\alpha_3} \quad (4.60)$$

The scalar potential is  $P^{(d)}$  and the upper label on it refers to the dimensions,  $d = 4$  and  $d = 5$ . The knowledge of the Killing vector (4.56) and the triplet of prepotentials determines the potential. The relation we need to exploit has been given in (4.14):

$$2n_H \vec{\mathcal{P}} = -\vec{J}_u^v \nabla_v K^u. \quad (4.61)$$

We note that a Fayet-Iliopoulos constant is present in our prepotential. Indeed when  $\zeta_1 = \zeta_2 = 0$  we find

$$\vec{\mathcal{P}} = 2f_d \alpha_3 (0, 0, 1). \quad (4.62)$$

Therefore, it is important to notice that a negative cosmological constant is associated only to the gauging along the  $\alpha_3$  direction. For this reason we prefer to isolate from the potential the contribution which is proportional to  $\beta$ . In four dimensions we find that,

$$P^{(4)}(\zeta_1, \zeta_2) = -\frac{2\alpha_3^2}{(1 - |\zeta_1|^2 - |\zeta_2|^2)^2} \left( V_{(3)}^{(4)} - V_{(3-8)}^{(4)} \right) \quad (4.63)$$

with

$$V_{(3)}^{(4)} = \left[ 12 - 16(|\zeta_1|^2 + |\zeta_2|^2) + 3(|\zeta_1|^4 + |\zeta_2|^4) - 10|\zeta_1|^2 |\zeta_2|^2 \right]$$

$$V_{(3-8)}^{(4)} = \gamma \left[ 4(\gamma - 1)|\zeta_1|^2 + 4(\gamma + 1)|\zeta_2|^2 - 3(\gamma - 2)|\zeta_1|^4 - 3(\gamma + 2)|\zeta_2|^4 - 6\gamma|\zeta_1|^2 |\zeta_2|^2 \right]$$

Similarly, in five dimensions the potential is given by,

$$P^{(5)}(\zeta_1, \zeta_2) = -\frac{2\alpha_3^2}{(1 - |\zeta_1|^2 - |\zeta_2|^2)^2} \left( V_{(3)}^{(5)} - V_{(3-8)}^{(5)} \right) \quad (4.64)$$

with

$$V_{(3)}^{(5)} = \left[ 8 - 11(|\zeta_1|^2 + |\zeta_2|^2) + 2(|\zeta_1|^4 + |\zeta_2|^4) + 8|\zeta_1|^2|\zeta_2|^2 \right]$$

$$V_{(3-8)}^{(5)} = \gamma \left[ (3\gamma - 2)|\zeta_1|^2 + (3\gamma + 2)|\zeta_2|^2 - 2(\gamma - 2)|\zeta_1|^4 - 2(\gamma + 2)|\zeta_2|^4 - 4\gamma|\zeta_1|^2|\zeta_2|^2 \right]$$

### 4.3 $\mathcal{N} = 8$ Supergravity in $d = 5$

Let us discuss the bosonic field of  $\mathcal{N} = 8$  supergravity in  $d = 5$  [100, 101, 102]. The  $R$ -symmetry group of the theory has an  $SU(4) \simeq SO(6)$  subgroup. We are interested in truncation of the bosonic sector of  $\mathcal{N} = 8$  supergravity where the retained fields correspond to a subset of the following fields<sup>5</sup>,

- gravity,
- the  $SO(6)$  adjoint<sup>6</sup> gauge fields  $A_\mu^{IJ}$ ,
- the 42 scalars  $V_{AB}^{ab}$  parametrizing the coset  $E_{6(6)}/Usp(8)$ .

The **42** scalars can be classified according to their representation under  $SO(6)$ . The decomposition is,

$$\mathbf{42} = \mathbf{20} + (\mathbf{10} + \overline{\mathbf{10}}) + \mathbf{1} + \mathbf{1} . \quad (4.65)$$

The scalars in the representation **20** and the gauge fields in the representation **15** can be collected in an elegant way as KK modes of the type IIB theory in ten dimensions [103]. The sector of type IIB which is relevant for the truncation is given by the metric  $ds_{10}^2$  and the self-dual five form  $F_{(5)}^+$ . This is itself a consistent truncation inside type IIB theory. Indeed type IIB theory contains other fields other than the metric and the five form but these can be safely set to zero. Then, the equations of motions simply reduce to,

$$R_{MN} = \frac{1}{96} F_{MPQRS} F_N^{PQRS}, \quad dF_{(5)} = 0 , \quad (4.66)$$

where  $R_{MN}$  is the Ricci tensor of the ten dimensional metric. The conventions for the exterior calculus and the Hodge dual forms are listed in Appendix (B).

<sup>5</sup>The full bosonic sector of  $\mathcal{N} = 8$  supergravity contains also a pair of twelve 2-forms gauge potentials.

<sup>6</sup>In the case of  $SO(N)$ , the dimension of the adjoint representation is  $N(N-1)/2$ , which is the dimension of an anti-symmetric  $N \times N$  matrix.

When type IIB theory is compactified on the five sphere, the scalars and the gauge bosons characterize the deformations of the metric and the five form. In particular, the twenty scalars parametrize a symmetric unimodular matrix

$$T \in SL(6, \mathbb{R}) , \quad T_{ij} = T_{ji} , \quad \det T = 1 ,$$

and the fifteen gauge potentials parametrize an anti-symmetric matrix

$$A_{(1)}^{ij} = -A_{(1)}^{ji} .$$

In both cases the latin indexes  $i$  and  $j$  label the  $\mathbf{6}$  of  $SO(6)$ . The type IIB ansatz is given in terms of  $T_{ij}$  and  $A_{(1)}^{ij}$  as follows [103],

$$ds_{10}^2 = \Delta^{1/2} ds_5^2 + g^{-2} \Delta^{-1/2} T_{ij}^{-1} D\mu^i D\mu^j , \quad (4.67)$$

$$H_{(5)} = G_{(5)} + \star G_{(5)} , \quad (4.68)$$

$$G_{(5)} = -gU\epsilon_{(5)} + g^{-1} (T_{ij} \star DT_{jk}) \wedge (\mu^k D\mu^i) \\ - \frac{1}{2} g^{-2} T_{ik}^{-1} T_{jl}^{-1} \star F_{(2)}^{ij} \wedge D\mu^k \wedge D\mu^l .$$

where we have defined,

$$\Delta \equiv T_{ij} \mu^i \mu^j , \quad U \equiv 2T_{ij} T_{jk} \mu^i \mu^k - \Delta T_{ii} , \\ F_{(2)}^{ij} = dA_{(1)}^{ij} + gA_{(1)}^{ik} \wedge A_{(1)}^{kj} , \quad DT_{ij} = dT_{ij} + gA_{(1)}^{ik} T_{kj} - gT_{ik} A_{(1)}^{kj} , \\ \mu^i \mu^i = 1 , \quad D\mu^i \equiv d\mu^i + gA_{(1)}^{ij} \mu^j . \quad (4.69)$$

The volume form on the five dimensional space-time is  $\epsilon_{(5)}$  and the coordinate  $\mu^i \mu^i = 1$  live on the internal five sphere.

The result of [103] provides a five dimensional Lagrangian whose solutions are also solutions of (4.66) through the ansatz (4.68), and therefore they are solutions of type IIB theory by construction. The five dimensional Lagrangian is given by

$$\mathcal{L}_{SO(6)}^{(5)} = \mathcal{R} - \frac{1}{4} T_{ij}^{-1} \star DT_{jk} T_{kl}^{-1} \wedge DT_{li} - \frac{1}{4} T_{ik}^{-1} T_{jl}^{-1} \star F_{(2)}^{ij} \wedge F_{(2)}^{kl} - P(T_{ij}) \\ - \frac{1}{48} \epsilon_{i_1 \dots i_6} \left( F_{(2)}^{i_1 i_2} F_{(2)}^{i_3 i_4} A_{(1)}^{i_5 i_6} - g F_{(2)} A_{(1)} A_{(1)} A_{(1)} + \frac{2}{5} g^2 A_{(1)} A_{(1)} A_{(1)} A_{(1)} A_{(1)} \right) \quad (4.70)$$

where the wedge products in the Chern-Simon terms (second line) are understood and the potential can be written in the compact form,

$$P(T_{ij}) = \frac{1}{2} g^2 (2T_{ij} T_{ji} - T_{ii}^2) . \quad (4.71)$$

The system (4.70) is a consistent bosonic truncation of  $\mathcal{N} = 8$  supergravity with  $SO(6)$  gauge group. We emphasize that *it is not supersymmetric* (even if fermions were to be included). This argument will be clarified in the discussion of Section 4.4. Nevertheless,  $\mathcal{L}_{SO(6)}^{(5)}$  contains three  $\mathcal{N} = 2$  bosonic truncations whose matter content is specified by the number of gauge fields [104]. In particular, we will find truncations with two vector multiplets, one vector multiplet and finally, no vector multiplets at all, just the graviphoton. The latter being the universal  $\mathcal{N} = 2$  minimal gauged supergravity. Before turning to this point we would like to make a further observation regarding the vacua of the theory. It is useful to write down the equations of motions for the scalars and also for the field strengths,

$$\begin{aligned}
D(T_{ik}^{-1}T_{jl}^{-1} \star F_{(2)}^{kl}) &= -2gT_{k[i}^{-1} \star DT_{j]k} - \frac{1}{8}\epsilon_{ijk_1\dots k_4} F_{(2)}^{k_1k_2} \wedge F_{(2)}^{k_3k_4} , \\
D(T_{ik}^{-1} \star DT_{kj}) &= -2g^2(2T_{ik}T_{jk} - T_{ij}T_{kk})\epsilon_{(5)} + T_{ik}^{-1}T_{lm}^{-1} \star F_{(2)}^{lk} \wedge F_{(2)}^{mj} \\
&\quad - \frac{1}{6}\delta_{ij} \left[ -2g^2(2T_{kl}T_{kl} - (T_{kk})^2)\epsilon_{(5)} + T_{pk}^{-1}T_{lm}^{-1} \star F_{(2)}^{lk} \wedge F_{(2)}^{mp} \right] .
\end{aligned}$$

By setting the gauge field to zero, a vacuum of the theory is provided by

$$\langle T_{ij} \rangle = \delta_{ij} . \quad (4.72)$$

The potential associated with this solution is non zero and gives a negative cosmological constant  $V = -12g^2$ . This means that an AdS solution exists in the theory. The coupling  $g$  coincides with the inverse radius of  $AdS_5$  because of the relation,

$$V(AdS_d) = -\frac{(d-2)(d-1)}{L^2} \quad \rightarrow \quad d = 5 \quad \leftrightarrow \quad V = -\frac{12}{L^2} . \quad (4.73)$$

In general, distinct vacua of the potential are labelled by the residual amount of  $SO(6)$  symmetry that they preserve. In (4.72), the symmetry preserved is maximal and this is the  $SO(6)$  invariant point of  $\mathcal{N} = 8$ . The mass of the scalars at the  $SO(6)$  invariant point are obtained by linearizing the equations of motions around this constant solution. The procedure simplifies because we have to consider group elements in  $SL(6)$  which are symmetric and close to the identity. They are of the form

$$T_{ij} = \delta_{ij} + \theta_\alpha \Lambda_{ij}^\alpha, \quad \text{with} \quad \text{Tr} \Lambda = 0 . \quad (4.74)$$

where the index  $\alpha$  runs over  $1, \dots, 20$  and the matrices  $\Lambda^\alpha$  are a subset of the generators of  $SL(6)$ . It is enough to work at first order in the variables  $\theta_\alpha$ .

Then, by expanding the r.h.s of the  $T_{ij}$  equations, we find that the  $\theta_\alpha$  have equal masses given by  $m^2 = -4g^2$ . This value corresponds to  $\Delta = 2$  operators and we will check that the scalars retained in the  $\mathcal{N} = 2$  truncations we are interested in belong to this category.

Firstly, we want to study a truncation of (4.70) with gauge group  $U(1)^3$ . In terms of the matrix  $T_{ij}$  and the one forms  $A^{ij}$ , the Lagrangian is described by the following block diagonal ansatz inside  $\mathcal{L}_{SO(6)}^{(5)}$ ,

$$T_{ij} = \mathbf{1}_{2 \times 2} \otimes \begin{pmatrix} \mathcal{X}_1 & 0 & 0 \\ 0 & \mathcal{X}_2 & 0 \\ 0 & 0 & \mathcal{X}_0 \end{pmatrix}, \quad \mathbf{1}_{2 \times 2} = \begin{pmatrix} 1 & 0 \\ 0 & 1 \end{pmatrix}, \quad (4.75)$$

$$A_{(1)}^{ij} = i\sigma_2 \otimes \begin{pmatrix} A_{(1)}^1 & 0 & 0 \\ 0 & A_{(1)}^2 & 0 \\ 0 & 0 & A_{(1)}^0 \end{pmatrix}, \quad i\sigma_2 = \begin{pmatrix} 0 & 1 \\ -1 & 0 \end{pmatrix} \quad (4.76)$$

Because  $T \in SL(6, \mathbb{R})$  the determinant of this matrix is fixed to unity and it is convenient to use the parametrization

$$\mathcal{X}_1 = e^{-\phi_1 - \phi_2}, \quad \mathcal{X}_2 = e^{-\phi_1 + \phi_2}, \quad \mathcal{X}_0 = e^{2\phi_1}. \quad (4.77)$$

The Maxwell action obtained by substituting the ansatz (4.76) in the Lagrangian (4.70) is,

$$\begin{aligned} \mathcal{L}_{SO(6)}^{(5)} \supset & -\frac{1}{2} \left( e^{2\phi_1 + 2\phi_2} \star F^1 \wedge F^1 + e^{2\phi_1 - 2\phi_2} \star F^2 \wedge F^2 + e^{-4\phi_1} \star F^0 \wedge F^0 \right) \\ & -\frac{1}{3} (F^1 \wedge F^2 \wedge A^0 + F^1 \wedge F^0 \wedge A^2 + F^2 \wedge F^0 \wedge A^1) \end{aligned} \quad (4.78)$$

In section 4.3.1 we spell out the full Lagrangian for this  $U(1)^3$  truncation. The other two truncations, previously mentioned, are  $\mathcal{N} = 2$  truncations within this model. The Lagrangian for the  $U(1)^3$  truncation will be conventionally indicated by  $\mathcal{L}^{\text{III}}$ : the upper label specifies that the gauge fields retained in the theory are three. Similarly, we define  $\mathcal{L}^{\text{II}}$  for the  $U(1)^2$  truncation and  $\mathcal{L}^{\text{I}}$  for the  $U(1)$  truncation. Their Lagrangians are explicitly written in the sections 4.3.2 and 4.3.3. In these sections we make evident the underlining  $\mathcal{N} = 2$  geometry. As we already know, because the matter fields are just vector multiplets in  $d = 5$ , the scalars will parametrize a real special manifold  $\mathcal{V}$ . It may be superfluous but we remind the reader that in the case of  $\mathcal{L}^{\text{III}}$  there are three gauge vectors but two vector multiplets, in the case of  $\mathcal{L}^{\text{II}}$  there are two gauge vectors but one vector multiplet and finally, in the case of  $\mathcal{L}^{\text{I}}$  there is just the graviphoton.

### 4.3.1 The $U(1)^3$ truncation

This is the parent truncation in  $\mathcal{N} = 8$  where three gauge fields are retained. The Einstein Hilbert action is understood,

$$e^{-1}\mathcal{L} = \mathcal{R} + \mathcal{L}_{scalars}^{\text{III}} + \mathcal{L}_{vectors}^{\text{III}} + \mathcal{L}_{CS}^{\text{III}} + \text{P}^{\text{III}} \quad (4.79)$$

and matter couplings are defined by,

$$\mathcal{L}_{scalars}^{\text{III}} = -3\partial_\mu\phi_1\partial^\mu\phi_1 - \partial_\mu\phi_2\partial^\mu\phi_2 \quad (4.80)$$

$$\mathcal{L}_{vectors}^{\text{III}} = -\frac{1}{4}\left(e^{2\phi_1+2\phi_2}F_{\mu\nu}^1F^{\mu\nu 1} + e^{2\phi_1-2\phi_2}F_{\mu\nu}^2F^{\mu\nu 2} + e^{-4\phi_1}F_{\mu\nu}^0F^{\mu\nu 0}\right)$$

$$\mathcal{L}_{CS}^{\text{III}} = +\frac{1}{4}\epsilon^{\mu\nu\rho\sigma\tau}F_{\mu\nu}^1F_{\rho\sigma}^2A_\tau^0 \quad (4.81)$$

$$\text{P}^{\text{III}} = -4c_R^2\left(e^{-2\phi_1} + e^{\phi_1+\phi_2} + e^{\phi_1-\phi_2}\right) \quad (4.82)$$

With respect to the potential  $\text{P}(T_{ij})$  written in (4.71), we prefer to use  $c_R^2$  instead of  $g^2$ . This notation makes contact with the  $\mathcal{N} = 2$  construction that we presented in Section 4.1.3. In that language, it will be clear that only the prepotentials  $P^r$  contribute to the final form of the potential (4.82). We now proceed with the  $\mathcal{N} = 2$  analysis of the Lagrangian.

The metric  $G_{xy}$  and the kinetic matrix  $a_{IJ}$  can be understood by means of the very special real geometry. This is defined as the  $n$  dimensional surface in  $\mathbb{R}^{n+1}$  satisfying the constraint,

$$C_{IJK}h^Ih^Jh^K = 1 \quad \text{with } C_{IJK} \text{ totally symmetric .} \quad (4.83)$$

In the above formula, the symbols  $h^I$ ,  $I = 0, \dots, n$  represent the coordinates of  $\mathbb{R}^{n+1}$ . In the case of  $U(1)^3$ , the  $C_{IJK}$  tensor can be taken all but  $C_{012}$  equal to zero. In particular the embedding is given by

$$C_{012} = \frac{\sqrt{3}}{2}, \quad \begin{cases} h^0 = e^{2\phi_1}/\sqrt{3} \\ h^1 = e^{-\phi_1-\phi_2}/\sqrt{3} \\ h^2 = e^{-\phi_1+\phi_2}/\sqrt{3} \end{cases} \quad (4.84)$$

We note that using the ansatz  $C_{012} \neq 0$ , the following formulas can be deduced,

$$i = 1, 2, 3 \quad a_{II} = \frac{1}{3} \left( \frac{1}{h^I} \right)^2, \quad (4.85)$$

$$i \neq j \quad a_{ij} = -2C_{ijk} h^k (1 - 6 C_{012} h^0 h^1 h^2), \quad (4.86)$$

$$x = 1, 2 \quad G_{xx} = \frac{1}{2} \sum_{I=0}^3 \left( \frac{\partial_x h^I}{h^I} \right)^2, \quad (4.87)$$

$$g_{12} = 0. \quad (4.88)$$

The kinetic matrix  $a_{IJ}$  is diagonal because of the relation  $C_{IJK} h^I h^J h^k = 1$  and the diagonal entries are given by,

$$a_{00} = e^{-4\phi_1}, \quad a_{11} = e^{2\phi+2\phi_2}, \quad a_{22} = e^{2\phi_1-2\phi_2}. \quad (4.89)$$

The induced metric  $G_{xy}$  is also diagonal and it is straightforward to show that

$$G_{11} = 3, \quad G_{22} = 1. \quad (4.90)$$

As a result, the kinetic term in  $\mathcal{L}_{scalars}^{\text{III}}$  agrees with the one obtained from  $\mathcal{L}_{scalars}^{(5)}$ . We now consider  $\mathcal{L}_{vectors}^{(5)}$  and for convenience we use the same notation of  $\mathcal{N} = 8$  indicating with  $(A^0, A^1, A^2)$  the three gauge fields. The redefinition  $A^I \rightarrow A^I/\sqrt{2}$  fixes the kinetic matrix in  $\mathcal{L}_{vectors}^{(5)}$  to the canonical form and the coefficient of the Chern-Simon term becomes

$$\left( \frac{1}{\sqrt{2}} \right)^3 \frac{1}{3\sqrt{6}} C_{IJK} \epsilon^{\mu\nu\rho\sigma\tau} F_{\mu\nu}^I F_{\rho\sigma}^J A_\tau^K = \frac{1}{4} \epsilon^{\mu\nu\rho\sigma\tau} F_{\mu\nu}^1 F_{\rho\sigma}^2 A_\tau^0. \quad (4.91)$$

The scalar potential can be deduced from the general formula (4.20) where the prepotentials  $\mathcal{P}^r$ ,  $r = 1, 2, 3$ , are taken to be Fayet-Iliopoulos constants,  $\vec{\mathcal{P}}_I = \mathfrak{f} (0, 0, 1)$ ,  $I = 0, 1, 2$ . Then, we have

$$P^3 = +\frac{\mathfrak{f}}{\sqrt{3}} \left( e^{2\phi_1} + e^{-\phi_1+\phi_2} + e^{-\phi_1-\phi_2} \right), \quad (4.92)$$

$$P_1^3 = -\frac{\mathfrak{f}}{\sqrt{2}} \left( 2e^{2\phi_1} - e^{-\phi_1+\phi_2} - e^{-\phi_1-\phi_2} \right), \quad (4.93)$$

$$P_2^3 = -\frac{\mathfrak{f}}{\sqrt{2}} \left( e^{-\phi_1+\phi_2} - e^{-\phi_1-\phi_2} \right). \quad (4.94)$$

We remark that  $P_1^3 = P_2^3 = 0$  iff  $\phi_1 = 0$  and  $\phi_2 = 0$ . An easy calculation shows that the potential (4.20) is given by,

$$\begin{aligned} V(\phi_1, \phi_2) = -2P^3 P^3 + P_x^3 P_y^3 G^{xy} &= -2P^3 P^3 + \frac{1}{3} P_1^3 P_1^3 + P_2^3 P_2^3 \quad (4.95) \\ &= -2 \mathfrak{f}^2 \left( e^{-2\phi_1} + e^{\phi_1+\phi_2} + e^{\phi_1-\phi_2} \right). \end{aligned}$$

The constant  $f$  can be adjusted so that (4.95) reproduces  $P^{\text{III}}$ .

### 4.3.2 The $U(1)^2$ truncation

Starting from  $\mathcal{L}^{\text{III}}$ , it is possible to truncate to  $U(1)^2$  by identifying two of the gauge fields,  $A^1 = A^2 = A/\sqrt{2}$  (along with  $F_{\mu\nu}^1 = F_{\mu\nu}^2 = F_{\mu\nu}/\sqrt{2}$ ). Consistency of the truncation requires a vanishing  $\phi_2$ . The result is,

$$\mathcal{L}_{scalars}^{\text{II}} = -3\partial_\mu\phi_1\partial^\mu\phi_1 \quad (4.96)$$

$$\mathcal{L}_{vectors}^{\text{II}} = -\frac{1}{4}\left(e^{2\phi_1}F_{\mu\nu}F^{\mu\nu} + e^{-4\phi_1}F_{\mu\nu}^0F^{\mu\nu 0}\right) \quad (4.97)$$

$$\mathcal{L}_{CS}^{\text{II}} = +\frac{1}{8}\epsilon^{\mu\nu\rho\sigma\tau}F_{\mu\nu}F_{\rho\sigma}A_\tau^0 \quad (4.98)$$

$$P^{\text{II}} = -4c_R^2\left(e^{-2\phi_1} + 2e^{\phi_1}\right) \quad (4.99)$$

The  $\mathcal{N} = 2$  analysis is similar to that of  $\mathcal{L}^{\text{III}}$  but formulas are slightly modified. In this case, the real geometry is given by,

$$C_{011} = \frac{\sqrt{3}}{4}, \quad \begin{cases} h^0 = e^{2\phi_1}/\sqrt{3} \\ h^1 = 2e^{-\phi_1}/\sqrt{3} \end{cases} \quad (4.100)$$

The kinetic matrix  $a_{IJ}$  is again diagonal with entries,

$$a_{00} = \frac{1}{3}\left(\frac{1}{h^0}\right)^2 = e^{-4\phi_1}, \quad a_{11} = \frac{2}{3}\left(\frac{1}{h^1}\right)^2 = \frac{1}{2}e^{2\phi_1}. \quad (4.101)$$

Similarly to the case of the  $U(1)^3$  truncation, the non diagonal term  $a_{12}$  vanishes because of the relation  $3C_{011}h^0h^1h^1 = 1$ . The same relation has been used to obtain the coefficient  $2/3$  in front of  $a_{11}$ . The notation for the gauge fields again follows that of  $\mathcal{N} = 8$  and we only need to rescale  $A^0 \rightarrow A^0/\sqrt{2}$  in order for  $\mathcal{L}_{vectors}^{(5)}$  to agree with  $\mathcal{L}_{vectors}^{\text{II}}$ . The Chern-Simon term also matches and is given by

$$\left(\frac{1}{\sqrt{2}}\right)\frac{1}{3\sqrt{6}}C_{IJK}\epsilon^{\mu\nu\rho\sigma\tau}F_{\mu\nu}^IF_{\rho\sigma}^JA_\tau^K = \frac{1}{8}\epsilon^{\mu\nu\rho\sigma\tau}F_{\mu\nu}F_{\rho\sigma}A_\tau^0 \quad (4.102)$$

The metric on the scalar manifold reduces to

$$G_{11} = \frac{1}{2}\left(\frac{\partial_1 h^0}{h^0}\right)^2 + \left(\frac{\partial_1 h^1}{h^1}\right)^2 = 3. \quad (4.103)$$

By considering Fayet-Iliopoulos constants,  $\vec{\mathcal{P}}_I = \mathfrak{f} (0, 0, 1)$ ,  $I = 0, 1, 2$ , the prepotentials and the potential can be easily found. A calculation equivalent to that of the  $U(1)^3$  truncation shows that,

$$P^3 = +\frac{\mathfrak{f}}{\sqrt{3}} \left( e^{2\phi_1} + 2e^{-\phi_1} \right) \quad (4.104)$$

$$P_1^3 = -\mathfrak{f}\sqrt{2} \left( e^{2\phi_1} - e^{-\phi_1} \right) \quad (4.105)$$

$$V(\phi_1) = -2P^3P^3 + P_x^3P_y^3G^{xy} = -2\mathfrak{f}^2 \left( e^{-2\phi_1} + 2e^{\phi_1} \right) \quad (4.106)$$

### 4.3.3 The minimal gauged $\mathcal{N} = 2$ supergravity

The truncation given by  $\mathcal{L}^{\text{II}}$  is not the whole story. It is indeed possible to retain just the graviton multiplet. The resulting theory is the minimal gauged  $\mathcal{N} = 2$  supergravity: the gauge group reduces to a single  $U(1)$  and there are no matter fields. We can obtain this theory from  $\mathcal{L}^{\text{III}}$  by considering the identification  $A^0 = A^1 = A^2 = A/\sqrt{3}$ . The consistency of the truncation requires  $\phi_1 = 0$  and  $\phi_2 = 0$ . The Lagrangian is

$$\mathcal{L}^{\text{I}} = \mathcal{R} - \frac{1}{4}F_{\mu\nu}F^{\mu\nu} + \frac{1}{12\sqrt{3}}\epsilon^{\mu\nu\rho\sigma\tau}F_{\mu\nu}F_{\rho\sigma}A_\tau + 12 \quad (4.107)$$

We can also obtain (4.107) from  $\mathcal{L}^{\text{II}}$ . In this case, first we need to consider  $A^0 = A/\sqrt{2}$ , then we have to normalize the gauge field in order to have a canonical kinetic term, i.e  $A \rightarrow \sqrt{2/3} A$ . The Chern-Simon term becomes,

$$\mathcal{L}_{CS}^{\text{II}} \rightarrow \frac{1}{8}\epsilon^{\mu\nu\rho\sigma\tau}F_{\mu\nu}F_{\rho\sigma} \left( \frac{1}{\sqrt{2}}A_\tau \right) \quad (4.108)$$

$$\rightarrow \frac{1}{8\sqrt{2}} \left( \sqrt{\frac{2}{3}} \right)^3 \epsilon^{\mu\nu\rho\sigma\tau}F_{\mu\nu}F_{\rho\sigma}A_\tau \quad (4.109)$$

and the coefficient equals the one given in (4.107).

The scalar manifold  $\mathcal{V}$  is trivial without the presence of vector multiplets and the relation  $C_{IJK}h^Ih^Jh^K = 1$  reduces to a single non trivial component,  $C_{000} = 1$ . It follows that  $h^0 = 1$  and  $a_{00} = 1$ . The coefficient of the Chern-Simon term, obtained from  $\mathcal{L}_{\text{vectors}}^{(5)}$ , matches that of (4.107) after the correct normalization of the gauge field. In this case the normalization of the  $\mathcal{N} = 2$  gauge field  $A$  is  $A \rightarrow A/\sqrt{2}$ . The resulting Chern-Simon term is,

$$\mathcal{L}_{CS}^{(5)} = \left( \frac{1}{\sqrt{2}} \right)^3 \frac{1}{3\sqrt{6}}\epsilon^{\mu\nu\rho\sigma\tau}F_{\mu\nu}F_{\rho\sigma}A_\tau = \frac{1}{12\sqrt{3}}\epsilon^{\mu\nu\rho\sigma\tau}F_{\mu\nu}F_{\rho\sigma}A_\tau. \quad (4.110)$$

## 4.4 The Incomplete Hypermultiplets

In this section we go back to the original  $\mathcal{N} = 8$  supergravity. The truncation described by  $\mathcal{L}_{SO(6)}$  is a consistent bosonic truncation with gauge group  $SO(6)$  and scalars in the adjoint. We have also proven that this model contains three abelian  $\mathcal{N} = 2$  supergravities given by  $\mathcal{L}^{III}$ ,  $\mathcal{L}^{II}$  and  $\mathcal{L}^I$ . In this framework, the scalars of the two vector multiplets have a simple embedding in terms of the matrix  $T_{ij}$ , in fact they are described by a diagonal matrix with entries  $X_1$ ,  $X_2$  and  $X_3$ , as defined in (4.77). This is a very nice result and we would like to see how this story is modified by the introduction of charged scalars.

From the  $\mathcal{N} = 2$  perspective it is natural to expect that the  $T_{ij}$  matrix has enough room to accommodate not only real scalars coming from vector multiplets but also complex scalars coming from hypermultiplets. Then, it should be possible to work out the couplings of this new theory by means of the  $\mathcal{N} = 2$  machinery. This idea is formalized by the following consideration. The field content of  $\mathcal{N} = 8$  supergravity can be decomposed into  $\mathcal{N} = 2$  multiplets under  $SU(3) \times U(1)$ , which is a subgroup of the full  $R$  symmetry group. The result of this branching is given in Table 4.1 and we can check with group theory arguments what  $\mathcal{N} = 2$  theories are expected to appear as consistent truncations within  $\mathcal{L}_{SO(6)}$ .

The analysis of Table 4.1 has two main outcomes. The first one is that the  $U(1)^3$  truncation, corresponding to  $\mathcal{L}^{III}$ , is obtained by retaining two out of the **8** vector multiplets that live in  $\mathcal{N} = 8$ . As a concrete example, we observe that the representation **8** of  $SU(3)$  is indeed the adjoint representation of  $SU(3)$ . In this case a complete set of generators is given in terms of the Gell-Mann matrices and the two diagonal generators are,

$$\Lambda_3 = \begin{pmatrix} 1 & 0 & 0 \\ 0 & -1 & 0 \\ 0 & 0 & 0 \end{pmatrix}, \quad \Lambda_8 = \frac{1}{\sqrt{3}} \begin{pmatrix} 1 & 0 & 0 \\ 0 & 1 & 0 \\ 0 & 0 & -2 \end{pmatrix} \quad (4.111)$$

The embedding of these two elements into the  $T_{ij}$  matrix is straightforward and the result is given in (4.75). We also observe that, by expanding the matrix  $T_{ij}$  for small  $\phi_1$  and  $\phi_2$ , we find the correspondence,

$$\Lambda_3 \otimes \mathbf{1}_{2 \times 2} \leftrightarrow \phi_1 \quad \Lambda_8 \otimes \mathbf{1}_{2 \times 2} \leftrightarrow \phi_2 \quad (4.112)$$

The second observation is that  $\mathcal{L}_{SO(6)}$  is not a supersymmetric truncation. To show this claim we consider the representation **20** of  $SO(6)$  and the splitting  $\mathbf{8} \oplus \mathbf{6} \oplus \bar{\mathbf{6}}$ . On one hand the scalars parametrizing the  $T_{ij}$  matrix have masses

| $\mathcal{N} = 2$ multiplet | fields                                    | $\Delta$ values                               | $SU(3) \times U(1)$  |
|-----------------------------|---|---|--|
| Graviton                    | $(g_{\mu\nu}, \psi_\mu, A_\mu)$           | $\left(4, \frac{7}{2}, 3\right)$              | $(\mathbf{1}_0, \mathbf{1}_{\pm 1}, \mathbf{1}_0)$   |
| Gravitino                   | $(\psi_\mu, A_\mu, B_{\mu\nu}, \lambda)$  | $\left(\frac{7}{2}, 3, 3, \frac{5}{2}\right)$ | $(\mathbf{3}_{\frac{1}{3}}, \mathbf{3}_{\frac{4}{3}}, \mathbf{3}_{-\frac{2}{3}}, \mathbf{3}_{\frac{1}{3}}) + \text{cc.}$   |
| Vector                      | $(A_\mu, \lambda, \phi)$                  | $\left(3, \frac{5}{2}, 2\right)$              | $(\mathbf{8}_0, \mathbf{8}_{\pm 1}, \mathbf{8}_0)$   |
| Tensor                      | $(\lambda, B_{\mu\nu}, \varphi, \lambda)$ | $\left(\frac{7}{2}, 3, 3, \frac{5}{2}\right)$ | $(\mathbf{3}_{\frac{1}{3}}, \mathbf{3}_{-\frac{2}{3}}, \mathbf{3}_{-\frac{2}{3}}, \mathbf{3}_{-\frac{4}{3}}) + \text{cc.}$ |
| Hypermatter (1)             | $(\varphi, \zeta, \varphi)$               | $\left(3, \frac{5}{2}, 2\right)$              | $(\mathbf{6}_{\frac{2}{3}}, \mathbf{6}_{-\frac{2}{3}}, \mathbf{6}_{-\frac{4}{3}}) + \text{cc.}$                            |
| Hypermatter (2)             | $(\varphi, \zeta, \varphi)$               | $\left(4, \frac{7}{2}, 3\right)$              | $(\mathbf{1}_0, \mathbf{1}_{-1}, \mathbf{1}_{-2}) + \text{cc.}$  |

Table 4.1: The field content of  $\mathcal{N} = 8$  written in terms of  $\mathcal{N} = 2$  multiplets under  $SU(3) \times U(1) \supset SU(4)$ . Adapted from [105].

$m^2 = -4g^2$ , on the other hand the representation  $\mathbf{6}$ , which describes operators with dimension  $\Delta = 2$  and therefore bulk scalars with mass  $m^2 = -4g^2$ , corresponds only to half of an hypermultiplet. Unfortunately, there are no hypermultiplets inside the  $T_{ij}$ .

Even if it is not possible to consider the embedding of a full hypermultiplet into the bosonic  $\mathcal{L}_{SO(6)}$ , it is still possible to find charged scalars in the  $T_{ij}$  matrix. Indeed, at the level of generators it is clear how to construct such charged scalars. By looking at the covariant derivative

$$dT_{ij} + gA_{(1)}^{ik}T_{kj} - gT_{ik}A_{(1)}^{kj} \sim dT + g[A, T] \quad (4.113)$$

we understand that charged scalars are associated with generators  $\Lambda_\alpha$ , of the form (4.74), whose commutator with  $A$  is non zero:  $[A, \Lambda_\alpha] \neq 0$ . In terms of the anti-symmetric matrix  $A_{(1)}^{ij}$ , the  $U(1)^3$  gauge fields are represented by a block diagonal ansatz in which each of the three blocks is proportional to  $i\sigma_2$ . Then, the scalars  $\mathcal{X}_i$  are proportional to the identity and for this reason they are neutral. Within the block diagonal ansatz implemented for the  $\mathcal{X}_i$ , we can find charged scalars either in the case  $\Lambda_\alpha = \sigma_1$  or in the case  $\Lambda_\alpha = \sigma_3$ . The underlying scalar manifold is  $SL(2)/SO(2)$ . Two nice parametrizations are the

following:

$$\mathcal{M}^{(1)} = e^{-i\sigma_2\theta/2} e^{\sigma_1\eta} e^{+i\sigma_2\theta/2} \quad (4.114)$$

or

$$\mathcal{M}^{(3)} = e^{-i\sigma_2\theta/2} e^{\sigma_3\eta} e^{+i\sigma_2\theta/2} \quad (4.115)$$

We observe that the condition  $\det\mathcal{M}^{(1)} = 1$  is ensured because of the product rule of the determinant. The same holds for  $\mathcal{M}^{(3)}$ . It is also easy to check that at first order in  $\eta$  the matrix  $\mathcal{M}^{(1)}$  is generated by  $\sigma_1$  whereas  $\mathcal{M}^{(3)}$  is generated by  $\sigma_3$ . In terms of a complex scalar,  $\eta$  represents a radial coordinate and  $\theta$  the relative phase. The most general block diagonal  $T_{ij}$  matrix is then,

$$T_{ij} = \begin{pmatrix} \mathcal{X}_1\mathcal{M}_1 & 0 & 0 \\ 0 & \mathcal{X}_2\mathcal{M}_2 & 0 \\ 0 & 0 & \mathcal{X}_0\mathcal{M}_0 \end{pmatrix} \quad (4.116)$$

where  $\mathcal{M}_i$  is one of the two matrices  $\mathcal{M}^{(1)}$  or  $\mathcal{M}^{(3)}$  and the lower label refers to the independent pairs  $\{\eta_i, \theta_i\}$ ,  $i = 0, 1, 2$ , each one parametrizing a single charged scalar. It is also clear that each  $\eta_i$  will be charged with respect to the corresponding gauge field  $A^i$ . The Lagrangian which follows from  $\mathcal{L}_{SO(6)}$  is a generalization of  $\mathcal{L}^{\text{III}}$  [105, 12]. Here we consider just the modified pieces: the scalar sector and the new potential are,

$$\mathcal{L}_{scalars}^{\text{III}} = -3\partial_\mu\phi_1\partial^\mu\phi_1 - \partial_\mu\phi_2\partial^\mu\phi_2 \quad (4.117)$$

$$-\frac{1}{2} \sum_{a=1}^3 [(\partial\eta_a)^2 + \sinh^2\eta_a(\partial\theta_a - 2gA_a)^2]$$

$$P^{\text{III}} = 2g^2 \left( \sum_{i=0}^2 (\mathcal{X}_i \sinh \eta_i)^2 - 2 \sum_{i<j} \mathcal{X}_i \mathcal{X}_j \cosh \eta_i \cosh \eta_j \right) \quad (4.118)$$

The choice of parametrization is not important,  $\mathcal{M}^{(1)}$  or  $\mathcal{M}^{(3)}$  lead to the same result. The other contributions to the full Lagrangian are the ones of  $\mathcal{L}^{\text{III}}$ . In particular, the kinetic matrix for field strengths and the Chern-Simon term remain unvaried. We note that the complex scalars have equal charges  $q_i = 2$ ,  $i = 0, 1, 2$  and these agree with the  $U(1)$  quantum numbers given in Table 4.1.

By looking at the parametrizations (4.114) and (4.115) we also understand the form of the potential  $P^{\text{III}}$ . In fact, by considering the cyclic property of the trace it is evident that the potential does not depend upon the phases  $\theta_i$  and the full calculation reduces to a combination of

$$\text{Tr } \mathcal{M} = \text{Tr } e^{\sigma_1\eta} = \text{Tr } e^{\sigma_3\eta} = 2 \cosh \eta, \quad (4.119)$$

$$\text{Tr } \mathcal{M}^2 = \text{Tr } e^{2\sigma_1\eta} = \text{Tr } e^{2\sigma_3\eta} = 2 \cosh 2\eta. \quad (4.120)$$

| SYM operator                       | desc       | SUGRA   | $\Delta$          | spin                         | $SU(4)$     |
|------------------------------------|------------|---|-------------------|------------------------------|-------------|
| $\text{tr}X^k$ $k \geq 2$          | -          | $h_\alpha^\alpha$ and $C_{\alpha\beta\gamma\delta}$ | $k$               | $(0, 0)$                     | $[0, k, 0]$ |
| $\text{tr}\lambda X^k$ $k \geq 1$  | $Q$        | fermion d.o.f.                                      | $k + \frac{3}{2}$ | $(\frac{1}{2}, 0)$           | $[1, k, 0]$ |
| $\text{tr}\lambda\lambda X^k$      | $Q^2$      | $C_{\alpha\beta}$                                   | $k + 3$           | $(0, 0)$                     | $[2, k, 0]$ |
| $\text{tr}\lambda\bar{\lambda}X^k$ | $Q\bar{Q}$ | $h_{\mu\alpha}$ and $C_{\mu\alpha\beta\gamma}$      | $k + 3$           | $(\frac{1}{2}, \frac{1}{2})$ | $[1, k, 1]$ |
| $\text{tr}FX^k$ $k \geq 1$         | $Q^2$      | $C_{\mu\nu}$  | $k + 2$           | $(1, 0)$                     | $[0, k, 0]$ |

Table 4.2: Example of SYM operators that belong to a definite superconformal multiplet with chiral primary operator  $\text{tr}X^k$   $k \geq 2$ . The range of  $k$  is  $k \geq 0$ , unless otherwise specified. We have defined  $h_{ij}$  as the ten dimensional metric in type IIB supergravity. Indexes  $\alpha, \beta, \gamma, \delta$  label the compact coordinates of the five-sphere. Other greek indexes label  $\text{AdS}_5$  directions. The form gauge fields are  $C_{(4)}$  and  $C_{(2)}$ . Adapted from [38].

When the charged scalars vanish,  $\eta_i = 0$   $i = 0, 1, 2$ , we recover the potential (4.82) written in terms of the  $\mathcal{X}_i$ .

$$P^{\text{III}} = -4g^2 (\mathcal{X}_1\mathcal{X}_2 + \mathcal{X}_1\mathcal{X}_3 + \mathcal{X}_2\mathcal{X}_3) . \quad (4.121)$$

## 4.5 Connecting with $\mathcal{N} = 4$ SYM

It is our interest to understand what dual field theory operators  $\mathcal{L}_{scalars}^{\text{III}}$  is describing. For this purpose, it is convenient to reconsider  $\mathcal{N} = 4$  SYM and in particular, the list of operators given in Table 2.2. As we will see, the matrix  $T_{ij}$  introduced in the previous sections makes the direct link among type IIB theory compactified on  $\text{AdS}_5 \times S^5$ ,  $\mathcal{N} = 4$  SYM and  $\mathcal{N} = 8$  supergravity in five dimensions.

We recall some basic facts about  $\mathcal{N} = 4$  SYM [2]. The R-symmetry group is  $SU(4)$  which is a cover of  $SO(6)$ . The theory has an  $SU(N)$  gauge field, **6** real scalar transforming as a vector of  $SO(6)$  and four Weyl fermions  $\lambda_\alpha^A$  transforming in the **4** of  $SU(4)$ . From the point of view of an  $\mathcal{N} = 1$  sub-algebra of the supersymmetry algebra, these fields can be assembled into three

chiral superfields  $\Phi^i$  with  $i = 1, 2, 3$  and a single gauge vector multiplet. The lowest component of each  $\Phi^i$  is thus a complex scalar field built out of two real scalar fields  $X^i$ . The superpotential is  $W = \epsilon_{ijk} \Phi^i [\Phi^j, \Phi^k]$  and in order to have the right  $R$ -charge assignment,  $R[W] = 2$ , we need  $R[\Phi^i] = 2/3$  for each  $i = 1, 2, 3$ .

The chiral primary operator that appears in Table 4.2 belongs to the class of operators defined by  $\mathcal{T}^{i_1 \dots i_k} = \text{tr}(\Phi^{i_1} \dots \Phi^{i_k})$  with  $k \geq 2$ . The indexes  $\{i_1, \dots, i_k\}$  are symmetrized so to ensure that descendants will not show up. Indeed, without this expedient, a descendant may appear in  $\mathcal{T}^{i_1 \dots i_k}$  because of the fact that the commutators  $[\Phi^i, \Phi^j]$  are derivatives of the superpotential  $W$ . The  $R$  charge of  $\mathcal{T}^{i_1 \dots i_k}$  is  $k$  times that of  $\Phi$ . Furthermore, these operators have (protected) dimension equals to  $k$  which implies a dual bulk mass equals to  $m^2 L^2 = k(k-4)$ . The most familiar description of  $\mathcal{T}^{i_1 \dots i_k}$  is perhaps given in terms of  $SO(6)$  symmetry. Then, the chiral operators we are considering are symmetric traceless tensors  $\mathcal{T}^{a_1, \dots, a_k}$  of order  $k$  and Dinkin label  $[0, k, 0]$ . For  $k = 2$  this representation has dimension **20** and the dual masses are  $m^2 L^2 = -4$ . We conclude that the  $T_{ij}$  bulk scalars correspond to

$$\text{tr} X^i X^j - \frac{1}{6} \delta^{ij} \text{tr} \sum_i (X^i)^2 . \quad (4.122)$$

However, since  $\mathcal{L}_{scalars}^{\text{III}}$  contains two real scalars  $\phi_1, \phi_2$  and three complex scalar  $(\eta_i, \theta_i)$  with  $i = 1, 2, 3$ , it would be more appropriate to use the complex basis  $\mathcal{T}^{ij} = \text{tr} \Phi^i \Phi^j$ . In particular, the three  $\Phi^i$  can be understood as a representation of  $SU(3)$  and we can rely on the decomposition given in Table 4.1,

$$\mathbf{20} = \mathbf{6} \oplus \bar{\mathbf{6}} \oplus \mathbf{8} .$$

Then, the product representations we are interested in are [44]

$$\mathbf{3} \otimes \mathbf{3} = \bar{\mathbf{3}}_A \oplus \mathbf{6}_S, \quad \bar{\mathbf{3}} \otimes \mathbf{3} = \mathbf{1} \oplus \mathbf{8} . \quad (4.123)$$

We notice that the adjoint of  $SU(3)$  is mapped to Gell-Mann matrices representation that we have already mentioned. The representation  $\mathbf{6}_S$  is given by

$$\text{tr}(\Phi^i)^2 \text{ with } i = 1, 2, 3, \quad \left\{ \begin{array}{l} \text{tr} \Phi^1 \Phi^2 \\ \text{tr} \Phi^1 \Phi^3 \\ \text{tr} \Phi^2 \Phi^3 \end{array} \right. \quad (4.124)$$

and its complex conjugate is obtained by the substitution  $\Phi \rightarrow \bar{\Phi}$ . The above operators may be understood as  $\text{tr}(\Phi^i S^{ij} \Phi^j)$  with  $S^{ij}$  a  $3 \times 3$  symmetric matrix.

This matrix makes the link with the tensor decomposition of  $T_{ij}$ . Indeed, on the gravity side, the charged scalar is obtained by considering the tensor product  $(SL(2)/SO(2)) \otimes S^{ij}$  and we conclude that the dual operator of the complex scalar  $(\eta_i, \theta_i)$  is  $\text{tr}(\Phi^i)^2$  for each  $i = 1, 2, 3$ . The  $R$  charge is  $R[(\Phi^i)^2] = 4/3$  and matches the  $U(1)$  quantum number given in Table 4.1.

The representation  $\mathbf{8}$  can be understood with a similar reasoning by considering operators of the form  $\text{tr}(\Phi^i \Lambda^{ij} \bar{\Phi}^j)$ . These are real and therefore their  $R$ -charge vanishes. In a given basis, the two Gell-Mann matrices  $\Lambda^{ij} = \Lambda_3, \Lambda_8$  define the operators dual to  $\phi_1$  and  $\phi_2$ . Explicitly, they are

$$\text{tr}(|\Phi^1|^2 + |\Phi^2|^2 - 2|\Phi^3|^2), \quad \text{tr}(|\Phi^1|^2 - |\Phi^2|^2) \quad (4.125)$$

As we have already seen, on the gravity side, these two operators are mapped to the tensor products of  $\Lambda_3 \otimes \mathbf{1}_{2 \times 2}$  and  $\Lambda_8 \otimes \mathbf{1}_{2 \times 2}$ . Sometimes in the literature they are written in terms of the real scalar fields  $X^i$ . The change of variable is quite immediate and the result is

$$\mathcal{T}_{\phi_1} = \text{tr}(X_1^2 + X_2^2 + X_3^2 + X_4^2 - 2X_5^2 - 2X_6^2), \quad (4.126)$$

$$\mathcal{T}_{\phi_2} = \text{tr}(X_1^2 + X_2^2 - X_3^2 - X_4^2). \quad (4.127)$$

# Chapter 5

## Hair in 5D $\mathcal{N} = 8$ Supergravity

Phenomenological models of holographic superconductivity have shown a variety of interesting phenomena. We have been able to engineer first order phase transitions, non standard critical exponents and Hall currents by tuning the functional form of a certain set of couplings that define the bulk Lagrangian. In this chapter we go beyond that approach looking for holographic superconductivity in supergravity and string theory. This is the so called “top-down” approach that in principle will provide a precise understanding of the “Cooper pair” state by means of the exact AdS/CFT mapping.

Matter couplings in supergravity have been introduced in the previous chapter. Here, we will see special geometries at work by considering vector multiplets coupled to charged scalars. The theory is an abelian gauge theory with three gauge bosons coupled to two neutral scalars coming from the vector multiplets and several  $SU(1, 1)/U(1)$  charged scalar. Black holes with finite charge density and neutral scalars turned on are usually called dilatonic black holes<sup>1</sup>. They differ substantially from the Reissner-Nördstrom black hole and some of them are better suited for condensed matter applications. Therefore, it is our interest to extend the phase diagrams of these theories looking for superconducting states. The outcome of our analysis will be quite counter intuitive with respect to our understanding based on the study of phenomenological models. For example, we will find condensates that only exists for temperatures above a certain critical temperature, the so called *retrograde* condensate.

---

<sup>1</sup>These geometries are the “STU” black holes in five dimensions first discovered by []. Sometimes the name “STU” is also referred to the three charged scalars that describe the special special Kähler geometry  $SU(1, 1)/U(1) \otimes SO(2, 2)/(SO(2) \times SO(2))$ .

## 5.1 Dilatonic Black Holes

Our starting point is the  $U(1)^3$  truncation presented in section 4.3. The uncondensed phase of this theory is defined, as usual, by considering the set of solutions, either extremal or thermal, with vanishing charged scalars. Concretely, the first task of this section is the search for black hole solutions which are a generalization of the AdS Reissner-Nördstrom black hole. In this context, we expect a couple of basic novelties. First, a generic solution will carry different charges depending on the configuration of the gauge fields. Second, even if the charged scalars are identically zero in the bulk, the dilaton fields  $\phi_1$  and  $\phi_2$  are necessarily switched on because of the couplings with the field strengths, i.e. because of the kinetic matrix  $a_{IJ}$ .

It is useful to write down the equations of motions for the matter fields. The set of Maxwell equations is,

$$\nabla^\mu (e^{-4\phi_1} F_{\mu\nu}^0) = 0 \quad (5.1)$$

$$\nabla^\mu (e^{2\phi_1+2\phi_2} F_{\mu\nu}^1) = 0 \quad (5.2)$$

$$\nabla^\mu (e^{2\phi_1-2\phi_2} F_{\mu\nu}^2) = 0 \quad (5.3)$$

and the equations for the two dilatons  $\phi_1$  and  $\phi_2$  are,

$$\nabla_\mu \nabla^\mu \phi_1 - \frac{1}{12} e^{2\phi_1} (e^{2\phi_2} F^1 F^1 + e^{-2\phi_2} F^2 F^2 - 2e^{-6\phi_1} F^0 F^0) = \frac{1}{6} \partial_1 \text{P}^{\text{III}} \quad (5.4)$$

$$\nabla_\mu \nabla^\mu \phi_2 - \frac{1}{4} e^{2\phi_1} (e^{2\phi_2} F^1 F^1 - e^{-2\phi_2} F^2 F^2) = \frac{1}{2} \partial_2 \text{P}^{\text{III}} \quad (5.5)$$

We used the notation  $F^i F^i \equiv F_{\mu\nu}^i F^{\mu\nu i}$  and  $\partial_i = \partial/(\partial\phi_i)$ . It is evident that the field strengths  $F^1$ ,  $F^2$  and  $F^0$  effectively source the equations of motion for the two scalars. Finally we also have,

$$\partial_1 \text{P}^{\text{III}} = -4c_R^2 (-2e^{-2\phi_1} + e^{\phi_1+\phi_2} + e^{\phi_1-\phi_2}) \quad (5.6)$$

$$\partial_2 \text{P}^{\text{III}} = -4c_R^2 (e^{\phi_1+\phi_2} - e^{\phi_1-\phi_2}) \quad (5.7)$$

The family of black holes that we want to investigate asymptote an *AdS* vacuum. In our case this vacuum is provided by the  $SO(6)$  fixed point of  $\mathcal{N} = 8$  supergravity, which corresponds to  $\phi_1 = 0$  and  $\phi_2 = 0$  and all the gauge fields set to zero. The value of the cosmological constant,  $\text{P}^{\text{III}}(0) = -12c_R^2$ , fixes the normalization of the constant  $c_R$ . We define  $c_R = 1/L$ , where  $L$  is the radius of  $\text{AdS}_5$ . In the previous chapter we have proven that the masses of the

scalars in the  $\mathbf{20}'$  are fixed to the value  $m^2 L^2 = -4$ . It is a simple calculation to check this result in the case of  $\phi_1$  and  $\phi_2$ . Indeed,

$$\frac{1}{6}\partial_1 \text{P}^{\text{III}} = -\frac{4}{L^2}\phi_1 + \dots, \quad \frac{1}{2}\partial_2 \text{P}^{\text{III}} = -\frac{4}{L^2}\phi_2 + \dots \quad (5.8)$$

We remind the reader the logic of the AdS/CFT correspondence in relation to our condensed matter studies. Given a certain theory, our first goal is to find black hole solutions in which gauge fields of the electric type have non trivial profile in the bulk, namely  $A^i = \Phi^i(r)dt$ . Concretely we will consider a metric of the form,

$$ds^2 = g_{\mu\nu}dx^\mu dx^\nu = e^{C(r)} \left( -f(r)e^{-\chi(r)} dt^2 + r^2 d\vec{x}^2 + \frac{dr^2}{f(r)} \right). \quad (5.9)$$

The Reissner-Nördstrom black hole is the simplest example we have studied. In the dual field theory, this charged black hole was found to describe a state with finite charge density. In particular, the charge density and the chemical potential are read from the asymptotics of the gauge field according to the discussion of section 3.6. In the present case, we are considering a truncation of  $\mathcal{N} = 8$  supergravity which retains three gauge field. Then, in the dual field theory, we can turn on at most three chemical potentials  $\mu_1, \mu_2, \mu_3$ , each one corresponding to its  $\Phi^i(r)$ ,  $i = 1, 2, 3$  bulk gauge field. Taking into account the equations of motions, the three gauge field source the two neutral scalar field and therefore we expect that  $\phi_1(r)$  and  $\phi_2(r)$  have a non trivial profile in the bulk. This is the main difference with respect to the Reissner-Nördstrom black hole: having a vector multiplet interaction implies that the gauge field comes along with its “partner”, the neutral scalar field.

The ansatz (5.9) is similar to that of section 3.2.1. In addition, we have only introduced the conformal factor  $e^{C(r)}$ . As usual the asymptotic boundary coincides with  $r \rightarrow \infty$ . We can say something more about the functions  $f(r)$ ,  $\chi(r)$  and  $C(r)$ . By considering the requirement that our black hole solutions asymptote the  $SO(6)$  AdS vacuum we find,

$$g_{xx} \equiv e^{C(r)} r^2 \approx r^2, \quad g_{rr} \equiv \frac{1}{f(r)} \approx \frac{1}{r^2}. \quad (5.10)$$

Therefore, we deduce that  $C(r)$  and  $\chi(r)$  vanish at the boundary whereas  $f(r)$  diverges like  $r^2$ . There is a gauge freedom in the choice of  $C(r)$  and  $\chi(r)$  which does not involve  $f(r)$ . This is related to the invariance of the Einstein equations under coordinate transformations, in our specific case, reparametrization

of the radial coordinate. In a coordinate system where the metric takes the form

$$ds^2 = e^{2A(r)} (-h(r)dt^2 + d\vec{x}^2) + e^{2B(r)} \frac{dr^2}{h(r)} \quad (5.11)$$

the function  $B(r)$  is a gauge function. The mapping between the two metrics (5.9) and (5.11) is given by,

$$e^{2A(r)} = e^{C(r)r^2}, \quad e^{2B(r)} = \frac{1}{r^2} e^{C(r)-\chi(r)}, \quad h(r) = \frac{f(r)}{r^2} e^{-\chi(r)}. \quad (5.12)$$

Our gauge fixing is  $C(r) = \alpha\chi(r)$  and the parameter  $\alpha$  can be used to simplify the equations of motion. Then, the metric components of the black hole are described just by two independent functions, which can be taken to be  $f(r)$  and  $\chi(r)$ . There is a simple choice of  $\alpha$  in any  $d$  dimensional space-time. This is dictated by the form of combination,

$$\sqrt{g} \mathcal{R} \sim e^{[(d-2)C(r)-\chi(r)]/2} \left( (d-3)(d-2)r^{d-4} + \text{Derivative terms} \right). \quad (5.13)$$

The choice  $\alpha = 1/(d-2)$  helps to get rid of the exponential term. We do not speculate any further on this point limiting our intuition to a computational understanding. The effective Lagrangian of the  $U(1)^3$  model becomes

$$\begin{aligned} \mathcal{L}_{eff}^{\text{III}} = & -r^3 f(r) \left[ \left( \frac{6}{r^2} + 3 \frac{f'(r)}{r f(r)} \right) - \frac{\chi'(r)}{2} + \frac{\chi'(r)^2}{6} \right] \\ & - 3r^3 f(r) \phi_1'^2 - r^3 f(r) \phi_2'^2 - e^{\chi(r)/3} r^3 \text{P}^{\text{III}}(\phi_1, \phi_2) \\ & + \frac{r^3}{2} e^{2\chi(r)/3 + 2\phi_1(r)} \left( e^{-6\phi_1} \Phi_0'(r)^2 + e^{+2\phi_2} \Phi_1'(r)^2 + e^{-2\phi_2} \Phi_2'(r)^2 \right) \end{aligned} \quad (5.14)$$

and considerably simplifies the derivation of the equations of motion.

The search for black hole solutions with the above characteristics dates back to [107] where an analytic family of black holes was constructed. This is a remarkable result because Einstein equations are non linear differential equations and in general there are no recipes on how to find such analytic solutions. In our case there is a chance to succeed because Maxwell equations can be integrated. This integration introduces three constants  $\mathcal{Q}_i$ ,  $i = 0, 1, 2$

and the result is

$$e^{2\chi/3} \partial_r \Phi^0(r) = e^{4\phi_1} \frac{Q_0}{r^3} \quad (5.15)$$

$$e^{2\chi/3} \partial_r \Phi^1(r) = e^{-2\phi_1 - 2\phi_2} \frac{Q_1}{r^3} \quad (5.16)$$

$$e^{2\chi/3} \partial_r \Phi^2(r) = e^{-2\phi_1 + 2\phi_2} \frac{Q_2}{r^3} . \quad (5.17)$$

It is important to observe that the gauge fields  $\Phi^i$  do not enter explicitly the Lagrangian and the field strengths  $F_{rt}^i = \partial_r \Phi^i$  can be completely eliminated from the equations of motion by means of (5.15)-(5.17). The fields involved in these equations, all but the gauge fields  $\Phi^i$ , vanish at boundary. Then, each electric field  $F_{rt}^i = \partial_r \Phi^i(r)$  at infinity behaves like  $Q^i/r^3$  and matches the expected fall-off of a generic electric field in AdS<sub>5</sub>. The  $Q^i$ 's represent the electric charges of the black hole and a generic black hole solution will depend at least on the three parameters.

The solution of [107] is built on a set of harmonic functions  $H_0(r)$ ,  $H_1(r)$ ,  $H_2(r)$ . The metric of the black hole is given by

$$ds^2 = H(r)^{1/3} \left( -\frac{f(r)}{H(r)} dt^2 + r^2 d\vec{x}^2 + \frac{dr^2}{f(r)} \right)$$

$$f(r) = \frac{r^2}{L^2} H - \frac{m}{r^2} , \quad H = H_0 H_1 H_2 , \quad H_i = 1 + \frac{Q_i^2}{r^2} \quad (5.18)$$

$$C(r) = \frac{1}{3} \chi(r), \quad \chi(r) = H(r)$$

and the matter fields are,

$$\Phi^i(r) = \left( \frac{Q_i \sqrt{m}}{r_h^2 + Q_i^2} - \frac{Q_i \sqrt{m}}{r^2 + Q_i^2} \right) \quad (5.19)$$

$$\phi_1(r) = -\frac{1}{3} \log H_0 + \frac{1}{6} \log H_1 + \frac{1}{6} \log H_2 \quad (5.20)$$

$$\phi_2(r) = +\frac{1}{2} \log H_1 - \frac{1}{2} \log H_2 \quad (5.21)$$

The number of parameters that specify the solution is four, they are  $Q_0$ ,  $Q_1$ ,  $Q_2$  and  $m$ . The electric charges  $Q_i$  are given by the combinations  $Q_i \sqrt{m}$ . The harmonic functions  $H_i(r)$  are positive definite and therefore the equation

$f(r) = 0$  has solutions only if  $m \neq 0$ . The parameter  $m$  is the non-extremality parameter and the position of the horizon  $r_h$  is the greatest root of  $f(r) = 0$ . If all the three charges are turned on,  $Q_i \neq 0$  for  $i = 0, 1, 2$ , this equation is third order in the variable  $r_h^2$ ,

$$(r_h^2 + Q_0^2)(r_h^2 + Q_1^2)(r_h^2 + Q_2^2) = mr_h^2 \quad (5.22)$$

and the solutions are complicated function of  $\{Q_0, Q_1, Q_2, m\}$ . On the other hand, special cases in which one or two charges are set to zero, can be handled without too much difficulties. The temperature is given by

$$T = \frac{1}{4\pi} f'(r) e^{-\chi(r)/2} \Big|_{r=r_h} . \quad (5.23)$$

and by means of (5.22) can be written in the following form,

$$T = \frac{1}{2\pi r_h^2} \left( 2r_h^6 + r_h^2 \sum_{i=0}^2 Q_i^2 - \prod_{i=0}^2 Q_i^2 \right) \left( \prod_{i=0}^2 \sqrt{r_h^2 + Q_i^2} \right)^{-1} . \quad (5.24)$$

### 5.1.1 Entropy: general features

We would like to understand some of the properties of this new family of black holes. As a warm up exercise, we consider the simplest configuration of gauge fields, namely  $Q_i = Q$  for  $i = 0, 1, 2$ . In this case the dilatons vanish and the metric takes the following form,

$$ds^2 = (r^2 + Q^2) \left( -\hat{f}(r) dt^2 + d\vec{x}^2 \right) + \frac{r^2}{(r^2 + Q^2)^2} \frac{dr^2}{\hat{f}(r)} \quad (5.25)$$

$$\hat{f}(r) = 1 - \frac{mr^2}{(r^2 + Q^2)^3}$$

The change of variable,

$$r^2 + Q^2 = \xi^2, \quad d\xi^2 = \frac{r^2}{(r^2 + Q^2)} dr^2 \quad (5.26)$$

brings (5.25) into the familiar form of the Reissner-Nördstrom black hole in five dimensions with charge  $\rho = Q\sqrt{m}$ ,

$$ds^2 = -F(r) dt^2 + \xi^2 d\vec{x}^2 + \frac{d\xi^2}{F(r)}, \quad F(r) = \left( \xi^2 - \frac{m}{\xi^2} + \frac{Q^2 m}{\xi^4} \right) \quad (5.27)$$

Having the benchmark of the Reissner-Nördstrom black hole is of great help. The idea is the following. We can look at the phase space of solutions (5.18)

by considering those physical quantities that are special to the Reissner-Nördstrom black hole. The first candidate we are thinking of is the entropy. Indeed, it is well known that the Fermi Liquid phase is described by ground states with vanishing entropy, but on the holographic side, this feature is not generic in black hole thermodynamics. For example, the entropy of the Reissner-Nördstrom black hole remains finite as the temperature is cooled. The resulting dual field theory is somehow exotic from the point of view of condensed matter physics whereas we would like to have black holes whose properties reproduce typical features (even if at strongly coupled) of condensed matter systems.

The entropy density of the black holes (5.18) is given by

$$s = \frac{2\pi}{k^2} \prod_{i=0}^3 \sqrt{r_h^2 + Q_i^2} = \frac{2\pi}{k^2} r_h \sqrt{m} . \quad (5.28)$$

The second equality follows from the relation (5.22). In the dual field theory we will work in the canonical ensemble. In the black hole solution, this is equivalent to fixing the values of the charges  $Q_i$ . Then, being  $Q_i \sqrt{m} = Q_i$ , the temperature and the position of the horizon are determined only by the parameter  $m$  through the relations (5.24) and (5.22).

Having chosen our thermodynamical ensemble, we can now study the general properties of the entropy. The first observation comes for free: when all the three charges are turned on, like in the case of the Reissner-Nördstrom black hole, the entropy is bounded from below and never vanishes. We understand that a necessary condition for  $s$  to vanish is having at least one of the charges set to zero. In this case, the entropy is proportional to  $r_h$  and we conclude that  $s = 0$  only if  $r_h = 0$ . Two easy calculations based on the equation (5.22) complete this analysis. If one of the charges is set to zero,  $r_h = 0$  implies  $m = Q_i^2 Q_j^2$ . If two of the charges are set to zero,  $r_h = 0$  implies  $m = 0$ . This last case may be singular because  $f(r)$  is strictly positive. For this reason, we actually need to check that  $m = Q_i^2 Q_j^2$  and  $m = 0$  do coincide with the zero temperature limit of the corresponding family of black holes. In Figure 5.1 we show a plot of the entropy as function of the temperature for three configurations of charges. These represent our three *guiding cases*:

- the red line corresponds to the Reissner-Nördstrom black hole,
- the black line corresponds to  $Q_0 = 0$  with  $Q_1 = Q_2 = 1$ ,
- the blue line corresponds to  $Q_0 = 1$  with  $Q_1 = Q_2 = 0$

The black curve has zero entropy at zero temperature. We point out that this family of black holes exhibits another feature valuable for the description of

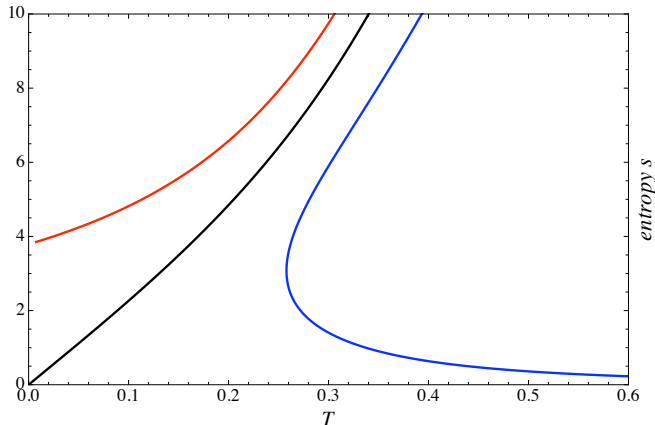


Figure 5.1: *The behavior of the entropy as function of the temperature for: the Reissner-Nördstrom black hole (red), the case  $\mathcal{Q}_0 = 0$  with  $\mathcal{Q}_1 = \mathcal{Q}_2 = 1$  (black), the case  $\mathcal{Q}_0 = 1$  with  $\mathcal{Q}_1 = \mathcal{Q}_2 = 0$  (blue).*

fermionic systems: it has linear specific heat at low temperature [106]. Therefore, it is definitely interesting to put forward the study of this background in the context of holographic superconductivity.

Figure 5.1 has several interesting characteristics. We can go from the black curve to the red one tuning  $\mathcal{Q}_0$  up to the value  $\mathcal{Q}_0 = 1$ . In all these cases there are three charges turned on and we expect the entropy to be bounded from below, similarly to the case of the Reissner-Nördstrom black hole. The family of black holes corresponding to  $\mathcal{Q}_0 = 1$  with  $\mathcal{Q}_1 = \mathcal{Q}_2 = 0$  shows a minimum temperature. As we suspected, the limit  $m = 0$  is singular and indeed corresponds to the limit of infinite temperature. The entropy is not a monotonic function and out of the two branches, the physical one is associated with a positive specific heat, i.e  $\partial s / \partial T > 0$ . This feature distinguishes the blue curve from the others. The existence of a minimum temperature raises the question of what are the possible gravitational solutions that contributes to the thermodynamics below such minimum temperature. One possibility is that the thermodynamically favored solution is actually a superconducting black hole configuration. We will explore this possibility when charged scalars will be introduced.

We conclude this section with a last remark. In the limit where of one the charges is taken to be very large, the solution goes to the configuration  $\mathcal{Q}_0 = 1$  with  $\mathcal{Q}_1 = \mathcal{Q}_2 = 0$ . In particular, no matter which gauge field among

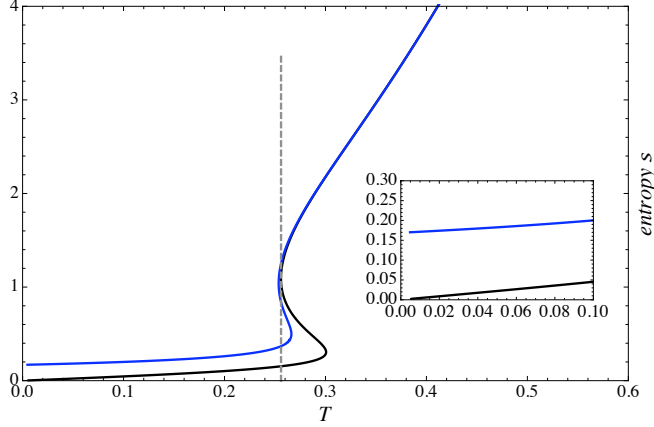


Figure 5.2: For a generic configuration of charges, we can take various limits. Entropy for two examples: the blue line corresponds to  $\mathcal{Q}_0 = 20$  and  $\mathcal{Q}_1 = \mathcal{Q}_2 = 1$ ; the black line corresponds  $\mathcal{Q}_0 = 20$  with  $\mathcal{Q}_1 = 0$  and  $\mathcal{Q}_2 = 1$ .

$\Phi_0, \Phi_1, \Phi_2$  is turned on, there is always a linear combination of  $\phi_1$  and  $\phi_2$  that brings the problem back to  $\mathcal{Q}_0 = 1$  with  $\mathcal{Q}_1 = \mathcal{Q}_2 = 0$ . This is exemplified in Figure 5.2. We also notice that, the difference between taking this limit from the Reissner-Nördstrom black hole or the configuration  $\mathcal{Q}_0 = 0$  with  $\mathcal{Q}_1 = \mathcal{Q}_2 = 1$ , respectively the red line and the black line in Figure 5.1, is the behavior of the entropy at zero temperature.

## 5.2 Linearized Analysis

For a generic choice of  $\{\mathcal{Q}_0, \mathcal{Q}_1, \mathcal{Q}_2\}$ , the temperature of the black hole (5.24), or equivalently  $m$ , describes a one parameter family of solutions inside the full “phase space” of the  $U(1)^3$  truncation. In principle, any of the charged scalars  $\eta_1, \eta_2, \eta_3$  can be turned on this background. The equations of motion for these scalars are

$$\eta_i'' + \eta_i' \left( \frac{3}{r} + \frac{f'}{f} \right) + 4 \frac{e^\chi}{f^2} \cosh \eta_i \sinh \eta_i \Phi_i^2 - D_i \text{P}^{\text{III}} \quad (5.29)$$

where we have defined,

$$D_i \text{P}^{\text{III}} = 4 \frac{e^{\chi/3}}{f} \mathcal{X}_i \sinh \eta_i \left( \mathcal{X}_i \cosh \eta_i - \sum_{j \neq i} \mathcal{X}_j \cosh \eta_j \right). \quad (5.30)$$

The indexes  $i, j$  run over  $0, 1, 2$ . The masses at the  $SO(6)$  fixed point are  $m^2 L^2 = -4$  in agreement with the arguments of  $\mathcal{N} = 8$  supergravity. Actually, in a general background  $\{\mathcal{Q}_0, \mathcal{Q}_1, \mathcal{Q}_2\}$ , the expansion of  $D_i \mathbf{P}^{\text{III}}$  is dominated at small  $\eta_i$  by the term,

$$-4 \frac{e^{\chi/3}}{f} \mathcal{X}_i \left( \mathcal{X}_i - \sum_{j \neq i} \mathcal{X}_j \right). \quad (5.31)$$

This is function of the dilatons whose asymptotic value is the mass of the scalar field,  $m^2 L^2 = -4$ . The expression (5.31) is a novelty with respect to the phenomenological models introduced in chapter 3. In that case, mass and charge were constants and independent of the Reissner-Nördstrom background. Our first thought goes to the critical temperature  $\mathcal{T}$  which is defined by the existence of superconducting black hole with a small condensate. It has been showed in section 3.6.2 that  $\mathcal{T}$  only depends on the phenomenological constants of the theory, among them, the mass and the charge of the scalar. Indeed, when the profile of the bulk scalar can be considered to be small, for example in the case of a second order phase transition at the critical temperature, we can linearize its equation of motion and look for solutions in the background of the uncondensed black hole. Then, the temperature of this solution gives the temperature  $\mathcal{T}$ . In section 3.4, the linearized equation for the charged scalar was found to depend just on three constants: the mass, the charge and the coefficient  $\kappa$ . As a result, these parameters determine the value of the temperature  $\mathcal{T}$  and for the case of second order phase transition, the value of the critical temperature.

The situation for the scalars  $\eta_1, \eta_2, \eta_3$  is modified by the presence of the dilatons. Let us assume from the beginning the case of a second order phase transition. At the critical temperature, it is still true that the profile of the scalar field is small, on the other hand, the dilatons  $\phi_1$  and  $\phi_2$ , which are part of the background, cannot be neglected. As a result, the linearized equation for a single  $\eta_i$  contains two substantially different terms,

- ▶ a standard coupling with the background gauge fields  $\Phi_i$ .
- ▶ a non trivial coupling with the dilaton fields through the term (5.31).

For a fixed configuration of charges such that two of them are equals, the corresponding  $\eta_i$  fields will be equally charged under the gauge fields, but their couplings with the dilatons  $\phi_1$  and  $\phi_2$  will be different. Therefore, we expect to find different critical temperatures depending on the couplings (5.31)

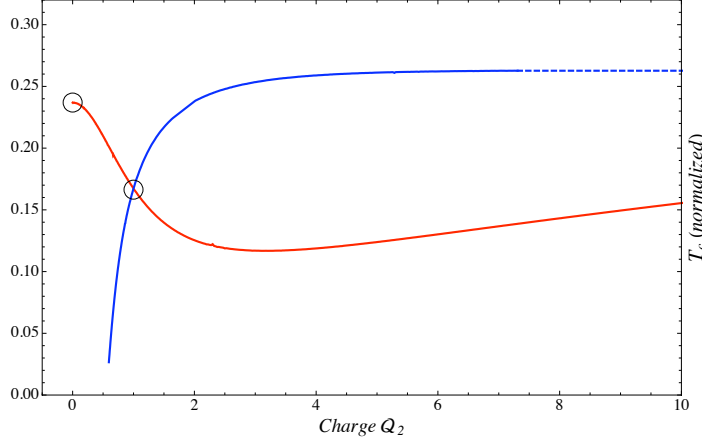


Figure 5.3: We consider black holes with  $Q_0 = Q_1 = 1$  and we tune the value of  $Q_2$  in the range  $[0, +\infty]$ . The critical temperature is normalized with respect to  $\rho_t^{1/3}$  where  $\rho_t = \sqrt{Q_1^2 + Q_2^2 + Q_3^2}$ . The red curve corresponds to  $\eta_0$  and the blue curve to  $\eta_1$ . The case  $Q_2 = 1$  is the Reissner-Nördstrom black hole.

under consideration. This is remarkable if we consider that the charged scalars all correspond to operators with the same dimension  $\Delta = 2$ . In Figure 5.3 we show the result of the linearized analysis for the scalars  $\eta_0$  and  $\eta_1$  in a background with  $Q_0 = Q_1 = 1$  and varying  $Q_2$ .

We anticipate that not every point in the Figure is associated with a second order phase transition. It would be desirable to have a complete map of second order phase transitions but unfortunately this is not the case. Nevertheless, we would like to imagine this ideal setup, where the transitions to the condensed phase are second order, to put forward the following interesting idea.

Let us consider a situation in which there are two order parameters, for concreteness let us take  $\eta_0$  and  $\eta_1$ . Each  $\eta_i$  is coupled to the corresponding gauge field  $A_i$  for  $i = 1, 2$ . Then, we may introduce in the system a doping parameter by increasing the value of one of the two charge densities, i.e.  $Q_0 - Q_1 \neq 0$ . This imbalance will produce a competition between the two order parameters and as a result only one will dominate the thermodynamics. This is expected because changing the value  $Q_i$  in the boundary, translates into a change of the bulk couplings of the scalar fields  $\eta_0$  and  $\eta_1$  with respect to the environment:  $\phi_1(r)$ ,  $\Phi^0(r)$  and  $\Phi^1(r)$ . We now describe in more detail this holographic mechanism.

We calculate the critical temperature for  $\eta_0$  and  $\eta_1$  in the background

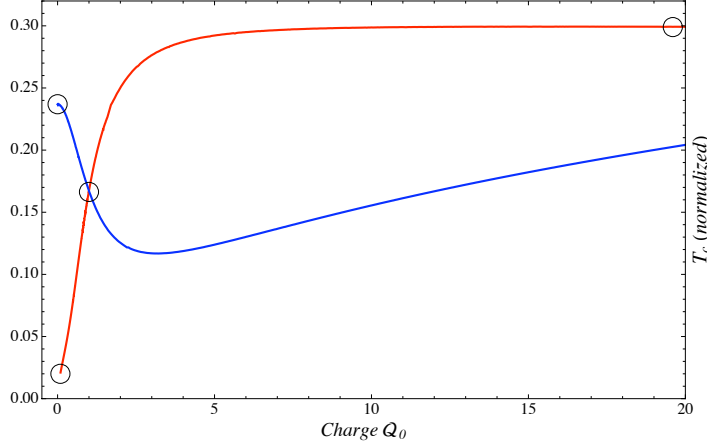


Figure 5.4: We consider black holes with  $Q_1 = Q_2 = 1$  and we tune the value of  $Q_0$  in the range  $[0, +\infty]$ . The critical temperature is normalized with respect to  $\rho_t^{1/3}$  where  $\rho_t = \sqrt{Q_1^2 + Q_2^2 + Q_3^2}$ . The red curve corresponds to  $\eta_0$  and the blue curve to  $\eta_1$ . The case  $Q_0 = 1$  is the Reissner-Nördstrom black hole.

configuration given by  $Q_1 = Q_2 = 1$  and varying  $Q_0$ . The result is shown in Figure 5.4 where the red curve corresponds to  $\eta_0$  and the blue curve to  $\eta_1$ . We describe the three *guiding* cases:

- $Q_0 = 1$ . The background is Reissner-Nördstrom and the dilatons vanish. This is a special case because the mass (5.31) is really a constant. We expect the standard arguments on  $T_c$  to apply and in fact Figure 5.4 shows that  $\eta_0$  and  $\eta_1$  have the same critical temperature.
- $Q_0 = 0$ . The gauge field  $\Phi^0$  vanishes and the scalar field  $\eta_0$  is effectively neutral on this background. We expect  $\eta_0$  not to condense and we have checked that it doesn't. In the range  $0 < Q_0 < 0.1$  it is numerically hard to see what happens. However, this study is not really relevant to our discussion and we avoid speculations. On the other hand, the scalar  $\eta_1$  is perfectly healthy on this background and has a finite critical temperature  $T_c \approx 0.236919$
- $Q_0 \rightarrow \infty$ . This case is the opposite of  $Q_0 = 0$ . At infinity, the family of black holes coincide with  $Q_0 = 1$  but  $Q_1 = Q_2 = 0$ . We expect  $\eta_0$  to condense with critical temperature given by the asymptotic value of the red curve  $\approx 0.3058$ . The case of  $\eta_1$  instead has different features. It is effectively neutral on this background and therefore we expect  $\eta_1$  not

condense. We have checked that there are no solutions to the symmetry breaking boundary conditions. Nevertheless, the blue line seems to keep increasing in the limit  $\mathcal{Q}_0 \gg 1$  and we conclude that it has to stop for a certain critical value of  $\mathcal{Q}_0$ . In the same limit  $\mathcal{Q}_0 \gg 1$ , the background shows a minimum temperature  $T_{min} \approx 0.257$  and probably this is the reason why the  $\eta_1$  condensate disappears.

Considering the hypothetical scenario in which Figure 5.4 gives a complete map of second order phase transitions. The superconducting phase will be determined by the dominant solution between the  $\eta_0$  superconductor and the  $\eta_1$  superconductor, namely the solution with greater critical temperature. As long as we increase  $\mathcal{Q}_0$  the  $\eta_1$ -condensate ceases to be the dominant solution and  $\eta_0$  takes his place. In this sense, the scalar field  $\eta_0$  and  $\eta_1$  compete. This is the bulk mechanism that we have mentioned before and it is driven by the difference  $\mathcal{Q}_0 - \mathcal{Q}_1 \neq 0$ . Unluckily, within the  $\mathcal{L}_{SO(6)}$  models that we are studying, the assumption of second order phase transitions turns out to be generically wrong. In the next sections we will consider this issue more accurately.

As a last remark, the reader may notice that Figure 5.4 and Figure 5.3 have something in common. The corresponding frameworks are understood and the two limits are:  $\mathcal{Q}_2 \rightarrow 0$  for  $\eta_0$  and  $\mathcal{Q}_0 \rightarrow 0$  for  $\eta_1$ . They coincide because both scalars have formally the same mass and are equally coupled with respect to the gauge fields. The situation is different in the limit where  $\mathcal{Q}_2 \rightarrow \infty$  and  $\mathcal{Q}_0 \rightarrow \infty$ . Even if the masses turns out to have the same limit, the gauge field configuration is different and in fact there is no common limit between the asymptotic of Figure 5.4 and the asymptotic of Figure 5.3.

### 5.3 Truncations to a single charge

Our approach is to pick a single  $U(1)$  out of the “phase space”  $\{\mathcal{Q}_0, \mathcal{Q}_1, \mathcal{Q}_2\}$ . In the context of holographic superconductivity this is the natural thing to do because guarantees that our dual field theory has a definite meaning of a global “electric” charge. The truncation to a single charge can be understood by means of group theoretical arguments. For example, we can define the preferred  $U(1)$  as the gauge field in  $A_{ij}$  left invariant by the action of an  $SO(6)$  element. Then, the scalar sector is identified with the set of fields in  $T_{ij}$  which survive the modding out [12]. Alternatively, we may work directly with the equations of motion by considering first the uncondensed phase (5.18).

From a computational point of view, the possibility of setting some of the scalar fields to zero minimizes the numerical effort needed to find the

superconducting solution. We begin this analysis starting with the equation of motion of the scalar field  $\phi_2$ ,

$$\nabla_\mu \nabla^\mu \phi_2 - \frac{1}{4} e^{2\phi_1} \left( e^{2\phi_2} F^1 F^1 - e^{-2\phi_2} F^2 F^2 \right) = \frac{1}{2} \partial_2 \text{P}^{\text{III}} \quad (5.32)$$

$$\partial_2 \text{P}^{\text{III}} = -\frac{4}{L^2} e^{\phi_1} (e^{\phi_2} - e^{-\phi_2}) . \quad (5.33)$$

We note the relation  $\partial_2 \text{P}^{\text{III}} = 0$  iff  $\phi_2 = 0$  and we deduce that

$$\phi_2(r) \equiv 0 \quad \rightarrow \quad F^1 = F^2 . \quad (5.34)$$

The opposite arrow may be false in general but it is true for the class of the black holes (5.18): setting  $\Phi^1 = \Phi^2$ , equivalently  $\mathcal{Q}_1 = \mathcal{Q}_2$ , forces  $H_1(r) = H_2(r)$  and  $\phi_2(r) = 0$ . Concluding, we have reduced the study of the uncondensed phase to the study of solutions belonging to  $\mathcal{L}^{\text{II}}$ .

The addition of the incomplete hypermultiplets is consistent if the two conditions  $\phi_2(r) = 0$  and  $\Phi^1 = \Phi^2$  are preserved. The equation of motion of  $\phi_2$  is modified by the presence of the full scalar potential (4.118). This potential contains couplings between dilatons and charged scalars and in particular we obtain,

$$\begin{aligned} \partial_2 \text{P}^{\text{III}} = & -\frac{4}{L^2} \left( (\mathcal{X}_1^2 \sinh^2 \eta_1 - \mathcal{X}_2^2 \sinh^2 \eta_2) + \right. \\ & \left. + \mathcal{X}_0 \cosh \eta_0 (\mathcal{X}_2 \cosh \eta_2 - \mathcal{X}_1 \cosh \eta_1) \right) . \end{aligned}$$

Imposing  $\phi_2(r) = 0$  leads to the constraint,

$$\begin{aligned} \partial_2 \text{P}^{\text{III}} = & \frac{4}{L^2} e^{-\phi_1} (\cosh \eta_2 - \cosh \eta_1) \times \\ & \times \left( -e^{2\phi_1} \cosh \eta_0 + e^{-\phi_1} (\cosh \eta_2 + \cosh \eta_1) \right) = 0 . \end{aligned} \quad (5.35)$$

The solution of this constraint in the  $\{\eta_1, \eta_2\}$  sector is  $\eta_1 = \eta_2$  but we need to check its consistency by looking at the equations of motion of the charged scalars. From (5.29) we find  $\Phi^1 = \Phi^2$  and

$$D_1 \text{P}^{\text{III}} = D_2 \text{P}^{\text{III}} \quad \rightarrow \quad \mathcal{X}_1 = \mathcal{X}_2 . \quad (5.36)$$

This last condition corresponds to  $\phi_2 = 0$ . Thus, the consistency of the truncation is proven. Summarizing, the Lagrangian that we are considering couples  $\mathcal{L}^{\text{II}}$  to two charged scalars coming from the incomplete hypermultiplets,

namely

$$\mathcal{L}^{II} = \mathcal{R} + \mathcal{L}_{vectors}^{II} + \mathcal{L}_{scalars}^{II} + \text{P}^{II} + \mathcal{L}_{CS}^{II} \quad (5.37)$$

$$\mathcal{L}_{vectors}^{II} = -\frac{1}{4} \left( e^{2\phi_1} F_{\mu\nu} F^{\mu\nu} + e^{-4\phi_1} F_{\mu\nu}^0 F^{\mu\nu 0} \right) \quad (5.38)$$

$$\begin{aligned} \mathcal{L}_{scalars}^{II} &= -3\partial_\mu \phi_1 \partial^\mu \phi_1 \\ &\quad -\frac{1}{2} \left( \partial_\mu \eta_0 \partial^\mu \eta_0 + \sinh^2 \eta_0 \left( \partial\theta_0 - \frac{2}{L} A_0 \right)^2 \right) \\ &\quad -\frac{1}{2} \partial_\mu \eta \partial^\mu \eta - \sinh^2 \frac{\eta}{\sqrt{2}} \left( \partial\theta - \frac{2}{L} \frac{A}{\sqrt{2}} \right)^2 \end{aligned} \quad (5.39)$$

$$\text{P}^{II} = -\frac{2}{L^2} \left( 2e^{-2\phi_1} + 4e^{\phi_1} \cosh \eta_0 \cosh \frac{\eta}{\sqrt{2}} - e^{4\phi_1} \sinh^2 \eta_0 \right) \quad (5.40)$$

$$\mathcal{L}_{CS}^{II} = +\frac{1}{8} \epsilon^{\mu\nu\rho\sigma\tau} F_{\mu\nu} F_{\rho\sigma} A_\tau^0 \quad (5.41)$$

where we have defined  $\eta_1 = \eta_2 = \eta/\sqrt{2}$  and  $A_1 = A_2 = A/\sqrt{2}$ , so to have canonical kinetic terms. It is important to remark that the charge of the scalar field  $\eta_0$  is  $qL = 2$  but the charge of the new field  $\eta$  is  $qL = \sqrt{2}$ . On the other hand, the masses of  $\eta_0$  and  $\eta$  are the same,  $m^2 L^2 = -4$ . The Chern Simons term does not play any role. There are two preferred  $U(1)$  gauge fields in this truncation,

$$\mathbf{A} : \Phi^0 \neq 0 \oplus \Phi = 0 \quad ; \quad \mathbf{B} : \Phi^0 = 0 \oplus \Phi \neq 0 . \quad (5.42)$$

Here  $\Phi$  is defined by  $A = \Phi(r)dt$ . The uncondensed phase of these two models is represented by a dilatonic black holes with a non trivial  $\phi_1(r)$ . We can turn on the charged scalars by considering,

$$\mathbf{A} : \eta_0 \neq 0 \oplus \eta = 0 \quad ; \quad \mathbf{B} : \eta_0 = 0 \oplus \eta \neq 0 \quad (5.43)$$

This is the only possible choice we can make. In fact, the scalar  $\eta_0$  is charged under  $\Phi^0$  but neutral under  $\Phi$  whereas the scalar  $\eta$  is charged under  $\Phi$  but neutral under  $\Phi^0$ .

We recognize that Model **A** and Model **B** correspond to two of the three guiding cases discussed in the previous section and highlighted in Figure 5.4. The missing case is the truncation to the Reissner-Nördstrom black hole. It is

not difficult to guess how the ansatz for this truncation will look like. Indeed, the Reissner-Nördstrom black hole coincides with the three equal charges configuration  $\mathcal{Q}_0 = \mathcal{Q}_1 = \mathcal{Q}_2 = 1$  and we expect the matrix  $T_{ij}$  to be diagonal and isotropic in the three blocks. The consistent truncation is

$$\mathbf{C} : \eta_0 = \eta_1 = \eta_2 = \frac{\eta_d}{\sqrt{3}} \oplus \Phi^0 = \Phi^1 = \Phi^2 = \frac{\Phi_d}{\sqrt{3}} \quad (5.44)$$

with  $\phi_1 = 0$ . The resulting Lagrangian is

$$\begin{aligned} \mathcal{L}^{\mathbf{I}} &= \mathcal{R} - \frac{1}{4} F^{\mu\nu} F_{\mu\nu} \\ &\quad - \frac{1}{2} \partial_\mu \eta_d \partial^\mu \eta_d - \frac{3}{2} \sinh^2 \left( \frac{\eta_d}{\sqrt{3}} \right) \left( \partial \theta_d + \frac{2}{L} \frac{A_d}{\sqrt{3}} \right)^2 - \mathbf{P}^{\mathbf{I}} \end{aligned}$$

with

$$\mathbf{P}^{\mathbf{I}} = -\frac{6}{L^2} \left( 1 + \cosh^2 \left( \frac{\eta_d}{\sqrt{3}} \right) \right). \quad (5.45)$$

The mass of the scalar  $\eta_d$  is  $m^2 L^2 = -4$  and the charge  $qL = 2/\sqrt{3}$ . We can obtain the equation of motions of the above theory from  $\mathcal{L}^{\mathbf{I}}$ . First we set  $\phi_1 = 0$ , then we consider  $\eta_0 = \eta/\sqrt{2}$  and  $\Phi^0 = \Phi/\sqrt{2}$ . Regarding the first identification, the intuition comes from the comparison between

$$\begin{aligned} \partial_{\eta_0} \mathbf{P}^{\mathbf{II}} \Big|_{\phi_1=0} &= 4 \cosh \frac{\eta}{\sqrt{2}} \sinh \eta_0 - 2 \cosh \eta_0 \sinh \eta_0 \quad (5.46) \\ \partial_\eta \mathbf{P}^{\mathbf{II}} \Big|_{\phi_1=0} &= 2\sqrt{2} \cosh \eta_0 \sinh \frac{\eta}{\sqrt{2}} \end{aligned}$$

These two terms become proportional after we impose  $\eta_0 = \eta/\sqrt{2}$ . The relation  $\Phi^0 = \Phi/\sqrt{2}$  has been used in section 4.3.3 to recover the minimal gauged  $\mathcal{N} = 2$  supergravity.

## 5.4 The condensed phase

The truncations obtained in the previous section can be described in terms of the following Lagrangian

$$\mathcal{L} = \sqrt{g} \left( \mathcal{R} - 3(\partial\varphi)^2 - \frac{1}{4} G(\varphi) F^{\mu\nu} F_{\mu\nu} - \frac{1}{2} (\partial\eta)^2 - \frac{1}{2} J(\eta) A_\mu A^\mu - V(\eta, \varphi) \right), \quad (5.47)$$

where the coupling functions  $G(\varphi)$ ,  $J(\eta)$  and the potential  $V(\eta, \varphi)$  are determined by the truncations  $\mathbf{A}$ ,  $\mathbf{B}$  and  $\mathbf{C}$ . In particular, the dilaton  $\phi$  and the charged scalar  $\eta$  denote the only scalars retained in these three models.

### 5.4.1 Equations of motion and asymptotic behavior

Our ansatz for the metric has been already given in (5.9) in terms of the functions  $f(r)$ ,  $\chi(r)$  and  $C(r)$ ,

$$ds^2 = g_{\mu\nu} dx^\mu dx^\nu = e^{C(r)} \left( -f(r) e^{-\chi(r)} dt^2 + r^2 d\vec{x}^2 + \frac{dr^2}{f(r)} \right). \quad (5.48)$$

The gauge fixing parameter  $\alpha$ , defined as  $C(r) = \alpha\chi(R)$ , was the only freedom left. In section 5.1 we have seen that the value  $\alpha = 1/3$  facilitates the search for simple analytic solutions. On the other hand, when  $\alpha \neq 1/3$  the analytic form of (5.18) can be quite complicated. For the numerical procedure this is not a problem and actually the convenient choice turns out to be  $\alpha = 0$ . In order to clarify this point we briefly review how the numerical procedure works paying special attention to  $\alpha$

In chapter 3, we described in detail the construction of a superconducting black hole. The same method can be employed to reproduce the family of solutions (5.18) once the charged scalar is set to zero. The asymptotic behavior of the dilaton  $\phi$  is

$$\phi(r) \rightarrow \frac{O_\phi}{r^2} + \frac{S_\phi}{r^2} \log r \quad (5.49)$$

and the boundary condition we need to impose is  $S_\phi = 0$ . When the Einstein equations are considered we find,

$$\begin{aligned} E_{\mu\nu} - T_{\mu\nu} &= 0, \\ \mathcal{R}_{\mu\nu} - \frac{1}{2} g_{\mu\nu} \mathcal{R} &\equiv E_{\mu\nu} \\ T_{\mu\nu} &\equiv 3\partial_\mu\phi\partial_\nu\phi + \frac{1}{2} \left( F_{\mu\gamma} F_\nu{}^\gamma - \frac{1}{2} g_{\mu\nu} FF \right) - \frac{1}{2} g_{\mu\nu} V(\phi). \end{aligned}$$

The only non trivial components of the Ricci tensor are  $\mathcal{R}_{tt}$ ,  $\mathcal{R}_{rr}$  and  $\mathcal{R}_{\vec{x}\vec{x}}$ , the latter being a diagonal matrix. The  $rr$  component is first order in  $\chi$  and  $f$  whereas  $\mathcal{R}_{tt}$  and  $\mathcal{R}_{\vec{x}\vec{x}}$  are second order. A convenient choice is,

$$\frac{e^\chi}{f^2} (E_{tt} - T_{rr}) + (E_{rr} - T_r) = 0 \quad (5.50)$$

$$E_{tt} - T_{tt} = 0. \quad (5.51)$$

The parameter  $\alpha$  appears explicitly in the above equations and we find,

$$\alpha \left( \chi'' - \frac{\alpha-1}{2} \chi'^2 \right) + \frac{\chi'}{r} + \frac{1}{2} \phi'^2 + \frac{1}{3} \eta'^2 + \frac{1}{3} \frac{e^\chi}{f^2} J(\eta) \Phi^2 = 0 \quad (5.52)$$

$$\alpha \mathfrak{A} + \frac{e^{(1-\alpha)\chi}}{2f} G(\phi) \Phi'^2 + \frac{6}{r^2} + \frac{3f'}{rf} + \frac{e^{\alpha\chi} V(\phi, \eta)}{f} + 3\phi'^2 = \mathfrak{B} \quad (5.53)$$

where  $\mathfrak{B}$  depends on the charged scalar and  $\mathfrak{A}$  is a certain combination of the metric functions (not really relevant for the discussion),

$$\mathfrak{A} = 3\alpha \left( \frac{3\chi'}{r} + \frac{\alpha\chi'^2}{2} + \chi'' \right) + \alpha \frac{3f'}{2f} \chi' \quad \mathfrak{B} = -\frac{1}{2} \left( \eta'^2 + J(\eta)e^\chi \frac{\Phi^2}{f^2} \right) \quad (5.54)$$

Matter fields satisfy,

$$\Phi'' + \Phi' \left( \frac{3}{r} + \frac{(1+\alpha)}{2} \chi' + \frac{\partial_\phi G}{G} \phi' \right) - e^{\alpha\chi} \frac{J(\eta)}{fG(\phi)} \Phi = 0 \quad (5.55)$$

$$\phi'' + \phi' \left( \frac{3}{r} - \frac{(1-3\alpha)}{2} \chi' + \frac{f'}{f} \right) + \frac{e^{(1-\alpha)\chi}}{12g} \partial_\phi G \Phi'^2 - e^{\alpha\chi} \frac{\partial_\phi V}{6f} = 0 \quad (5.56)$$

$$\eta'' + \eta' \left( \frac{3}{r} - \frac{(1-3\alpha)}{2} \chi' + \frac{f'}{f} \right) + \frac{e^\chi}{2f^2} \partial_\eta J(\eta) \Phi^2 - e^{\alpha\chi} \frac{\partial_\eta V}{f} = 0 \quad (5.57)$$

Black hole solutions are defined postulating the existence of the horizon located at  $r_h$ . This is implemented by considering a finite  $\chi(r_h) \neq 0$  and the following series expansion for the function  $f$ ,

$$f(r) \approx f'(r_h)(r - r_h) + \frac{1}{2} f''(r_h)(r - r_h)^2 + \dots, \quad f'(r_h) \neq 0. \quad (5.58)$$

Terms of the form  $1/f$  are potentially dangerous when evaluated at the horizon and a regular solution of the equations of motion is obtained only by imposing certain relations among  $M(r_h)$  and  $M'(r_h)$ , where  $M$  is the vector  $M = (\Phi, \phi, \eta)$ . These relations ensure that the equations of motion are not divergent at  $r_h$ . For convenience we define  $\phi(r_h) \equiv \phi_h$ ,  $\eta(r_h) \equiv \eta_h$ ,  $\chi(r_h) \equiv \chi_h$  and  $\Phi'(r_h) \equiv E_h$ . The analysis of (5.55), (5.56) and (5.57) leads to the constraints

$$\Phi(r_h) = 0 \quad (5.59)$$

$$f'(r_h) \phi'(r_h) = \frac{e^{\alpha\chi_h}}{6} \partial_\phi V(\phi_h, \eta_h) - \frac{e^{(1-\alpha)\chi_h}}{12} \partial_\phi G(\phi_h) E_h^2 \quad (5.60)$$

$$f'(r_h) \eta'(r_h) = e^{\alpha\chi_h} \partial_\eta V(\phi_h, \eta_h) \quad (5.61)$$

The first one is such that  $\Phi/f$  is finite, the others regularize derivative terms proportional to  $1/f$ . Equation (5.53) has similar divergences and the value of  $f'(r_h)$  is determined by the condition

$$\left( \alpha \frac{\chi'(r_h)}{2} + \frac{1}{r_h} \right) f'(r_h) = -\frac{1}{3} \left[ e^{\alpha\chi} V(\phi_h, \eta_h) + \frac{1}{2} e^{(1-\alpha)\chi_h} G(\phi_h) E_h^2 \right] \quad (5.62)$$

For a generic value of  $\alpha$ , the independent variables we are left with are:  $E_h$ ,  $\phi_h$ ,  $\eta_h$ ,  $\chi_h$  and  $\chi'(r_h)$ . The case of  $\chi(r)$  is substantially different from the case of the scalar fields or the gauge field. Indeed, equation (5.52) does not involve  $f(r)$  and it is regular at the horizon. We conclude that,  $\chi'(r_h)$  is not determined by the regularity condition and appears as a free parameter. Two scaling symmetries,

$$r \rightarrow ar, \quad (t, \vec{x}) \rightarrow a^{-1}(t, \vec{x}), \quad f \rightarrow a^2 f, \quad \Phi \rightarrow a\Phi \quad (5.63)$$

and

$$e^x \rightarrow a^2 e^x, \quad t \rightarrow at, \quad \Phi \rightarrow a\Phi, \quad (5.64)$$

can be used to fix  $r_h = 1$  and  $\chi_h = 1$ . Then, the Cauchy problem is specified by four independent variables:  $E_h$ ,  $\phi_h$ ,  $\eta_h$ ,  $\chi'(r_h)$ . If we set  $\eta = 0$  from the beginning and we consider the boundary condition  $S_\phi = 0$ , our numerics should reproduce the analytic black holes given in (5.18). We remind the reader that, fixing  $r_h = 1$  in the case of a single charge, is the same as fixing the charge density (or the chemical potential) and therefore we expect to find a one parameter family of solutions. However, we have three values to specify,  $E_h$ ,  $\phi_h$  and  $\chi'(r_h)$ , but one boundary condition,  $S_\phi = 0$ . An additional constraint need to be imposed. In order to have a better understanding of this problem we reconsider the analytic solutions (5.18). The function  $\chi(r)$  has a closed expression and it is not difficult to find the UV boundary behavior of the various fields,

$$\chi(r) = \frac{Q_0^2 + Q_1^2 + Q_2^2}{r^2} + \dots \quad (5.65)$$

$$\phi_1(r) = \frac{-2Q_0^2 + Q_1^2 + Q_2^2}{6r^2} + \dots \quad (5.66)$$

$$\phi_2(r) = \frac{-Q_1^2 + Q_2^2}{2r^2} + \dots \quad (5.67)$$

$$\Phi'_0(r) = -2\frac{\sqrt{m}Q_0}{r^3} + \dots \quad (5.68)$$

$$\Phi'_1(r) = -2\frac{\sqrt{m}Q_1}{r^3} + \dots \quad (5.69)$$

$$\Phi'_2(r) = -2\frac{\sqrt{m}Q_2}{r^3} + \dots \quad (5.70)$$

The radial scaling symmetry is not enough to determine the multi-charge thermodynamical ensemble and we have to fix two ratios, for example  $Q_1/Q_0$  and  $Q_2/Q_0$ . This correspond to a fine tuning of the values of  $\Phi'_1(r_h)$  and

$\Phi_2'(r_h)$ . We are lead to the following relation,

$$2(Q_0^2 + Q_1^2 + Q_2^2) + (Q_1^2 + Q_2^2 - 2Q_0^2) = 3Q_1^2 + 3Q_2^2 . \quad (5.71)$$

This is an identity between the charges and the asymptotics of  $\chi(r)$  and  $\phi_1(r)$ . In particular we understand (5.71) as a constraint on the asymptotic of  $\chi(r)$ . It is interesting to investigate the kernel of the equation (5.52), namely the solution of  $\chi(r)$  in the absence of matter fields. We find that

$$\chi(r) = \chi_\infty + \frac{2}{1-\alpha} \log \left( \alpha S_\chi r^{1-\frac{1}{\alpha}} + 1 \right) \quad (5.72)$$

For the case  $\alpha = 1/3$  the asymptotics of  $\chi(r)$  contains a term of order  $S_\chi/r^2$  and generically, there will a contribution of order  $S_\chi/r^2$  to the expansion (5.65). However, this is not detectable from the asymptotics of  $\chi(r)$  because the numerical output will be just a number corresponding to the sum  $S_\chi + \sum_i Q_i^2$ . The condition  $S_\chi = 0$  is obtained indirectly by the constraint (5.71). From a numerical point of view, we have to use this (additional) UV constraint to solve for  $\chi'(r_h)$ . We conclude that  $\alpha \neq 0$  is not the better option from a computational point of view. The optimal value is  $\alpha = 0$ . In this case, the equation (5.52) is reduced to a first order equation and  $\chi'(r_h)$  is automatically determined by the equations. We will use this gauge to solve the equations of motion.

It is useful to write down the UV asymptotic behavior when  $\alpha = 0$ ,

$$\phi(r) = \frac{O_\phi}{r^2} + \frac{S_\phi}{r^2} \log r + \dots \quad (5.73)$$

$$\Phi(r) = \mu - \frac{\rho}{r^2} + \dots \quad (5.74)$$

$$\eta(r) = \frac{O_\eta}{r^2} + \frac{S_\eta}{r^2} \log r + \dots \quad (5.75)$$

$$e^{-\chi} f(r) = e^{-\chi_\infty} \left( \frac{r^2}{L^2} - \frac{M}{r^2} + \dots \right) , \quad (5.76)$$

$$\chi = \chi_\infty + \frac{1}{r^4} (\# + O(\log r) + O(\log^2 r)) + \dots \quad (5.77)$$

The symbol  $\#$  stands for a quadratic combination of  $\{O_\phi, S_\phi\}$  and  $\{O_\eta, S_\eta\}$  whose precise form is not relevant. We just remark that the asymptotics of  $\chi$  is completely determined. Field theory quantities can be calculated reading the values of

$$(\rho \quad \mu), \quad M, \quad O_\phi \quad O_\eta \quad (5.78)$$

Log terms appear not only in  $\chi(r)$  but also as sub-leading terms in the expansion of  $f$ ,  $\phi$ ,  $\eta$ ,  $\Phi$ . However, their coefficients are only proportional to  $S_\phi$  or  $S_\eta$  and vanish when the boundary conditions  $S_\eta = 0$  and  $S_\phi = 0$  are imposed.

### 5.4.2 Numerical Results

It is useful to remind which are the physical quantities that characterize the phase diagram of the theory. These are field theory quantities and are obtained from the boundary data analyzed in the previous section. In particular, the energy, the charge density and the entropy are,

$$E_{ft} = \frac{3m}{16\pi G_N}, \quad \rho_{ft} = \frac{\rho}{8\pi G_N}, \quad s = \frac{r_h^3}{4G_N}. \quad (5.79)$$

Then, the free energy is given by the combination,

$$f = E_{ft} - Ts = \frac{1}{8\pi G_N} \left( \frac{3}{2}M - 2\pi r_h^3 T \right) \quad (5.80)$$

Sometimes it is convenient to multiply the above quantities by a factor  $2G_N/\pi$ . In this case

$$\rho_{ft} = \frac{\rho}{4\pi^2}, \quad f = \frac{1}{4\pi^2} \left( \frac{3}{2}M - 2\pi r_h^3 T \right) \quad (5.81)$$

In the canonical ensemble the charge density is fixed and we may define thermodynamical dimensionless quantities by considering appropriate ratios. This is a consequence of the fact that the equations of motion are invariant under the radial scaling (5.63). For the relevant cases we find,

$$\frac{T}{\rho^{1/3}}, \quad \frac{f}{\rho^{4/3}}, \quad \frac{s}{\rho}. \quad (5.82)$$

It is clear that we can switch from  $\rho_{ft} = 1$  to  $\rho = 1$  with a simple scaling. In the next three sections we study the condensed phases of Model **A**, **B** and **C**.

**Condensation in sector A.** This model is defined by the couplings  $G(\eta)$ ,  $J(\eta)$  and the potential  $V(\phi, \eta)$  given in section 5.3. For convenience we report the results in the following box:

$$\begin{aligned} G(\phi) &= e^{-4\phi}, & J(\eta) &= 4 \sinh^2 \eta, \\ V(\phi, \eta) &= -2 \left( 2e^{-2\phi} + 4e^\phi \cosh \eta - e^{-4\phi} \sinh^2 \eta \right). \end{aligned}$$

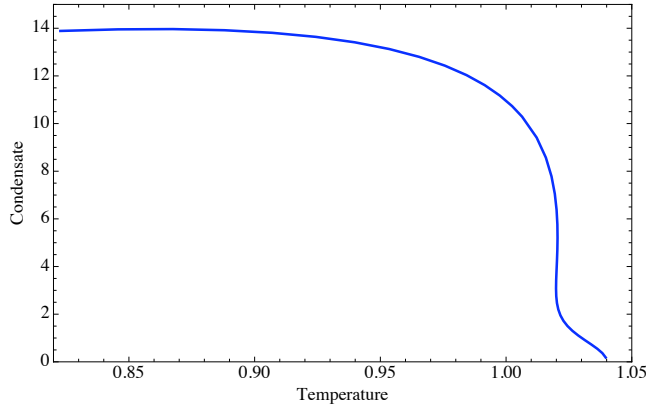


Figure 5.5: *Condensate in the sector **A**. The normalization is  $\rho = (4\pi^2)^{1/3}$ . Adapted from [12].*

The linearized analysis carried out in section 5.2 implies that a condensate turns on at the critical temperature  $T_c \approx 0.306(4\pi^2)^{1/3}$ . In fact, a superconducting black hole solution shows up at  $T_c$ . This solution exists for temperature  $T \leq T_c$  however, the shape of the condensate is not comparable with the HHH model and it is actually numerically hard to study the black hole at low temperature. In Figure 5.5 we zoom on the most interesting aspect of this condensate.

At some lower temperature  $T_1 \cong 1.02$  the second derivative of the condensate with respect to the temperature changes sign. This could be an indication of a new phase transition as it implies that the fourth order term of the free energy in terms of the condensate must have a strong temperature dependence near  $T_1$ . In Landau-Ginzburg theory, it is normally assumed that the fourth order coefficient is not strongly temperature dependent around the critical point  $T_c$ , but it is in principle possible that there is some new temperature scale below  $T_c$  where this coefficient also starts to change. In particular, if it goes to zero or becomes negative then this term no longer stabilizes the condensate, and higher order coefficients (if present) become important. Because of this, the behavior of the condensate can change and indeed can blow up at this new temperature scale, as indeed occurs in the present model.

From the gravitational point of view, the fact that on one hand, the critical temperature is close to the minimum temperature  $T_m \approx 0.88$  of the uncondensed phase, on the other hand, the charge of the bulk scalar is relatively small, may explain the reason why the condensate shows the drastic change at

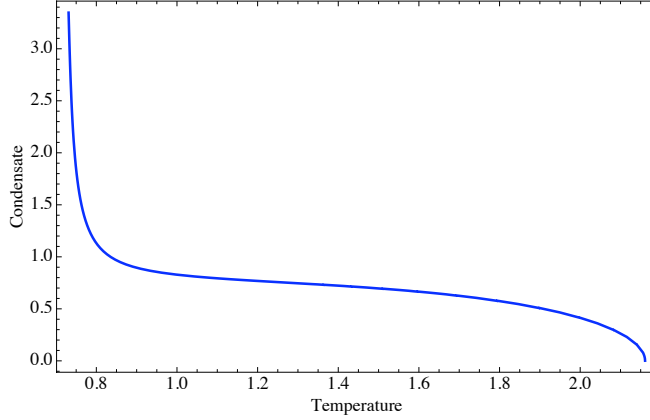


Figure 5.6: *Condensate in the sector  $\mathbf{A}$  with fictitious charge  $q = 16$ . The normalization is  $\rho = (4\pi^2)^{1/3}$ . Adapted from [12].*

the temperature  $T_1$ . As a matter of fact, considering a large fictitious charge  $q$  in front of the coupling  $J(\eta)$ , the resulting condensate is more stable and the temperature  $T_1$  is moved to low temperatures. In Figure 5.6 we show an example for  $q = 16$ .

Regarding the existence of the extremal solution, it is interesting to note that at any finite  $q$ , the potential has a saddle point at  $\phi = (\log 3)/6$  and  $\eta = (\log 3)/2$ . Then, the horizon data of the superconducting solutions are driven towards the tachyonic direction and it is not clear how the geometry backreact to this endless flow. We believe that most likely the free energy of the superconducting black hole will resemble the free energy of the uncondensed black hole. This is show in Figure 5.7. The motivation comes from the study of similar superconducting solutions carried out in [15]. Unfortunately, for Model  $\mathbf{A}$  it is numerically hard to get a reasonable picture of the thermodynamics. Instead, we will try to describe what we expect to happen. We can see from the Figure that the free energy of the uncondensed black hole has two branches and only the branch with lower free energy is physical. Actually, there are two critical temperatures for the superconducting instability. One is attached to the lower branch at  $T_c \approx 0.306(4\pi^2)^{1/3} \approx 1.0414$  and the other one is attached to the upper branch at  $T_c \approx 0.55(4\pi^2)^{1/3} \approx 1.87$ . We observe that the first critical temperature coincides with the asymptotic value that we read from Figure 5.4. In particular, in section 5.2 we have described only one superconducting instability. Here, we observe that  $\eta_0$  (and only  $\eta_0$ ) has sec-

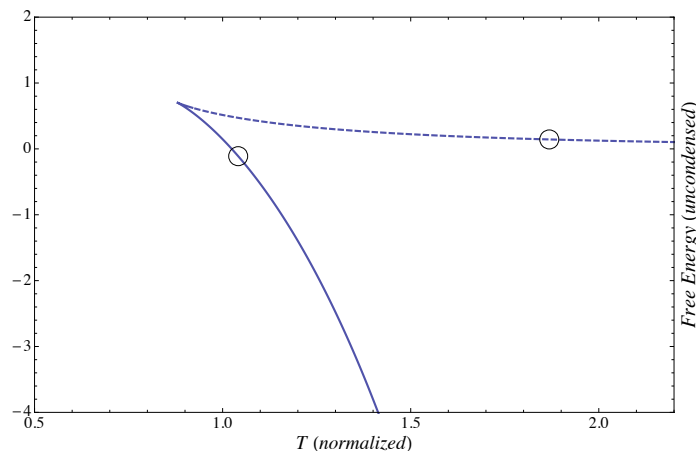


Figure 5.7: *Free energy of the uncondensed black holes of Model A. There are two branches: solid and dashed line. The first is thermodynamically favored. The two circles indicates the critical temperature of the superconducting instability.*

ond critical temperature starting from  $\mathcal{Q}_0 \gtrsim 36$ . Established the existence of this second branch of solutions, we conjecture that at some finite temperature, the superconducting branch arising at  $T_c \approx 1.0414$  joins the superconducting branch coming from  $T_c \approx 1.87$ . Then, the condensed phase has a new minimum temperature, lower than  $T_c \approx 0.88$  but the thermodynamics is similar to that of the uncondensed phase. In particular, only the lower branch, the one with less free energy, has a physical interpretation.

**Condensation in sector B.** This model still has a non vanishing dilaton and it is characterized by the following couplings,

$$\begin{aligned}
 G(\phi) &= e^{2\phi} , & J(\eta) &= 4 \sinh^2 \frac{\eta}{\sqrt{2}} , \\
 V(\phi, \eta) &= -4 \left( e^{-2\phi} + 2e^\phi \cosh \frac{\eta}{\sqrt{2}} \right) .
 \end{aligned}$$

The condensate is described by the curve of Figure 5.8. The result is quite surprising and unexpected. We find that there exists a family of hairy black

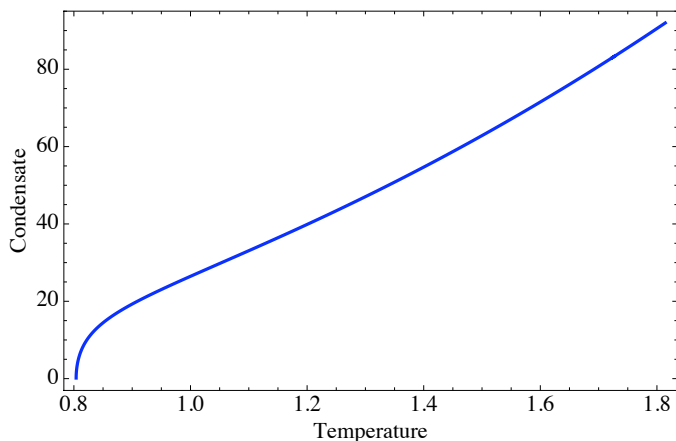


Figure 5.8: *The retrograde condensate of Model B. The normalization is  $\rho = (4\pi^2)^{1/3}$ . Adapted from [12]*

holes but for temperatures greater than the critical temperature. We notice that the critical temperatures agrees with the value found in the linearized approximation  $T_c \approx 0.237(4\pi^2)^{1/3} \approx 0.807$ . For condensation to actually take place at  $T_c$ , the free energy of the superconducting solution has to be less than the free energy of the uncondensed solution. We find that the free energy of our superconducting black holes is at all temperatures  $T > T_c$  greater than the free energy of the uncondensed black hole. Therefore, these hairy black holes represent an unstable branch that does not contribute to the thermodynamics. We will refer to this subdominant condensate as *retrograde condensate*<sup>2</sup>.

In analogy to the case of a first order phase transition (see for example Figure 3.2 ) we may also wonder if the curve of the condensate loops back at higher temperatures. We do not expect this to happen. Indeed, Figure 5.8 includes temperatures that are high enough to be above any dimensionful scale of the problem and furthermore, the curve seems to have already reached a well defined asymptotic behavior.

Several features of the uncondensed phase of Model **B** were common to the thermodynamics of a Fermi system and encouraged the search for a superconducting solution. Unfortunately, there is no holographic superconductivity at low temperature.

---

<sup>2</sup>The term “retrograde condensation” was first used by Kuenen in 1892 [108] to describe the behavior of a binary mixture during isothermal compression above the critical temperature of the mixture (a discussion can be found in [109]). Such a system also displays the phenomenon of a subdominant condensate in some temperature range.

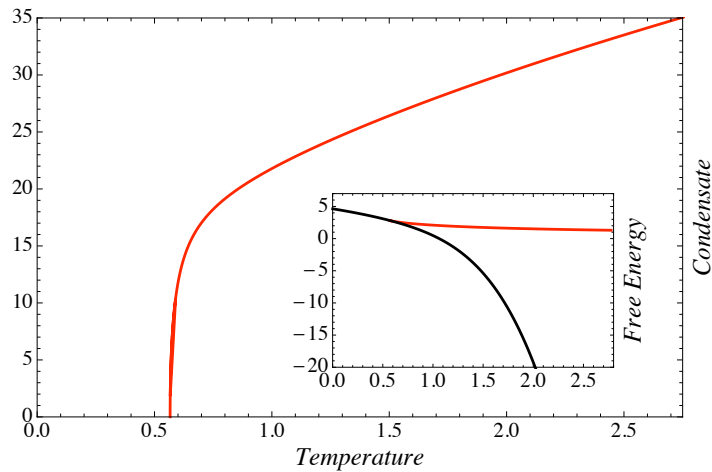


Figure 5.9: *The retrograde condensate of Model C. The free energy of the retrograde condensate (in red) is greater than the free energy of the uncondensed phase (in black) and therefore there is no phase transition.*

**Condensation in sector C.** This model has no dilatons and it is closest one to the phenomenological models that we studied in chapter 3. The functions  $J(\eta)$  and  $G(\eta)$  are,

$$J(\eta) = 4 \sinh^2 \frac{\eta}{\sqrt{3}}, \quad V(\eta) = -6 \left( 1 + \cosh^2 \frac{\eta}{\sqrt{3}} \right). \quad (5.83)$$

In this case, the uncondensed phase is described by the Reissner-Nördstrom black hole and there is a single gauge field. As Figure 5.9 shows, we again find retrograde condensation: the hairy black hole solution exists only for  $T > T_c$ . In the same Figure we show a plot of the free energies. The analysis is similar to that of Model B and in conclusion there is no phase transition.

## 5.5 Summary of results

In this chapter we have considered the  $U(1) \times U(1) \times U(1) \subset SO(6)$  sector of  $\mathcal{N} = 8$  supergravity. This is an  $\mathcal{N} = 2$  truncation in which only vector multiplets are retained. With respect to the phenomenological superconductors, black hole solutions in this model support neutral scalar fields, the dilatons, and have more than one electric field turned on. In the dual field theory these black holes correspond to states characterized by three different chemical po-

tentials. By studying general features of the entropy we have identified three *guiding* models classified according to the configuration of charges,

- One single charge turned on and two charges set to zero,
- Two equals charges turned on and one charge set to zero,
- Three equals charges turned on.

Then, we have introduced  $SU(1,1)/U(1)$  charged scalars and we have investigated whether these dilatonic black holes were unstable towards the formation of a charged hair. As a general strategy, we wanted to reproduce the minimal setup of the phenomenological models considering in addition a single neutral dilaton. Then, we have restricted our attention to Model **A**, **B** and **C**. The numerical problem came with subtle which we fixed by choosing an appropriate ansatz for the metric. The results we have found are the following.

- The condensation in Model **A** is compatible with an interesting phenomenology in which the minimum of the Landau-Ginzburg potential suddenly runaway and then stabilize. This could be an indication that the potential strongly depends on the temperature since the uncondensed phase has an effective minimum temperature which may act like a barrier against the condensation.
- Regarding Model **B** and Model **C**, the outcome of our analysis has been quite unexpected since the retrograde condensate has appeared. This is a negative result for supergravity however, we simply have to face the fact that in some cases the complicated dynamics which comes from string theory cannot be reduced to the study of a simple truncation.



# Chapter 6

## Dynamical Hypermultiplets I

In the previous chapter we have studied a certain non supersymmetric truncations of  $\mathcal{N} = 8$  supergravity in five dimensions. We now consider the one parameter family of  $\mathcal{N} = 2$  supergravity theories constructed in chapter 4. Our main interest is to understand the role of quaternionic geometry in the context of holographic superconductivity and in particular, analyze the dynamics of the two charged hyperscalars which parametrize the coset space  $SU(2, 1)/U(2)$ . We remind that our class of  $\mathcal{N} = 2$  supergravity is a one-parameter family of abelian supergravities where  $\gamma$  is the parameter that picks out the gauging direction in the isotropy group of the scalar manifold. We will consider special values of  $\gamma$  and study the resulting  $\mathcal{N} = 2$  supergravity.

In five dimensions the  $\gamma = 1$  model describes the universal hypermultiplet that appears in a large class of type IIB compactifications. These compactifications are based on Sasaki-Einstein manifolds and include a single gauge field and a massive charged scalar. We review the construction first made by Gubser and collaborators in [110] and as a concrete example, we show how the universal hypermultiplet is realized in  $\mathcal{N} = 8$  supergravity. Then, we discuss an interesting matching between the  $\gamma = 0$  model and the  $\mathcal{N} = 1$  superconformal theory of Witten and Klebanov dual to type IIB theory compactified on  $AdS_5 \times T^{1,1}$ . Finally we study the  $\gamma = 1/3$  model and its feasible relation with  $\mathcal{N} = 8$  supergravity.

The  $\gamma = 0$  model is also characterized by the appearance of a retrograde condensate. From the field theory point of view, there is a priori no special interest in the retrograde condensate. However, we would like to understand why it is there. In particular, we are motivated by the general observation that a large class of supergravities have a potential which is unbounded from below and therefore the scalar fields will always fall down along the runaway direction. Then, differently from the case of the W-shaped potentials it is not clear

which geometry describes the extremal solution. The situation is qualitatively similar to the case of potential defined just by the negative mass term but as we know very well, the condensate in the familiar HHH model admits a zero temperature limit whereas there is no looping back solution in the retrograde condensate. Despite the retrograde condensation, there is a general procedure to generate extremal IR geometries in supergravity theories. We will see how these geometries may play a role in the holographic superconductivity.

## 6.1 The $\gamma$ -family of $SU(2, 1)/U(2)$ Hypers in 5D

The bosonic sector of 5D  $\mathcal{N} = 2$  supergravity coupled to the  $SU(2, 1)/U(2)$  hypermultiplet is

$$e^{-1}\mathcal{L}_{\mathcal{H}} = \mathcal{R} - \frac{1}{4}F^{\mu\nu}F_{\mu\nu} - 2h_{i\bar{j}}D^\mu\zeta_i\overline{D_\mu\zeta_j} - \mathsf{P}^{(5)}(\zeta_1, \zeta_2) . \quad (6.1)$$

We briefly recall the notation from section 4.2. The metric  $h_{i\bar{j}}$  on the quaternionic manifold is

$$h_{i\bar{j}}d\zeta_i d\bar{\zeta}_j = \frac{d\zeta_1 d\bar{\zeta}_1 + d\zeta_2 d\bar{\zeta}_2}{(1 - |\zeta_1|^2 - |\zeta_2|^2)} + \frac{(\bar{\zeta}_1 d\zeta_1 + \bar{\zeta}_2 d\zeta_2)(\zeta_1 d\bar{\zeta}_1 + \zeta_2 d\bar{\zeta}_2)}{(1 - |\zeta_1|^2 - |\zeta_2|^2)^2} . \quad (6.2)$$

The covariant derivatives are

$$\begin{cases} D_\mu\zeta_1 \equiv \partial_\mu\zeta_1 - iA_\mu\frac{\sqrt{3}}{2}(\gamma + 1)\zeta_1 \\ D_\mu\zeta_2 \equiv \partial_\mu\zeta_2 - iA_\mu\frac{\sqrt{3}}{2}(\gamma - 1)\zeta_2 \end{cases} \quad (6.3)$$

and the potential is

$$\mathsf{P}^{(5)}(\zeta_1, \zeta_2) = -\frac{3}{2}\frac{8 - \mathsf{V}^{(5)}}{(1 - |\zeta_1|^2 - |\zeta_2|^2)^2} \quad (6.4)$$

$$\begin{aligned} \mathsf{V}^{(5)} &= (11 - 2\gamma + 3\gamma^2)|\zeta_1|^2 + (11 + 2\gamma + 3\gamma^2)|\zeta_2|^2 \\ &\quad - 2(\gamma - 1)^2|\zeta_1|^4 - 2(\gamma + 1)^2|\zeta_2|^4 - 4(\gamma^2 + 2)|\zeta_1|^2|\zeta_2|^2 \end{aligned} \quad (6.5)$$

The reader may refer to section 4.2 for a detailed analysis of the gauging procedure needed to construct this model. Here, we are mainly interested

in studying gravitational solutions related to condensed matter applications. In the context of  $\mathcal{N} = 2$  supergravity, the Lagrangian (6.1) corresponds to the minimal setting for holographic superconductivity. It contains a single gauge field  $A$ , coming from the graviton multiplet, and a single hypermultiplet parametrized by the two charged scalars  $\zeta_1$  and  $\zeta_2$ . The field strength is defined as usual by  $F_{\mu\nu} = \partial_{[\mu}A_{\nu]}$ . The AdS vacuum corresponds to  $\zeta_1 = \zeta_2 = 0$  and the value of the cosmological constant has been chosen so that the radius  $L$  of  $AdS$  is normalized to unity. This is a choice of normalization of the Killing vector and the only meaningful parameter is  $\gamma$ . In the absence of vector multiplets or dilatonic couplings the black hole solution with vanishing hyperscalars is the Reissner-Nördstrom black hole. We will implicitly assume the Reissner-Nördstrom black hole to represent the uncondensed phase for all the  $\gamma$  models of  $\mathcal{N} = 2$  supergravity.

Technically, the parameter  $\gamma$  picks a  $U(1)$  direction in the isotropy group  $SU(2)_R \times U(1)$  of the scalar manifold but from the point of view of the AdS/CFT correspondence this is not much information. Instead, it is more interesting to relate  $\gamma$  with the masses calculated at the AdS vacuum. We still have in mind the  $\mathcal{N} = 8$  supergravity and therefore we would like to see whether or not the  $SU(2,1)/U(2)$  hypermultiplet belongs to  $\mathcal{N} = 8$  supergravity for specific values of  $\gamma$ . This is certainly motivated by the exact bulk to boundary dictionary that  $\mathcal{N} = 8$  supergravity offers, nevertheless other values of  $\gamma$  may be relevant for a general discussion about holographic superconductivity.

| $\gamma$      | $(m_1^2, m_2^2)$                            | $(r_1, r_2)$                             | $(\Delta_1, \Delta_2)$                  |
|---------------|---|--|---|
| $\frac{1}{3}$ | $(-4, -3)$                                  | $\left(\frac{4}{3}, -\frac{2}{3}\right)$ | $(2, 3)$                                |
| 1             | $(-3, 0)$                                   | $(2, 0)$                                 | $(3, 4)$                                |
| 0             | $\left(-\frac{15}{4}, -\frac{15}{4}\right)$ | $(1, -1)$                                | $\left(\frac{3}{2}, \frac{5}{2}\right)$ |

Table 6.1: Masses, charges, and dimensions of the dual field theory operators which correspond to a fixed  $\gamma$ . The charges  $(r_1, r_2)$  are defined to be  $q_i = \sqrt{3}/2r_i$  where  $r_i = \gamma - (-)^i$ .

The kinetic term of the scalars is not standard and is related to the metric of the quaternionic manifold. However, at the AdS vacuum, the masses can be read directly from the potential by evaluating a standard Hessian matrix. They are given by

$$m_1^2 L^2 = -\frac{3}{4}(1+\gamma)(5-3\gamma) \quad m_2^2 L^2 = -\frac{3}{4}(1-\gamma)(5+3\gamma) \quad (6.6)$$

We observe that the Lagrangian (6.1) is symmetric under  $\zeta_1 \leftrightarrow \zeta_2$  with  $\gamma \leftrightarrow -\gamma$  and therefore, without loss of generality, we can assume  $\gamma \geq 0$ . In the Table 6.1 we provide a list of significant values of  $\gamma$ . The first two,  $\gamma = 1/3$  and  $\gamma = 1$ , are obtained by matching the value of  $m_1^2$  with the values of the masses in  $\mathcal{N} = 8$  supergravity. In fact, we recall from Table 6.2 that  $\mathcal{N} = 8$  scalars are classified into  $\mathcal{N} = 2$  hypermultiplets according to  $SU(3) \times U(1)$  representations. It is interesting to note the perfect agreement between quantum numbers of Hypermatter (1) and (2) with respect to masses and charges of  $\zeta_1$  and  $\zeta_2$  for  $\gamma = 1/3$  and  $\gamma = 1$ . In this last case, the  $\mathcal{N} = 8$  hypermultiplet is a singlet under  $SU(3)$  and we have good chances that our  $\mathcal{N} = 2$  supergravity is a truncation of  $\mathcal{N} = 8$  supergravity. The same conclusion may be false in the case of  $\gamma = 1/3$  given the more complicated  $SU(3)$  structure. Before turning to these embeddings we comment on the quantum numbers that have been found in the case  $\gamma = 0$ .

The  $\gamma = 0$  model does not belong to  $\mathcal{N} = 8$  supergravity because the masses are excluded from the spectrum. Instead,  $m_1$  and  $m_2$  are equal and coincide with the conformal mass  $m_C L$  in AdS<sub>5</sub> [111], namely

$$\text{in } AdS_{d+1}, \quad m_C^2 L^2 \equiv \frac{-d^2+1}{4} \quad \rightarrow \quad m_C^2 L^2 = -\frac{15}{4} \quad (6.7)$$

We note that for this particular value of the mass, standard and alternative

|     | Hypermatter                 | $\Delta$                         | $SU(3) \times U(1)$   |
|-----|-----------------------------|----------------------------------|---|
| (1) | $(\varphi, \zeta, \varphi)$ | $\left(3, \frac{5}{2}, 2\right)$ | $(\mathbf{6}_{\frac{2}{3}}, \mathbf{6}_{-\frac{1}{3}}, \mathbf{6}_{-\frac{4}{3}}) + \text{cc.}$ |
| (2) | $(\varphi, \zeta, \varphi)$ | $\left(4, \frac{7}{2}, 3\right)$ | $(\mathbf{1}_0, \mathbf{1}_{-1}, \mathbf{1}_{-2}) + \text{cc.}$                                 |

Table 6.2: The hypers of  $\mathcal{N} = 8$  decomposed under  $SU(3) \times U(1) \supset SU(4)$ . Adapted from [105].

quantization are both allowed. Also the charges do not match with the spectrum of  $\mathcal{N} = 8$  supergravity.

The non linear  $SU(2, 1)/U(2)$  sigma model slightly complicates the analysis of the Lagrangian (6.1) and it turns out convenient to work directly with the equations of motions. In the complex variables  $\zeta_1$  and  $\zeta_2$  we find,

$$(\nabla_\mu - ig_1 A_\mu)(\nabla^\mu - ig_1 A^\mu)\zeta_1 + (\partial_\mu \zeta_1 - ig_1 A_\mu \zeta_1)\mathcal{X}^\mu - DV_1 \zeta_1 = 0, \quad (6.8)$$

$$(\nabla_\mu - ig_2 A_\mu)(\nabla^\mu - ig_2 A^\mu)\zeta_2 + (\partial_\mu \zeta_2 - ig_2 A_\mu \zeta_2)\mathcal{X}^\mu - DV_2 \zeta_2 = 0, \quad (6.9)$$

where  $g_1$  and  $g_2$  can be read from the definitions of  $D_\mu \zeta_1$  and  $D_\mu \zeta_2$  and

$$\mathcal{X}_\mu = \frac{2}{1 - |\zeta_1|^2 - |\zeta_2|^2} \left( \bar{\zeta}_1 D_\mu \zeta_1 + \bar{\zeta}_2 D_\mu \zeta_2 \right). \quad (6.10)$$

Our analysis will focus mostly on the following two quantities:

$$DV_1 = -\frac{3}{4}(1 + \gamma) \left[ \frac{-5 + 3\gamma + (7 - \gamma)|\zeta_1|^2 + (3 - \gamma)|\zeta_2|^2}{(1 - |\zeta_1|^2 - |\zeta_2|^2)} \right] \quad (6.11)$$

$$DV_2 = -\frac{3}{4}(1 - \gamma) \left[ \frac{-5 - 3\gamma + (7 + \gamma)|\zeta_2|^2 + (3 + \gamma)|\zeta_1|^2}{(1 - |\zeta_1|^2 - |\zeta_2|^2)} \right] \quad (6.12)$$

The symmetry under  $\zeta_1 \leftrightarrow \zeta_2$  with  $\gamma \leftrightarrow -\gamma$  is preserved. From the above formulas we also recover the masses  $m_1^2$  and  $m_2^2$  given in (6.6) and obtained by expanding around the AdS vacuum.

In the next sections we calculate explicitly  $DV_1$ ,  $DV_2$  and the potential of the  $\mathcal{N} = 2$  theories that correspond to  $\gamma = 1$ ,  $\gamma = 1/3$  and  $\gamma = 0$ . We will study in detail their superconducting phases.

**Review of the Thermodynamical ensemble.** We have already introduced in the previous chapters the machinery needed to construct a superconducting solution. In particular, for any value of  $\gamma$ , the  $\mathcal{N} = 2$  supergravity (6.1) can be treated within the general setup of the phenomenological model. The ansatz for the metric and the gauge field is

$$ds^2 = -f(r)e^{-\chi} dt^2 + d\vec{x}^2 + \frac{dr^2}{f(r)}, \quad A_\mu dx^\mu = \Phi(r) dt. \quad (6.13)$$

It is useful to recall the UV asymptotic behavior of a generic superconducting solution. This is

$$\zeta_i(r) = \frac{O^{\Delta_i}}{r^{\Delta_i}} + \dots \quad (6.14)$$

$$\Phi(r) = \mu - \frac{\rho}{r^2} + \dots \quad (6.15)$$

$$e^{-\chi} f(r) = e^{-\chi_\infty} \left( \frac{r^2}{L^2} - \frac{M}{r^2} + \dots \right), \quad (6.16)$$

$$\chi = \chi_\infty + O\left(\frac{1}{r^{2(\Delta_1+1)}}\right) + O\left(\frac{1}{r^{2(\Delta_2+1)}}\right) \quad (6.17)$$

where  $i = 1, 2$  and  $\Delta_1, \Delta_2$  are the dimensions of the dual condensates. They are defined by the standard quantization scheme. In the special cases, the alternative quantization scheme may also be considered. The energy, the charge density and the entropy of the field theory are defined as,

$$E_{ft} = \frac{3M}{16\pi G_N}, \quad \rho_{ft} = \frac{\rho}{8\pi G_N}, \quad s = \frac{r_h^3}{4G_N}. \quad (6.18)$$

The free energy is given by the combination,

$$f = E_{ft} - Ts = \frac{1}{8\pi G_N} \left( \frac{3}{2}M - 2\pi r_h^3 T \right). \quad (6.19)$$

We will work in the canonical ensemble where the charge density of the field theory is fixed, i.e  $\rho = 1$ .

## 6.2 The $\gamma = 1$ Holographic Superconductor

This model is defined by,

$$P^{(5)}(\zeta_1, \zeta_2) \Big|_{\gamma=1} = -6(1 - |\zeta_2|^2) \left[ \frac{2 - 3|\zeta_1|^2 - 2|\zeta_2|^2}{(1 - |\zeta_1|^2 - |\zeta_2|^2)^2} \right] \quad (6.20)$$

$$DV_1 = -3 \left[ \frac{1 - 3|\zeta_1|^2 - |\zeta_2|^2}{1 - |\zeta_1|^2 - |\zeta_2|^2} \right] \quad (6.21)$$

$$DV_2 = 0$$

It is interesting to observe that  $DV_2 \equiv 0$ . As a consequence, the  $\zeta_2$  field has trivial dynamics and we can focus on the field theory dual to  $\zeta_1$ . The redefinition

$$\zeta_1 = \tanh \frac{\eta}{2} e^{i\theta} \quad (6.22)$$

brings the  $\mathcal{N} = 2$  scalar Lagrangian into the standard form,

$$\mathcal{L}_{scalar}^{\gamma=1} = -\frac{1}{2} \left[ \partial_\mu \eta \partial^\mu \eta + \sinh^2 \eta (\partial\theta - \sqrt{3}A)^2 \right] - 3 \cosh^2 \frac{\eta}{2} (5 - \cosh \eta) \quad (6.23)$$

Then, we can study the superconducting phase by considering the general strategy discussed in chapter 3.2. In particular, the Lagrangian (6.23) corresponds to a phenomenological model with given potential and  $J(\eta) = 3 \sinh^2 \eta$ . The AdS vacuum is set at  $r \rightarrow \infty$  and the asymptotic of the scalar in the off-shell configuration is

$$\eta(r) \rightarrow \frac{S^{(1)}}{r} + \frac{O^{(3)}}{r^3} + \dots \quad (6.24)$$

The symmetry breaking condition requires  $S^{(1)} = 0$  and the condensate has dimension  $\Delta = 3$ . In Figure 6.1 we show the numerical results. At the critical temperature  $T_c \approx 0.0835$  we find a second order phase transition from the uncondensed phase represented by the Reissner-Nördstrom black to a superconducting phase where  $\eta(r) \neq 0$ .

The topology of the potential plays an important role in the construction of the holographic superconducting phase. In particular, we can understand how the zero temperature solution will look like by following the evolution of the horizon data as the temperature is cooled. In other words, the flow of the scalar field along the potential encodes part of the information regarding the superconducting ground-state and classically, this flows is determined by the topology of the potential. The zero temperature solution is a charged domain wall and we now describe how to obtain this solution [112]. First of all, let us note that the existence of the domain wall can be guessed by considering that  $DV_1 = 0$  has a non trivial solution for finite  $\zeta_1$  and an IR AdS vacuum emerges. Numerically we have verified that the low temperature superconducting solutions approach the charged domain wall background and in particular, the value of the scalar field at zero temperature coincides with the limit  $\zeta_1 \rightarrow 1/\sqrt{3}$ . This is actually a fixed point and the metric takes the form,

$$ds^2 = \frac{r^2}{L_{IR}^2} (-dt^2 + d\vec{x}^2) + \frac{L_{IR}^2}{r^2} dr^2 \quad \cosh \eta = 2 \quad L_{IR}^2 = \frac{8}{9} \quad (6.25)$$

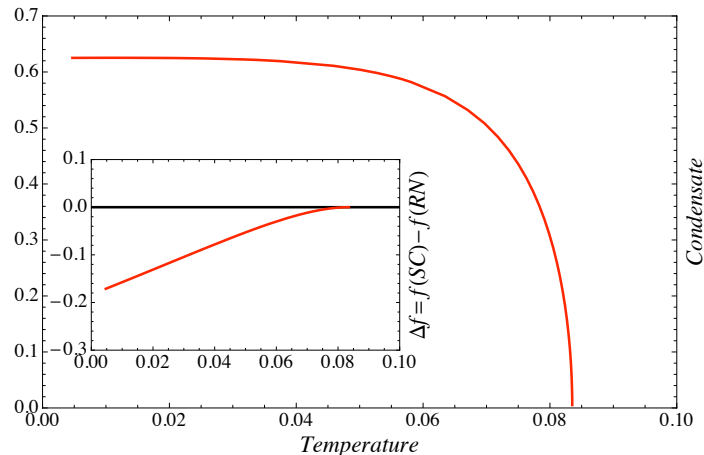


Figure 6.1: The condensate of dimension  $\Delta = 3$  and difference of free energy between the uncondensed phase (RN) and the superconducting phase (SC) as function of the temperature ( $\rho = 1$ ). The phase transition is second order.

In this geometry the scalar field sits at the minimum of the potential and the gauge field vanishes, i.e.  $\Phi(r) = 0$ . Because the gauge field must carry flux at the boundary, we have to move from (6.25) exciting irrelevant perturbations, in particular the sub-leading modes of the fields  $\Phi(r)$  and  $\eta(r)$ . These perturbations are,

$$\eta(r) \approx r^{e_\eta}, \quad e_\eta = 2(\sqrt{3} - 1) \quad ; \quad \Phi(r) \approx r^{e_\Phi}, \quad e_\Phi = 2 \quad (6.26)$$

The zero temperature solution is then obtained by integrating the full system of equations up to the UV boundary where the shooting method is applied to match the condition  $S^{(1)} = 0$ . We mention that  $e_\eta$  and  $e_\Phi$  do correspond to IR irrelevant perturbations in the sense of the RG flow. When this condition is not satisfied, Lifshitz solutions need to be considered and we refer to [113] for a more comprehensive discussion.

### 6.2.1 Type IIB Sasaki-Einstein Truncations.

The present  $\mathcal{N} = 2$  supergravity model can be consistently embedded in type IIB theory. First we consider the embedding of the charged  $\zeta_1$  scalar field and then we add the  $\zeta_2$  field. We proceed following this order because it is not hard to figure out which field in type IIB theory corresponds to the  $\zeta_2$  scalar. This has to be a complex chargeless scalar field with  $DV_2 = 0$  and

dimension  $\Delta = 4$ . There is only one candidate with these characteristics: the axio-dilaton  $\tau = C_0 + ie^{-\phi}$ . Thus, the incorporation of  $\tau$  in the Lagrangian, even if not completely trivial, will be almost straightforward once the ansatz for the  $\zeta_1$  truncation has been understood.

The embedding of the charged  $\zeta_1$  scalar has been assembled in [110]. It is our interest to spell out some of the details of the construction. To do so we follow the reference [114, 115]. A similar procedure has been successfully applied also to eleven dimensional supergravity [116].

We begin by recalling that a regular Sasaki Einstein manifold  $Y$  can be seen as a  $U(1)$  fibration over a Kähler-Einstein base manifold  $B_{KE}$ :

$$ds_Y^2 = ds_B^2 + \xi \otimes \xi \quad (6.27)$$

where  $\sigma$  is a globally defined 1-form dual to the Reeb Killing Vector [117]. All Sasaki-Einstein manifolds are characterized by three globally defined real 2-forms  $J^x$  satisfying,

$$J^x \wedge J^y = 2\delta^{xy} \text{vol}(B), \quad i_\xi(J^x) = 0 \quad (6.28)$$

$$d\Omega_2 = 3i \xi \wedge \Omega_2 \quad d\xi = 2\omega \quad (6.29)$$

In the second line, we have defined  $J^1 = \omega$  and  $\Omega_2 = J^2 + iJ^3$ . We will keep this notation throughout the construction. “ $\text{vol}(B)$ ” denotes the volume form on the base manifold. We also note the two relations,

$$\star \xi = \text{vol}(B), \quad \star J^x = J^x \wedge \xi \quad (6.30)$$

The starting point is to write down a decomposition of the ten dimensional fields of type IIB theory according to the structure of possible deformations of the Sasaki-Einstein manifold. We implicitly assume the Einstein frame for the ten dimensional metric. Then we find,

$$\begin{aligned} ds^2 &= G_{MN} dx^M dx^N \\ &= e^{-\frac{2}{3}(4U+V)} ds_5^2 + e^{2U} ds_B^2 + e^{2V} (\xi + A) \otimes (\xi + A) \end{aligned} \quad (6.31)$$

where  $M, N = 0, \dots, 9$ . The fields  $U(x)$  and  $V(x)$  are scalars whereas  $A(x)$  is a 1-form on the five dimensional space-time. In particular,  $x^\mu$  with  $\mu = 0, \dots, 4$  are coordinates for  $ds_5^2$  and  $y^m$  with  $m = 5, \dots, 9$  are coordinates for  $Y$ . The scalars  $U$  and  $V$  parametrize the “breathing mode” and the “squashing mode” of the compact transverse manifold: the combination  $(4U + V)$  controls the overall volume, while the other combination  $U - V$  modifies the relative size of the  $U(1)$  fiber with respect to the size of the base manifold.

The study of the other fields of type IIB theory is more involved. The only exceptions are the dilaton  $\varphi$  and the axion  $C_0$  that have trivial dependence on the internal coordinates  $y^m$ . The 2-forms  $B_2$  and  $C_2$  and the self-dual 4-form  $C_4^+$  need a more careful analysis because they are tensor fields and therefore have legs on the compact space. In general these legs cannot be consistently truncated unless the tensor field itself vanishes. By following [118], we implement the Kaluza-Klein reduction of these fields by performing an expansion in the structure forms  $\xi$ ,  $\omega$  and  $\Omega_2$ . Before proceeding, we point out that a five dimensional gauge transformation is induced by a reparametrization of the fiber coordinate. A more familiar example is perhaps that of toroidal compactifications where the metric is written as

$$\begin{aligned} ds^2 &= G_{MN} dx^M dx^N \\ &= G_{\alpha\beta} dx^\alpha dx^\beta + e^{2V} (d\xi + A_\alpha dx^\alpha)^2 \end{aligned} \quad (6.32)$$

The compact dimension is  $x^9 \equiv \xi$  and the ten dimensional metric is split under  $SO(1, 8)$  into a vector  $A_\mu(x) \sim G_{\alpha 9}$ , a scalar  $V(x) \sim G_{99}$  and the lower dimensional metric  $G_{\alpha\beta}$  on the non compact manifold. Reparametrizations of the form  $\xi \rightarrow \xi + k(x)$  induce the transformation  $A_\alpha(x) \rightarrow A_\alpha(x) + \partial_\alpha k(x)$  which in turn implies that  $A_\mu$  is a gauge field. The scalar  $V(x)$  is invariant under gauge transformations.

In the case of the Sasaki-Einstein compactification, since we would like the reduction ansatz to be gauge covariant we need to understand how the ten dimensional fields transform under this reparametrization. In order to do so, we consider the Lie derivative along the the Killing vector of the fiber isometry. We indicate this vector with  $K = k(x)\partial/\partial\xi$  and we refer to the Lie derivative with  $L_K$ . Then,  $L_K = \iota_X \cdot d + d \cdot \iota_X$  and we obtain

$$L_K \omega = 0, \quad L_K \Omega_2 = 3ik(x)\Omega_2 \quad (6.33)$$

We conclude that  $J$  is invariant under gauge transformations but  $\Omega_2$  is not. Thus, five dimensional harmonics of  $\Omega_2$  appearing in the expansion of  $B_2$ ,  $C_2$  and  $C_4^+$  will be charged under the  $U(1)$  gauge field. Ten dimensional forms have to be expanded in terms of  $\xi + A$  rather than just  $\xi$ . The complete expansion of the ten dimensional fields can be found in [114]. In our case, the ansatz for the  $\zeta_1$  truncation with  $C_0$  to zero and constant dilaton is given by,

$$\begin{aligned} e^{2V} &= \cosh \frac{\eta}{2}, & e^{-2U} &= \cosh \frac{\eta}{2}, \\ B_2 &= \text{Re} (b^\Omega \Omega_2), & b^\Omega &= L^2 \tanh \frac{\eta}{2} e^{i\theta}, \\ C_2 &= \text{Im} (c^\Omega \Omega_2), & c^\Omega &= ib^\Omega \end{aligned} \quad (6.34)$$

The self-dual five form  $F_5^+$  is given by

$$\begin{aligned}
\mathcal{F} &= \cosh^2 \frac{\eta}{2} (5 - \cosh \eta) \text{vol}(ds_5^2) - L^3 (\star_5 dA) \wedge \omega \\
&\quad + \frac{L^4}{4} e^{8U} \sinh^2 \eta (d\theta - 3A) \wedge \omega \wedge \omega \\
\star \mathcal{F} &= \frac{L^4}{2} e^{4U} (\cosh \eta - 5) (\xi + A) \wedge \omega \wedge \omega + L^4 dA \wedge (\xi + A) \wedge \omega \\
&\quad + \frac{L}{2} \sinh^2 \eta (\star_5 (d\theta - 3A)) \wedge (\xi + A) \\
F_5^+ &= \mathcal{F} + \star \mathcal{F} \tag{6.35}
\end{aligned}$$

We observe that  $F_5$  admits the following form decomposition

$$F_5 = f_5 + f_0 \omega \wedge \omega \wedge (\xi + A) \tag{6.36}$$

$$+ f_3^\omega \wedge \omega + f_2^\omega \wedge \omega \wedge (\xi + A) \tag{6.37}$$

$$+ f_4 \wedge (\xi + A) + f_1 \wedge \omega \wedge \omega \tag{6.38}$$

where the self duality condition imposes

$$f_5 = -2e^{-\frac{32}{3}U - \frac{8}{3}V} \star_5 f_0 \tag{6.39}$$

$$f_4 = 2e^{-8U} \star f_1, \tag{6.40}$$

$$f_3^\omega = -e^{-\frac{4}{3}(U+V)} \star f_2^\omega \tag{6.41}$$

By comparing with (6.35) we read

$$f_0 = 3\text{Im}(b^\Omega \bar{c}^\Omega) + 2 \tag{6.42}$$

$$f_1 = \frac{1}{2} \{ \text{Re} [ b^\Omega (d\bar{c}^\Omega + 3iA\bar{c}^\Omega) ] - (b^\Omega \leftrightarrow c^\Omega) \} \tag{6.43}$$

$$f_2^\omega = L^3 dA \tag{6.44}$$

Finally, the truncated action reads

$$\mathcal{L}_{IIB}^{\zeta_1} = \mathcal{R} - \frac{3L^2}{2} (\star_5 dA) \wedge dA + A \wedge dA \wedge dA \quad (6.45)$$

$$- \frac{1}{2} \left( d\eta^2 + \sinh^2 \eta (d\theta - 3A)^2 - 6 \cosh^2 \frac{\eta}{2} (5 - \cosh \eta) \right) \quad (6.46)$$

### 6.2.2 The Universal Hypermultiplet.

It is clear that  $\mathcal{L}_{IIB}^{\zeta_1}$  coincides with (6.23). From the point of view of  $\mathcal{N} = 2$  we have retained only half of the hypermultiplet, i.e the  $\zeta_1$  field. By giving dynamics to the axio-dilaton we expect to recover the full  $\gamma = 1$  supergravity theory. This is done by considering the axio-dilaton action already present in type IIB theory together with the identification,

$$c^\Omega = b^\Omega \tau = e^{\phi/2} e^{i\theta} \tanh \frac{\eta}{2} \quad (6.47)$$

The result is

$$\mathcal{L}_{\mathcal{H}} - \mathcal{L}_{IIB}^{\zeta_1} = -\frac{1}{2} \cosh^2 \frac{\eta}{2} \left( d\phi^2 + e^{2\phi} \cosh^2 \frac{\eta}{2} dC_0^2 \right) \quad (6.48)$$

$$- \frac{1}{2} e^\phi \sinh^2 \eta dC_0 (d\theta - 3A) \quad (6.49)$$

The  $SU(2,1)/U(2)$  kinetic term we are familiar with involves the complex coordinates  $\{\zeta_1, \zeta_2\}$  and can be conveniently written by means of the Kähler potential (4.31). In order to match the above expression with the kinetic term of the  $\gamma = 1$   $\mathcal{N} = 2$  supergravity written in (6.1), we need to find the correct change of variable. Explicitly, the field redefinition we seek is<sup>1</sup>,

$$\zeta_1 = \sqrt{1 - |\zeta_2|^2} e^{i\theta} \tanh \frac{\eta}{2} \sqrt{\frac{1 + i\bar{\tau}}{1 - i\tau}}, \quad \zeta_2 = \frac{1 + i\tau}{1 - i\tau}. \quad (6.50)$$

Then, our  $\mathcal{N} = 2$  supergravity describes the universal hypermultiplet that belongs to the class (6.31) of Sasaki-Einstein compactifications. The dual field theory is a  $\mathcal{N} = 1$  Conformal Field Theory whose  $R$ -symmetry is geometrically realized by the gauging of the connection  $A$ . Here, we see how this  $U(1)$  fiber is embedded into the  $U(1) \times SU(2)_R$  isotropy group of the quaternionic scalar manifold. Since we have not specified the base space of the Sasaki-Einstein manifold, the compactification that we have provided contains a large class of theories. In particular, the five sphere is a Sasaki-Einstein manifold and  $\mathcal{N} = 8$

<sup>1</sup>We thank Jorge Russo for this result.

supergravity in five dimensions arises from type IIB theory compactified on  $\text{AdS}_5 \times \text{S}^5$ . Thus, the resulting  $\mathcal{N} = 2$  supergravity is by construction contained into  $\mathcal{N} = 8$  supergravity. As a result, we have proven that our  $\gamma = 0$   $\mathcal{N} = 2$  supergravity describes Hypermatter (2) in  $\mathcal{N} = 8$  supergravity (see Table 6.2 for the reference).

### 6.3 The $\gamma = 0$ Holographic Superconductor

This model is defined by,

$$P^{(5)}(\zeta_1, \zeta_2) \Big|_{\gamma=0} = -\frac{3}{2} \left[ \frac{8 - 11(|\zeta_1|^2 + |\zeta_2|^2) + 2(|\zeta_1|^2 + |\zeta_2|^2) + 6|\zeta_1|^2|\zeta_2|^2}{(1 - |\zeta_1|^2 - |\zeta_2|^2)^2} \right]$$

$$DV_1 = -\frac{3}{4} \left[ \frac{5 - 7|\zeta_1|^2 - 3|\zeta_2|^2}{1 - |\zeta_1|^2 - |\zeta_2|^2} \right] \quad (6.51)$$

$$DV_2 = DV_1 \quad (6.52)$$

In this theory, the scalars have not only equal masses  $m_{1/2}^2 = -15/4$  but also equal interactions,  $DV_1 = DV_2$ . Thus, there exist two natural truncations to a single charged scalar field. They are

$$\text{I} \quad \zeta_1 = \tanh \frac{\eta}{2} e^{i\theta} \quad \text{and} \quad \zeta_2 = 0$$

$$\text{II} \quad \zeta_1 = \zeta_2 = \zeta \quad \text{with} \quad \zeta = \frac{1}{\sqrt{2}} \tanh \frac{\eta}{2} e^{i\theta}.$$

We can treat both cases within the framework of phenomenological models by reading the potential given in (6.51) and defining the function  $J(\eta)$  through the coupling with the gauge field. The resulting Lagrangians are,

$$\mathcal{L}_{scalar}^{\gamma=0} = -\frac{1}{2} \partial_\mu \eta \partial^\mu \eta - \frac{1}{2} J^{(i)}(\eta) A^2 - V^{(i)} \quad (6.53)$$

where we have defined the two sets of couplings

$$\text{Model I} \quad \left\{ \begin{array}{l} J^I = \frac{3}{4} \sinh^2 \eta \\ V^I = \frac{3}{8} (\cosh^2 \eta - 12 \cosh \eta - 21) \end{array} \right. \quad (6.54)$$

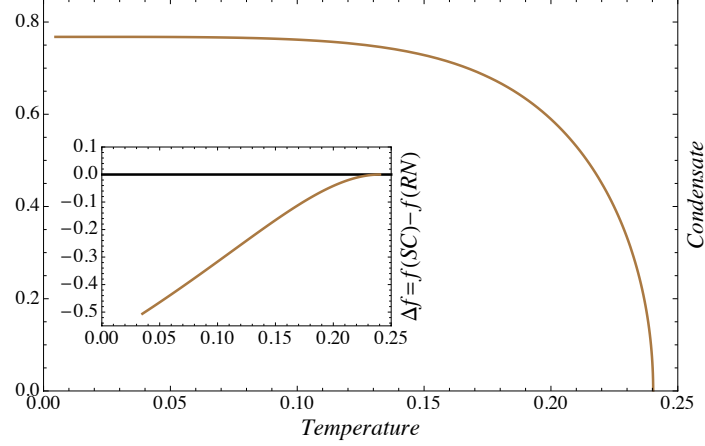


Figure 6.2: *The condensate of dimension  $\Delta = 3/2$  in Model I and the difference of free energy between the uncondensed phase (RN) and the superconducting phase (SC) as function of the temperature ( $\rho = 1$ ). The phase transition is second order.*

and

$$\text{Model II} \quad \begin{cases} J^{II} = 3 \sinh^2 \frac{\eta}{2} \\ V^{II} = \frac{3}{2} \left( 3 + 5 \cosh^2 \frac{\eta}{2} \right) \end{cases} \quad (6.55)$$

The identification  $\zeta_1 = \zeta_2$  in Model II does not affect the value of the mass and the asymptotic behavior of  $\eta$  in both these models is,

$$\eta(r) \rightarrow \frac{O^{(1)}}{r^{3/2}} + \frac{O^{(2)}}{r^{5/2}} + \dots \quad (6.56)$$

We also observe that the first non vanishing contribution in the above expansion comes at order  $r^{7/2}$ . The value  $-15/4$  lies in the range of masses for which both standard and alternative quantization are allowed. In the case of alternative quantization, we search for a condensate of dimension  $\Delta = 3/2$  by requiring  $O^{(2)} = 0$ . In the case of standard quantization, we look for a condensate of dimension  $\Delta = 5/2$  by imposing  $O^{(1)} = 0$  [13].

**The results for Model I.** We show in Figure 6.2 and Figure 6.3 the two condensates that Model I describes. Curiously, the transition to the superconducting phase is second order for the  $\Delta = 3/2$  condensate and first order for

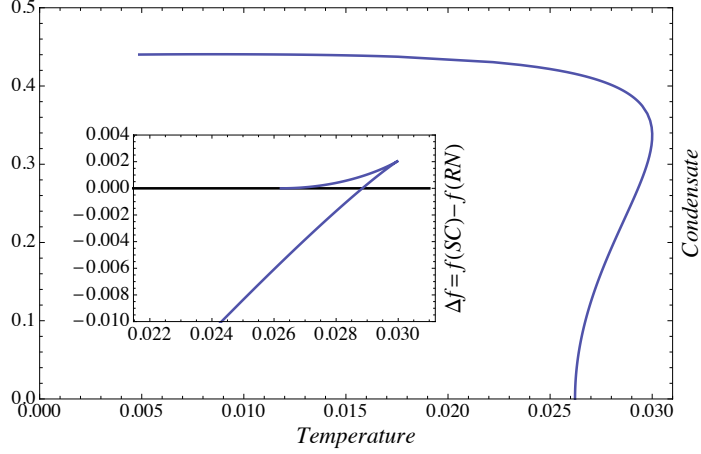


Figure 6.3: The condensate of dimension  $\Delta = 5/2$  in Model I and the difference of free energy between the uncondensed phase (RN) and the superconducting phase (SC) as function of the temperature ( $\rho = 1$ ). The solution has two branches and the phase transition is first order. It takes place at the critical temperature  $T_c \approx 0.029$ .

the  $\Delta = 5/2$  condensate. The zero temperature solution is understood as a charged domain wall between an IR AdS and the AdS vacuum at the boundary. The difference between the two Figures is the choice of quantization: the IR fixed point is the same. This is characterized by  $\cosh \eta_{IR} = 6$  and AdS radius  $L_{IR}^2 = 32/57$ . With the same conventions as in (6.26), perturbations of matter fields are governed by the positive exponents,

$$e_\eta = -2 + 2\sqrt{\frac{89}{19}} \quad ; \quad e_\Phi = -1 + \sqrt{\frac{299}{19}} \quad (6.57)$$

**The Retrograde Condensate.** Another interesting aspect of the  $\gamma = 0$  supergravity is the appearance of a retrograde condensate. This solution exists in Model II and for both types of quantizations. In Figure 6.4 we show the retrograde condensate of dimension  $\Delta = 3/2$ . We observe that the linearized analysis for both Model I and Model II is the same and therefore the corresponding operators condense at the same temperature. As for Model C in  $\mathcal{N} = 8$  supergravity, there is no phase transition and the retrograde condensate is a subdominant solution.

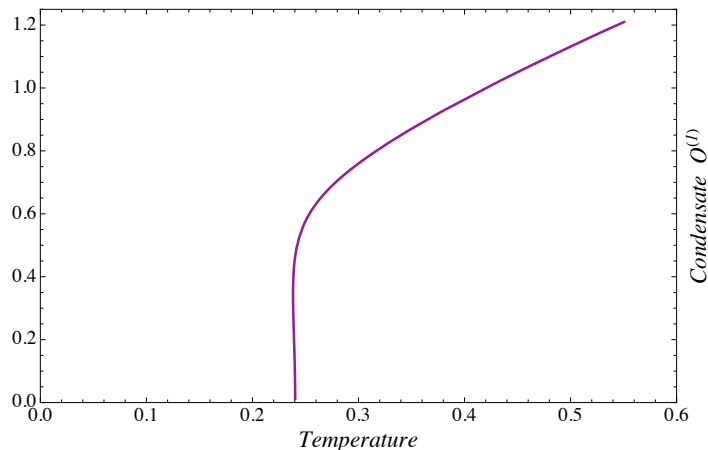


Figure 6.4: *The retrograde condensate of dimension  $\Delta = 3/2$  in Model II ( $\rho = 1$ ).*

### 6.3.1 Connecting with Type IIB theory on $\text{AdS}_5 \times \text{S}^5$

The study of the  $\gamma = 0$  supergravity is also motivated by a feasible connection between type IIB superstring. We pointed out that  $\mathcal{N} = 8$  supergravity rules out scalars with masses  $m^2 L^2 = -15/4$ . In particular, the spectrum of type IIB theory on  $\text{AdS}_5 \times \text{S}^5$  does not support Kaluza-Klein modes with this value of the mass. Other internal manifolds, different from  $S^5$ , may do the job. One such manifold is the homogeneous space  $T^{1,1} = (SU(2) \times SU(2))/U(1)$  with  $U(1)$  being the diagonal subgroup of  $SU(2) \times SU(2)$ . The dual field theory was found by Klebanov and Witten in [119] and we quickly outline the idea of the construction. Their starting point is a geometrical characterization of  $T^{1,1}$ , identified with the transverse space of a Calabi-Yau three-fold  $Y_6$ . This manifold is a cone defined by the  $SU(2) \times SU(2) \times U(1)$  symmetry. As a concrete realization of  $Y_6$  we consider the surface

$$z_1^2 + z_2^2 + z_3^2 + z_4^2 = 0, \quad (6.58)$$

where the  $z_i$  are homogeneous coordinates on  $\mathbb{CP}^4$ . An equivalent characterization of this surface is,

$$z_1 z_2 - z_3 z_4 = 0. \quad (6.59)$$

At the conical singularity the metric will take the form of a cone over  $T^{1,1}$ , namely

$$ds_Y^2 = dr^2 + r^2 ds_T^2 \quad (6.60)$$

where  $ds_T^2$  is the metric of the homogeneous manifold. The Calabi-Yau threefold  $Y_6$  is Ricci-flat and  $T^{1,1}$  is an Einstein manifold with positive curvature. By taking advantage of this construction, the dual field theory is identified by studying a stack of  $N$  D3-branes placed at the conical singularity. This idea mimics the original Maldacena derivation of the AdS/CFT correspondence but in a different setup. In particular, supersymmetry is reduced from  $\mathcal{N} = 4$  to  $\mathcal{N} = 2$  and the resulting field theory is a  $4D$   $\mathcal{N} = 1$  superconformal theory with gauge group  $SU(N) \times SU(N)$ . Together with the two chiral gauge superfields  $W_{1\alpha}$  and  $W_{2\alpha}^2$ , there are the chiral superfields  $(A_1, A_2)$  and  $(B_1, B_2)$ . Respectively,  $A_1$  and  $B_2$  transform in the fundamental representation of  $SU(N)$ , whereas  $A_2$  and  $B_1$  transform in the anti-fundamental. We can think of them as  $N \times N$  matrices whose eigenvalues parametrize the position of the D3-branes. The global symmetry group is  $SU(2)_A \times SU(2)_B$  where the labels  $A$  and  $B$  refer to the corresponding chiral superfields. In other words,  $A_k$  and  $B_l$  transform as two doublets under the global symmetry. This is evident when the equation (6.59) is solved by writing

$$z_1 \rightarrow A_1 B_1, \quad z_2 \rightarrow A_2 B_2, \quad z_3 \rightarrow A_1 B_2, \quad z_4 \rightarrow A_2 B_1. \quad (6.61)$$

Finally, the  $\mathcal{N} = 1$  theory has a unique superpotential given by

$$W \sim \varepsilon^{ij} \varepsilon^{kl} \text{Tr} A_i B_k A_j B_l. \quad (6.62)$$

The precise conjecture is: Type IIB string theory on  $AdS_5 \times T^{1,1}$ , with  $N$  units of Ramond-Ramond flux on  $T^{1,1}$ , should be equivalent an  $SU(N) \times SU(N)$  gauge theory, with chiral matter fields  $(N, \bar{N}) \oplus (\bar{N}, N)$  flowing to an infrared fixed point and perturbed by the superpotential (6.62).

The point we would like to emphasize about this theory is the following. For  $\gamma$  integer, the masses and the charges of the  $SU(2, 1)/U(2)$  hypermultiplet, are in precise correspondence with those of the chiral  $AdS$  multiplets for type IIB on  $AdS_5 \times T^{1,1}$ , with specific global  $SU(2) \times SU(2)$  quantum numbers  $(j, l)$ . In particular, we are interested in:

- Kaluza-Klein tower originating from the complex zero- and two-forms with  $2j = 2l = \gamma - 1$ ,  $\gamma \geq 1$ . This is dual to field theory operators of the form

$$\Phi^{\gamma-1} = \text{Tr}[(W_1^2 + W_2^2)(A_k B_l)^{\gamma-1}]$$

---

<sup>2</sup>Given the two vector superfields  $V_1$  and  $V_2$ , the chiral superfields  $W_{i\alpha}$  are defined through the standard relation  $W_{i\alpha} = \overline{D}D(e^{V_i} D_\alpha e^{-V_i})$  where  $D_\alpha$  and  $\overline{D}_{\dot{\alpha}}$  are the covariant derivatives in the superspace formalism.

- Kaluza-Klein tower originating from the metric, the four-form and the complex two form with  $2j = 2l = \gamma + 1$ ,  $\gamma \geq 0$ . This is dual to field theory operators of the form

$$S^{\gamma+1} = \text{Tr}[(A_k B_l)^{\gamma+1}]$$

A precise discussion about the Kaluza-Klein compactification on  $T^{1,1}$  and the exact mapping with the dual CFT can be found in the pioneer work [120]. For our purpose it is enough to recall that:

- i) At the conformal point, the dimension  $\Delta$  of  $\Phi^{\gamma-1}$  and  $S^{\gamma+1}$  is protected, meaning that  $\Delta$  is related to the  $R$ -charge which in turns is quantized<sup>3</sup>.
- i) The chiral superfields  $A$  have  $j = 1/2$ ,  $l = 0$  whereas the chiral superfields  $B$  have  $j = 0$ ,  $l = 1/2$ . At the conformal point, both  $A$  and  $B$  have anomalous conformal dimension  $\Delta = 3/4$  and  $R$ -charge  $1/2$ . It follows that,

$$\Delta(S) = \frac{3}{2} (\gamma + 1) . \quad (6.63)$$

Then, the lowest state in the Kaluza-Klein tower has  $\gamma = 0$  and  $\Delta = 3/2$ .

- iii) The chiral gauge superfields  $W_{1\alpha}$  and  $W_{2\alpha}$  have dimensions  $\Delta = 3/2$  and  $R$ -charge 1. It follows that,

$$\Delta(\Phi) = 3 + \frac{3}{2} (\gamma - 1) . \quad (6.64)$$

Then, the lowest state in the Kaluza-Klein tower has  $\gamma = 1$  and  $\Delta = 3$ .

Interestingly enough, these same relations hold for the  $SU(2, 1)$  hypermultiplet of our  $\mathcal{N} = 2$  supergravities when  $\gamma$  is taken to be integer.

We can borrow the type IIB embedding presented in the previous paragraph and valid for every Sasaki-Einstein manifold, including  $Y_6$ , to claim that the lowest Kaluza-Klein state in the first tower corresponds to the  $SU(2, 1)/U(2)$  hypermultiplet with  $\gamma = 1$ . As we know, the corresponding masses are,  $m^2 L^2 = -3$  and  $m^2 \tilde{L}^2 = 0$ . The  $SU(2) \times SU(2)$  quantum numbers are  $j = l = 0$  meaning that this hypermultiplet is a singlet under the global symmetry group. This is the same situation as in  $\mathcal{N} = 8$  supergravity where Hypermatter (2) was actually a singlet under  $SU(3)$ . On the other hand, the lowest Kaluza-Klein state in the second tower has  $\gamma = 0$  and  $SU(2)$  quantum

---

<sup>3</sup>Unlike  $\mathcal{N} = 4$ , operators with protected dimensions have conformal dimension different from their free-field value.

numbers  $j = l = 1/2$ . At this point it is natural to ask, is the  $\gamma = 0$   $\mathcal{N} = 2$  supergravity a consistent truncation within type IIB theory compactified on  $T^{1,1}$ . Symmetries are not of help because the hypermultiplet is not a singlet under  $SU(2) \times SU(2)$ , as we have seen  $j = l = 1/2$ . This is a major obstruction to the consistency of the truncation. Nevertheless, it only means that we should find this hypermultiplet by retaining the full  $SU(2) \times SU(2)$  matter content<sup>4</sup>. Therefore, it may be the case that our  $\gamma = 0$   $\mathcal{N} = 2$  supergravity arises as a particular truncation. After all, this is suggested by the fact that  $\gamma = 0$  corresponds to the lower states in the Kaluza-Klein tower. We leave this issue for a future study.

**Competition between Condensates.** We suppose that the  $\gamma = 0$   $\mathcal{N} = 2$  supergravity belongs to the  $T^{1,1}$  compactification of type IIB superstring. As we have shown, the full  $AdS_5 \times T^{1,1}$  theory has two charged operators in the lowest Kaluza-Klein towers,  $S^{\gamma+1}$  for  $\gamma = 0$  and  $\Phi^{\gamma-1}$  for  $\gamma = 1$ . They have different charges and therefore we expect the condensate of dimension  $\Delta = 3$  to compete with the condensate of dimension  $\Delta = 3/2$ . In order to have a better understanding of this statement, we recall the study of the linearized approximation discussed in the cases of phenomenological models. The critical temperature for the superconducting instability only depends on the mass and the charge of the dual scalar field. In the cases of negative masses, we showed that this critical temperature increases if either one of the following conditions is satisfied: the mass is decreased and the charge is increased. The first condition, written in terms of the dimension of the dual operator, implies that the critical temperature increases if the dimension increases. Then, the scalar of Model I, which has mass the lowest mass  $m^2 L^2 = -15/4$ , it has not the greatest charge, i.e.  $r = 1$  versus  $r = 2$  of the universal hypermultiplet. Therefore, we cannot conclude which condensate between  $\Delta = 3$  and  $\Delta = 3/2$  is going to condense first unless we construct the superconducting black hole. By comparing Figure 6.2 with Figure 6.1, we see that the “dominant” solution is the one associated with the  $\Delta = 3/2$  condensate.

It worth noting that we do not know whether the  $\Delta = 3/2$  condensate controls the low energy physics of the  $\mathcal{N} = 1$  superconformal theory. The bulk scalar certainly corresponds to the lowest Kaluza-Klein state in the dual field theory but the above claim involves a much more complicated dynamical

---

<sup>4</sup>We point out that it not consistent to retain just the massless  $SU(2) \times SU(2)$  vector fields [121]. We also remind that in the harmonic analysis of [120], the scalars of mass  $m^2 L^2 = -15/4$  belong to VM type I and come out of the 4-form and the metric: they are  $b$  and  $\phi$  respectively with R charges  $r$  and  $r - 2$ . (See table 1, table 7 and discussion on page 30).

analysis of the superconducting branch, that lies outside our simple framework.

## 6.4 $\gamma = 1/3$ and Hypers of $\mathcal{N} = 8$ supergravity

This model is defined by,

$$P^{(5)}(\zeta_1, \zeta_2) \Big|_{\gamma=\frac{1}{3}} = -\frac{2}{3} \left[ \frac{18 - 24|\zeta_1|^2 + 2|\zeta_1|^4 - 27|\zeta_2|^2 + 8|\zeta_2|^4 + 19|\zeta_1|^2|\zeta_2|^2}{(1 - |\zeta_1|^2 - |\zeta_2|^2)^2} \right]$$

$$DV_1 = -\frac{4}{3} \left[ \frac{3 - 5|\zeta_1|^2 + 2|\zeta_2|^2}{1 - |\zeta_1|^2 - |\zeta_2|^2} \right] \quad (6.65)$$

$$DV_2 = -\frac{1}{3} \left[ \frac{9 - 5|\zeta_1|^2 + 11|\zeta_2|^2}{1 - |\zeta_1|^2 - |\zeta_2|^2} \right] \quad (6.66)$$

It is consistent to truncate either to  $\zeta_1 = 0$  and  $\zeta_2 \neq 0$  or to  $\zeta_1 \neq 0$  and  $\zeta_2 = 0$ . Then, we can study holographic superconductivity in the two sectors independently. Our interest is motivated by the precise matching between the quantum numbers of the  $\{\zeta_1, \zeta_2\}$  hyperscalars with the quantum numbers of the scalar fields in  $\mathcal{N} = 8$  supergravity. In particular, the field  $\zeta_1$  has mass  $m^2 L^2 = -4$  and charge  $qL = \sqrt{3}/2r_+ = 2/\sqrt{3}$  and therefore it has the same critical temperature of the charged scalar  $\eta_d$  in Model **C**. However, the potential of the  $\mathcal{N} = 2$  supergravity makes a strong difference. Indeed  $P^{(5)}(\zeta_1, 0)$  has an Higgs-like shape whose minimum describes an IR AdS fixed point. Then, the condensate goes to zero temperature and the extremal solution is one of the charged domain walls that we know how to construct. This intuition has been confirmed by the numerical simulation.

Let's suppose we know how to embed the  $\gamma = 1/3$   $SU(2, 1)/U(2)$  hypermultiplet in  $\mathcal{N} = 8$  supergravity. It would be interesting to see how this model is related to the retrograde condensate that shows up in Model **C**. Indeed, differently from what we have seen in the  $\gamma = 0$   $\mathcal{N} = 2$  supergravity, the retrograde condensate does not appear as a result of an identification between the two scalars of the same hypermultiplet. Instead, we need to glue together different hyperscalars coming from the representation **6** of the  $SU(3)_R$ . For a given hypermultiplet with scalars  $\zeta_1$  and  $\zeta_2$ , the masses are already fixed by imposing the relation  $|\Delta_1 - \Delta_2| = 1$  together with the constraint  $m_1^2 L^2 = -4$ . Then,  $m_2^2 L^2 = -3$  and we conclude that Model **C** does not admit an  $\mathcal{N} = 2$  description unless we consider a quaternion manifold supporting at least two hypermultiplets. In the worst-case scenario, we should consider a quaternion manifold supporting all the **6** hypermultiplets of  $\mathcal{N} = 8$  supergravity. After a

proper truncation of the quaternionic manifold, one of these hypermultiplets may be described by the  $\gamma = 1/3$   $SU(2,1)/U(2)$  hypermultiplet. Unfortunately, the proof that  $\gamma = 1/3$   $\mathcal{N} = 2$  supergravity is a truncation in  $\mathcal{N} = 8$  supergravity turns out to be a complicated task and we were not able to show whether this theory admits such embedding. We leave this issue for a future study.

## 6.5 Comments of the Retrograde Condensate

The study of holographic superconductivity in phenomenological models has proven the stability of the holographic condensation against a vast range of “coupling” modifications. Indeed, this dynamics seemed to be a universal feature of charged gravitational backgrounds whenever a charged scalar field could be turned on. The results obtained for Model **C** in  $\mathcal{N} = 8$  supergravity and for Model II in  $\gamma = 0$   $\mathcal{N} = 2$  supergravity, clash our general expectations.

From the point of view of the dual field theory, the retrograde condensate does not represent the ground state of the system and it is irrelevant to the dynamics. From the point of view of supergravity, the presence of these solutions poses the following question. The superconducting instability is understood as a violation of the Breitenlohner-Freedman bound. In particular, both the UV mass and the charge of the scalar conspire so that the IR mass violates the Breitenlohner-Freedman bound of the  $AdS_2$  region that emerges at extremality. This argument is quite general and certainly holds for the scalars of Model **C** and Model II. Therefore, it is still true that the Reissner-Nördstrom black hole at zero temperature is unstable when this charged scalar is turned on, nevertheless there is no family of superconducting black holes that resolves the instability. Instead, the retrograde condensate appears.

### 6.5.1 Novel Extremal Solutions from a Superpotential

We want to reconsider Model **C** and Model II and look for zero temperature solutions having in mind the charged domain wall solutions found in section 6.2. Our purpose is to find an IR geometry with certain characteristics and see whether or not we can evolve this geometry to match a superconducting solution in the UV. We will assume that the charge of the extremal black hole is carried only by the charged scalar across the bulk and therefore  $\Phi(r) \approx 0$  is a good approximation in the IR. We believe this to be valid only if dilatonic couplings with the gauge field are absent, i.e  $G = 1$  in the phenomenological Lagrangian.

By considering the above setup, we first look for exact geometry with vanishing gauge field. Then, we are left with three equations of motion,

$$\eta'' + \eta' \left( \frac{3}{r} - \frac{\chi'}{2} + \frac{f'}{f} \right) - \frac{\partial_\eta V}{f} = 0, \quad (6.67)$$

$$\frac{\chi'}{r} + \frac{1}{3}\eta'^2 = 0, \quad (6.68)$$

$$\frac{6}{r^2} + \frac{3f'}{rf} + \frac{V}{f} + \frac{1}{2}\eta'^2 = 0, \quad (6.69)$$

The equations (6.68)-(6.69) can be solved for  $\chi'(r)$  and  $f(r)$  by considering the additional relation  $g_{tt} = e^{-\chi(r)}f(r) = r^2$ . Indeed we remind the reader that  $\Phi = 0$  and therefore the stress energy tensor  $\mathcal{T}_{\mu\nu}$  that appears on the right hand side of the Einstein equations satisfies the property  $\mathcal{T}_{tt} = \mathcal{T}_{xx}$  for any spacial component. We find

$$\frac{1}{f} = \frac{1}{V} \left( \frac{1}{2}\eta'^2 - \frac{12}{r^2} \right), \quad \frac{\chi'}{r} = -\frac{1}{3}\eta'^2. \quad (6.70)$$

We point out that having  $g_{tt} = r^2$  is not automatically synonymous of zero temperature. We will come back to the meaning of taking the zero temperature limit at the end of this section. The construction of the IR geometry follows by plugging formulas (6.70) into the equation of motion for  $\eta$ . The result is,

$$\eta'' + \frac{5}{r}\eta' - \frac{r}{6}\eta'^3 + \frac{\partial_\eta V}{V} \left( \frac{1}{2}\eta'^2 - \frac{12}{r^2} \right) = 0. \quad (6.71)$$

A nice property of this equation is that it can be reduced to a first order equation by using a superpotential (a nice analysis can be found in [122]). In our case, the existence of the superpotential is guaranteed because of supersymmetry. However, it is instructive to obtain the first order equations from scratch by considering the following definitions,

$$V = \gamma(\partial_\eta W)^2 + \beta W^2 \quad \eta' = -\frac{\gamma}{r} \frac{\partial_\eta W}{W}. \quad (6.72)$$

The parameter  $\gamma$  and  $\beta$  are constant not depending on  $\eta$ . Starting from the

two relations (6.72) we can prove that,

$$\eta'' - \frac{\gamma}{r^2} \frac{\partial_\eta W}{W} + \frac{\gamma}{r} \frac{\partial_\eta^2 W}{W} \eta' - \frac{\gamma}{r} \left( \frac{\partial_\eta W}{W} \right)^2 = 0 \quad (6.73)$$

$$V = \frac{W^2 r^2}{\gamma} \left( \eta'^2 + \frac{\beta\gamma}{r^2} \right) \quad (6.74)$$

$$\frac{\partial_\eta^2 W}{W} \eta' = -\frac{r}{\gamma} \frac{\partial_\eta V}{V} \left( \frac{1}{2} \eta'^2 + \frac{\beta\gamma}{2r^2} \right) + \frac{\beta}{r} \frac{\partial_\eta W}{W} \quad (6.75)$$

Then, the equation (6.73) can be brought in form similar to (6.71)

$$\eta'' + \frac{1-\beta}{r} \eta' - \frac{r}{\gamma} \eta'^3 + \frac{\partial_\eta V}{V} \left( \frac{1}{2} \eta'^2 + \frac{\beta\gamma}{2r^2} \right) = 0 \quad (6.76)$$

and a direct comparison between these two equations shows that the values of the constants are  $\gamma = 6$  and  $\beta = -4$ . In conclusion, given a potential  $V$ , the definition of the superpotential  $W$  reads,

$$V = 6(\partial_\eta W)^2 - 4W^2 \quad (6.77)$$

We observe that the product  $\beta\gamma/2$  that appears in (6.76) or in (6.74) has to match the value of the cosmological constants of  $AdS_5$ . Therefore, it is straightforward to generalize the above formulas to space-time dimensions  $d+1$ . We obtain,

$$\gamma = 2(d-1), \quad \beta = -d \quad \rightarrow \quad V = 2(d-1)(\partial_\eta W)^2 - d W^2 \quad (6.78)$$

The form of (6.78) strictly holds for our set of equations of motion. A different normalization of the kinetic terms in the Lagrangian (5.47) obviously affects the definition of  $\beta$  and  $\gamma$ .

As a concrete example, we consider the following family of superpotentials,

$$W(\eta) = \mathfrak{f} \cosh(\sigma\eta) \quad (6.79)$$

The overall normalization is always fixed so that  $V(0)$  equals the value of the cosmological constant of  $AdS_{d+1}$ . The result is  $\mathfrak{f}^2 = (d-1)$ . Indeed  $\partial W \sim \sinh \eta$  and vanishes when  $\eta = 0$ , whereas  $W(0) = \mathfrak{f}$ . In  $AdS_5$ , the potential (6.78) becomes,

$$V = -3 \left( 6\sigma^2 + (4 - 6\sigma^2) \cosh^2(\sigma\eta) \right) \quad (6.80)$$

and it is easy to see that  $\sigma = 1/\sqrt{3}$  reproduces the potential of model **C**,

$$P^I = -6 \left( 1 + \cosh^2 \frac{\eta}{\sqrt{3}} \right) \quad (6.81)$$

At this point we are left with a first order equation for  $\eta$  to solve. It is still convenient to consider space-time dimensions  $d+1$  because no further calculations will be needed in order to generalize our formulas. The class of superpotentials (6.79) is integrable and the solution of  $\eta(r)$  is given by

$$\eta(r) = \frac{1}{\sigma} \operatorname{arcsinh} \left( (r/C_\eta)^{-2(d-1)\sigma^2} \right) . \quad (6.82)$$

The constant  $C_\eta$  is a dimensionful parameter. On the other hand, the function  $f(r)$  only depends on the potential, the field  $\eta$  and the cosmological constant through the relation,

$$\frac{1}{f} = \frac{1}{V} \left( \frac{1}{2} \eta'^2 - \frac{d(d-1)}{r^2} \right) . \quad (6.83)$$

A short calculation shows that the metric takes the form

$$f(r) = r^2 \left( 1 + (r/C_\eta)^{-4(d-1)\sigma^2} \right) \quad (6.84)$$

$$ds^2 = r^2 (-dt^2 + d\vec{x}^2) + \frac{dr^2}{r^2 [1 + (r/C_\eta)^{-4(d-1)\sigma^2}]} \quad (6.85)$$

By considering Model **C**, namely  $\sigma = 1/\sqrt{3}$  and  $d = 4$ , we obtain the solution,

$$ds^2 = r^2 (-dt^2 + d\vec{x}^2) + \frac{dr^2}{r^2 [1 + (r/C_\eta)^{-4}]} \quad (6.86)$$

By considering Model **II**, namely  $\sigma = 1/2$  and  $d = 4$ , we obtain the solution,

$$ds^2 = r^2 (-dt^2 + d\vec{x}^2) + \frac{dr^2}{r^2 [1 + (r/C_\eta)^{-3}]} \quad (6.87)$$

At this point the line of reasoning proceeds as follows. First, we want to understand if the above solutions can be promoted to a superconducting solution. Then, we want to consider these solutions as the extremal limit of a family of superconducting black holes. Implicitly we are making a stronger assumption about the low temperature superconducting black holes that we are supposed

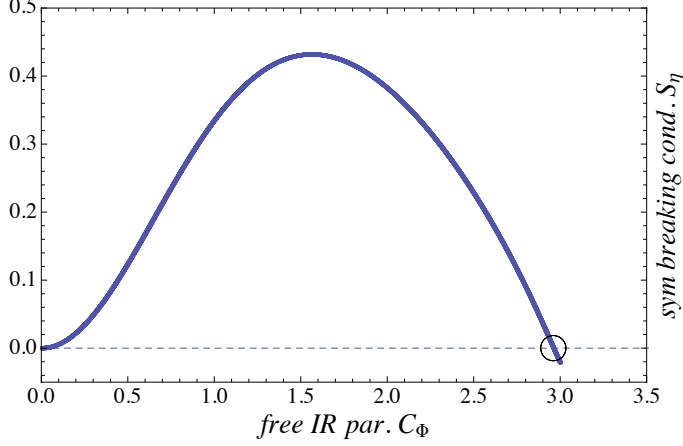


Figure 6.5: We show a plot of the symmetry breaking condition  $S_\eta$  as function of the free IR parameter  $C_\Phi$ . There exist only one solution highlighted by the circle.  $S_\eta = 0$  corresponds  $C_\Phi \approx 2.96$  and for  $C_\Phi \gtrsim 3$ . there are no numerical solutions.

to know: we are saying that the near-horizon region of these black holes is well approximated by a metric of the form,

$$ds^2 = \mathcal{F}(r)dt^2 + r^2d\vec{x}^2 + \frac{dr^2}{\mathcal{F}(r)[1 + (r/C_\eta)^{-4}]} \quad (6.88)$$

$$\mathcal{F}(r) \approx \#_1(r - r_h) + \#_2(r - r_h)^2 + \dots \quad (6.89)$$

Thus, we make sense of the zero temperature limit by considering  $\#_1 \rightarrow 0$  as  $r_h \rightarrow 0$  with  $\#_2 \neq 0$ . The novelty of our zero temperature construction is encoded in the knowledge of the radial component of the metric, where the metric departs from the usual AdS solutions, namely

$$g_{rr} \sim \left[1 + (r/C_\eta)^{-4(d-1)\sigma^2}\right]^{-1}. \quad (6.90)$$

Indeed, deviation of  $g_{rr}$  from the conformal case certainly becomes important in relation to the IR behavior of several physical observables.

By considering the above machinery, we are curious to see if Model **C** or Model **II** admit an extremal solution whose IR geometry coincides with (6.85). The procedure is to build a series expansion that allows the background to flow from the IR geometry (6.85) where  $\Phi = 0$  to the UV boundary where the electric field is turned on. Along the way, we expect the charged scalar field to get correction with respect to the solution (6.82).

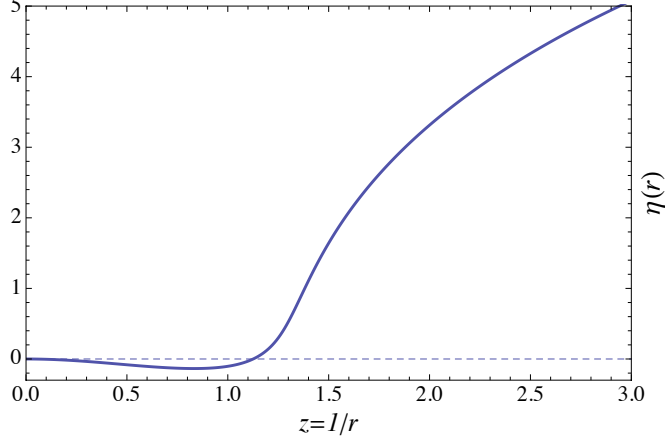


Figure 6.6: The profile of  $\eta(r)$  at large  $r$  for the value  $C_\Phi \approx 2.96$ . This solution has a negative condensate,  $O_\eta \approx -0.85$ , and it is not monotonic ( $\rho = 1$ ).

**Model C.** The starting point is the following expansion valid at small  $r$

$$\eta(r) \approx \frac{\sqrt{3}}{2} \log \frac{4C_\eta^2}{r^4} + I_\eta^{[2]} r^2 + I_\eta^{[4]} r^4 + \dots \quad (6.91)$$

$$\Phi(r) \approx C_\Phi r^2 + I_\Phi^{[4]} r^2 + I_\Phi^{[6]} r^6 \dots \quad (6.92)$$

$$e^{\chi(r)} \approx \frac{C_\eta^4}{r^4} + I_\chi^{[0]} + I_\chi^{[2]} r^2 + \dots \quad (6.93)$$

$$e^{-\chi(r)} f(r) \approx r^2 + I_f^{[4]} r^4 + \dots \quad (6.94)$$

The coefficients  $I$  are determined in terms of  $C_\eta$  and  $C_\Phi$ . It is also clear that for  $C_\Phi = 0$  the above series expansion provides the analytic solution found in (6.82) and (6.86). We can fix  $C_\eta$  by invoking the radial scaling

$$r \rightarrow ar, \quad (t, \vec{x}) \rightarrow a^{-1}(t, \vec{x}), \quad f \rightarrow a^2 f, \quad \Phi \rightarrow a\Phi. \quad (6.95)$$

Then, we are left with one free parameter,  $C_\Phi$ , and one condition at the UV,  $S_\eta = 0$ . Figure 6.5 represents a plot of  $S_\eta$  as function of  $C_\Phi$ . The solution that we find is shown in Figure 6.6 and it is not physical. We conclude that there are no extremal holographic superconductors in model **C** whose IR geometry belongs to the class of solutions (6.85).

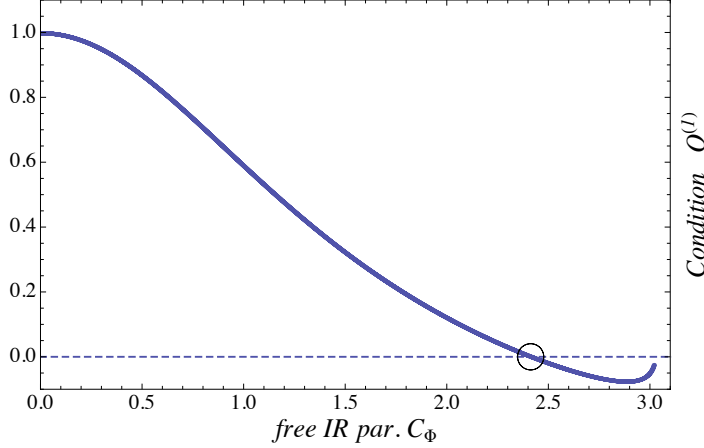


Figure 6.7: Plot of  $O^{(1)}$  as function of the free parameter  $C_\Phi$ . The value of the condensate is  $O^{(1)} \approx 1.108$  ( $\rho = 1$ ).

**Model II.** We implement a series expansion similar to that Model **C**. This time the gauge field is a perturbation with IR asymptotics,

$$\Phi(r) = C_\Phi r^{3/2} + \dots \quad (6.96)$$

For vanishing  $C_\Phi$  we recover the exact solution (6.87). According to the analysis of the symmetry breaking condition, we can impose either  $O^{(1)} = 0$  or  $O^{(2)} = 0$ . The two cases lead to different results and we prefer to comment on them separately.

- **Standard Quantization.** In Figure 6.7 we show a plot of  $O^{(1)}$  as function of the free IR parameter  $C_\Phi$ . There exists a superconducting solution for  $C_\Phi \approx 2.41$ . The corresponding geometry is physical and in particular the functions  $\{f(r), \chi(r), \Phi(r), \eta(r)\}$  are positive and monotonic. In the plot we have choose  $C_\eta^{3/2} = 1/2$  and we can check that the numerics correctly reproduces the asymptotic expansion of the exact solution  $\eta(r)$  for  $C_\Phi = 0$ , namely  $\eta(r) \approx r^{3/2} + O(r^{9/2})$ .
- **Alternative Quantization.** It turns out that Model II, considered in the alternative quantization scheme suffers of the same problem of Model **C** and the solution gives a negative condensate.

The existence of a candidate zero temperature solution in Model II, at least in the standard quantization scheme, is remarkable. Nevertheless, the family

of retrograde condensates does not loop back to zero temperature and we conclude that the two solutions represent two disjoint points in the phase space of the theory. Thus, the question that comes naturally is the following, is it possible to heat up extremal solutions like the one constructed in this section? We will answer to this question in the next chapter, giving a concrete example in the context of  $\mathcal{N} = 8$  supergravity in four dimensions. The setup will be that of  $\mathcal{N} = 2$  supergravity coupled to  $SU(2, 1)/U(2)$  hypermultiplet. In particular, we will consider the same gauging that led to the  $\gamma = 0$  theory, i.e. gauging  $\sigma_3$  direction in the  $SU(2)_R$  isotropy group. The reasons why we prefer to work in four dimensions will become clear throughout the discussion.

# Chapter 7

## Dynamical Hypermultiplets II

In four dimensions, there is a preferred  $\mathcal{N} = 2$  supergravity which also has  $\gamma = 0$ . This theory can be embedded in four dimensional  $\mathcal{N} = 8$  supergravity and it describes the  $SO(3) \times SO(3)$  truncation constructed in [138]. We focus on this model because it has several special features. Some of them are also present in the five dimensional theory but the string embedding is not as clear as in four dimensions. The model contains a zero temperature superconducting domain wall but it also contains a retrograde condensate. For a clearer mental picture it is convenient to associate these two solutions to special points in the potential.

Apart from the standard vacuum solution at the origin, the scalar potential has a saddle point and two tachyonic directions which run towards a common infinite fixed point. More precisely, one of the two tachyonic directions originates from the saddle point, the other is independent and both join at infinity. By restricting the scalar field profile on a particular direction, the saddle point becomes a minimum and out this minimum we construct the extremal charged domain wall superconductor. Along the independent tachyonic direction we find the retrograde condensate. Remarkably, out of the runaway direction originating from the saddle point we find a novel family of extremal superconductors characterized by an IR cone geometry. The latter belongs to the class of exact solutions that we derived in the previous chapter by using the superpotential technique.

We will probe the novel superconducting solutions in two different ways: by calculating the entanglement entropy and by studying the conductivity at low frequencies. The results can be understood in terms of the IR cone geometry and are also quite intuitive. In particular, the solution introduces an energy scale that determines the departure of the novel superconductors from the conformal IR behavior of the charged domain wall solution.

The dual field theory mechanisms that drives the physics towards the new IR geometries is very interesting. We will see that a marginal deformation shows up in the UV and that the AdS/CFT correspondence maps this marginal deformation to a topologically flat direction in the scalar potential. This UV marginal deformation flows in the infrared to a relevant deformation and the end point of the flow is the new IR geometry that we construct. We will explain in more details what we mean by that. Here, we just emphasize that the topology of the scalar manifold plays a fundamental role.

## 7.1 The 4D $\mathcal{N} = 2$ Supergravity

We consider the bosonic sector of 4D  $\mathcal{N} = 2$  supergravity theory coupled to matter fields for a special value of the gauging parameter. The procedure to obtain the Lagrangian has been illustrated in section 4.2 and the result is the following,

$$e^{-1}\mathcal{L}_{\mathcal{H}} = \mathcal{R} - \frac{1}{4}F^{\mu\nu}F_{\mu\nu} - 2h_{i\bar{j}}D^\mu\zeta_i\overline{D_\mu\zeta_j} - P^{(4)}(\zeta_1, \zeta_2) . \quad (7.1)$$

where the covariant derivatives are

$$\left\{ \begin{array}{l} D_\mu\zeta_1 \equiv \partial_\mu\zeta_1 - iA_\mu\frac{1}{2}(\gamma+1)\zeta_1 \\ D_\mu\zeta_2 \equiv \partial_\mu\zeta_2 - iA_\mu\frac{1}{2}(\gamma-1)\zeta_2 \end{array} \right. \quad (7.2)$$

and the potential is

$$P^{(4)}(\zeta_1, \zeta_2) = -\frac{1}{2}\frac{12 - V^4}{(1 - |\zeta_1|^2 - |\zeta_2|^2)^2} \quad (7.3)$$

$$\begin{aligned} V^{(4)} &= (16 - 4\gamma + 4\gamma^2)|\zeta_1|^2 + (16 + 4\gamma + 4\gamma^2)|\zeta_2|^2 \\ &\quad - 3(\gamma - 1)^2|\zeta_1|^4 - 3(\gamma + 1)^2|\zeta_2|^4 - (6\gamma^2 - 10)|\zeta_1|^2|\zeta_2|^2 \end{aligned} \quad (7.4)$$

The AdS vacuum corresponds to  $\zeta_1 = \zeta_2 = 0$  and the value of the cosmological constant is  $V^{(4)}(0) = -6^1$ . According to this normalization the AdS radius is fixed to  $L = 1$ .

---

<sup>1</sup>This is choice of normalization of the Killing vector and it corresponds to set  $\alpha_3^2 = 1/4$  in the Lagrangian of section 4.2. The only meaningful parameter is  $\gamma$ .

In this chapter we will consider just the case  $\gamma = 0$  because this particular model can be embedded as consistent truncation of  $\mathcal{N} = 8$  supergravity in four dimension. The dual field theory is the  $\mathcal{N} = 6$  superconformal Chern-Simons matter theory on the world-volume of M2-branes [67]. The AdS/CFT dictionary is also known and we may rely on it to understand, at least in principle, what operators condenses in the dual field theory. In order to do so, the details of the embedding into  $\mathcal{N} = 8$  supergravity will be certainly relevant. However, we will not need them for the purpose of the present discussion and we refer to [123] and references therein for a more comprehensive analysis.

### 7.1.1 Geometrical description

The masses of the scalars  $\zeta_1$  and  $\zeta_2$  can be read from

$$\mathcal{DV}_1 = -\frac{1}{2} \frac{4 - 5|\zeta_1|^2 - 3|\zeta_2|^2}{1 - |\zeta_1|^2 - |\zeta_2|^2}, \quad (7.5)$$

$$\mathcal{DV}_2 = -\frac{1}{2} \frac{4 - 5|\zeta_1|^2 - 3|\zeta_2|^2}{1 - |\zeta_1|^2 - |\zeta_2|^2}, \quad (7.6)$$

They are equals and coincide with  $m^2 L^2 = -2$ . Then, the fall-off behavior of the scalars field at the AdS vacuum is determined by the condition

$$\Delta(\Delta - 3) = -2 \quad (7.7)$$

whose solutions are  $\Delta = 1$ ,  $\Delta = 2$ . The value of the mass  $m^2 L^2 = -2$  allows both standard and alternative quantization. Our starting point is the truncation to a single scalar sector. We define Model I and Model II.

► Model I,

$$\zeta_1 = \tanh \frac{\eta}{2}, \quad \zeta_2 = 0, \quad \mathcal{P} = \frac{1}{2} \left( \sinh^4 \left( \frac{\eta}{2} \right) - 4 (2 + \cosh \eta) \right), \quad (7.8)$$

corresponds to [123]

$$\mathcal{L} = R - \frac{1}{2} F^2 - \frac{1}{2} (\partial\eta)^2 - \frac{1}{4} \sinh^2 \eta A^2 - \mathcal{P}. \quad (7.9)$$

The study of superconducting solutions qualitatively reproduces the same results and the same plots that we obtained in the five dimensional case. In particular, choosing the alternative quantization scheme for  $\zeta_1$  a superconducting black hole is found for  $T_c \approx 0.121\rho^{1/2}$ , the phase transition is second

order and the solution can be cooled down to zero temperature. It is the thermodynamically preferred phase and at  $T = 0$  the bulk geometry is understood as a charged domain wall between two  $\text{AdS}_4$  regions with different radius. Regarding the  $\Delta = 2$  condensate, we find that the transition to the superconducting phase is first order. Other details of these two condensate are not relevant in the present discussion and we refer to [123] for completeness.

► Model II,

$$\zeta_1 = \frac{1}{\sqrt{2}} \tanh \frac{\eta}{2}, \quad \zeta_2 = \frac{1}{\sqrt{2}} \tanh \frac{\eta}{2}, \quad \mathcal{P} = -2(2 + \cosh \eta), \quad (7.10)$$

corresponds to [124]

$$\mathcal{L} = R - \frac{1}{2}F^2 - \frac{1}{2}(\partial\eta)^2 - \sinh^2\left(\frac{\eta}{2}\right)A^2 - \mathcal{P}. \quad (7.11)$$

The critical temperature of the hairy black hole solutions is the same of Model I,  $T_c \approx 0.121\rho^{1/2}$ , but the superconducting condensate exists only for temperatures above  $T_c$ . The solution is not thermodynamical preferred and the system always stays in the uncondensed phase. This is the “retrograde condensate” found in [124]. We will show a plot of this retrograde condensate in the next section.

Model I and Model II corresponds to two different scalar configurations however, they share a common feature,  $|\zeta_1|^2 + |\zeta_2|^2 = \tanh^2(\eta/2)$ . This observation suggests that there is a larger class of black holes in our theory<sup>2</sup>. In this new class of solutions Model I and Model II are only isolated points. By considering a more sensible parametrization of the scalar manifold we will make clear how the topology of the scalar manifold enters the construction of this large class of black holes. Indeed, the coset space  $SU(2,1)/U(2)$  is topologically a ball in  $\mathbb{C}^2$  and can be parametrized by one radial coordinate  $\tau$  and three angles,

$$\zeta_1 = \tau \cos \frac{\theta}{2} e^{i(\varphi+\psi)/2}, \quad \zeta_2 = \tau \sin \frac{\theta}{2} e^{-i(\varphi-\psi)/2}. \quad (7.12)$$

This parametrization has been already introduced in section 4.2. We also define  $\tau = \tanh(\eta/2)$  to make contact with the single charged scalar of Model I and Model II. The coordinates  $\{\theta, \varphi, \psi\}$  represent the Hopf fibration of the three sphere. In our setup, one of the two phases,  $\varphi$ , identifies the charge of the complex scalars and therefore can be gauged away by a redefinition. The

---

<sup>2</sup>We thank Jorge Russo for this very important comment.

other phase,  $\psi$ , can be taken to be a constant when superconducting solutions are considered. We will set  $\psi = 0$  for convenience. Concretely, the Lagrangian that we are studying is,

$$\mathcal{L} = \mathcal{R} - \frac{1}{4}\mathcal{F}^2 - \frac{1}{2}\sinh^2\left(\frac{\eta}{2}\right)(\partial\theta)^2 - \frac{1}{2}(\partial\eta)^2 - \frac{1}{2}J(\eta, \theta)\mathcal{A}_\mu\mathcal{A}^\mu - \mathcal{P}(\eta, \theta). \quad (7.13)$$

The potential and the coupling  $J(\eta, \theta)$  in the field variables  $\{\eta, \theta\}$  are,

$$\mathcal{P}(\eta, \theta) = \frac{1}{2}\left(\sinh^4\left(\frac{\eta}{2}\right)\cos^2\theta - 4(2 + \cosh\eta)\right), \quad (7.14)$$

$$J(\eta, \theta) = \sinh^2\left(\frac{\eta}{2}\right)\left(1 + \cos^2\theta\sinh^2\left(\frac{\eta}{2}\right)\right). \quad (7.15)$$

It is easy to recognize that Model I and Model II are obtained by setting respectively  $\theta = 0$  and  $\theta = \pi/2$ . Thus, our idea is to study in more details the critical points of the potentials including  $\theta$  as dynamical field. First, it is useful to write down the equations of motion for the new theory (7.13) and it turns out convenient to slightly modify the usual parametrization of metric by defining

$$ds^2 = -f(r)dt^2 + \frac{r^2}{L^2}(dx^2 + dy^2 + dz^2) + \frac{dr^2}{f(r)h(r)^2}, \quad A = \Phi(r)dt. \quad (7.16)$$

The field  $h(r)$  plays the same role of the field  $\chi(r)$  in the phenomenological setting<sup>3</sup>. In particular, we can derive the equations of motion for  $f(r)$  and  $h(r)$  by considering linear combinations of the general equations of motions given in section 3.2.1. For simplicity, we summarize the result. Regarding the metric fields,  $h(r)$  and  $f(r)$  we find,

$$\frac{h'}{rh} + \frac{1}{4}\eta'^2 + \frac{1}{4}\sinh^2\left(\frac{\eta}{2}\right)\theta'^2 + J(\eta, \theta)\frac{\Phi^2}{4f^2h^2} = 0 \quad (7.17)$$

$$-\frac{1}{4}\eta'^2 - \frac{1}{4}\sinh^2\left(\frac{\eta}{2}\right)\theta'^2 + \frac{\Phi'^2}{4f} + \frac{f'}{rf} + \frac{1}{r^2} + \frac{1}{2fh^2}\mathcal{P}(\eta, \theta) - J(\psi, \varphi)\frac{\Phi^2}{4f^2h^2} = 0 \quad (7.18)$$

---

<sup>3</sup>We would like to point out that  $f(r)$  defined in (7.16) is not the  $f(r)$  used in (3.2.1) where  $g_{tt} = f(r)e^{-\chi(r)}$ . They are related by a simple redefinition:  $f_{here} = f_{there}e^{-\chi}$  and  $h = e^{\chi/2}$ .

Regarding the matter fields,  $\Phi(r)$  and  $\eta(r)$  we find,

$$\Phi'' + \left(\frac{2}{r} + \frac{h'}{h}\right)\Phi' - J(\eta, \theta)\frac{\Phi}{fh^2} = 0 \quad (7.19)$$

$$\eta'' + \left(\frac{2}{r} + \frac{f'}{f} + \frac{h'}{h}\right)\eta' - \frac{1}{4}\sinh\eta\theta'^2 + \partial_\eta J(\eta, \theta)\frac{\Phi^2}{2f^2h^2} - \frac{1}{fh^2}\partial_\eta \mathcal{P}(\eta, \theta) = 0 \quad (7.20)$$

Finally, the equations for the new field  $\theta(r)$ ,

$$\begin{aligned} \theta'' + \left(\frac{2}{r} + \frac{f'}{f} + \frac{h'}{h}\right)\theta' + \coth\left(\frac{\eta}{2}\right)\eta'\theta' + \\ + \frac{1}{\sinh^2(\eta/2)}\left(\partial_\theta J(\eta, \theta)\frac{\Phi^2}{2f^2h^2} - \frac{1}{fh^2}\partial_\theta \mathcal{P}(\eta, \theta)\right) = 0 \end{aligned} \quad (7.21)$$

The derivatives  $\partial_\eta \mathcal{P}$  and  $\partial_\theta \mathcal{P}$  are,

$$\partial_\eta \mathcal{P} = -g^2 \sinh\eta \left(4 - \cos^2\theta \sinh^2\left(\frac{\eta}{2}\right)\right) \quad (7.22)$$

$$\partial_\theta \mathcal{P} = -2g^2 \sin 2\theta \sinh^4\left(\frac{\eta}{2}\right) \quad (7.23)$$

For the special point  $\eta = 0$ , no matter what value of  $\theta \in [0, \pi)$  we fix,  $\partial_\eta \mathcal{P}$  and  $\partial_\theta \mathcal{P}$  vanish automatically. Since the functions  $\mathcal{P}(\eta, \theta)$  and  $J(\eta, \theta)$  are  $\pi/2$ -periodic it's sufficient to consider,

$$\mathcal{M}_\theta = \{(\eta = 0, \theta) \mid \theta \in [0, \pi/2]\} . \quad (7.24)$$

Then, the set  $\mathcal{M}_\theta$  resembles a flat direction of the potential but not in the usual sense<sup>4</sup>. Technically, the reason is that both scalars,  $\zeta_1$  and  $\zeta_2$ , have non zero mass,  $m^2 L^2 = -2$ . Instead,  $\mathcal{M}_\theta$  appears as a flat direction only in the variables  $\{\eta, \theta\}$ . Under the change of coordinates (7.12),  $\eta = 0$  (or  $\tau = 0$ ) implies  $\zeta_1 = \zeta_2 = 0$  and  $\mathcal{M}_\theta$  is mapped to the origin  $\zeta_1 = \zeta_2 = 0$ . Therefore, the interpretation of  $\theta$  is obtained by considering the ratio  $\zeta_2/\zeta_1$  which gives a term proportional to  $\tan(\theta/2)$ . The choice of  $\theta$  fixes the direction of departure from the origin towards the boundary. This is a consequence of the topology of  $SU(2, 1)/U(2)$  that can be seen as the open ball in  $\mathbb{C}^2$ . We refer to  $\mathcal{M}_\theta$  as a topologically flat direction.

---

<sup>4</sup>In supersymmetric theories, as well as in supergravity theories, a classical flat direction in the potential is parametrized by a massless field whose expectation value sets the mass spectrum of the theory.

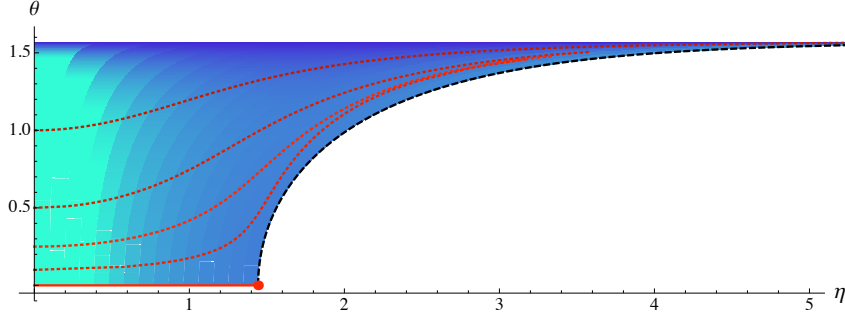


Figure 7.1: *Density plot of the potential  $\mathcal{P}$ . The potential gets steeper as the color becomes darker. The red dot is the saddle point  $\theta = 0$ ,  $\eta = 2 \operatorname{arccosh}\sqrt{5}$ . The horizontal axis has been rescaled by a factor 0.5. The dashed black line is the set  $\{(\theta, \eta) \mid \partial_\eta \mathcal{P} = 0\}$ . The red lines represent the interpolating solutions described in section 7.2.*

In Figure 7.1 we show a density plot of  $\mathcal{P}(\eta, \theta)$  for a generic value of  $\theta$ . The black dashed line is the set of points  $\{(\theta, \eta) \mid \partial_\eta \mathcal{P} = 0\}$ . This line separates the plane  $(\eta, \theta)$  in two regions according to the sign of  $\partial_\eta \mathcal{P}$ . In the colored region this derivative is negative and the potential decreases. In the white region the potential increases and it behaves like  $\mathcal{P} \approx \exp 2\eta$  in the large  $\eta$  limit. In summary, Figure 7.1 shows that along the slices of constant  $\theta \neq \pi/2$  the potential is bounded from below but, on the slice  $\theta = \pi/2$ , the potential is negative definite and decreases like  $\mathcal{P} \approx -\exp \eta$ . A second isolated critical point  $\mathfrak{S}$  exists for  $\theta = 0$  and  $\eta = 2 \operatorname{arccosh}\sqrt{5}$  and according to the above analysis  $\mathfrak{S}$  is a saddle point.

Independently of  $\eta$ , the condition  $\partial_\theta \mathcal{P} = 0$  is satisfied by the two isolated values  $\theta = \pi/2$  and  $\theta = 0$ . These two particular values of  $\theta$  can be promoted to a constant bulk solution and correspond to Models I and II. The existence of the space  $\mathcal{M}_\theta$  implies that  $\theta$  can be chosen arbitrarily when  $\eta$  vanishes. On the other hand  $\eta$  vanishes if and only if  $\zeta_1 = 0$  and  $\zeta_2 = 0$ . In a superconducting solution this last condition is satisfied at the boundary of the geometry, where the space is asymptotically *AdS*. Therefore it is natural to think that black hole solutions with fixed UV value of  $\theta_\infty \in \mathcal{M}_\theta$  can be constructed. In particular, thermal superconducting solutions with  $\theta_\infty \in \mathcal{M}_\theta$  interpolate between Model I and Model II.

We explore this possibility by analyzing the asymptotic behavior of the variables  $\{\eta(r), \theta(r)\}$  in the *AdS* background. Expanding the equations of motion to lowest order in the  $\eta$  field, we find

$$\frac{f'}{rf} + \frac{1}{r^2} - \frac{6}{f} + \frac{\Phi'^2}{4f} = 0, \quad (7.25)$$

$$\Phi'' + \left(\frac{2}{r} + \frac{h'}{h}\right) \Phi' = 0, \quad (7.26)$$

$$\eta'' + \left(\frac{2}{r} + \frac{f'}{f} + \frac{h'}{h}\right) \eta' - \frac{1}{4} \eta \theta'^2 + \frac{\Phi^2}{4f^2 h^2} \eta + 4 \frac{\eta}{f h^2} = 0, \quad (7.27)$$

$$\theta'' + \left(\frac{2}{r} + \frac{f'}{f} + \frac{h'}{h}\right) \theta' + 2 \frac{\eta'}{\eta} \theta' = 0. \quad (7.28)$$

The equation for  $h(r)$  is trivial,  $h'(r) = 0$ . We suppose that the term  $\theta'^2$  is sub-leading. Thus the first three equations decouple and (at leading order) are solved by the AdS metric together with,

$$\eta(r) = \frac{O_\eta^{(1)}}{r} + \frac{O_\eta^{(2)}}{r^2} + \dots \quad (7.29)$$

$$\Phi(r) = \mu - \frac{\rho}{r} + \dots \quad (7.30)$$

Substituting into (7.28) we find that the choice of quantization scheme for  $\eta(r)$  crucially affects the asymptotics of  $\theta(r)$ . The equation,

$$\theta'' + \frac{4}{r} \theta' + 2 \frac{\eta'}{\eta} \theta' = 0 \quad (7.31)$$

has the desired solution only if  $O_\eta^{(2)} = 0$ . Only in this case we find the admissible asymptotic behavior,

$$\theta(r) = \theta_\infty + \frac{\xi}{r} + \dots \quad (7.32)$$

As  $\theta'^2$  is of order  $1/r^4$  we find that the assumption we made was correct. At this stage, we can think of  $\xi$  as the condensate relative to  $\theta_\infty$ . In the next section we construct superconducting black holes with the following boundary conditions:  $\theta_\infty \in \mathcal{M}_\theta$  and  $O_\eta^{(2)} = 0$ . The coefficient  $O_\eta^{(1)} \equiv O_\eta$  define the condensate. These are the interpolating solutions that we want to construct. Our solutions offer a rich (and quite unexpected) framework where all the physical properties associated with them have a simple explanation.

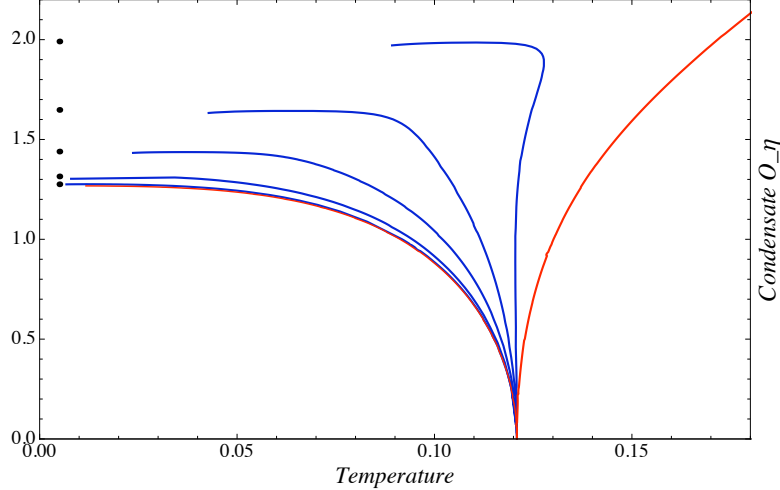


Figure 7.2: The condensate  $O_\eta(T, \theta_\infty)$  studied by letting the value of  $\theta_\infty$  vary. Black dots are obtained from our new zero temperature solutions. From bottom to top the curves correspond to  $\theta_\infty = 0, 0.1, 0.25, 0.5, 0.75, 1$ . The rightmost red curve is the retrograde condensation which corresponds to  $\theta_\infty = \pi/2$ . Strictly speaking the curves should be represented in a three dimensional space according to their value of  $\theta_\infty$ . For simplicity we have collected the results in a single picture.

## 7.2 $\Delta = 1$ Interpolating Solutions

We study the full system of equations (7.17)-(7.21) with the asymptotic conditions defined in the previous section. The condensate  $O_\eta = O_\eta(T, \theta_\infty)$  is associated with an operator of dimension  $\Delta = 1$  and it is function of the temperature  $T$  and of the angle  $\theta_\infty$ . Figure 7.2 shows the temperature dependence of the condensate when the value of  $\theta_\infty$  is varied in the range  $[0, \pi/2]$ .

All the curves originate from the same branch at  $T \approx 0.121$ . This fact is easily understood considering the linearized approximation around the Reissner-Nordström black hole [11]. Indeed the critical temperature is only determined by the quadratic terms in the equation of the charged scalar  $\eta(r)$ . In the present case all the terms depending on the field  $\theta(r)$  are suppressed and therefore only the mass,  $m^2 L^2 = -2$ , and charge,  $qL = 1/2$ , enter in the analysis. It follows that the critical temperature for the onset of a small superconducting black holes does not depend on  $\theta_\infty$ .

Important changes happen when the value of  $\theta_\infty$  is tuned up to the value  $\pi/2$ . As we expected, the shape of the curve  $O_\eta(T, \theta_\infty)$  gets closer to the retro-

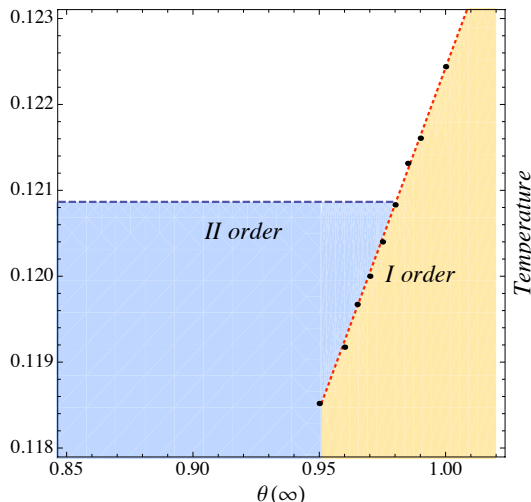


Figure 7.3: Phase diagram of the system as function of the temperature and the parameter  $\theta_\infty$ . Colored region represent the superconducting phase. The color distinguishes between different degrees of freedom according to the type of phase transition that the system experience.

grade condensate, but for intermediate values, for example  $\theta_\infty = 1$ , something interesting happens. In this case the shape of the curve brings to mind the case of a first order phase transition [10]. Calculating the free energy of the superconducting black holes and comparing the result with the Reissner-Nordström case, we find that the order of the phase transition depends on  $\theta_\infty$ . The situation is clarified by Figure 7.3. In the white region the uncondensed solution is the only allowed configuration. When the temperature is cooled, the superconducting phase is thermodynamically favored. In the blue region the phase transition takes place at  $T_c^{sec} \approx 0.121$  and it is second order. In the yellow region and for temperatures above  $T_c^{sec}$  the phase transition is first order. The critical temperature of the first order phase transition, extrapolated from the free energy, can be read from the contour of the yellow region: it increases along the dashed red line. In this case the curve of the condensate has two branches, the lower branch is not thermodynamically favored and when the temperature approaches the critical temperature the system jumps into the superconducting phase.

When the phase transition is still second order something new happens, even if the system has entered the superconducting phase, the free energy shows a discontinuity at some temperature smaller than  $T_c^{sec}$ . This new be-

havior starts approximately at  $\theta^{crit} \approx 0.95$  and the discontinuity is of first order type. The discontinuity is physically interpreted as a change in the nature of the degrees of freedom that are responsible for the phase transition. Indeed, a pictorial feature of the curves  $O_\eta(T, \theta_\infty)$  when  $\theta_\infty$  is not small is the presence of a plateau that starts at some intermediate value of the temperature and describes the remaining part of the curve as the zero temperature is reached. The extension of the plateau grows with  $\theta_\infty$  and when the phase transition is first order it basically represents the entire curve. In the next sections we give more details about these phenomena by calculating the entanglement entropy of the superconducting ground state. Before, we discuss the existence of the zero temperature solutions.

### 7.2.1 Zero temperature solutions

Figure 7.2 indicates that for several values of  $\theta_\infty \in \mathcal{M}_\theta$  the numerical black holes converge to a zero temperature solution. The case  $\theta_\infty = 0$  is well studied and for completeness we review the argument.

In a superconducting solution the value of the  $\eta(r_h)$  generically runs along the potential. Small values of  $\eta(r_h)$  correspond to temperatures in a neighborhood to the left of the critical temperature. In the case  $\theta_\infty = 0$ , the field  $\theta(r)$  vanishes in the bulk and thus the value of  $\eta(r_h)$  is tied to the slice  $\{\eta, \mathcal{P}(\eta, 0)\}$ . When the temperature is cooled,  $\eta(r_h)$  hits the critical point  $\mathfrak{S}$ . The situation is graphically realized by the solid red line in Figure 7.1. At the critical point there is an emergent AdS<sub>4</sub> space with radius  $L^2 = 3/7$  and the solution of the equations of motion is,

$$f(r) = \frac{7}{3}r^2, \quad h(r) = 1, \quad \eta(r) = 2 \operatorname{arccosh}\sqrt{5}, \quad \Phi(r) = 0. \quad (7.33)$$

Because the gauge field must carry flux at the boundary, we have to move from (7.33) exciting irrelevant perturbations, i.e sub-leading modes of the fields  $\Phi(r)$  and  $\eta(r)$ . On this background the small perturbations,  $\delta\eta(r)$  and  $\delta\Phi(r)$ , are governed by the equations

$$\delta\Phi'' + \frac{2}{r}\delta\Phi' - \frac{60}{7}\frac{\delta\Phi}{r^2} = 0, \quad \delta\eta'' + \frac{4}{r}\delta\eta' - \frac{60}{7}\frac{\delta\eta}{r^2} = 0,$$

and the solutions we have exponents,

$$e_\eta = -\frac{3}{2} + \sqrt{\frac{303}{28}} \quad ; \quad e_\Phi = \frac{1}{2} + \sqrt{\frac{247}{28}} \quad (7.34)$$

The extremal solution is obtained by integrating the full system of equations up to the UV boundary where the shooting method is applied to match the

condition  $O_\eta^{(2)} = 0$ . Sometimes we will refer to this solution as the conformal domain wall.

For the cases  $\theta_\infty \neq 0$  one could be suspicious about the zero temperature limit. We have already observed that the potential has a runaway direction from the saddle point  $\mathfrak{S}$  towards the value  $\theta = \pi/2$ . Exactly for  $\theta(r) = \pi/2$  the condensation is retrograde and one might think that all the curves corresponding to  $\theta_\infty \neq 0$  have to be retrograde at some point. Indeed Figure 7.1 shows that for fixed  $0 < \theta_\infty < \pi/2$  the numerics of the solutions when  $T \rightarrow 0$  converges to  $\theta(r_h) \rightarrow \pi/2$ . In the same regime  $\eta(r_h)$  grows and  $\Phi'(r_h)$  takes small values. On the other hand, if the extremal limit of the finite temperature black holes exists, we should look for a solution of the equations of motion with the following behavior:  $\theta(r) = \pi/2$ ,  $\Phi(r) = 0$  and divergent scalar field  $\eta(r)$ . Surprisingly, an analytic solution can be found and it is given by,

$$ds^2 = r^2(-dt^2 + d\vec{x}^2) + \frac{dr^2}{r^2 + C_\eta^2}, \quad \theta(r) = \frac{\pi}{2}, \quad (7.35)$$

$$\eta(r) = 2 \operatorname{arcsinh} \frac{C_\eta}{r}, \quad \Phi(r) = 0. \quad (7.36)$$

This solution is one of the exact solutions that come out of the superpotential calculation of section 6.5. In particular, it corresponds to  $d = 4$  and  $\sigma = 1/2$ . Interestingly, the value  $\sigma = 1/2$  also characterizes the solution in five dimension, precisely in (6.87). We believe this value to be uniquely tied to the scalar manifold  $SU(2, 1)/U(2)$ .

We are now in the position to construct the extremal black hole. We look for irrelevant perturbations  $\delta\theta(r)$  and  $\delta\Phi(r)$  on the background (7.35). Linearizing the equations for  $\Phi(r)$  and  $\theta(r)$  we find that the perturbations are governed by the equations,

$$\delta\Phi'' + \frac{1}{r}\delta\Phi' - \frac{2}{r^2}\delta\Phi = 0, \quad \delta\theta'' + \frac{1}{r}\delta\theta' - \frac{2}{r^2}\delta\theta = 0, \quad (7.37)$$

and the solutions are,

$$\delta\Phi(r) = C_\Phi^{(1)}r + \frac{C_\Phi^{(-1)}}{r}, \quad \delta\theta(r) = C_\theta^{(1)}r + \frac{C_\theta^{(-1)}}{r}. \quad (7.38)$$

Imposing  $C_\Phi^{(-1)} = 0$  and  $C_\theta^{(-1)} = 0$ , we integrate the full system of equations, from small radial scales up to the UV boundary. There are three parameters left,  $\{C_\eta, C_\theta, C_\Phi\}$ . We use the radial scaling to set  $C_\eta$  to unity and the

shooting method technique to match the boundary conditions. In particular we want to fix  $\theta_\infty$  in the range  $(0, \pi/2)$  and we need to impose  $O_\eta^{(2)} = 0$ . From these new zero temperature solutions we extrapolate the values of the condensates. Figure 7.2 shows the result, the zero temperature value of the condensate, for fixed  $\theta_\infty$ , agrees with the limit  $O_\eta(T \rightarrow 0, \theta_\infty)$  taken from the finite temperature black holes.

In the approximation  $C_\eta \rightarrow 0$  the metric in (7.35) matches with AdS<sub>4</sub> and the divergent behavior of the scalar field is turned off. One might wonder if in that limit the expansion (7.33) is somehow recovered. We want to point out that this is not the case: for arbitrary small values of  $\theta_\infty > 0$  the limit  $\theta(r \rightarrow 0)$  is always  $\pi/2$ . The correct interpretation of the statement is to think about the IR values,  $\theta = 0$  and  $\theta = \pi/2$ , as “order parameters” that distinguish two different phases of the theory<sup>5</sup>. This consideration implies that the IR physics described by the conformal domain wall and the new zero temperature solution is different. Indeed, a new scale appears in the solution:  $C_\eta$ . The first geometrical feature related to  $C_\eta$  is evident: in the region  $r \ll C_\eta$  the metric looks like a cone in which the transverse space  $M$  is the Minkowsky space,

$$ds^2 \approx dr^2 + C_\eta^2 r^2 (-dt^2 + d\vec{x}^2). \quad (7.39)$$

The cone structure can be seen explicitly through a formal construction,

- For  $0 < C_\eta < 1$  we define  $\cos \alpha = C_\eta$  and we consider the following embedding. The curve  $z/r = \pm \tan \alpha$  with  $r \geq 0$ , defines a “surface of revolution” in the 5-dimensional space given by  $ds^2 = dz^2 + dr^2 + r^2 dM^2$ . The resulting 4-dimensional metric is  $ds^2 = dr^2 + r^2 \cos^2 \alpha dM^2$ .
- For  $C_\eta > 1$  we define  $\cosh \alpha = C_\eta$  and we consider a similar embedding. The curve  $z/r = \pm \tanh \alpha$  with  $r \geq 0$ , defines a “surface of revolution” in the 5-dimensional space given by  $ds^2 = -dz^2 + dr^2 + r^2 dM^2$ . The resulting 4-dimensional metric is  $ds^2 = dr^2 + r^2 \cosh^2 \alpha dM^2$ .

The construction is formal in the sense that, unless one of the transverse direction in  $M$  is compact, there are no angles that can be used to rotate the curve  $z = z(r)$ . At  $r = 0$ , the bulk caps off with a “good” conical singularity. Indeed, according to the usual criteria, the on-shell potential is bounded from above [125]. We can check the statement looking at the value of the potential at origin  $r = 0$ . In this case  $\theta(0) = \pi/2$  and  $\mathcal{P}(\eta(r), \pi/2) = -2(2 + \cosh \eta) = -2(3 + 2C_\eta^2/r^2)$  goes to  $-\infty$  in the limit  $r \rightarrow 0$ . On the other hand, for

---

<sup>5</sup>We thank R. Myers for a discussion which led to this line of thought.

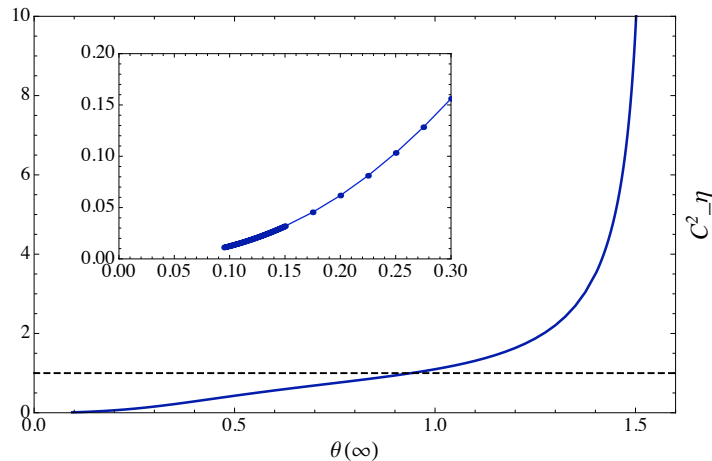


Figure 7.4: The function  $C_\eta^2(\theta_\infty)$ . Zero temperature solutions are normalized taking  $\rho = 1$ . The dashed black line highlights the value  $C_\eta = 1$  which distinguishes between the two 5d embeddings of the IR cone geometry.

intermediate scales  $C_\eta \ll r \ll \tilde{r}$ , where  $\tilde{r}$  is such that deviations of the bulk solution from (7.35) are important, the metric still looks like  $\text{AdS}_4$ . A quantity that may be able to distinguish the differences between the conformal domain wall and the new zero temperature solution is the entanglement entropy. We dedicate the next section to this calculation.

Figure 7.4 shows the relations between  $C_\eta$  and  $\theta_\infty$ . We already know two limits of these curves. The first one is obtained for  $\theta_\infty \rightarrow 0$ . In this case the solution is close to the conformal domain wall, we can check that  $C_\eta$  is converging to zero whereas the condensate is approaching the expected value  $O_\eta(T = 0, \theta_\infty = 0) \approx 1.265$ . The second limit is  $\theta_\infty \rightarrow \pi/2$ . We know that the condensation is retrograde and according to the numerical data the curve has no turning point towards zero temperature. As a matter of fact, both values of  $C_\eta$  and  $O_\eta(T = 0)$  become singular meaning that the extremal solution blows up. This behavior agrees with the expectation that the curve of the condensate exists only for temperatures above  $T_c$ .

The last observation about the properties of the solution regards the electric flux. The electric flux  $\mathcal{F}(r)$  is given by the expression,  $\mathcal{F}(r) = r^2 h(r) \Phi'(r)$ . In the region  $r \ll C_\eta$  it behaves like  $\mathcal{F}(r) \approx C_\eta C_\Phi r$  and therefore, in the limit  $r \rightarrow 0$ , the flux vanishes. From this observation we learn that the density charge  $\rho$  of the field theory originates only from the charged matter in the extra coordinate. Indeed, integrating once the equation (7.19) we obtain the

Gauss law for the superconducting solution. It relates the  $U(1)$  charge  $\rho$ , the electric flux at the origin and the integral of the coupling  $J(\eta, \theta)$  across the bulk. Since the flux vanishes at  $r = 0$ , the field theory charge  $\rho$  originates only from the integral of  $J(\eta, \theta)$ .

## 7.2.2 Comments on the Extremal Limit

In this paragraph we provide further evidence that the extremal limit of our interpolating superconducting solutions is actually given by the zero temperature geometries constructed in the previous section. From Figure 7.2, we already know that for a given  $\theta_\infty$ , the value of condensate at small temperatures asymptotes to the zero temperature result. However this is a non trivial check from the point of view of the boundary and we would like to test our solutions also from the IR. In particular we will check that for a given  $\theta_\infty$ , the horizon geometry of the black hole solutions converges to the IR geometry (7.35) in the limit  $T \rightarrow 0$ . The way we imagine this matching to happen is the following.

The superconducting solution at finite temperature are constructed by imposing that  $f(r)$  has a simple zero at the horizon, i.e

$$f(r) \approx \#_1(r - r_h) + \#_2(r - r_h)^2 + \dots \quad (7.40)$$

where  $\#_1$  and  $\#_2$  are two coefficients and  $\#_1$  essentially represents the finite temperature of the solution. At zero temperature we expect  $\#_1$  to vanish and  $\#_2$  to be finite so to recover the exact solution (7.35). In this sense, as the temperature is cooled, for example at order  $\epsilon$ ,  $\#_1$  will become smaller but still we will have to impose  $\#_1 \neq 0$  in order to construct the solution. Thus all the information we are seeking has to be encoded into  $h(r)$ . In particular, we will show that IR near extremal solutions behave like

$$ds^2 = f(r)dt^2 + r^2d\vec{x}^2 + \frac{dr^2}{f(r)[1 + (r/C_\eta)^{-2}]} \quad (7.41)$$

$$f(r) \approx \#_1(r - r_h) + \#_2(r - r_h)^2 + \dots \quad (7.42)$$

with  $f(r)$  given in (7.40).

In Figure 7.5 we show a plot of  $h(r)$  for different values of  $\theta_\infty$  and for the lowest temperature available from the numerics. We observe that all the solid lines stop at some small  $r = r_h$ . We also see that in the range  $r_h \leq r < 1$  the function  $h(r)$  is well approximated by a divergent function and we have checked

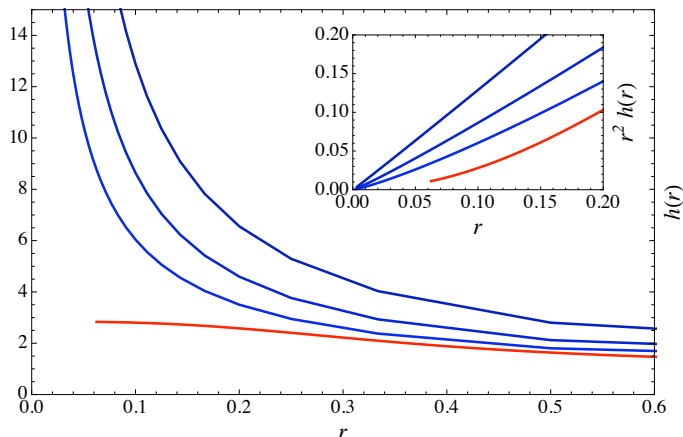


Figure 7.5: A plot of  $h(r)$  and  $r^2 h(r)$  for different values of  $\theta_\infty$ . From bottom to top, the curves correspond to  $\theta_\infty = 0, 0.5, 0.75, 1$ . The temperature is the lowest temperature available from the numerics and can be read from Figure 7.2. The normalization of the black holes is fixed by choosing  $\rho = 1$ . We observe that  $h(r)$  goes to a constant in the IR of the charged domain wall background and so does the corresponding low temperature superconducting solution. Then,  $r^2 h(r) \approx r^2$  if  $\theta_\infty = 0$  whereas  $r^2 h(r) \approx r$  in all the other cases.

that indeed  $h(r)$  behaves like  $1/r$ . This confirms our conjecture and provides a direct numerical proof that for  $\theta_\infty \neq 0$ , our zero temperature solutions coincides with the extremal limit of the thermal holographic superconductors. We anticipate that the study of the entanglement entropy will provide further evidence that at low temperatures,  $\theta_\infty \neq 0$  solutions, are effective cone geometries in the IR.

### 7.3 The Entanglement entropy

The entanglement entropy (EE) of a region  $\mathcal{E}$  in the boundary field theory is computed holographically according to the proposal of [126]. It is calculated by considering the area of bulk surfaces  $\gamma_{\mathcal{E}}$  whose boundary is given by  $\partial\mathcal{E}$ . According to the proposal, the entanglement entropy is the minimal area,

$$S_{\mathcal{E}} = \frac{2\pi \text{Area}(\gamma_{\mathcal{E}})}{\kappa^2} . \quad (7.43)$$

The strategy is to rewrite the problem as a variational problem. The solution of the equations of motion provides the profile of the minimal area surface

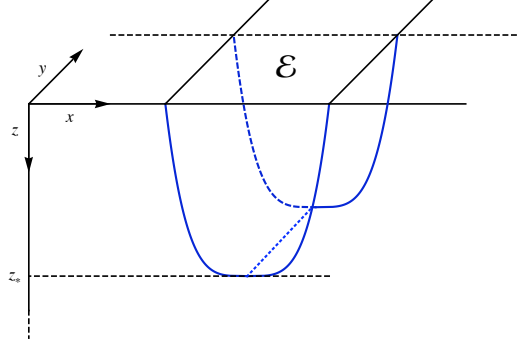


Figure 7.6: *Cartoon of the bulk surface  $\gamma_{\mathcal{E}}$  used in the calculation of the entanglement entropy. The surface is connected and the configuration has a turning point located at  $z = z_{\star}$ .*

and allows one to compute the entanglement entropy of the configuration. It's convenient to use the variable  $z = 1/r$  writing the spatial part of the metric in the form

$$ds_{\text{spatial}}^2 = \frac{L^2}{z^2} (dx^2 + dy^2 + U(z)dz^2) , \quad U(z) = \frac{1}{z^2 f(z) h^2(z)} . \quad (7.44)$$

The UV boundary is located at  $z = 0$ . We are interested in boundary surfaces with strip shape,

$$\mathcal{E} = \{(x, y) \mid -\frac{l_x}{2} \leq x \leq \frac{l_x}{2}, 0 \leq y \leq l_y\} . \quad (7.45)$$

We parametrize the bulk surface  $\gamma_{\mathcal{E}}$  choosing coordinate  $y$  and  $x = x(z)$  as schematically depicted in Figure 7.6. The area functional is given by,

$$\text{Area}(\gamma_{\mathcal{E}}) = 2L^2 l_y \int_{\epsilon}^{z_{\star}} \frac{dz}{z^2} \sqrt{U(z) + x'(z)^2} . \quad (7.46)$$

In the formula  $z_{\star}$  is the turning point of the configuration whereas  $\epsilon$  is an  $UV$  regulator. The variational problem for  $x(z)$  has a conservation law that allows to eliminate  $x'(z)$  from the integral (7.46). The conservation law is,

$$\frac{x'(z)}{z^2 \sqrt{U(z) + x'(z)^2}} = \frac{1}{z_{\star}^2} . \quad (7.47)$$

We solve for  $x'(z)$  and we use the result to write the area functional in the form,

$$\text{Area}(\gamma_{\mathcal{E}}) = 2L^2 l_y \int_0^{z_{\star}} \frac{dz}{z^2} \sqrt{\frac{U(z)}{1 - (z/z_{\star})^4}} . \quad (7.48)$$

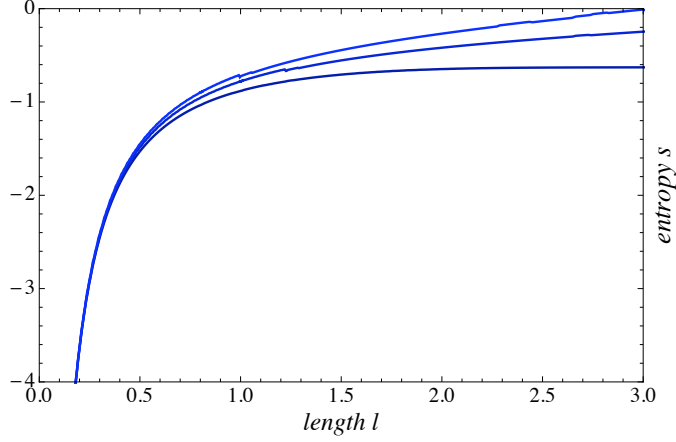


Figure 7.7: Numerical plots of the entanglement entropy as function of the length  $l_x$ . The case  $\theta_\infty = 0.5$  is displayed for different temperatures. From bottom to top  $T \approx 0.04, 0.095, 0.11$ .

Integrating the conservation law we find the relation between  $l_x$  and  $z_*$ ,

$$\frac{l_x}{2} = \int_0^{l_x/2} dx = \int_0^{z_*} dz \frac{z^2}{z_*^2} \sqrt{\frac{U(z)}{1 - (z/z_*)^4}}. \quad (7.49)$$

The entanglement entropy is divergent in the limit  $\epsilon \rightarrow 0$ . The origin of the divergence is easily understood: it corresponds to the integration of the short distances degrees of freedom and geometrically is due to the fact that the minimal surface reaches all the way to the boundary. This leading divergent term is the “boundary area law” of the entanglement entropy. Subtracting the divergence, we can write  $S_{\mathcal{E}}$  in terms of the finite quantity  $s$  defined by,

$$S_{\mathcal{E}} = \frac{4\pi L^2}{\kappa^2} l_y \left( s + \frac{1}{\epsilon} \right). \quad (7.50)$$

Formula (7.50) is proportional to the ratio  $L^2/\kappa^2$ , where  $L$  is the *AdS* radius and  $1/\kappa^2$  is the gravitational constant of the 4D model. According to the gauge/gravity correspondence  $L^2/\kappa^2$  is a function of the numbers of colors of the dual gauge theory. The present model is not based on a string construction thus, the precise relation is not fixed. However, in the large  $N$  limit the dependence  $L^2/\kappa^2 \sim N^{3/2}$  is to be expected [127]. The overall coefficient is not determined but the  $N^{3/2}$  dependence is a robust feature.

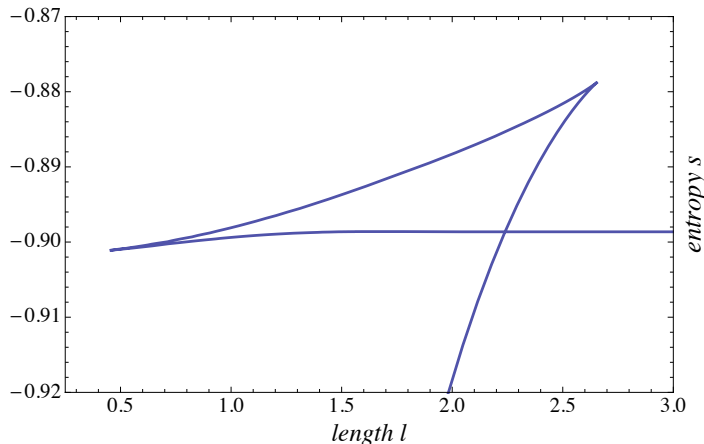


Figure 7.8: We show a zoom of the swallow-tail curve which characterizes a first order phase transition,  $\theta_\infty = 1$  and  $T \approx 0.082$ .

### 7.3.1 EE at Finite Temperature.

A distinction between first order and second order phase transition in the condensate phase diagram is necessary.

We first consider the case in which the phase transition is second order. In Figure 7.7 we show the plots of  $s = s(l_x)$  for the two values,  $\theta_\infty = 0.1$  and  $\theta_\infty = 0.5$ . When the temperature is close to the critical temperature, the large lengths behavior of the entropy shows a linear dependence. Lowering the temperature, the slope drops to zero and the entropy approaches a constant value. If the region  $\mathcal{E}$  has a relatively small size then  $z_*$  is close to the boundary and thus the pure AdS<sub>4</sub> result  $1/l_x$  is recovered [128].

When the phase transition becomes first order, the entanglement entropy is multi-valued at some length  $l_k$ . The swallow-tail curve, typical of this cases, is displayed in Figure 7.8. For  $l > l_k$  the slope of the curve  $s(l_x)$  suddenly changes and the entropy saturates to a fixed value.

### 7.3.2 EE at Zero Temperature

We now turn to the zero temperature solutions. For the conformal domain wall the picture does not show any substantial novelty with respect to the general analytical arguments reviewed in [129, 130]. We consider directly our new numerical results. We repeat a simple scaling argument that captures the main feature of the zero temperature solution when  $\theta_\infty \neq 0$  [131].

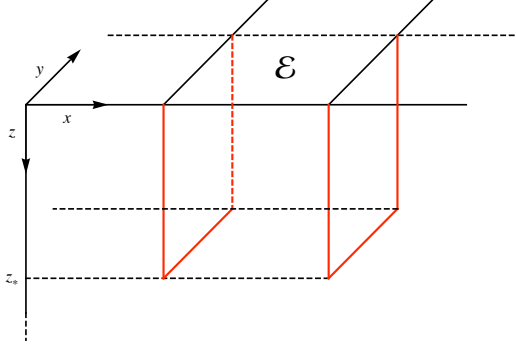


Figure 7.9: *Cartoon of the bulk surface  $\gamma_{\mathcal{E}}$  used in the calculation of the entanglement entropy. The surface is disconnected, the two planes are located at fixed  $x$ -coordinate and they are extended in the  $z$  direction, from the boundary up to  $z = z_*$ .*

If  $z \gg 1$  the function  $U(z)$  is given by the radial component of the metric in (7.35),

$$U(z) = (1 + C_{\eta}^2 z^2)^{-1} \approx (C_{\eta}^2 z^2)^{-1} \quad z \gg 1/C_{\eta} \quad \text{R}_1, \quad (7.51)$$

$$\approx 1 \quad \tilde{z} \ll z \ll 1/C_{\eta} \quad \text{R}_2, \quad (7.52)$$

where  $\tilde{z} = 1/\tilde{r}$ . If the length  $l_x$  is probing the intermediate region  $\text{R}_2$  then we expect the known behavior, however deep in the IR something new happens. We can estimate the integral (7.49) by considering (7.51) and the change of variables  $z \rightarrow z/z_*$ ,

$$\frac{l_x}{2} = z_* \int_0^1 dz \frac{z^2}{\sqrt{1-z^4}} U(z z_*)^{1/2} \sim \text{const } z_* \left( \frac{1}{z_* C_{\eta}} \right) \sim \text{const } \frac{1}{C_{\eta}}. \quad (7.53)$$

A maximum length  $l_x^{max}$  exists and the above relation shows that it is proportional to  $C_{\eta}^{-1}$ . According to the interpretation of the radial coordinate as energy scale,  $l_x^{max}$  and  $C_{\eta}$  are correctly related. It might seem surprising that in the limit of large  $z_*$  the length  $l_x$  remains tied to the value  $l_x^{max}$ . However, it does not mean that there are no configurations with  $l_x \geq l_x^{max}$ . It is important to keep in mind that the previous calculation considered only smooth and connected surfaces  $\gamma_{\mathcal{E}}$ , but in addition we have disconnected configurations. This class of surfaces consist of two disconnected planes located at  $x = \pm l_x/2$  that are extended in the  $z$  direction for a length equal to  $z_*$ . The entanglement entropy as a function of the length  $l_x$  is constant and only depends on

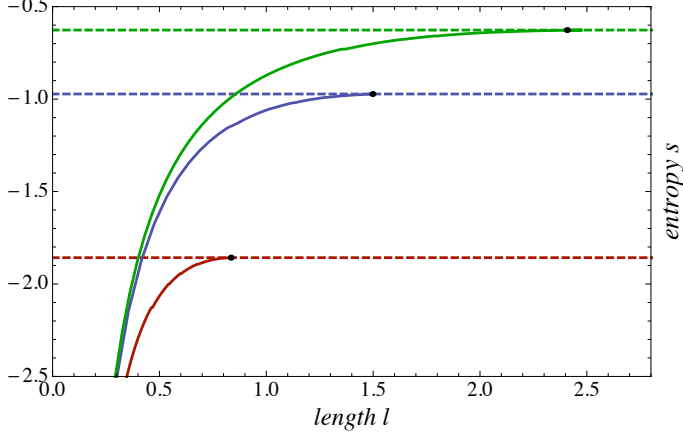


Figure 7.10: Behavior of the entanglement entropy for several cases. We present the result for the new zero temperature solutions. Along the solid lines the entropy has been calculated making use of the connected surface  $\gamma_{\mathcal{E}}$ . Dashed lines correspond to the contribution of the infinitely long disconnected surfaces. The maximum length  $l^{max}$  is indicated by the black dots. From top to bottom the various cases correspond  $\theta_{\infty} = 0.5, 1, 1.4$ . At  $l^{max}$  the solid lines merge with the dashed lines and the confinement/deconfinement transition takes place. Interestingly, for  $\theta_{\infty} = 1$ ,  $l_k$  is of the same order as  $l^{max}$ .

$z_*$  through the following formula,

$$S_{\mathcal{E}} = \frac{4\pi L^2}{\kappa^2} l_y \int_0^{z_*} \frac{dz}{z^2} \sqrt{U(z)} = \frac{4\pi L^2}{\kappa^2} l_y \left( s + \frac{1}{\epsilon} \right). \quad (7.54)$$

Figure 7.10 shows that when the size of  $\mathcal{E}$  is stretched up to  $l_x^{max}$ , there is a transition from the connected to the disconnected surface. In the limit  $z_* \gg 1/C_{\eta}$ , the contribution to the entanglement entropy coming from the disconnected configuration converges to the value reached by the connected surface when  $l_x = l^{max}$ .

**The confined cohesive phase.** At this point we can give a more exhaustive answer to the following question: what is the effective field theory that describes the low energy properties of our zero temperature superconductors? In the case  $\theta_{\infty} = 0$  we know that this is a conformal field theory because of the emergent  $\text{AdS}_4$  region. In the case  $\theta_{\infty} \neq 0$ , the hint comes from the transition that we have discovered in the previous paragraph. This transition is similar to the confinement/deconfinement transition that has been studied in [133].

The authors of [133] calculate the entanglement entropy in confining field theories with a known holographic dual [134, 135] and find that the entanglement entropy shows a transition from a connected to a disconnected solution. The existence of such transition is argued to be a necessary condition for the theory to be confining and should occur in any confining large  $N$  gauge theory. Finally, they relate the existence of this transition to the internal geometry of the gravitational backgrounds. In particular, these confining gravitational backgrounds typically have a type of cigar geometry because of an internal cycle which smoothly contracts and approaches zero size at the infrared where the space time ends.

We borrow the above results and we conjecture that our zero temperature solutions are dual to a confining theory. We also note that in our geometries the IR cone plays the role of the cigar tip. The idea of a cohesive phase is also suitable and we can strengthen our understanding by considering the rate of change of the entanglement entropy with the length  $l_x$ , i.e.  $\partial_l S$ . For connected configurations  $\partial_l S \sim N^{3/2}$  and the degrees of freedom that form the ground state are in a deconfined phase. When the topology of the bulk surface changes to the disconnected configuration, the degrees of freedom living in  $\mathcal{E}$  are not correlated with the ones of  $\mathcal{E}^c$ . This situation characterizes the large length scales and indeed the entanglement entropy is a constant for  $l_x > l_x^{max}$ : for disconnected configuration  $\partial_l S$  vanishes. In this sense we think of  $l_x^{max}$  as a sort of cohesion length which the entanglement entropy is able to probe. According to the classification introduced in [136], a confined cohesive phase is emerging in the IR of our model.

The calculation of this section helps to understand what characteristic length can be associated with the superconducting state, in order to distinguish between first or second order phase transition. We consider the case  $\theta_\infty = 1$  which is particularly instructive. The phase diagram of  $O_\eta(T, 1)$  shows a clear first order phase transition. It means that correlation lengths are finite when the temperature approaches the critical temperature. Because there are only two scales in our gravitational solutions,  $C_\eta$  and  $T_c$ , all other scales will be functions of  $C_\eta$  and  $T_c$ . Then, we can characterize the first order phase transition with the value of  $l_x^{max}$  (at zero temperature).

For a generic  $\theta_\infty$  we need a more careful analysis. Indeed, we know that the maximum length  $l_x^{max}$  exists for each value of  $\theta_\infty$  but the phase transition is not always first order. In particular, for small values of  $\theta_\infty$  the scale  $C_\eta \ll 1$  and therefore  $l_x^{max} \gg 1$ . In these cases the phase transition is second order. We can make a qualitative comment about this phenomenon reconsidering the discussion of section 7.2. When  $\theta_\infty$  increases, the curve of the condensate develops a plateau (see Figure 7.2). This plateau grows until the phase tran-

sition becomes first order. At the same time  $l_x^{max}$  decreases towards a critical value related to  $\theta^{crit}$ . This critical value of the length  $l_x^{max}$  is the one that we associate to a “strong” cohesion of the ground state.

In summary, by calculating the entanglement entropy we have unfolded the interesting features that were encoded in our extremal geometries (7.35). As a result, the scale  $C_\eta$  characterizes the typical length scale of the entanglement entropy when the system enters the superconducting phase at  $\theta_\infty \neq 0$ .

## 7.4 Optical Conductivity

In this section we show that the low energy excitations above the zero temperature background are gapped. In particular, we perturb the geometry and we extract dynamical informations for the optical conductivity. We will use results of section 3.7 that we briefly recall.

In order to obtain the conductivity we need to solve for a linearized perturbation of the vector potential  $A_x(r, t) = a_x(r)e^{-i\omega t}$ . The perturbation is found to satisfy

$$a_x'' + \left( \frac{f'}{f} - \frac{\chi'}{2} \right) + \left[ \left( \frac{w^2}{f^2} - \frac{\Phi'(r)^2}{f} - \frac{J(\eta, \theta)}{f} \right) \right] a_x = 0 \quad (7.55)$$

This equation makes use of the following metric,

$$ds^2 = -f(r)e^{-\chi(r)/2} dt^2 + r^2 d\vec{x}^2 + \frac{dr^2}{f(r)}, \quad (7.56)$$

which is not in the same coordinate system of the metric (7.16). Nevertheless, since we are interested in the extremal solution (7.35) the change of variables is almost straightforward. In the IR this reads

$$e^\chi = 1 + \frac{C_\eta^2}{r^2} + \dots, \quad f(r) = r^2 + C_\eta^2 + \dots, \quad f(r)e^{-\chi} = r^2 + \dots$$

The irrelevant perturbations that we used to shoot at the UV will not play any role and we omit them for simplicity. Equation (7.55) can be recast in a Schrodinger-like equation by introducing a new radial variable,

$$dz = \frac{e^{\chi(r)/2}}{f(r)} dr \quad - a_{x,zz} + V_{sh}(z)a_x = w^2 a_x \quad (7.57)$$

and defining the potential,

$$V_{sh}(z) = f(r) \left[ \Phi'(r)^2 + J(\eta(r), \theta(r))e^{-\chi(r)} \right] \quad (7.58)$$

At large  $r$ ,  $dz = dr/r^2$  and we can choose the integration constant so that  $z = -1/r$ . Then, the UV limit corresponds to  $z \rightarrow 0^-$ . In the opposite limit,  $r = 0$  we find,

$$dz = \frac{e^{\chi(r)/2}}{f(r)} dr \sim \frac{dr}{r}, \quad (7.59)$$

therefore, the extremal horizon corresponds to  $z = -\infty$ . Near  $z = 0$ , the Schrödinger potential is finite and goes to  $V(z) = q^2 O_\eta^2$ . This behavior is determined by the boundary condition that defines the  $\Delta = 1$  condensate. Along the semi-axis  $z > 0$  we extend the definition of the potential by setting  $V(z) = 0$ . The knowledge of the potential in the IR is crucial for the understanding of the optical conductivity without relying on numerical simulations. This is the great advantage of considering the formulation in terms of Schrödinger equation. Indeed, as show in section 3.7, the conductivity is

$$\sigma(w) = -\frac{i}{w} \frac{a_x^{(1)}}{a_x^{(0)}} = \frac{1-R}{1+R} \quad (7.60)$$

where  $R$  is amplitude of the reflected wave  $a_x = e^{-i\omega z} + R e^{i\omega z}$ . Here  $a_x \sim e^{-i\omega t}$  is the incoming wave that goes through the potential barrier. This wave travels from  $z = +\infty$  towards  $z = 0^+$ . Since, the transmitted wave is purely ingoing at the horizon, this satisfies the desired boundary conditions for the perturbation  $A_x(r, t)$ . In a range of frequencies below the height of the barrier, the probability of transmission will be small and  $R$  will be close to one. This means that  $\sigma(w)$  will be small. In order to have  $\sigma(w)$  strictly zero, the potential  $V_{sh}(z)$  has to be gapped at the horizon. In fact, when  $w^2$  lies below the gap there will be no transmitted wave and the probability  $R$  will be maximal, which means  $R = 1$  identically.

A short calculation shows that for our extremal solutions

$$V_{sh}(z) \rightarrow C_\eta^2(1 + C_\Phi^2) \quad \text{as} \quad z \rightarrow -\infty \quad (7.61)$$

and we conclude that the optical conductivity has a gap at low frequencies. This gap is directly proportional to the scale  $C_\eta$  that characterizes the IR geometry. Since  $C_\eta$  is ultimately related to the condensate  $O_\eta$ , the gap is fixed by the value of condensate.

We recall that in the BCS theory the superconducting phase is gapped, the gap  $\omega_g$  being proportional to the condensate (see section 1.2 for a review). On the gravitational side, the proof of this statement requires analytic control over the zero temperature solution. For the HHH model and for the conformal domain wall it has been proven that the conductivity has no gap at low frequency. In the second case, since there is an emergent IR conformal fixed point,

a scaling relation of the type  $\sigma(\omega) \sim \omega^\gamma$  is expected. However, the absence of a gap in the HHH model was somehow unexpected. Our model overcomes this discrepancy and provide a superconducting state with a strongly coupled “Cooper-pair”, a gap at low frequency in the spectrum and finite correlation length for the entanglement entropy. All these interesting and novel aspects of our model are turned on only at  $\theta_\infty \neq 0$ . In the next section we make contact between the classical gravitational picture of the  $\theta_\infty \neq 0$  solutions and the field theory dynamics that it is responsible for the non trivial RG flow of the theory.

## 7.5 Dual field theory and marginal deformations

Having studied the model in the variables  $\{\eta, \theta\}$  it is convenient to go back to the original ones  $\{z_1, z_2\}$ . The asymptotic expansion for the two complex scalar fields is known: they both have the same near-boundary behavior,

$$z_1(r) = \frac{\mathcal{O}_1^{(1)}}{r} + \frac{\mathcal{O}_1^{(2)}}{r^2} + \dots, \quad z_2(r) = \frac{\mathcal{O}_2^{(1)}}{r} + \frac{\mathcal{O}_2^{(2)}}{r^2} + \dots. \quad (7.62)$$

We use the definition of  $z_1$  and  $z_2$  in terms of  $\eta$  and  $\theta$ , i.e.  $z_1(r) = \tau \cos(\theta/2)$  and  $z_2(r) = \tau \sin(\theta/2)$ , to relate the coefficients  $\theta_\infty$ ,  $\xi$  and  $O_\eta$  to the four parameters appearing in (7.62). The result is the following,

$$\mathcal{O}_1^{(1)} = \frac{1}{2} O_\eta \cos \frac{\theta_\infty}{2}, \quad \mathcal{O}_1^{(2)} = -\frac{1}{4} O_\eta \xi \sin \frac{\theta_\infty}{2}, \quad (7.63)$$

$$\mathcal{O}_2^{(1)} = \frac{1}{2} O_\eta \sin \frac{\theta_\infty}{2}, \quad \mathcal{O}_2^{(2)} = \frac{1}{4} O_\eta \xi \cos \frac{\theta_\infty}{2}. \quad (7.64)$$

Given a superconducting solution with fixed  $\theta_\infty$  none of the above coefficients is independent of the temperature. Nevertheless, defining the constant  $\lambda \equiv \tan(\theta_\infty/2)$ , the following relations hold,

$$\mathcal{O}_2^{(1)} = \lambda \mathcal{O}_1^{(1)} \quad (7.65)$$

$$\mathcal{O}_1^{(2)} = -\lambda \mathcal{O}_2^{(2)} \quad (7.66)$$

$$\mathcal{O}_1^{(1)} \mathcal{O}_1^{(2)} + \mathcal{O}_2^{(1)} \mathcal{O}_2^{(2)} = 0 \quad (7.67)$$

We observe that  $\lambda$  has zero dimension. From the expressions (7.65) and (7.66) we recognize all the imprints of the double trace deformation in the AdS/CFT

setup [61]. In the following we explain the details of this deformation. They are important in order to understand the dual description which is behind the relations (7.65) and (7.66). A useful technique in this context is the holographic renormalization approach. In particular, we want to evaluate the euclidean action on the bulk of a given solution.

Standard methods allow one to compute the euclidean action  $S_E$  as a total derivative [73, 74],

$$\begin{aligned} S_E = - \int d^4x \sqrt{-g} \mathcal{L} &= \frac{1}{2\kappa^2} \int d^3x \int_{r_h}^{\infty} dr \partial_r (2rh(r)f(r)) \\ &= \frac{1}{2\kappa^2} \int d^3x \left( 2rh(r)f(r) \right) \Big|_{r \rightarrow \infty}, \end{aligned} \quad (7.68)$$

where  $\mathcal{L}$  is given in (7.1). The surface term at the horizon vanishes both at finite temperature and at zero temperature. At finite temperature the term  $r_h h(r_h)$  is finite but  $f(r_h) = 0$  by construction. At zero temperature the term  $rh(r)$  is bounded by  $C_\eta$  in the limit  $r \rightarrow 0$  but  $f(r)$  vanishes like  $r^2$ . The surface term at infinity, i.e. in the limit  $r \rightarrow \infty$ , is not finite and needs to be renormalized. At the boundary we find two types of divergences,

$$\left( 2rh(r)f(r) \right) \Big|_{r \rightarrow \infty} = 2r^3 + \sum_{i=1,2} \mathcal{O}_i^{(1)} \mathcal{O}_i^{(1)} r - 2M + \frac{8}{3} \sum_{i=1,2} \mathcal{O}_i^{(1)} \mathcal{O}_i^{(2)}. \quad (7.69)$$

The  $r^3$  term originates from the integration over the AdS space and it is regulated by the Gibbons-Hawking term plus a boundary cosmological constant,

$$S_{GH} = \frac{1}{2\kappa^2} \int d^3x \sqrt{-g_B} \left( 2K + \frac{4}{L} \right). \quad (7.70)$$

The metric  $g_B$  is the induced metric at the boundary and  $K$  is the trace of the extrinsic curvature defined by

$$K^{\mu\nu} = -\frac{1}{2} (\nabla^\mu n^\nu + \nabla^\nu n^\mu), \quad (7.71)$$

with  $n^\mu$  outward pointing unit vector, normal to the boundary.

The term which is linearly divergent in  $r$  comes from the integration over the radial profile of the scalar fields. Counterterms are not uniquely specified unless the choice of quantization scheme is fixed. In the present case, the mass of the scalar fields is  $m^2 L^2 = -2$  and therefore both scalars can be quantized in the two possible schemes. However, there is no ambiguity. Indeed, we recall that  $\zeta_1$  and  $\zeta_2$  are part of an hypermultiplet in the  $\mathcal{N} = 2$  theory. Thus, their

quantum numbers in  $AdS$  are  $\Delta = 1$  and  $\Delta = 2$  and the natural choice is to quantize them in different ways. For concreteness we consider the alternative quantization scheme for  $z_1$  and the standard quantization scheme for  $z_2$ .

The scalar field  $z_1$  is dual to an operator of dimension  $\Delta = 1$  whereas the scalar field  $z_2$  is dual to an operator of dimension  $\Delta = 2$ . The boundary values  $\mathcal{O}_1^{(1)}$  and  $\mathcal{O}_2^{(2)}$  are interpreted as condensates whereas,  $\mathcal{O}_1^{(2)}$  and  $\mathcal{O}_2^{(1)}$  are the sources. This choice is in agreement with the dynamics studied in section 7.2 for the value  $\theta_\infty = 0$ . In this case we have set the scalar field  $\zeta_2$  to zero and the condensation has been associated with the operator with dimension  $\Delta = 1$  dual to  $\zeta_1$ . According to this choice, the counterterm for the  $z_2$  scalar is

$$S_2 = \frac{1}{2\kappa^2} \int d^3x \sqrt{-g_B} 2 z_2^2 / L , \quad (7.72)$$

whereas the counterterm for the  $z_1$  scalar is

$$S_1 = -\frac{1}{2\kappa^2} \int d^3x \sqrt{-g_B} ( 4 z_1 n^\mu \partial_\mu z_1 + 2 z_1^2 / L ) . \quad (7.73)$$

The renormalized euclidean action is finite and it is given by,

$$\mathcal{S}_{ren} = S_E + S_{GH} + (S_1 + S_2) = \frac{1}{\kappa^2} \int d^3x \left( -\frac{M}{2} + \frac{4}{3} \mathcal{O}_1^{(1)} \mathcal{O}_1^{(2)} - \frac{2}{3} \mathcal{O}_2^{(1)} \mathcal{O}_2^{(2)} \right) . \quad (7.74)$$

Taking into account the relations (7.65) and (7.66), the final result is,

$$-\mathcal{S}_{ren} = \frac{1}{\kappa^2} \int d^3x \left( \frac{M}{2} + 2\lambda \mathcal{O}_1^{(1)} \mathcal{O}_2^{(2)} \right) . \quad (7.75)$$

From the above expression we understand the consequence of having identified the sources with the condensates. The double trace deformation  $\mathcal{O}_1^{(1)} \mathcal{O}_2^{(2)}$ , with marginal coupling  $\lambda$ , shows up as a finite contribution to the renormalized action. In order to be completely general, we note that the identification between sources and condensates given in (7.65) and (7.66) takes into account only the “radial” part of the complex fields  $\zeta_1$  and  $\zeta_2$ . Indeed, looking for black hole solutions we dropped the phases from our Lagrangian however, the double trace deformation has to involve complex operators. We can easily restore the phases because the most general solution, according to our ansatz (7.12), has the phases  $\psi$  and  $\varphi$  constants. Therefore we simply consider that  $\zeta_1 = z_1(r) \exp(i(\varphi + \psi)/2)$  and  $\zeta_2 = z_2(r) \exp(-i(\varphi - \psi)/2)$ . Then, from the asymptotic expansion of  $z_1(r)$  and  $z_2(r)$  given in (7.62), we obtain complex sources and complex condensates. The relations (7.65) and (7.66) are generalized taking into account the following observation: it is only consistent to

identify operators with the same quantum numbers thus, the charges of the scalar fields fix the relation between sources and condensate. This means that  $\zeta_1$  is related to  $\zeta_2^\dagger$ . Proceeding with the identification we find

$$\mathcal{O}_2^{(1)\dagger} = \lambda_C \mathcal{O}_1^{(1)} , \quad \mathcal{O}_1^{(2)} = -\bar{\lambda}_C \mathcal{O}_2^{(2)\dagger} , \quad \text{with } \lambda_C = \lambda e^{-i\psi} . \quad (7.76)$$

The marginal deformation is then,

$$\delta\mathcal{S} = \int d^3x \left( \lambda_C \mathcal{O}_1 \mathcal{O}_2 + \bar{\lambda}_C \mathcal{O}_1^\dagger \mathcal{O}_2^\dagger \right) , \quad (7.77)$$

where we have dropped the upper indexes and we have defined  $\{\mathcal{O}_1, \mathcal{O}_2\}$  as the complex operators dual to the scalars  $\{\zeta_1, \zeta_2\}$ . Remarkably the deformation is invariant under the  $U(1)$  action,

$$\mathcal{O}_1 \rightarrow e^{i\alpha} \mathcal{O}_1 , \quad \mathcal{O}_2 \rightarrow e^{-i\alpha} \mathcal{O}_2 , \quad (7.78)$$

and this global  $U(1)$  symmetry of the field theory is not explicitly broken by  $\delta\mathcal{S}$ . It is worthwhile to mention that the operator  $\mathcal{O}_1^{(1)} \mathcal{O}_2^{(2)}$  is strictly marginal only in the planar limit.

The understanding of  $\theta_\infty$  in the gravitational description is now clear: the parameter  $\theta_\infty$  is mapped to the marginal coupling  $\lambda$  in the dual field theory through the relation  $\lambda = \tan(\theta_\infty/2)$ . It is therefore tempting to consider the dependence on the extra coordinate  $r$  of the field  $\theta(r)$  in an RG fashion. In fact, it is a general feature in the AdS/CFT scheme to interpret the evolution of the (zero temperature) geometry, from the AdS boundary towards the bulk, as the flow of the UV microscopic theory towards a low energy regime. In this sense the interpolating solutions represent a novelty of this thesis: whenever  $\theta_\infty \neq 0$  the theory enters a low energy confining phase. However, the double trace deformation that we have identified does not break conformal invariance and therefore cannot be responsible for the RG flow. On the other hand, it is certainly evident, from the analysis of the potential in Figure 7.1, that  $\theta_\infty \neq 0$  drives the theory towards the  $\theta = \pi/2$  well, away from the conformal fixed point represented by  $\mathfrak{S}$ . This is a consequence of  $\mathfrak{S}$  being a saddle and cannot be avoided in the classical approximation to supergravity. Therefore, we conclude that conformal invariance is somehow broken. To approach this issue we consider the asymptotic behavior of  $\theta(r)$ ,

$$\theta(r) = \theta_\infty + \frac{\xi}{r} + \dots .$$

In a superconducting solution we have seen that  $\xi \equiv 0$  implies  $\theta(r)$  constant in the bulk. The value  $\theta_\infty = 0$  belongs to this case and even if it represents a

trivial example, because  $\lambda = 0$ , it matches the expectation that conformal invariance is not explicitly broken. Therefore,  $\xi \neq 0$  parametrizes our ignorance of how conformal invariance is broken in the UV [137]. This observation suggests that a relevant deformation is turned on at a certain high energy scale. The same relevant deformation is then responsible for the RG flow. The intuition on  $\xi \neq 0$  can be further specified by considering another important relation which holds between the two condensates:

$$\mathcal{O}_2^{(2)} = \frac{1}{2}\xi\mathcal{O}_1^{(1)} . \quad (7.79)$$

This is an “on-shell” relation which is not specified by the boundary data given in (7.65) and (7.66). Instead, it arises from the bulk dynamics of the interpolating solution, in particular from (7.63) and (7.64). Because we want to keep the  $U(1)$  invariance manifest, it is convenient to work with the complex version of (7.79),

$$\mathcal{O}_2^{(2)\dagger} = \frac{1}{2}\xi\mathcal{O}_1^{(1)}e^{-i\psi} . \quad (7.80)$$

According to our interpretation of  $\delta\mathcal{S}$  as double trace deformation, the coefficient  $\xi$  assumes the role of an energy scale proportional to the beta function of the coupling  $\lambda$ , i.e.  $r\theta'(r) \propto \xi/r$ . We conclude that the relation (7.80), which introduces the UV scale  $\xi$  in the definition of the condensates, breaks conformal invariance and provides the relevant deformation which initiates the RG flow. Indeed, by substituting the above relation (7.80) in  $\delta\mathcal{S}$ , we find an effective UV action of the form,

$$\delta\mathcal{S}_{eff} \propto \lambda\xi\mathcal{O}_1^\dagger\mathcal{O}_1 . \quad (7.81)$$

This effective action has the expected RG behavior and in fact, by using dimensional analysis, we find that  $\int d^3x \delta\mathcal{S}_{eff} \propto (\xi/E)$ . Once the RG flow is initiated the coupling  $\lambda$  runs. Its value in the IR, given by  $\theta(0) = \pi/2$ , characterizes the effective low energy confining phase with respect to the conformal point identified by  $\mathfrak{S}$ . In particular, the field theory dynamics of the tachyonic direction at the saddle point can be explored with the following argument. The coordinates  $\zeta_1$  and  $\zeta_2$  also diagonalize the Hessian in a neighborhood of  $\mathfrak{S}$ . The  $\zeta_2$  direction corresponds to a scalar with the negative mass  $m^2L^2 = -12/7^6$ , dual to a relevant operator in the IR conformal theory. Then, any mixing between  $\zeta_1$  and  $\zeta_2$  in the UV will source this IR relevant perturbation. In other words, even if  $\xi$  is of order  $\epsilon$ , and the theory stays arbitrarily close to

---

<sup>6</sup>Note that the mass value is above the BF bound and therefore  $\mathfrak{S}$  is a stable non supersymmetric fixed point [138].

the conformal point  $\mathfrak{S}$  at an intermediate scale, the mentioned IR relevant perturbation will drive the flow along the tachyonic direction. The above intermediate scale is  $C_\eta$ . This fact can be seen both from the radial component of the metric in (7.35) and from the log term that appears in the IR expansion of  $\eta(r)$ , i.e.  $\eta(r) \approx \log(C_\eta^2/r^2)$  for  $r \ll C_\eta$ .

Finally, the deformation  $\delta\mathcal{S}$  is exactly marginal only for the two cases  $\theta_\infty = 0$  and  $\theta_\infty = \pi/2$ . It is therefore interesting to note that when  $\theta_\infty \neq 0$  the coupling flows along the flat direction towards  $\theta = \pi/2$ . If  $\theta = \pi/2$  was a second fixed point, this kind of flow would be the expected running of an exactly marginal operator when some massive field is integrated out [139]. It is a nice property of our model that  $\theta(0) = \pi/2$  still characterizes the IR effective theory even if it does not correspond to any fixed point. In this sense the supergravity interpretation, that  $\theta_\infty = 0$  and  $\theta_\infty = \pi/2$  are better understood as “order parameters” for the different phases of the model, is also valid in the dual field theory. In the next section, we seriously take into account the properties of  $\delta\mathcal{S}$  by considering how our model satisfies some general statement about Landau-Ginzburg theories.

Despite the remarkable interpretation of our extremal interpolating solutions in terms of RG flow dynamics, a field theoretical argument able to explain the reason why the retrograde condensate does not loop back to zero temperature is still absent. It remains an open problem and unfortunately our analysis of Section 7.2.1 only provides other evidence for the non existence of a zero temperature solution associated with the retrograde condensate.

### 7.5.1 Additional Comments about the dual field theory

We want to suggest a feasible connection between the existence of the moduli space  $\mathcal{M}_\theta$  and the existence of a marginal operator in the dual field theory. We borrow part of the story from the theory of the  $\mathcal{N} = 2$  Landau-Ginzburg models in two dimensions. Reviewing these ideas we closely follow [140].

We recall the notion of moduli in the Landau-Ginzburg model. A pedagogical example, which is also useful to understand the nature of phase transitions, is the mean field theory of a single scalar field  $\varphi$ . The potential of the theory is given by

$$V = m^2(T)\varphi^2 + \bar{\lambda}\varphi^4 . \tag{7.82}$$

with  $T$  a continuous parameter (the temperature) and with  $\lambda$  constant, positive and greater than zero. In a stable configuration the scalar is seated at the minimum of the potential. A smooth phase transition is realized if the parameter  $m^2(T)$  takes negative values in some range of temperatures. If  $m^2(T)$

behaves as follow,

$$\begin{cases} m^2(T) < 0 & \text{for } T < T_c , \\ m^2(T) = 0 & \text{for } T = T_c , \\ m^2(T) > 0 & \text{for } T > T_c , \end{cases} \quad (7.83)$$

the extrema of the potential, which is a solution of the equation,

$$\partial_\varphi V(T, \varphi) \Big|_{\varphi=\varphi_0} = 0 , \quad (7.84)$$

changes with the temperature. Above the critical temperature the potential is a sum of positive quantities and the only solution to (7.84) is  $\varphi_0 = 0$ . Below the critical temperature the value  $\varphi_0 = 0$  becomes a local maximum and the new minimum,

$$\varphi_0 = \sqrt{\frac{-m^2(T)}{\bar{\lambda}}} , \quad (7.85)$$

is the stable configuration. We want to emphasize a feature of  $V(T_c)$  that is physically crucial. At the critical temperature the equation

$$\partial_\varphi V(T_c, \varphi) \Big|_{\varphi_0} = \bar{\lambda} \varphi_0^3 = 0 \quad (7.86)$$

has solution  $\varphi_0 = 0$  which is three times degenerate: we say that  $V(T_c, \varphi)$  is critical. Starting from this example we analyze a more general situation. The definition of a critical potential falls into the framework of *singularity* functions. By considering  $n$  field variables, we define a (polynomial) potential  $\mathcal{V}(X_1, \dots, X_n)$  to be critical, or a *singularity* function, if its critical points are degenerate.

The possible deformations of  $\mathcal{V}(X_1, \dots, X_n)$  are polynomials in the original field variables and are classified according to the renormalization group as: relevant, marginal and irrelevant. Relevant perturbations split the degeneracy, but marginal deformation do not. The presence of marginal operators reveals that the critical potential is not isolated, but rather it is an element of a family  $\mathcal{M}_V$  of functions. If  $k$  is the number of marginal operators then the elements of  $\mathcal{M}_V$  are labeled by  $k$  continuous parameters  $\{\lambda_1, \dots, \lambda_k\}$  which are the coefficients of the marginal perturbations. In other words, an element of  $\mathcal{M}_V$  is of the form,

$$\mathcal{V}(X_1, \dots, X_n, \lambda_1, \dots, \lambda_k) = \mathcal{V}(X_1, \dots, X_n) + \sum_i^k \bar{\lambda}_i \mathcal{F}_i , \quad (7.87)$$

where  $\mathcal{F}_i$  is a marginal operator. The space  $\mathcal{M}_V$  has the structure of a ring and the coefficients  $\{\lambda_1, \dots, \lambda_k\}$  are called moduli. Each potential living in  $\mathcal{M}_V$  admits a critical point which is degenerate.

If we want to relate the degeneracy of the potentials in  $\mathcal{M}_V$  to our theory, Figure 7.2 clearly shows that all the condensates arises from the same branch at  $T \approx 0.121$ , independently of  $\theta_\infty$ . We can say more about the relation between the spaces  $\mathcal{M}_V$  and  $\mathcal{M}_\theta$ . Taking into account the results of the previous section we can collect the following chain of observations. First, the double trace operator  $\mathcal{F} = \mathcal{O}_1\mathcal{O}_2$  is a marginal operator which belongs to  $\mathcal{M}_V$  in the dual field theory. Second, the modulus  $\lambda$  associated with  $\mathcal{F}$  is geometrically the parameter  $\theta_\infty$  which belongs to  $\mathcal{M}_\theta$ . Thus, the AdS/CFT correspondence maps the modulus associated with  $\mathcal{F}$  to the space  $\mathcal{M}_\theta$ . More precisely, the relation  $\lambda_C = \tan(\theta_\infty/2)e^{-i\psi}$ , together with the restriction  $\theta_\infty \in [0, \pi/2]$ , which defines  $\mathcal{M}_\theta$ , implies that  $\lambda_C$  parametrizes the unit ball on the complex plane. We remove from this set the circle  $S^1$  because of the retrograde condensate and we refer to the open ball as  $\mathcal{B}(0, 1)$ .

At this point we can rephrase the analysis of the previous section by considering the action of the renormalization group flow on the open ball. We know that the origin is a fixed point and therefore we focus on the set  $\mathcal{B}(0, 1) \setminus \{0\}$ . In this case the renormalization group flow acts as an projection and the IR image of  $\mathcal{B}(0, 1) \setminus \{0\}$  is the unit circle.

At the classical level one might expect  $\lambda_C$  to vary in the entire complex plane. Instead, we find that  $\lambda_C \in \mathcal{B}(0, 1)$ . It is natural to ask what happens to the complement of  $\mathcal{B}(0, 1)$ . In this case  $\theta_\infty$  takes values in the range  $[\pi/2, \pi]$ . We already know the dynamics of the model simply because the potential is  $\pi/2$ -periodic: when  $\theta_\infty$  is increased from  $\pi/2$  to  $\pi$ , the condensate goes backwards from the retrograde condensate to the conformal domain wall. These solutions are related to the ones found for  $\theta_\infty \in \mathcal{M}_\theta$  but they are not the same. In fact, for  $\theta_\infty = \pi$  the scalar field  $\zeta_1$  is set to zero and the condensation is driven by  $\zeta_2$ . This situation is the opposite of the case  $\theta_\infty = 0$ . Let us see what is the boundary description in this case. The relations

$$\mathcal{O}_2^{(1)} = \lambda\mathcal{O}_1^{(1)}, \quad \mathcal{O}_1^{(2)} = -\lambda\mathcal{O}_2^{(2)}, \quad (7.88)$$

are always valid, even in the range  $\theta_\infty \in [\pi/2, \pi]$ . In the limit  $\theta_\infty \rightarrow \pi$ , the coupling  $\lambda$  blows up and the relations (7.88) make sense only if  $\mathcal{O}_1^{(1)} \rightarrow 0$  and  $\mathcal{O}_2^{(2)} \rightarrow 0$ . These two conditions are suitable for the opposite quantization scheme from that adopted in  $\mathcal{B}(0, 1)$ : the condensates are now  $\mathcal{O}_2^{(1)}$  and  $\mathcal{O}_1^{(2)}$ , the sources instead are  $\mathcal{O}_1^{(1)}$  and  $\mathcal{O}_2^{(2)}$ . Thus, the conformal domain wall in the case  $\theta_\infty = \pi$  has to be associated with the condensation of the operator  $\mathcal{O}_2^{(1)}$

with  $\mathcal{O}_2^{(2)} = 0$ . In summary, in the region  $\mathbb{C} \setminus \overline{\mathcal{B}(0,1)}$  the quantization scheme is exchanged with respect to the region  $\mathcal{B}(0,1)$ .



## Chapter 8

# Conclusions and Outlook

With a view towards condensed matter physics, let us recall the main conceptual difficulty with the problem of high- $T_c$  superconductivity. The normal phase of the high- $T_c$  superconductors above optimal doping is described by Non Fermi Liquid physics. In this region of the phase diagram the standard description of the fermionic excitations in terms of long-lived electrons at the Fermi Surface is not applicable because the system is strongly interacting. Thus, the concept of “Cooper pair” cannot be used to describe the superconducting phase because there are no electrons to form a bound state. The problem is then how to describe the phenomenon of superconductivity in these materials, or more generally in strongly coupled theories.

In this thesis we have shown that the AdS/CFT correspondence provides an intrinsic definition of the superconductivity in strongly coupled theories with an holographic dual. The logical leap it to rephrase the problem as a gravitational problem in asymptotically AdS spaces. In this framework, condensation of Cooper-pairs is described in terms of a gravitational background that spontaneously develops a charged hair. The dual field theory enters a new phase in which a charged condensate is turned on and the phenomenology of ordinary weakly coupled superconductors appears as a consequence of a London type equation. Being much more than ordinary superconductors, gravitational backgrounds with these properties have been called *holographic superconductors*. By considering first phenomenological models of holographic superconductivity and then strongly coupled theories originating from string theory, we have shown that the phase diagram of these theories contains a sector in which the system enters the holographic superconducting phase. Thus, we conclude that superconductivity is a general phenomenon not only at weak coupling but also in strongly coupled large  $N$  field theories.

In chapter 3 we analyzed holographic models inspired by the Landau-Ginzburg theory. The analysis carried out in this chapter aims at the classification of holographic phase transitions in terms of the phenomenological couplings introduced in the holographic description. Much of our findings have a direct analog in the Landau-Ginzburg theory however, it should be emphasized that the classical nature of the gravitational description arises because of the large  $N$  limit: the holographic description is not at all comparable with a mean field approximation. Remarkably, in our strongly coupled theories, the critical exponents at the phase transition satisfy the Rushbrooke identity and the possible forms of the critical behavior are characterized in terms of universality classes. It is interesting to observe that this result, which follows from renormalization group arguments in the standard field theory derivation, is exactly reproduced by a classical calculation in the gravity background.

Despite the similarities with the Landau-Ginzburg theory, there is a natural way to promote our phenomenological holographic superconductors into a full microscopic description. This is done by considering top-down models obtained from string theory in which the precise knowledge of the AdS/CFT dictionary gives the microscopic description of the condensing operator. In chapter 5 we have analyzed a first example in the context of  $\mathcal{N} = 4$  SYM. In particular, we have studied the complex scalar fields  $Z_i = \eta_i e^{i\theta_i}$ ,  $i = 1, 2, 3$ , with mass  $m^2 L^2 = -4$  and charge  $qL = 2$ , which are dual to the BPS operators

$$O_i = \text{Tr}[\Phi_i^2] , \tag{8.1}$$

where the  $\Phi_i$  are the three chiral superfields of  $\mathcal{N} = 4$  SYM. In section 6.2 we studied the universal multiplet and the charged scalar field dual the gluino bilinear,

$$\tilde{O} \sim \text{Tr}[\lambda\lambda] + \text{h.c.} , \tag{8.2}$$

where  $\lambda$  is a particular combination of the  $SU(4)$  fermions of  $\mathcal{N} = 4$  SYM. Our analysis shows that the operators  $O_i$  compete with the gluino bilinear but the latter is the one that condenses. It would be interesting to analyze the full phase diagram of the theory but we limited our search to sectors of the theory in which the superconducting instability plays a prominent role.

In chapter 6, the investigation of top-down model was based on  $\mathcal{N} = 2$  supergravity. Our main finding has been a feasible connection between the so called  $\gamma$ -models and the spectrum of type IIB supergravity compactified on  $\text{AdS}_5 \times \text{T}^{1,1}$ . The dual theory is also well understood and represents the Klebanov-Witten theory. Assuming that our models live in this theory we have studied competing condensates and we have found a sector of the theory

that exhibits holographic superconductivity. Even in this case, we conclude that holographic superconductivity is a generic phenomenon.

With respect to the known holographic superconductors obtained from string theory, the superconductor constructed in chapter 7 revealed additional features. The model has an interesting IR dynamics and several new ingredients coexist in the phase diagram. These are, the interpolating solutions constructed in section 7.2, the properties of the zero temperature solutions outlined in section 7.2.1 and the notion of double trace deformation in AdS/CFT. Each of them can be related to the existence of the space  $\mathcal{M}_\theta$  which is completely tied to the nature of the hypermatter scalar manifold  $SU(2,1)/U(2)$ . We emphasize the topological aspect of the manifold  $SU(2,1)/U(2)$  which is homeomorphic to a ball in  $\mathbb{C}^2$ . The three-sphere can be parametrized in terms of the Hopf fibration and as we go towards the center of the scalar manifold a “topological” degeneracy shows up: this is the moduli space  $\mathcal{M}_\theta$  which describes the onset of marginal deformations. Turning on this marginal deformation, generates a novel IR dynamics characterized by a confinement/deconfinement transition in the entanglement entropy of the ground state.

In  $\mathcal{N} = 4$  SYM, we found the first obstruction to the phenomenon of holographic superconductivity. This was related to the appearance of the retrograde condensate. We encountered this obstruction also in two different  $\mathcal{N} = 2$  truncations considered respectively in chapter 7 and chapter 7. In light of the results obtained in chapter 7, we now understand that there is no real problem with the retrograde condensate because it only represents a specific solution in a bigger phase space. This bigger phase space is associated to a marginal double trace deformation of the theory. In the context of the  $\mathcal{N} = 2$  truncations it was also evident how the marginal deformation appeared in the holographic description because this was encoded in the topology of the scalar manifold. The same construction does not hold for  $\mathcal{N} = 8$  supergravity and therefore it would be interesting to find how the marginal deformation shows up in this case. We leave this problem for the future.

The kind of holographic superconductors that we have studied are *s*-wave whereas the gap in the cuprates has a *d*-wave structure. In this sense, we should improve our models in order to describe *d*-wave superconductivity. Nevertheless, we believe that much of the results obtained in the *s*-wave case are valid in the case of holographic *d*-wave superconductors. Building a *d*-wave superconductors represents one of the current problems in AdS/CMT [141].

Finally we would like to stress that the normal phase of the holographic superconductors can be described either by the Reissner-Nördstrom black or by dilatonic black holes. The Reissner-Nördstrom black hole has the impor-

tant characteristic of being akin to the strange metals [142]. Indeed, several works have shown that fermionic excitations on top of the Reissner-Nördstrom black hole are governed by a nontrivial infrared fixed point which exhibits non analytic scaling behavior. This fixed point is the near horizon region of the extremal solution, namely  $\text{AdS}_2 \times \mathbb{R}^2$ . The scaling behavior that is found has the same form advocated for the cuprates and used as an input in the study of heavy fermion criticality. On the other hand, the dilatonic black holes introduce multiples  $U(1)$  charges and are probably better suited for the study of LOFF phases that we now mention [143, 144]. The different  $U(1)$ s may describe system of particles where different species coexist and the population of each specie may be unbalanced by tuning the corresponding bulk electric field. In the weak coupling theory, when the superconducting instability is turned on, the system is expected to develop inhomogeneous superconducting phases, where the Cooper pairs have non-zero total momentum. This phenomenon may also occur in  $\mathcal{N} = 4$  SYM at strong coupling. In fact, despite the cases of retrograde condensation that appeared in these models, there could be a different kind of instability which precisely involves a condensate with non zero momentum. We leave this issue for a future study.

# Appendix A

## QFT and Statistical Mechanics: Some Results

Perturbative methods of quantum field theories are very well review in standard textbooks [18, 19]. However, it may be convenient to revisit the particle physics approach from the point of view of condensed matter systems. Indeed, even if most of the perturbative techniques can be easily applied many body problems of bosons and fermions, the fact that the ground state of the free fermions theory is a Fermi surface requires a special analysis.

We remind the reader that in quantum mechanics time evolution can be equally introduced by using the Schrödinger representation or by using the Heisenberg representation. The principal difference is the following. In the Heisenberg representation the wave functions do not depend on time and the time dependence is transferred to operators according to the law,

$$\partial_t O = i[\mathcal{H}, O] \quad (\text{A.1})$$

where  $\mathcal{H}$  is the Hamiltonian of the physical system. In the Schrödinger representation instead, the operators are time independent and the wave functions depends on time.

**Setting up the perturbative expansion.** We consider the Hamiltonian,

$$\mathcal{H}(\lambda) = \int d^4\mathbf{r} \frac{1}{2m} \nabla \psi_\alpha^\dagger(\mathbf{r}) \cdot \nabla \psi_\alpha(\mathbf{r}) + \quad (\text{A.2})$$

$$+ \frac{1}{2} \int d\mathbf{r} d\mathbf{r}' \psi_\alpha^\dagger(\mathbf{r}) \psi_\beta^\dagger(\mathbf{r}') \lambda_{\alpha\beta\gamma\delta}(\mathbf{r}, \mathbf{r}') \psi_\gamma(\mathbf{r}') \psi_\delta(\mathbf{r}) \quad (\text{A.3})$$

or its Fourier transform (1.4). This Hamiltonian is of the form  $\mathcal{H}(\lambda) = \mathcal{H}_{free} + \lambda \mathcal{H}_{int}$ . Because of the interactions, the exact form of the eigenstates will be in general difficult to obtain and certainly it will not be given in terms of simple plane waves. The strategy is to define a field  $\psi_I$  whose time evolution

is determined just by the free Hamiltonian  $\mathcal{H}_{free}$ . Then, for a given reference time  $t = t_0$  we have

$$\psi_I(t, \mathbf{r}) = e^{i\mathcal{H}_{free}(t-t_0)}\psi_I(t_0, \mathbf{r})e^{-i\mathcal{H}_{free}(t-t_0)}. \quad (\text{A.4})$$

The next step is to express the Heisenberg field  $\psi$  in terms of  $\psi_I$ . By setting  $\tau = t - t_0$ , it is a short calculation to show that,

$$\psi(t, \mathbf{r}) = e^{i\mathcal{H}\tau}\psi(t_0, \mathbf{r})e^{-i\mathcal{H}\tau} = \quad (\text{A.5})$$

$$= e^{i\mathcal{H}\tau}e^{-i\mathcal{H}_{free}\tau}\psi_I(t, \mathbf{r})e^{i\mathcal{H}_{free}\tau}e^{-i\mathcal{H}\tau} \quad (\text{A.6})$$

We observe that  $[\mathcal{H}_{free}, \mathcal{H}] \neq 0$  and therefore

$$U(\tau) \equiv \exp\left(i\mathcal{H}_{free}(\tau)\right)\exp\left(-i\mathcal{H}(\tau)\right) \neq \exp\left(i(\mathcal{H}_{free} - \mathcal{H})(\tau)\right) \quad (\text{A.7})$$

The operator  $U$  defines the evolution in the *interaction picture*. It also satisfies the relation

$$U(\tau) = T\left\{\exp\left[-i\int_{t_0}^t dt' \mathcal{H}_I(t')\right]\right\}, \quad (\text{A.8})$$

$$\mathcal{H}_I(t) = e^{i\mathcal{H}_{free}(t-t_0)}\mathcal{H}_{int}e^{-i\mathcal{H}_{free}(t-t_0)}. \quad (\text{A.9})$$

We remind that the exponential is defined by its Taylor expansion with boundary condition  $U(0) = 1$ . The time-ordering  $T$  means that all terms in the Taylor expansion are time ordered. Then, the basic textbook formula for the n-point Green's Functions is,

$$\langle 0|T\{\psi(r_1)\dots\psi(r_n)\}|0\rangle = e^{-i\alpha}\langle 0|T\{\psi(r_1)\dots\psi(r_n)\exp\left[-i\int_{-\infty}^{+\infty} dt' \mathcal{H}_I(t)\right]\}|0\rangle \quad (\text{A.10})$$

where  $r_i = (t_i, \mathbf{r}_i)$  and

$$e^{-i\alpha} = \langle 0|T\left\{\exp\left[-i\int_{-\infty}^{\infty} dt' \mathcal{H}_I(t')\right]\right\}|0\rangle \quad (\text{A.11})$$

The case of the Green's Function can be easily deduced,

$$G(r, r') = -i\frac{\left\langle T\left\{\psi(r)\psi^\dagger(x)\exp\left[-i\int_{-\infty}^{+\infty} dt' \mathcal{H}_I(t)\right]\right\}\right\rangle}{\left\langle \exp\left[-i\int_{-\infty}^{+\infty} dt' \mathcal{H}_I(t)\right]\right\rangle}. \quad (\text{A.12})$$

Feynman diagrams are generated by expanding the exponential terms. This is a one to one correspondence, determined by the Wick Theorem, between a certain set of graphs and the terms that appear in series expansion of (A.10).

In this way, calculating the perturbative series reduces to forming all the possible Feynmann diagrams. The use of this technology is of great help. For example, a first simplification of the diagrammatic expansion is the following. Feynman diagrams are naturally classified as connected diagrams and disconnected diagrams. Then, it can be proved that the series expansion obtained by summing up all the disconnected diagrams is a phase factor that multiplies the amplitude generated by evaluating connected diagrams. This phase factor cancels with the  $e^{-i\alpha}$  and the net result is that the generalized n-points Green's Functions (A.10) are only specified by the series of connected Feynman diagrams. In the particular case of the two point function we find,

$$G(r, r') = -i \left\langle T \left\{ \psi(r) \psi^\dagger(x) \exp \left[ -i \int_{-\infty}^{+\infty} dt' \mathcal{H}_I(t) \right] \right\} \right\rangle_{conn} \quad (\text{A.13})$$

A second simplification of the diagrammatic expansion is related to a more careful analysis of the connected diagrams. Indeed, the knowledge of a certain set of diagrams, called 1-particle irreducible diagrams, is enough to generate all the connected Feynman diagrams. An irreducible diagrams is by definition a connected diagram which cannot be divided into two parts just by removing a free propagator. The, we can assemble all the connected diagrams by considering all the possible combinations of irreducible diagrams joint together by free propagators. The series of diagrams constructed in this way is usually called self energy.

**Fermi Surface: the kinematical constraint.** We calculate the one loop contribution to the  $2 \rightarrow 2$  scattering amplitude. By considering (A.13), this integral is given by,

$$(-i\lambda)^2 \int d\mathfrak{M} \langle p_1, p_2 | T \left\{ (a_{k_1}^\dagger a_{k_2}^\dagger a_{k_3} a_{k_4}) \Big|_t (a_{q_1}^\dagger a_{q_2}^\dagger a_{q_3} a_{q_4}) \Big|_0 \right\} | p_3, p_4 \rangle \quad (\text{A.14})$$

where we have defined

$$d\mathfrak{M} = \prod_{i=1}^4 \frac{dk_i}{(2\pi)^4} \frac{dq_i}{(2\pi)^4} \delta(k_1 + k_2 - k_3 - k_4) \delta(q_1 + q_2 - q_3 - q_4) . \quad (\text{A.15})$$

A connected diagram is obtained if only if the internal Wick's contractions couple operators at time  $t$  with operators at time 0. From a simple counting, it

follows that there are basically three type of pairings divided into two category. Three is the number of ways one can choose a pair of momenta out of set of four momenta having fixed the first component of the pair. The two categories are,

$$(1) \quad \overbrace{a_{k_1}^\dagger(t)a_{q_3}(0)} \quad \underbrace{a_{k_2}^\dagger(t)a_{q_4}(0)} \quad (A.16)$$

$$(2) \quad \overbrace{a_{k_1}^\dagger(t)a_{q_3}(0)} \quad \underbrace{a_{k_3}(t)a_{q_2}^\dagger(0)} \quad (A.17)$$

It follows that in the first case (A.16), the vertex at time  $t$  destroy the incoming particles  $|p_1, p_2\rangle$  whereas the vertex at time 0 create the final state  $|p_3, p_4\rangle$ , i.e.

$$G(k_1)G(k_2)\delta(k_1 - q_3)\delta(k_2 - q_4) \langle p_1, p_2 | \left\{ a_{k_3} a_{k_4} \Big|_t a_{q_1}^\dagger a_{q_2}^\dagger \Big|_0 \right\} | p_3, p_4 \rangle \quad (A.18)$$

In the case (A.16), each vertex connects one incoming and one outgoing particle,

$$G(k_1)G(k_3)\delta(k_1 - q_3)\delta(k_3 - q_2) \langle p_1, p_2 | \left\{ a_{k_2}^\dagger a_{k_4} \Big|_t a_{q_1}^\dagger a_{q_4} \Big|_0 \right\} | p_3, p_4 \rangle . \quad (A.19)$$

The final result is summarized by the following kernels,

$$(1) \quad \rightarrow \quad (-i\lambda)^2 \int \frac{dk}{(2\pi)^4} G(k)G(p_1 + p_2 - k), \quad (A.20)$$

$$(2a) \quad \rightarrow \quad (-i\lambda)^2 \int \frac{dk}{(2\pi)^4} G(k)G(p_1 - p_3 + k), \quad (A.21)$$

$$(2b) \quad \rightarrow \quad (-i\lambda)^2 \int \frac{dk}{(2\pi)^4} G(k)G(p_1 - p_4 + k) \quad (A.22)$$

where  $k$  is the momentum which runs in the loop, (2a) and (2b) represents the two different diagrams of Figure A.1 and Figure A.2. The delta function of momentum conservation,  $\delta(p_1 + p_2 - p_3 - p_4)$ , is understood. The above kernels are usually called pair bubble diagrams. For the purpose of this paragraph, the integrals (2a) and (2b) are formally equivalent and can be treated in the same way. We refer to them as the integrals of type (2). As we are going to show, the main difference between (1) and (2) comes from the domain of integration over the momentum  $\mathbf{k}$ . We remind that  $E_{\mathbf{k}}$  is not a positive quantity and it is defined as the energy measured with respect to the chemical potential,  $E_{\mathbf{k}} = \mathbf{k}^2/2m - \mu$ , where  $\mu = |\mathbf{k}_F|^2/2m$ .

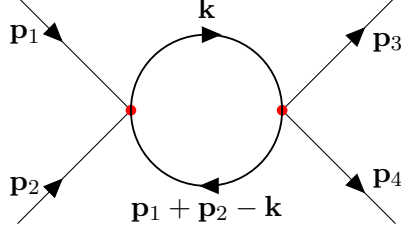


Figure A.1: *One Loop contribution to the scattering  $2 \rightarrow 2$  in the  $s$  channel.*

The integral (A.20) becomes

$$s \equiv p_1 + p_2 = (w_0, \mathbf{s}) \quad (\text{A.23})$$

$$(1) \rightarrow (-i\lambda)^2 \int \frac{d\mathbf{k}}{(2\pi)^3} \frac{d\omega}{(2\pi)} \left( \frac{1}{\omega - E_{\mathbf{k}} + i\delta_{\mathbf{k}}} \right) \left( \frac{1}{-\omega + w_0 - E_{\mathbf{s}-\mathbf{k}} + i\delta_{\mathbf{s}-\mathbf{k}}} \right)$$

The  $\omega$  integration can be carried out by using the Residue theorem. The denominators have poles in

$$\omega = E_{\mathbf{k}} - i\delta_{\mathbf{k}} \quad ; \quad \omega = w_0 - E_{\mathbf{s}-\mathbf{k}} + i\delta_{\mathbf{s}-\mathbf{k}} \quad (\text{A.24})$$

and therefore there are only two possible contributions, i.e. the ones which come from poles with opposite imaginary parts,

$$A(1) = \{\mathbf{k} \mid |\mathbf{k}| > k_F \cap E_{\mathbf{s}-\mathbf{k}} > 0\}, \quad (\text{A.25})$$

$$B(1) = \{\mathbf{k} \mid |\mathbf{k}| < k_F \cap E_{\mathbf{s}-\mathbf{k}} < 0\}. \quad (\text{A.26})$$

By considering the integral (A.21) we find,

$$t \equiv p_1 - p_3 = (w_0, \mathbf{t}) \quad (\text{A.27})$$

$$(2) \rightarrow (-i\lambda)^2 \int \frac{d\mathbf{k}}{(2\pi)^3} \frac{d\omega}{(2\pi)} \left( \frac{1}{\omega - E_{\mathbf{k}} + i\delta_{\mathbf{k}}} \right) \left( \frac{1}{\omega + w_0 - E_{\mathbf{t}+\mathbf{k}} + i\delta_{\mathbf{t}+\mathbf{k}}} \right)$$

and the denominators have poles in

$$\omega = E_{\mathbf{k}} - i\delta_{\mathbf{k}} \quad ; \quad \omega = -w_0 + E_{\mathbf{t}+\mathbf{k}} - i\delta_{\mathbf{t}+\mathbf{k}} \quad (\text{A.28})$$

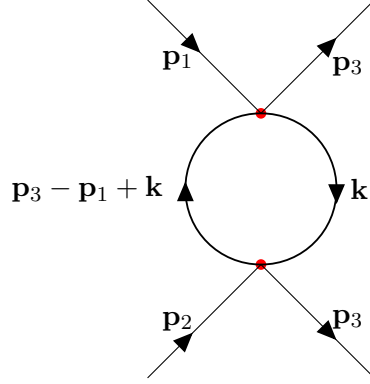


Figure A.2: *One Loop contribution to the scattering  $2 \rightarrow 2$  in the  $\mathbf{t}$  channel.*

Therefore, the only two possible contributions are

$$A(2) = \{\mathbf{k} \mid |\mathbf{k}| > k_F \cap E_{\mathbf{t}+\mathbf{k}} < 0\}, \quad (\text{A.29})$$

$$B(2) = \{\mathbf{k} \mid |\mathbf{k}| < k_F \cap E_{\mathbf{t}+\mathbf{k}} > 0\}. \quad (\text{A.30})$$

The constrain on  $E_{\mathbf{q}+\mathbf{k}}$ , where  $\mathbf{q}$  can be either  $\mathbf{s}$  or  $\mathbf{t}$ , depends on the angle  $\theta$  which is defined by the scalar product  $\mathbf{q} \cdot \mathbf{k} = |\mathbf{q}||\mathbf{k}| \cos \theta$ . It is convenient to partially fix the invariance under rotations and choose a reference frame in the  $\mathbf{k}$ -space such that  $\mathbf{q} = (|\mathbf{q}|, \vec{0})$ . For small momentum transfer,  $|\mathbf{q}| \ll k_f$ , the inequalities in  $A(1)$  and  $A(2)$  becomes approximately,

$$A(1) = \{(|\mathbf{k}|, \theta) \mid |\mathbf{k}| > k_F \cap |\mathbf{k}| > k_F + |\mathbf{s}| \cos \theta\} \quad (\text{A.31})$$

$$A(2) = \{(|\mathbf{k}|, \theta) \mid |\mathbf{k}| > k_F \cap |\mathbf{k}| < k_F - |\mathbf{t}| \cos \theta\} \quad (\text{A.32})$$

The same happens for the  $B$  sets. It is clear that  $A(2)$  only accounts for a window above  $k_F$  whereas  $A(1)$  do not. In the next paragraph we carry out the first explicit calculation of Feynman diagram and we actually see how the Fermi surface kinematics affects the result.

**Two Loop approximation from the bubble pair diagrams.** A self energy diagram contributing to  $\Sigma$  can be obtained from the above  $2 \rightarrow 2$  scattering amplitude by gluing two external legs. This diagram is relevant to the Fermi Liquid theory because its imaginary part determines whether the quasiparticle is stable or not. It also represents the leading order quantum

correction in the four Fermi interaction. The calculation is a two loop calculation that can be easily carried out by contracting another pair of operator in (A.14). We observe that, contrary to the pair bubble diagrams, we expect only one type of integral. The result is the following,

$$\Pi(p) \rightarrow (-i\lambda)^2 \int \frac{dt}{(2\pi)^4} G(p-t) \left\{ \int \frac{dk}{(2\pi)^4} G(k)G(k+t) \right\} \quad (\text{A.33})$$

where  $p$  is the external momentum. We recognize that the integral in parenthesis is formally the integral of type (2) introduced in the pair bubble diagrammatic,

$$(-i\lambda)^2 \int \frac{d\mathbf{k}}{(2\pi)^3} \frac{d\omega}{2\pi} \left( \frac{1}{\omega - E_{\mathbf{k}} + i\delta_{\mathbf{k}}} \right) \left( \frac{1}{\omega + w_0 - E_{\mathbf{t}+\mathbf{k}} + i\delta_{\mathbf{t}+\mathbf{k}}} \right). \quad (\text{A.34})$$

Therefore, we begin our calculation by considering the integral (2a) and we explicitly carry out the frequency integration on  $A(2)$  and  $B(2)$ . The result is

$$(2a) \rightarrow \Pi_2^A(\mathbf{t}, w_0) + \Pi_2^B(\mathbf{t}, w_0), \quad (\text{A.35})$$

$$\Pi_2^A(\mathbf{t}, w_0) = -i\lambda^2 \int_{A(2)} \frac{d\mathbf{k}}{(2\pi)^3} \frac{1}{-w_0 + E_{\mathbf{t}+\mathbf{k}} - E_{\mathbf{k}} + i\delta}, \quad (\text{A.36})$$

$$\Pi_2^B(\mathbf{t}, w_0) = -i\lambda^2 \int_{B(2)} \frac{d\mathbf{k}}{(2\pi)^3} \frac{1}{w_0 - E_{\mathbf{t}+\mathbf{k}} + E_{\mathbf{k}} + i\delta}. \quad (\text{A.37})$$

We examine first the two loop integral that involves the  $\Pi_2^B$  term. By defining  $p = (\omega, \mathbf{p})$  we find,

$$\Sigma^B(\omega, \mathbf{p}) = -i\lambda^2 \int \frac{d\mathbf{t}}{(2\pi)^3} \frac{dw_0}{2\pi} \int_{B(2)} \frac{d\mathbf{k}}{(2\pi)^3} \mathcal{I}^B(\omega, \mathbf{p}), \quad (\text{A.38})$$

$$\mathcal{I}^B(\omega, \mathbf{p}) \equiv \left( \frac{1}{\omega - w_0 - E_{\mathbf{p}-\mathbf{t}} + i\delta_{\mathbf{p}-\mathbf{t}}} \right) \left( \frac{1}{w_0 - E_{\mathbf{t}+\mathbf{k}} + E_{\mathbf{k}} + i\delta} \right). \quad (\text{A.39})$$

The poles are

$$w_0 = \omega - E_{\mathbf{p}-\mathbf{t}} + i\delta_{\mathbf{p}-\mathbf{t}}, \quad w_0 = E_{\mathbf{t}+\mathbf{k}} - E_{\mathbf{k}} - i\delta, \quad (\text{A.40})$$

and the contour in the complex plane is the same as before. The second pole is in the lower half plane, thus we need  $E_{\mathbf{p}-\mathbf{t}} > 0$ . The domain of integration becomes

$$B(2) = \{(\mathbf{k}, \mathbf{t}) \mid |\mathbf{k}| < k_F \cap E_{\mathbf{t}+\mathbf{k}} > 0 \cap E_{\mathbf{p}-\mathbf{t}} > 0\}. \quad (\text{A.41})$$

and the integration over  $w_0$  yields,

$$\Sigma^B(\omega, \mathbf{p}) = \lambda^2 \int \frac{d\mathbf{t}}{(2\pi)^3} \frac{d\mathbf{k}}{(2\pi)^3} \frac{1}{\omega + E_{\mathbf{k}} - E_{\mathbf{t}+\mathbf{k}} - E_{\mathbf{p}-\mathbf{t}} + i\delta} . \quad (\text{A.42})$$

The calculation of  $\Sigma^A$  is straightforward and the result is

$$\Sigma^A(\omega, \mathbf{p}) = -\lambda^2 \int \frac{d\mathbf{t}}{(2\pi)^3} \frac{d\mathbf{k}}{(2\pi)^3} \frac{1}{\omega + E_{\mathbf{k}} - E_{\mathbf{t}+\mathbf{k}} - E_{\mathbf{p}-\mathbf{t}} - i\delta} . \quad (\text{A.43})$$

The domain of integration is  $A(2) \cap \{\mathbf{t} \mid E_{\mathbf{p}-\mathbf{t}} > 0\}$ . Real and imaginary part of  $\Sigma = \Sigma^A + \Sigma^B$  determine respectively, the leading order correction to the energy  $E_{\mathbf{p}}$  and the lifetime  $\tau_{\mathbf{p}}$  of the quasiparticle. We can focus on the imaginary part of  $\Sigma^B$ , analogous result will hold for  $\text{Im}\Sigma^A$ . We make use of the identity,

$$\frac{1}{a + i\eta} = \text{P} \left[ \frac{1}{a} \right] - i\pi\delta(a) . \quad (\text{A.44})$$

Then,

$$\text{Im}\Sigma^B(\omega, \mathbf{p}) = -\lambda^2 \int d\mathbf{t} d\mathbf{k} \delta(\omega + E_{\mathbf{k}} - E_{\mathbf{t}+\mathbf{k}} - E_{\mathbf{p}-\mathbf{t}}) \quad (\text{A.45})$$

It is useful to consider the change of variable  $\mathbf{t} + \mathbf{k} = \mathbf{n}$  so that

$$\mathbf{p} - \mathbf{t} = \mathbf{p} - \mathbf{n} + \mathbf{k} , \quad (\text{A.46})$$

$$B(2) = \{(\mathbf{k}, \mathbf{n}) \mid |\mathbf{k}| < k_F \cap |\mathbf{n}| > k_F \cap |\mathbf{p} - \mathbf{n} + \mathbf{k}| > k_F\} . \quad (\text{A.47})$$

We also define the positive quantities,  $\mathcal{E}_{\mathbf{k}}$ ,  $\mathcal{E}_{\mathbf{n}}$ ,  $\mathcal{E}_{\mathbf{p}-\mathbf{n}+\mathbf{k}}$ , by considering

$$E_{\mathbf{k}} = \mu - \mathcal{E}_{\mathbf{k}} , \quad (\text{A.48})$$

$$E_{\mathbf{n}} = \mu + \mathcal{E}_{\mathbf{n}} , \quad (\text{A.49})$$

$$E_{\mathbf{p}-\mathbf{n}+\mathbf{k}} = \mu + \mathcal{E}_{\mathbf{p}-\mathbf{n}+\mathbf{k}} . \quad (\text{A.50})$$

The delta function constraint becomes

$$\omega - \mu = \mathcal{E}_{\mathbf{k}} + \mathcal{E}_{\mathbf{n}} + \mathcal{E}_{\mathbf{p}-\mathbf{n}+\mathbf{k}} \quad (\text{A.51})$$

and being the r.h.s. positive definite it is necessary that  $\omega - \mu > 0$ . Since  $E_{\mathbf{k}} < 0$ , the maximum value of  $\mathcal{E}_{\mathbf{k}}$  for a given  $\omega - \mu$  is evidently  $\omega - \mu$ . In this case  $\mathcal{E}_{\mathbf{n}}$  and  $\mathcal{E}_{\mathbf{p}-\mathbf{n}+\mathbf{k}}$  are zero. Hence, the integration over  $\mathbf{k}$  restricts to

$[\mu - \omega, \mu]$ . A similar reasoning applies to the integration over  $\mathbf{n}$ . Then, the delta function reduce the integral to

$$\text{Im}\Sigma^B(\omega, \mathbf{p}) = -\lambda^2 \int dS(n) dS(k) \int_{k_F}^{k_F+\Delta} dn \int_{k_F-\Delta}^{k_F} dk n^2 k^2 \quad (\text{A.52})$$

where  $n = |\mathbf{n}|$ ,  $k = |\mathbf{k}|$ ,  $S$  are angle variables and  $\Delta = m(\omega - \mu)/k_F$ . The estimate (1.18) follows by setting  $n = l = k_F$  and multiplying the result for  $\Delta^2$ .

**Superconducting Instability.** In this paragraph, we go back to the amplitudes (A.20), (A.21) and (A.22). We have seen how the calculation of  $\Sigma(\omega, \mathbf{p})$  is reduced to a two step calculation in which we first evaluated the integral of type (2). Here, we would like to see what happens for the integral of type (1):

$$(-i\lambda)^2 \int \frac{d\mathbf{k}}{(2\pi)^3} \frac{d\omega}{(2\pi)} \left( \frac{1}{\omega - E_{\mathbf{k}} + i\delta_{\mathbf{k}}} \right) \left( \frac{1}{-\omega + w_0 - E_{\mathbf{s}-\mathbf{k}} + i\delta_{\mathbf{s}-\mathbf{k}}} \right) \quad (\text{A.53})$$

We consider the integration in  $d\omega$  over  $A(1)$  and  $B(1)$ ,

$$(1) \rightarrow \Pi_1^A(\mathbf{s}, w_0) + \Pi_1^B(\mathbf{s}, w_0), \quad (\text{A.54})$$

$$\Pi_1^A(\mathbf{s}, w_0) = -i\lambda^2 \int_{A(1)} \frac{d\mathbf{k}}{(2\pi)^3} \frac{1}{-w_0 + E_{\mathbf{s}-\mathbf{k}} + E_{\mathbf{k}} - i\delta}, \quad (\text{A.55})$$

$$\Pi_1^B(\mathbf{s}, w_0) = -i\lambda^2 \int_{B(1)} \frac{d\mathbf{k}}{(2\pi)^3} \frac{1}{w_0 - E_{\mathbf{s}+\mathbf{k}} - E_{\mathbf{k}} - i\delta}. \quad (\text{A.56})$$

The integral over  $A(1)$  and  $B(1)$  is not constrained by the Fermi Surface kinematic. However, we can think of situations in which it is also natural to introduce a cut off on the energies  $E_{\mathbf{k}}$ . For example, two circumstances that are quite important are, the case of RG transformations and the case of the electron-phonon interactions. In both cases, the cut off is  $|E_{\mathbf{q}}| < \Lambda$  with  $\Lambda \ll \mu$  and it is valid  $\forall \mathbf{q}$ . It is interesting to carry out this analysis for  $A(1)$  and  $A(2)$  as well. Indeed, the sign of this inequality does not dependent on the delta function  $i\delta_{\mathbf{k}}$  and the constraint have to be considered on top of these two domains. As a result, regardless of the specific case  $A(1)$  or  $A(2)$ , the constraint  $|E_{\mathbf{k}}| < \Lambda$  implies that  $\mathbf{k}$  lives in a thin shell around the Fermi surface.

At this point, it is convenient to define  $\mathbf{l} = \mathbf{k} - \mathbf{k}_F$ . Then, the measure of integration in (A.55) and (A.56) is well approximated by the formula

$$\int d\mathbf{k} = 4\pi \int |\mathbf{k}|^2 d|\mathbf{k}| d\cos\theta \approx 4\pi k_F^2 \int d|\mathbf{l}| \int_{-1}^1 dx \quad (\text{A.57})$$

( $x \equiv \cos \theta$ ) and the difference of energies becomes,

$$\begin{aligned}
E_{\mathbf{s}+\mathbf{k}} + E_{\mathbf{k}} &= \frac{|\mathbf{k}|^2}{m} - 2\mu - \frac{|\mathbf{s}||\mathbf{k}| \cos \theta}{m} + \frac{|\mathbf{s}|^2}{2m} \\
&= \frac{2k_F}{m} |\mathbf{l}| - \frac{|\mathbf{s}|k_F}{m} \cos \theta + |\mathbf{s}| \mathcal{O}(|\mathbf{s}|, |\mathbf{l}| \cos \theta) + \mathcal{O}(|\mathbf{l}|^2), \\
&\approx \frac{2k_F}{m} |\mathbf{l}| - \frac{|\mathbf{s}|k_F}{m} \cos \theta.
\end{aligned} \tag{A.58}$$

where in the second line we have defined  $\mathbf{k} = \mathbf{k}_F + \mathbf{l}$ . It is convenient to introduce the Fermi velocity  $v = k_F/m$  and change variable  $\xi = |\mathbf{l}|k_F/m$ . Then, we obtain

$$\begin{aligned}
\Pi_1^A(\mathbf{s}, w_0) &= -i\lambda^2 mk_F \int_0^\Lambda \frac{d\xi}{2\pi^2} \int_{-1}^1 dx \frac{1}{+2\xi - w_0 - v|\mathbf{s}|x - i\delta}, \\
\Pi_1^B(\mathbf{s}, w_0) &= -i\lambda^2 mk_F \int_{-\Lambda}^0 \frac{d\xi}{2\pi^2} \int_{-1}^1 dx \frac{1}{-2\xi + w_0 + v|\mathbf{s}|x - i\delta},
\end{aligned}$$

We are mainly interested in the imaginary part of the above expression evaluated at  $\mathbf{s} = 0$ . This is the relevant case for the BCS instability. We also note the term  $-i\delta$  that appears in both denominators, to be contrasted with the term  $+i\delta$  that appeared in  $\Sigma(\omega, \mathbf{p})$ . By using again the identity (A.44) we find,

$$\begin{aligned}
\text{Im}(\Pi_1^A + \Pi_1^B)_{\mathbf{s}=0} &= -i\lambda^2 mk_F \left\{ i\pi \int_0^\Lambda d\xi [\delta(w_0 + 2\xi) + \delta(2\xi - w_0)] \right\} \\
&= -i\lambda^2 mk_F \left\{ i\frac{\pi}{2} \int_0^{2\Lambda} d\xi' [\delta(w_0 + \xi') + \delta(-w_0 + \xi')] \right\} \\
&= -i\lambda^2 mk_F \left\{ i\frac{\pi}{2} \left[ \int_{w_0}^{2\Lambda+w_0} \delta(\xi') d\xi' + \int_{-w_0}^{2\Lambda-w_0} \delta(\xi') d\xi' \right] \right\} \\
&= -i\lambda^2 mk_F \left\{ i\frac{\pi}{2} \theta_{2\Lambda+w_0} \otimes \theta_{2\Lambda-w_0} \right\}.
\end{aligned} \tag{A.59}$$

Then we recover the result (1.32). The integration of the real part is elementary and yields the logarithm.

# Appendix B

## Menagerie of $\mathcal{N} = 2$ geometry

**Conventions for the differential forms.** In this short paragraph, we give some informations regarding the use of differential forms, exterior calculus and Hodge dual forms, in the context of  $\mathcal{L}_{SO(6)}$ . We supposed the reader is already familiar with these concepts. The sum over repeated indexes is always understood but sometimes we can make it explicit in order to clarify the formula. We always consider an ambient space which is the space of the one forms  $\{dx^i\}$  of dimension  $d$ . The nature of this vector space is not required to be specified.

- Form fields are defined with the following conventions,

$$A_{(1)} = A_\mu dx^\mu \quad (\text{B.1})$$

$$F_{(2)} = \frac{1}{2} F_{\mu\nu} dx^\mu \wedge dx^\nu \quad (\text{B.2})$$

$$F_{(p)} = \frac{1}{p!} F_{\mu_1 \dots \mu_p} dx^{\mu_1} \wedge \dots \wedge dx^{\mu_p} . \quad (\text{B.3})$$

- Exterior derivative are given by

$$dF_p = \frac{1}{p!} \partial_\mu F_{\mu_1 \dots \mu_p} dx^\mu \wedge dx^{\mu_1} \wedge \dots \wedge dx^{\mu_p} . \quad (\text{B.4})$$

A familiar example, which goes back to Maxwell electrodynamics, is that of the electro-magnetic field strength  $F_{(2)}$ ,

$$F_{(2)} \equiv dA_{(1)} = \partial_\mu A_\nu dx^\mu \wedge dx^\nu = \frac{1}{2} (\partial_\mu A_\nu - \partial_\nu A_\mu) dx^\mu \wedge dx^\nu . \quad (\text{B.5})$$

It follows that  $F_{\mu\nu} = \partial_\mu A_\nu - \partial_\nu A_\mu$ .

- The wedge product is simply expressed as multiplications of forms,

$$F_{(p)} \wedge \Omega_{(q)} = \frac{1}{p!q!} F_{i_1 \dots i_p} \Omega_{j_1 \dots j_q} dx^{i_1} \wedge \dots \wedge dx^{i_p} \wedge dx^{j_1} \wedge \dots \wedge dx^{j_q} \quad (\text{B.6})$$

The product vanishes if  $p + q > d$ .

- The Hodge operator is a mapping between differential forms. It is defined on the basis of  $p$ -forms  $dx^{\mu_1} \wedge \dots \wedge dx^{\mu_p}$ , with  $p \leq d$  and it is usually indicated as a  $\star$  operation. The definition goes as follows:

$$\star(dx^{\mu_1} \wedge \dots \wedge dx^{\mu_p}) = \frac{\sqrt{-g}}{p!} dx^{\alpha_1} \wedge \dots \wedge dx^{\alpha_q} \epsilon_{\alpha_1 \dots \alpha_q}^{\mu_1 \dots \mu_p} \quad (\text{B.7})$$

where  $p + q = d$  and the LeviCivita tensor  $\epsilon_{\alpha_1 \dots \mu_p} = \pm 1$ , depending on the sign of the permutation  $(\alpha_1 \dots \alpha_q, \mu_1 \dots \mu_p)$ . The indexes are raised with the inverse metric  $g^{\alpha\mu}$ . For example, in  $d = 5$ , the 3-form  $\star F_{(2)}$  is given by,

$$\star F_{(2)} = \frac{\sqrt{-g}}{3! \cdot 2} F^{\mu\nu} \epsilon_{\alpha_1 \alpha_2 \alpha_3 \mu\nu} dx^{\alpha_1} \wedge dx^{\alpha_2} \wedge dx^{\alpha_3} \quad (\text{B.8})$$

where the components of  $\star F_{(2)}$  have anti-symmetric indexes  $\alpha_1 \alpha_2 \alpha_3$  and are explicitly given by  $(1/2)\sqrt{-g} \epsilon_{\alpha_1 \alpha_2 \alpha_3 \mu\nu} F^{\mu\nu}$ . In general the components of a  $q$ -form defined as  $\Omega_{(q)} = \star w_{(p)}$  are,

$$\Omega_{\alpha_1 \dots \alpha_q} = \frac{\sqrt{-g}}{p!} \epsilon_{\alpha_1 \dots \alpha_q \beta_1 \dots \beta_p} w^{\beta_1 \dots \beta_p} . \quad (\text{B.9})$$

With the above definitions it can be proved that

$$\star F_{(p)} \wedge F_{(p)} = \frac{1}{p!} \sqrt{-g} F^{\mu_1 \dots \mu_p} F_{\mu_1 \dots \mu_p} \quad (\text{B.10})$$

This relation makes use of a property of the Levi-Civita tensor:

$$\sum_{j_1 \dots j_q} \epsilon_{j_1 \dots j_q i_1 \dots i_p} \epsilon_{j_1 \dots j_q k_1 \dots k_p} = q! \delta_{i_1 \dots i_p}^{k_1 \dots k_p} \quad (\text{B.11})$$

where the  $\delta$  symbol is introduced by

$$\delta_{i_1 \dots i_p}^{k_1 \dots k_p} = \sum_{\sigma \in \mathfrak{S}} \text{sign}(\sigma) \delta_{\sigma(i_1)}^{k_1} \dots \delta_{i_p}^{k_p} . \quad (\text{B.12})$$

The rest of the formula follows because the components of form fields are anti-symmetric and therefore,

$$\sum_{I,K} F_{i_1 \dots i_p} F^{k_1 \dots k_p} \delta_{i_1 \dots i_p}^{k_1 \dots k_p} = \sum_I p! F_{i_1 \dots i_p} F^{i_1 \dots i_p} . \quad (\text{B.13})$$

For example we can calculate,

$$\delta_{\mu\nu}^{\alpha\beta} = \delta_\mu^\alpha \delta_\nu^\beta - \delta_\nu^\alpha \delta_\mu^\beta \quad (\text{B.14})$$

$$F_{\mu\nu} F^{\alpha\beta} \delta_{\mu\nu}^{\alpha\beta} = F_{\mu\nu} F^{\mu\nu} - F_{\mu\nu} F^{\nu\mu} = 2 F_{\mu\nu} F^{\mu\nu} \quad (\text{B.15})$$

**Special Geometry.** This three paragraphs are meant as a collection of useful formulas in the context of special geometry. They completely characterize the Lagrangian of  $\mathcal{N} = 2$  supergravity in dimensions  $d = 5$  and  $d = 4$ . We refer to section 4.1.3 and in particular to (4.17) and (4.22). In that section we gave the basic ingredients in order to understand the notation of  $\mathcal{N} = 2$  supergravity with matter couplings but we skipped the details.

- We begin with the case of real special geometry. This geometry describes vector multiplets in  $d = 5$ . The scalar manifold  $\mathcal{V}$  is the  $n$  dimensional surface in  $\mathbb{R}^{n+1}$  defined by the constraint

$$C_{IJK} h^I(\phi) h^J(\phi) h^k(\phi) = 1 \quad (\text{B.16})$$

The tensor  $C_{IJK}$  is completely symmetric in the lower indexes and the symbols  $h^I$  are coordinates for  $\mathbb{R}^{n+1}$ . The indexes  $IJK$  run over  $0, \dots, n_V$  and therefore the graviphoton is included in the list. The coordinates on the surface are the  $\phi_x$  with  $x = 0, n_V - 1$ . The kinetic matrix  $a_{IJ}$  and the metric on the scalar manifold are,

$$a_{IJ} \equiv -2 C_{IJK} h^k + 3 C_{IKL} h^k h^L C_{JMN} h^M h^N \quad (\text{B.17})$$

$$G_{xy} \equiv \frac{3}{2} \partial_x h^I \partial_y h^J a_{IJ} \quad (\text{B.18})$$

where we have also defined

$$h_x^I = -\sqrt{\frac{3}{2}} \partial_x h^I(\phi) \quad (\text{B.19})$$

A non abelian structure (in the absence of tensor multiplets see [86, 89] should satisfy

$$C_{L(IJ)}f_{KM}^L = 0 , \quad K_I^x = \sqrt{3}2h_k f_{JI}^k h^{jx} \quad (\text{B.20})$$

which implies

$$h_I f_{JK}^I h^K = 0 , \quad \rightarrow \quad K_I^x h^I = 0 . \quad (\text{B.21})$$

where  $K_I^x$  are the Killing vectors.

• Quaternionic Geometry is relevant for the description of hypermultiplets. The total number of real coordinates is  $4n_H$ . The geometry can be formulated completely in terms of more fundamental objects: these are the  $4n_H$ -beins  $f_u^{iA}$  with the  $SU(2)$  index  $i = 1, 2$  and the  $Sp(2n_H)$  index  $A = 1, \dots, 2n_H$ . The indexes are raised and lowered by the symplectic metrics  $C_{AB}$  and  $\varepsilon_{ij}$ . These matrices can be brought into the standard form,

$$\varepsilon_{ij} = i\sigma_2, \quad C_{AB} = \begin{pmatrix} 0 & \mathbf{1}_{n_H \times n_H} \\ -\mathbf{1}_{n_H \times n_H} & 0 \end{pmatrix} . \quad (\text{B.22})$$

The metric on the hyperscalar space is given by,

$$H_{uv} \equiv f_u^{iA} f_v^{iB} \varepsilon_{ij} C_{AB} \quad (\text{B.23})$$

The inverse vielbeins  $f_{iA}^u$  are defined by,

$$f_u^{iA} f_{iA}^u = \delta_v^u, \quad f_u^{iA} f_{jB}^u = \delta_j^i \delta_B^A . \quad (\text{B.24})$$

The triplet of complex structure is introduced as follows,

$$2f_u^{iA} f_{jA}^v = \delta_u^v \delta_j^i + \vec{\tau}_j^i \cdot \vec{J}_u^v, \quad \vec{J}_u^v = -i f_u^{iA} f_{jA}^v \vec{\sigma}_i^j . \quad (\text{B.25})$$

These hypercomplex structures are only covariantly constant up to a rotation between them,

$$\nabla_m (J^x)_n^v + 2\varepsilon^{xyz} \omega_m^y (J^z)_n^v = 0 , \quad (\text{B.26})$$

$$\nabla_m (J^x)_n^v = \partial_m (J^x)_n^v - \Gamma_{mn}^p (J^x)_p^v + \Gamma_{mp}^v (J^x)_n^p . \quad (\text{B.27})$$

The  $\Gamma_{mn}^p$  tensor is the Levi Civita connection given in terms of the metric  $H_{uv}$ . The  $\omega_m^y$  are the connections of the  $SU(2)$  bundle. They do not exist in global supersymmetry. In that case the complex structures are covariantly constants. The connections relative to the  $Sp(2n_H)$  bundle, called  $\Upsilon_{vj}^i$ , exist

even in the global case and in general they are obtained by requiring that the frame fields  $f_u^{iA}$  have vanishing covariant derivative. The condition is

$$\partial_v f_u^{iA} + f_u^{iB} \omega_{vB}^A + f_u^{jA} \Upsilon_{vj}^i - \Gamma_{uv}^w f_w^{iA} = 0 \quad (\text{B.28})$$

There are three type of connections on  $\mathcal{H}$ :  $\Gamma$ ,  $\omega$  and  $\Upsilon$ . Therefore, we can define three type of curvature,

$$\begin{aligned} R_{uv}{}^m{}_n &\equiv 2\partial_{[u}\Gamma_{v]n}^m + 2\Gamma_{y[u}^m\Gamma_{v]n}^y \\ \vec{\mathcal{R}}_{uv} &\equiv 2\partial_{[u}\omega_{v]} + 2\vec{\omega}_u \times \vec{\omega}_v \\ \mathcal{R}_{uvB}{}^A &\equiv 2\partial_{[u}\Upsilon_{v]B}^A + \Upsilon_{uC}^A\Upsilon_{vB}^C - \Upsilon_{vC}^A\Upsilon_{uB}^C \end{aligned} \quad (\text{B.29})$$

These curvatures are not independent and the following relation holds,

$$R_{uv}{}^m{}_n = f_{iA}^m f_n^{iB} \mathcal{R}_{uvB}{}^A - \vec{J}_n{}^m \cdot \vec{\mathcal{R}}_{uv}. \quad (\text{B.30})$$

Regarding the  $SU(2)$  bundle, we already stated that the most significant identity occurs between the curvature of the  $\omega$  connection and the Kähler form, namely

$$\vec{\mathcal{R}}_{uv} = \frac{1}{2} H_{up} \vec{J}_u{}^p \quad (\text{B.31})$$

Finally, we point out that quaternionic manifolds turn out to be Einstein:

$$R_{uv} \equiv R_{uv}{}^n{}_n = \frac{1}{4n_H} H_{uv} R. \quad (\text{B.32})$$

- Special Kähler Geometry is associated with vector multiplets in  $d = 4$ . It differs substantially from the case of real special geometry. First, it involves a complex manifold with certain properties and second, it as a non trivial first Chern class.

In a local frame, we consider a set of complex coordinates  $\{X^I, \bar{X}^I\}$  and an holomorphic function  $F(X)$  homogeneous of second degree in  $X^I$ . The index  $I$  runs over  $0, \dots, n_V$  and therefore the graviphoton is included.  $\mathcal{N} = 2$  supersymmetry impose the constraint

$$N_{IJ} X^I \bar{X}^J = -1, \quad N_{IJ} = 2\text{Im}F_{IJ} = -iF_{IJ} + i\bar{F}_{IJ}. \quad (\text{B.33})$$

where  $F_{IJ}$  are the second derivatives of  $F(X)$ . The very definition of  $F(X)$  implies that  $F_{IJ} X^J$  is the first derivative of  $F(X)$  with respect to  $X^I$ . Then, we observe that

$$N_{IJ} X^I \bar{X}^J = i(X^I, F_{IJ} X^J) \begin{pmatrix} 0 & 1 \\ -1 & 0 \end{pmatrix} \begin{pmatrix} \bar{X}^I \\ \bar{F}_{IJ} \bar{X}^J \end{pmatrix} \quad (\text{B.34})$$

By defining the ‘‘symplectic section’’

$$V = \begin{pmatrix} X^I \\ F_I \end{pmatrix} \quad (\text{B.35})$$

and the symplectic scalar product ,

$$\langle V|\bar{V}\rangle = V^t \begin{pmatrix} 0 & 1 \\ -1 & 0 \end{pmatrix} \bar{V} \quad (\text{B.36})$$

we can recast the constraint in the form  $i\langle V|V\rangle = -1$ . Let remind to the reader that in  $\mathcal{N} = 1$  a similar constraint also appears but supersymmetry fixes the scalar product to another value, i.e.  $i\langle V|V\rangle = -3$ . In any case, we can think of special Kähler geometry as a surface in the  $\mathbb{C}^{n_V+1}$  defined by the function  $F(X)$  and by the constraint (B.33). Then, the coordinates of this surface are  $\{z^\alpha, \bar{z}^{\bar{\alpha}}\}$  with  $\alpha = 1, \dots, n_V$  and the metric is given by

$$g_{\alpha\bar{\beta}} = N_{IJ}\partial_\alpha X^I \partial_{\bar{\beta}} \bar{X}^J = i\partial_\alpha \partial_{\bar{\beta}} \langle V|\bar{V}\rangle. \quad (\text{B.37})$$

This intuition is formalized by the choice of a convenient parametrization where the  $X^I$  coordinates take the form  $X^I = yZ^I(z)$ . The parameter  $y$  is taken to be real,  $y = \bar{y}$ . We are referring to  $y$  as a parameter and not as a coordinate because we want to use it in the following way. By plugging the above parametrization in (B.33) we find the relation,

$$y^2 = -(N_{IJ}X^I \bar{X}^J)^{-1}. \quad (\text{B.38})$$

Then, we can get the Kähler potential by defining,

$$\mathcal{K} = -\log(-N_{IJ}Z^I \bar{Z}^J), \quad y = e^{\mathcal{K}(z,\bar{z})/2}. \quad (\text{B.39})$$

We also observe that

$$N_{IJ}Z^I \bar{Z}^J = i\langle W|\bar{W}\rangle \quad W = \begin{pmatrix} Z^I \\ F_I \end{pmatrix} \quad (\text{B.40})$$

which implies that the Kähler form is determined only by the scalar product of the symplectic section. By using a more appropriate terminology, we say that the symplectic section (B.35) defines a line bundle  $\pi : L \rightarrow \mathcal{S}$  over the special Kähler manifold  $\mathcal{S}$ . In general, the first Chern class of a line bundle is defined in terms of the hermitian metric  $h = h(z, \bar{z})$  on the fiber  $L$ ,

$$c_1(L) \sim \bar{\partial}(h^{-1}\partial h) = \bar{\partial}\partial \log h. \quad (\text{B.41})$$

For a special Kähler geometry, formulas (B.39) and (B.40) show that  $h = i\langle W|\overline{W}\rangle$ . Then, the first Chern class of the line bundle is proportional to the Kähler form:  $c_1(L) = [K]$ . An alternative way to define a special Kähler geometry is by means of this fundamental relation,  $c_1(L) = [K]$ .

We understood that the line bundle is not flat and a proper covariant derivative, in the coordinates  $\{z^\alpha, \bar{z}^{\bar{\alpha}}\}$ , has to be introduced. By construction of the symplectic sections  $V = yW$  we obtain,

$$\nabla_{\bar{\alpha}}V \equiv \partial_{\bar{\alpha}}V - \partial_{\bar{\alpha}}\mathcal{K} V = 0 , \quad (\text{B.42})$$

$$\nabla_{\alpha}\bar{V} \equiv \partial_{\alpha}\bar{V} - \partial_{\alpha}\mathcal{K} \bar{V} = 0 . \quad (\text{B.43})$$

Then, it is natural to extend this definition to  $\nabla_{\alpha}V$  and  $\bar{\nabla}_{\bar{\alpha}}\bar{V}$ :

$$\nabla_{\alpha}V \equiv \partial_{\alpha}V + \partial_{\alpha}\mathcal{K} V , \quad (\text{B.44})$$

$$\bar{\nabla}_{\bar{\alpha}}\bar{V} \equiv \partial_{\bar{\alpha}}\bar{V} + \partial_{\bar{\alpha}}\mathcal{K} \bar{V} . \quad (\text{B.45})$$

It is important to emphasize that the connection  $\partial\mathcal{K}$  is a supergravity effect and it is absent in rigid supersymmetry. The derivative of  $\mathcal{K}$  can be taken over  $z^\alpha$  or  $\bar{z}^{\bar{\alpha}}$ . There is a natural way to build a single one form connection  $Q$  out of the two  $\partial\mathcal{K}$ . Indeed, we can map a line bundle  $\pi : L \rightarrow \mathcal{S}$  onto a  $U(1)$  principal bundle by the following procedure. If  $\exp[f_{\alpha\beta}(z)]$  is a transition function between two local charts of the line bundle, namely  $f_{\alpha\beta} : U^\alpha \rightarrow U^\beta$ , then the transition function in the corresponding  $U(1)$  principal bundle is  $\exp[i \text{Im}(f_{\alpha\beta}(z))]$ . The Kähler potential transforms as

$$\mathcal{K}\Big|_{U^\beta} = \mathcal{K}\Big|_{U^\alpha} + f_{\alpha\beta} + \bar{f}_{\alpha\beta} . \quad (\text{B.46})$$

At the level of the connections this correspondence is formulated by defining the  $U(1)$  connection,

$$Q \equiv -\frac{i}{2} (\partial_{\alpha}\mathcal{K}dz^{\alpha} - \partial_{\bar{\alpha}}\mathcal{K}d\bar{z}^{\bar{\alpha}}) . \quad (\text{B.47})$$

The two covariant derivatives (B.44) and (B.45) do not vanish. Indeed, they are used to define another geometrical object that it is fundamental in the special Kähler geometry. In the  $\mathcal{N} = 2$  language, this is the tensor  $C_{IJK}$  that specifies the magnetic couplings of the Lagrangian (4.25). It appears by considering the relation,

$$U_{\beta} = \nabla_{\beta}V , \quad (\text{B.48})$$

$$\nabla_{\alpha}U_{\beta} = iC_{\alpha\beta\gamma}g^{\gamma\bar{\sigma}}\bar{U}_{\bar{\sigma}} , \quad (\text{B.49})$$

(We remind the reader that the second covariant derivative acts on a tensor field and therefore it contains not only the connection  $\partial\mathcal{K}$  but also the Levi-civita connection). Another useful formula is

$$C_{\alpha\beta\gamma} = i\langle\nabla_\alpha\nabla_\beta V, \nabla_\gamma V\rangle = iF_{IJK}\nabla_\alpha X^I\nabla_\beta X^J\nabla_\gamma X^K. \quad (\text{B.50})$$

It can be checked that (B.49) is compatible with (B.50) upon using (B.37). The  $C_{\alpha\beta\gamma}$  tensor is holomorphic and symmetric in the indexes  $\alpha\beta\gamma$ . Finally, the curvature of the special Kähler geometry is fixed by the knowledge of the metric  $g_{\alpha\bar{\beta}}$  and the coefficients  $C_{\alpha\beta\gamma}$ ,

$$R_{\alpha\bar{\alpha}\beta\bar{\beta}} = 2g_{\alpha(\bar{\alpha}g_{\beta)\bar{\beta}} - C_{\alpha\beta\gamma}g^{\gamma\bar{\gamma}}\bar{C}_{\bar{\alpha}\bar{\beta}\bar{\gamma}}. \quad (\text{B.51})$$

As for the case of real geometry in five dimensions, the kinetic matrix for the gauge fields is also determined by the special Kähler geometry. The expression of  $\mathcal{N}_{IJ}$  in a local frame is,

$$\mathcal{N}_{IJ}(z, \bar{z}) = \bar{F}_{IJ} + i \frac{N_{IK}X^K N_{JL}X^L}{N_{MN}X^M X^N}. \quad (\text{B.52})$$

It can be easily proven that

$$\text{Im}\mathcal{N}_{IJ}X^I\bar{X}^J = -\frac{1}{2}. \quad (\text{B.53})$$

This relation is important because fixes the normalization of the kinetic matrix in the trivial case  $n_V = 0$ , when just the graviphoton is considered. We used this fact in (4.58).

Regarding the special geometry there is a last observation to be made. The physical quantities that enter the  $\mathcal{L}_{vectors}$  have been defined in terms of the holomorphic function  $F(X)$ . We also stressed that this is true in a local frame. It is possible to give a definition of these quantities without relying on the existence of the holomorphic function  $F(X)$ . This is called the symplectic formulation and it is based on the concept of holomorphic sections and symplectic transformations. We refer to the literature for a more detailed explanation. Here we only want to point out that the relation between the symplectic formulation and the local formulation is given by considering the non-holomorphic section  $X^I = yZ^I(z)$  together with the hidden assumption that  $(\partial_y X^I, \partial_\alpha X^I)$  is an invertible matrix.

**Composite Connections.** Fermionic fields were not the central object of our study. Furthermore, it is always consistent to truncate the supergravity action to its bosonic sector. On the other hand, there are several obvious reason to include fermions in our discussion. The first on being that an action invariant under supersymmetry needs by definition the introduction of fermionic degrees of freedom.

Regarding the set of  $\mathcal{N} = 2$  supermultiplets, the notation we use indicates with the upper or the lower position of the index the right and the left chirality of the spinor. We remind the reader that the graviton multiplet contains the  $SU(2)$  doublet of gravitini  $\Psi^i, \Psi_i$  where  $i = 1, 2$ , the  $n_V$  vector multiplets contain the  $SU(2)$  doublets of gaugini  $\lambda_i^\alpha, \lambda^{i\bar{\alpha}}$  where  $\alpha = 1, \dots, n_V$  and the  $n_H$  hypermultiplets contain the hyperini  $\psi_A, \psi^A$  where  $A = 1, \dots, 2n_H$ . Technically, there is a difference between five and four dimensions. In five dimensions fermions are symplectic Majorana. In four dimensions, fermions are Majorana. Then, the chiral projection is used to obtain for example  $\Psi^i$  and  $\Psi_i$ .

Fermions are section on the scalar manifolds. In the ungauged supergravity the covariant derivatives are

$$\nabla_\mu \Psi_{\nu i} = \left( \partial_\mu + \frac{1}{4} \mathfrak{S}_\mu^{ab} \gamma_{ab} - \frac{i}{2} Q_\mu \right) \Psi_{\nu i} - (\omega_u)_i^j \partial_\mu q^u \Psi_{\nu j} \quad (\text{B.54})$$

$$\nabla_\mu \lambda_i^\alpha = \left( \partial_\mu + \frac{1}{4} \mathfrak{S}_\mu^{ab} \gamma_{ab} - \frac{i}{2} Q_\mu \right) \lambda_i^\alpha + \Gamma_{\beta\gamma}^\alpha \lambda_i^\gamma \partial_\mu z^\beta - (\omega_u)_i^j \partial_\mu q^u \lambda_j^\alpha \quad (\text{B.55})$$

$$\nabla_\mu \psi^A = \left( \partial_\mu + \frac{1}{4} \mathfrak{S}_\mu^{ab} \gamma_{ab} + \frac{i}{2} Q_\mu \right) \psi^A + \Upsilon_{uB}^A \partial_\mu q^u \psi^B \quad (\text{B.56})$$

The connection  $\mathfrak{S}$  is the spin connection. The composite connections are  $Q, \omega, \Upsilon$  and the Levi Civita connection on  $\mathcal{S}$ , which is  $\Gamma_{\beta\gamma}^\alpha$ .  $Q$  and  $\omega$  are a supergravity effect. The gauging procedure gauge the composite connection by using covariant derivatives on the scalars and by introducing the prepotentials  $\mathcal{P}^0$  and  $\mathcal{P}^x, x = 1, 2, 3$ . The result is,

$$\Gamma_{\beta\gamma}^\alpha \partial_\mu z^\gamma \rightarrow \Gamma_{\beta\gamma}^\alpha D_\mu z^\gamma - A_\mu^I \partial_\beta K_I^\alpha \delta_\gamma^\beta \quad (\text{B.57})$$

$$\Upsilon_{uB}^A \partial_\mu q^u \rightarrow \Upsilon_{uB}^A \partial_\mu q^u - A_\mu^I t_{IB}^A \quad (\text{B.58})$$

$$Q_\mu \rightarrow Q_\mu + A_\mu^I \mathcal{P}_I^0 \quad (\text{B.59})$$

$$(\omega_u)_i^j \partial_\mu q^u \rightarrow (\omega_u)_i^j \partial_\mu q^u + \frac{1}{2} A_\mu^I (\mathcal{P}_I)_i^j \quad (\text{B.60})$$

where we have defined

$$t_{IB}{}^A = \frac{1}{2} f_{iA}^v \nabla_v K_I^u f_u^{iB} . \quad (\text{B.61})$$

The structure of the covariant derivatives (B.54)-(B.56) is the same, but now the composite connection are gauged. Analogous formulas can be obtained for  $\Psi^i$ ,  $\lambda^{i\bar{\alpha}}$  and  $\psi_A$ . Indeed  $\Psi_i \equiv P_R \Psi_i$  and

$$\Psi^i \equiv P_L \Psi^i = (\Psi_i)^C, \quad \Psi = \Psi^C = B^{-1} \Psi^* . \quad (\text{B.62})$$

In five dimension, the only difference with respect to the above formulation is the absence of the  $U(1)_R$  form  $Q$ .

# Bibliography

- [1] J. M. Maldacena, “The Large N limit of superconformal field theories and supergravity,” *Adv. Theor. Math. Phys.* **2**, 231 (1998) [hep-th/9711200].
- [2] E. Witten, “Anti-de Sitter space and holography,” *Adv. Theor. Math. Phys.* **2**, 253 (1998) [hep-th/9802150].
- [3] S. S. Gubser, I. R. Klebanov and A. M. Polyakov, “Gauge theory correlators from noncritical string theory,” *Phys. Lett. B* **428**, 105 (1998) [hep-th/9802109].
- [4] K. G. Wilson, “The renormalization group and critical phenomena,” *Rev. Mod. Phys.* **55**, 583 (1983).
- [5] I. Heemskerck and J. Polchinski, “Holographic and Wilsonian Renormalization Groups,” *JHEP* **1106**, 031 (2011) [arXiv:1010.1264 [hep-th]].
- [6] J. Polchinski, “Effective field theory and the Fermi surface,” [hep-th/9210046].
- [7] G. T. Horowitz, J. E. Santos and D. Tong, “Optical Conductivity with Holographic Lattices,” *JHEP* **1207**, 168 (2012) [arXiv:1204.0519 [hep-th]].
- [8] G. T. Horowitz, J. E. Santos and D. Tong, “Further Evidence for Lattice-Induced Scaling,” *JHEP* **1211**, 102 (2012) [arXiv:1209.1098 [hep-th]].
- [9] S. A. Hartnoll, C. P. Herzog and G. T. Horowitz, “Holographic Superconductors,” *JHEP* **0812**, 015 (2008) [arXiv:0810.1563 [hep-th]].
- [10] F. Aprile and J. G. Russo, “Models of Holographic superconductivity,” *Phys. Rev. D* **81**, 026009 (2010) [arXiv:0912.0480 [hep-th]].

- [11] F. Aprile, S. Franco, D. Rodriguez-Gomez and J. G. Russo, “Phenomenological Models of Holographic Superconductors and Hall currents,” JHEP **1005**, 102 (2010) [arXiv:1003.4487 [hep-th]].
- [12] F. Aprile, D. Roest and J. G. Russo, “Holographic Superconductors from Gauged Supergravity,” JHEP **1106**, 040 (2011) [arXiv:1104.4473 [hep-th]].
- [13] F. Aprile, A. Borghese, A. Dector, D. Roest and J. G. Russo, “Superconductors for superstrings on  $AdS_5 \times T^{1,1}$ ,” arXiv:1205.2087 [hep-th].
- [14] F. Aprile, “Holographic Superconductors in a Cohesive Phase,” JHEP **1210**, 009 (2012) [arXiv:1206.5827 [hep-th]].
- [15] F. Aprile, D. Rodriguez-Gomez and J. G. Russo, “p-wave Holographic Superconductors and five-dimensional gauged Supergravity,” JHEP **1101**, 056 (2011) [arXiv:1011.2172 [hep-th]].
- [16] “The Nobel Prize in Physics 1987”. Nobelprize.org. 14 Jun 2013 [http://www.nobelprize.org/nobel\\_prizes/physics/laureates/1987/index.html](http://www.nobelprize.org/nobel_prizes/physics/laureates/1987/index.html)
- [17] Neil W. Ashcroft, N. David Mermin “Solid State Physics,” Holt Rinehart & Winston (1976).
- [18] A.A.Abrikosov, L.P.Gorkov, I.E. Dzyaloshinski, “Methods of Quantum Field Theory in Statistical Physics” Dover Publications; Revised edition (1975).
- [19] Richard D. Mattuck, “A Guide to Feynman Diagrams in the Many-Body Problem,” Dover Publications; 2 edition (1992).
- [20] L. P. Pitaevskii (Author), E.M. Lifshitz (Author), “Statistical Physics, Part 2: Volume 9 (Course of Theoretical Physics Vol. 9),” Butterworth-Heinemann (1980).
- [21] A. B. Migdal, Soviet JETP **5**, 333 (1957). J. M. Luttinger, Phys. Rev. **119**, 1153 (1960).
- [22] S. A. Hartnoll and D. M. Hofman, “Locally Critical Resistivities from Umklapp Scattering,” Phys. Rev. Lett. **108**, 241601 (2012) [arXiv:1201.3917 [hep-th]].
- [23] J. bardeen, L. Cooper, J. R. Schrieffer, Phys.Rev. **108**, 1175-1204 (1957).

- [24] S. L. Budko, G. Lapertot, C. Petrovic, C. E. Cunningham, N. Anderson and P. C. Canfield, Phys. Rev. Lett. **86**, 1877 (2001).
- [25] W. L. McMillan and J.M. Rowell, In: “Superconductivity,” Vol I, pag 561, Edited by R.D. Parks, Marull, Dekker Inc. N.Y. (1969).
- [26] D. J. Scalapino, In: “Superconductivity,” Vol I, pag 449, Edited by R.D. Parks, Marull, Dekker Inc. N.Y. (1969).
- [27] R. Shankar, “Renormalization Group Approach to Interacting Fermions,” Rev. Mod. Phys., **66** (1994) 129.
- [28] Y.Kamihara, T. Watanabe, M. Hirano, H. Hosono, “Iron-based layered superconductors  $\text{LaO}_{1-x}\text{F}_x\text{As}$  ( $x \sim 0.05 - 0.12$ ) with  $T_c = 26\text{K}$ ” J.Am.Chem.Soc. **130**, 3296 (2008).
- [29] Hashimoto *et al.* Science **336**, 1554 (2012)
- [30] A. Abanov, A. V. Chubukov, and J. Schmalian, Adv. Phys., **52**, 119 (2003).
- [31] M. A. Metlitski and S. Sachdev, “Quantum phase transitions of metals in two spatial dimensions: II. Spin density wave order,” Phys. Rev. B **82**, 075128 (2010) [arXiv:1005.1288 [cond-mat.str-el]].
- [32] R. Mahajan, D. M. Ramirez, S. Kachru and S. Raghu, “Quantum critical metals in  $d = 3 + 1$ ,” arXiv:1303.1587 [cond-mat.str-el].
- [33] T. Valla *et al.*, Science **285**, 2110 (1999).
- [34] A.Kaminski *et al.*, Phys. Rev. Lett. **84**, 1788 (2000).
- [35] e.g. A. Punchkov, D. Basov and T. Timusk, J.Phys. Cond. Matter **8**, 10049 (1996).
- [36] R. C. Yu et al, Phys. Rev. Lett. **69**, 1431 (1992); S.J. Hagen, Z.Z. Wang and N.P. Ong, Phys. Rev. B **40**, 9389 (1989).
- [37] S. Sachdev, M. A. Metlitski and M. Punk, “Antiferromagnetism in metals: from the cuprate superconductors to the heavy fermion materials,” J. Phys. Condens. Matter **24**, 294205 (2012) [arXiv:1202.4760 [cond-mat.str-el]].
- [38] E. D’Hoker and D. Z. Freedman, “Supersymmetric gauge theories and the AdS / CFT correspondence,” hep-th/0201253.

- [39] J. M. Maldacena, “TASI 2003 lectures on AdS / CFT,” hep-th/0309246.
- [40] S. R. Coleman and J. Mandula, “All Possible Symmetries Of The S Matrix,” Phys. Rev. **159**, 1251 (1967).
- [41] M. F. Sohnius, “Introducing Supersymmetry,” Phys. Rept. **128**, 39 (1985).
- [42] J. Wess and J. Bagger, Supersymmetry and Supergravity, Princeton Univ. Press 1983
- [43] P. West, “Introduction to Supersymmetry and Supergravity,” World Scientific Publishing Co. Pte. Ltd. (1990) .
- [44] J. Terning, “Modern Supersymmetry: Dynamics and Duality,” (International Series of Monographs on Physics) Oxford University Press, USA (2009) .
- [45] J. Polchinski, “String Theory volume II, Superstring Theory and Beyond,” Cambridge University Press (1998) .
- [46] D. Freedman and A. Van Proeyen, “Supergravity,” Cambridge University Press (2012) .
- [47] P. S. Howe and P. C. West, “The Complete N=2, D=10 Supergravity,” Nucl. Phys. B **238**, 181 (1984).
- [48] J. H. Schwarz and P. C. West, “Symmetries and Transformations of Chiral N=2 D=10 Supergravity,” Phys. Lett. B **126**, 301 (1983).
- [49] C. Montonen and D. I. Olive, “Magnetic Monopoles as Gauge Particles?,” Phys. Lett. B **72**, 117 (1977).
- [50] E. Witten and D. I. Olive, “Supersymmetry Algebras That Include Topological Charges,” Phys. Lett. B **78**, 97 (1978).
- [51] R. Grimm, M. Sohnius and J. Wess, “Extended Supersymmetry and Gauge Theories,” Nucl. Phys. B **133**, 275 (1978).
- [52] V. K. Dobrev and V. B. Petkova, “On The Group Theoretical Approach To Extended Conformal Supersymmetry: Classification Of Multiplets,” Lett. Math. Phys. **9**, 287 (1985).
- [53] J. L. Petersen, “Introduction to the Maldacena conjecture on AdS / CFT,” Int. J. Mod. Phys. A **14**, 3597 (1999) [hep-th/9902131].

- [54] G. T. Horowitz and A. Strominger, “Black strings and P-branes,” Nucl. Phys. B **360**, 197 (1991).
- [55] J. Polchinski, “Tasi lectures on D-branes,” hep-th/9611050.
- [56] G. W. Gibbons and P. K. Townsend, “Vacuum interpolation in supergravity via super p-branes,” Phys. Rev. Lett. **71**, 3754 (1993)
- [57] M. Gunaydin and N. Marcus, “The Spectrum of the s\*\*5 Compactification of the Chiral N=2, D=10 Supergravity and the Unitary Supermultiplets of U(2, 2/4),” Class. Quant. Grav. **2**, L11 (1985).
- [58] B. de Wit and I. Herger, “Anti-de Sitter supersymmetry,” Lect. Notes Phys. **541**, 79 (2000) [hep-th/9908005].
- [59] P. Breitenlohner and D. Z. Freedman, “Positive Energy in anti-De Sitter Backgrounds and Gauged Extended Supergravity,” Phys. Lett. B **115**, 197 (1982).
- [60] I. R. Klebanov and E. Witten, “AdS / CFT correspondence and symmetry breaking,” Nucl. Phys. B **556**, 89 (1999) [hep-th/9905104].
- [61] E. Witten, “Multitrace operators, boundary conditions, and AdS / CFT correspondence,” hep-th/0112258.
- [62] S. A. Hartnoll, “Lectures on holographic methods for condensed matter physics,” Class. Quant. Grav. **26**, 224002 (2009) [arXiv:0903.3246 [hep-th]].
- [63] J. McGreevy, “Holographic duality with a view toward many-body physics,” Adv. High Energy Phys. **2010**, 723105 (2010) [arXiv:0909.0518 [hep-th]].
- [64] G. T. Horowitz, “Introduction to Holographic Superconductors,” arXiv:1002.1722 [hep-th].
- [65] C. P. Herzog, “Lectures on Holographic Superfluidity and Superconductivity,” J. Phys. A **42**, 343001 (2009) [arXiv:0904.1975 [hep-th]].
- [66] Leo P. Kadanoff “Statistical Physics: Statics, Dynamics and Renormalization,” World Scientific Pub Co Inc (July 2000).

- [67] O. Aharony, O. Bergman, D. L. Jafferis and J. Maldacena, “N=6 superconformal Chern-Simons-matter theories, M2-branes and their gravity duals,” JHEP **0810**, 091 (2008) [arXiv:0806.1218 [hep-th]].
- [68] Alexander Altland, Ben D. Simons “Condensed Matter Field Theory” Cambridge University Press; 2 edition (April 30, 2010).
- [69] S. S. Gubser, “Breaking an Abelian gauge symmetry near a black hole horizon,” Phys. Rev. D **78**, 065034 (2008) [arXiv:0801.2977 [hep-th]].
- [70] S. A. Hartnoll, C. P. Herzog and G. T. Horowitz, “Building a Holographic Superconductor,” Phys. Rev. Lett. **101**, 031601 (2008) [arXiv:0803.3295 [hep-th]].
- [71] S. Franco, A. Garcia-Garcia and D. Rodriguez-Gomez, “A General class of holographic superconductors,” JHEP **1004**, 092 (2010) [arXiv:0906.1214 [hep-th]].
- [72] S. S. Gubser and A. Nellore, “Low-temperature behavior of the Abelian Higgs model in anti-de Sitter space,” JHEP **0904**, 008 (2009) [arXiv:0810.4554 [hep-th]].
- [73] K. Skenderis, “Lecture notes on holographic renormalization,” Class. Quant. Grav. **19**, 5849 (2002) [hep-th/0209067].
- [74] J. T. Liu and W. A. Sabra, “Mass in anti-de Sitter spaces,” Phys. Rev. D **72**, 064021 (2005) [hep-th/0405171].
- [75] S. Franco, A. M. Garcia-Garcia and D. Rodriguez-Gomez, “A Holographic approach to phase transitions,” Phys. Rev. D **81**, 041901 (2010) [arXiv:0911.1354 [hep-th]].
- [76] R. Gregory, S. Kanno and J. Soda, JHEP **0910** (2009) 010 [arXiv:0907.3203 [hep-th]].
- [77] K. Maeda, M. Natsuume and T. Okamura, “Universality class of holographic superconductors,” Phys. Rev. D **79**, 126004 (2009) [arXiv:0904.1914 [hep-th]].
- [78] R. Werner. “Low-temperature electronic properties of Sr<sub>2</sub>RuO<sub>4</sub>. II. Superconductivity,” Phys. Rev. B **67**, 014505 (2003).
- [79] G. T. Horowitz and M. M. Roberts, “Holographic Superconductors with Various Condensates,” Phys. Rev. D **78**, 126008 (2008) [arXiv:0810.1077 [hep-th]].

- [80] S. A. Hartnoll and C. P. Herzog, “Ohm’s Law at strong coupling: S duality and the cyclotron resonance,” *Phys. Rev. D* **76**, 106012 (2007) [arXiv:0706.3228 [hep-th]].
- [81] Thomsen C., Cardona M., Friedl B., Rodriguez C.O., Mazin I.I., Andersen O.K. “Phonon self-energies and the gap of high-temperature superconductors.” *Solid State Communications* **75** 219-23, 1990.
- [82] A. Trajnerowicz, A. Golnik, C. Bernhard, et al. “Isotope effect on the optical phonons of YBa<sub>2</sub>Cu<sub>4</sub>O<sub>8</sub> studied by far-infrared ellipsometry and Raman scattering” *Phys. Rev. B* **74**, 104513 (2006)
- [83] G. T. Horowitz and M. M. Roberts, “Zero Temperature Limit of Holographic Superconductors,” *JHEP* **0911**, 015 (2009) [arXiv:0908.3677 [hep-th]].
- [84] S. A. Hartnoll and P. Kovtun, “Hall conductivity from dyonic black holes,” *Phys. Rev. D* **76**, 066001 (2007) [arXiv:0704.1160 [hep-th]].
- [85] D. Z. Freedman and A. K. Das, “Gauge Internal Symmetry in Extended Supergravity,” *Nucl. Phys. B* **120**, 221 (1977).
- [86] A. Ceresole and G. Dall’Agata, “General matter coupled N=2, D = 5 gauged supergravity,” *Nucl. Phys. B* **585**, 143 (2000) [hep-th/0004111].
- [87] L. Andrianopoli, M. Bertolini, A. Ceresole, R. D’Auria, S. Ferrara and P. Fre’, “General matter coupled N=2 supergravity,” *Nucl. Phys. B* **476**, 397 (1996) [hep-th/9603004].
- [88] L. Andrianopoli, M. Bertolini, A. Ceresole, R. D’Auria, S. Ferrara, P. Fre and T. Magri, “N=2 supergravity and N=2 superYang-Mills theory on general scalar manifolds: Symplectic covariance, gaugings and the momentum map,” *J. Geom. Phys.* **23**, 111 (1997) [hep-th/9605032].
- [89] M. Gunaydin and M. Zagermann, “The Gauging of five-dimensional, N=2 Maxwell-Einstein supergravity theories coupled to tensor multiplets,” *Nucl. Phys. B* **572**, 131 (2000) [hep-th/9912027].
- [90] B.A. Dubrovin, A.T. Fomenko, S.P. Novikov, “Modern Geometry Methods and Applications: Part I. The Geometry of Surfaces, Transformation Groups, and Fields,” (Graduate Texts in Mathematics) Springer; 1990 edition

- [91] B.A. Dubrovin, A.T. Fomenko, S.P. Novikov, “Modern Geometry Methods and Applications: Part II. The Geometry and Topology of Manifolds,” (Graduate Texts in Mathematics) Springer; 1990 edition
- [92] B. de Wit and H. Nicolai, “N=8 Supergravity,” Nucl. Phys. B **208**, 323 (1982).
- [93] B. de Wit, M. Rocek and S. Vandoren, JHEP **0102**, 039 (2001) [hep-th/0101161].
- [94] S. Ferrara and S. Sabharwal, “Quaternionic Manifolds for Type II Superstring Vacua of Calabi-Yau Spaces,” Nucl. Phys. B **332**, 317 (1990).
- [95] R. Britto-Pacumio, A. Strominger and A. Volovich, “Holography for coset spaces,” JHEP **9911**, 013 (1999) [hep-th/9905211].
- [96] A. Ceresole, G. Dall’Agata, R. Kallosh and A. Van Proeyen, “Hypermultiplets, domain walls and supersymmetric attractors,” Phys. Rev. D **64**, 104006 (2001) [hep-th/0104056].
- [97] A. Lukas, B. A. Ovrut and D. Waldram, “Heterotic M theory vacua with five-branes,” Fortsch. Phys. **48**, 167 (2000) [hep-th/9903144].
- [98] K. Behrndt, C. Herrmann, J. Louis and S. Thomas, “Domain walls in five-dimensional supergravity with nontrivial hypermultiplets,” JHEP **0101**, 011 (2001) [hep-th/0008112].
- [99] A. C. Cadavid, A. Ceresole, R. D’Auria and S. Ferrara, “Eleven-dimensional supergravity compactified on Calabi-Yau threefolds,” Phys. Lett. B **357**, 76 (1995) [hep-th/9506144].
- [100] M. Gunaydin, L. J. Romans and N. P. Warner, “Gauged N=8 Supergravity in Five-Dimensions,” Phys. Lett. B **154**, 268 (1985).
- [101] M. Pernici, K. Pilch and P. van Nieuwenhuizen, “Gauged N=8 D=5 Supergravity,” Nucl. Phys. B **259**, 460 (1985).
- [102] B. de Wit, “Supergravity,” hep-th/0212245.
- [103] M. Cvetič, H. Lu, C. N. Pope, A. Sadrzadeh and T. A. Tran, “Consistent SO(6) reduction of type IIB supergravity on S<sup>5</sup>,” Nucl. Phys. B **586**, 275 (2000) [hep-th/0003103].

- [104] M. Cvetič, M. J. Duff, P. Hoxha, J. T. Liu, H. Lu, J. X. Lu, R. Martinez-Acosta and C. N. Pope *et al.*, “Embedding AdS black holes in ten-dimensions and eleven-dimensions,” Nucl. Phys. B **558**, 96 (1999) [hep-th/9903214].
- [105] J. T. Liu, H. Lu, C. N. Pope and J. F. Vazquez-Poritz, “New supersymmetric solutions of N=2, D=5 gauged supergravity with hyperscalars,” JHEP **0710**, 093 (2007) [arXiv:0705.2234 [hep-th]].
- [106] S. S. Gubser and F. D. Rocha, “Peculiar properties of a charged dilatonic black hole in  $AdS_5$ ,” Phys. Rev. D **81**, 046001 (2010) [arXiv:0911.2898 [hep-th]].
- [107] K. Behrndt, M. Cvetič and W. A. Sabra, “Nonextreme black holes of five-dimensional N=2 AdS supergravity,” Nucl. Phys. B **553**, 317 (1999) [hep-th/9810227].
- [108] J.P. Kuenen, *Measurements on the surface of Van der Waals for mixtures of carbonic acid and methyl chloride*, Commun. Phys. Lab. Univ. Leiden, No 4 (1892).
- [109] D. Katz and F. Kurata, *Retrograde condensation*, Ind. Eng. Chem. **32**, pp. 817-827 (1940).
- [110] S. S. Gubser, C. P. Herzog, S. S. Pufu and T. Tesileanu, “Superconductors from Superstrings,” Phys. Rev. Lett. **103**, 141601 (2009) [arXiv:0907.3510 [hep-th]].
- [111] P. K. Townsend, “Positive Energy And The Scalar Potential In Higher Dimensional (super)gravity Theories,” Phys. Lett. B **148**, 55 (1984).
- [112] S. S. Gubser and F. D. Rocha, “The gravity dual to a quantum critical point with spontaneous symmetry breaking,” Phys. Rev. Lett. **102**, 061601 (2009) [arXiv:0807.1737 [hep-th]].
- [113] S. S. Gubser and A. Nellore, “Ground states of holographic superconductors,” Phys. Rev. D **80**, 105007 (2009) [arXiv:0908.1972 [hep-th]].
- [114] D. Cassani, G. Dall’Agata and A. F. Faedo, “Type IIB supergravity on squashed Sasaki-Einstein manifolds,” JHEP **1005**, 094 (2010) [arXiv:1003.4283 [hep-th]].

- [115] J. T. Liu, P. Szepietowski and Z. Zhao, “Consistent massive truncations of IIB supergravity on Sasaki-Einstein manifolds,” *Phys. Rev. D* **81**, 124028 (2010) [arXiv:1003.5374 [hep-th]].
- [116] J. P. Gauntlett, S. Kim, O. Varela and D. Waldram, “Consistent supersymmetric Kaluza-Klein truncations with massive modes,” *JHEP* **0904**, 102 (2009) [arXiv:0901.0676 [hep-th]].
- [117] D. Martelli, J. Sparks and S. -T. Yau, “Sasaki-Einstein manifolds and volume minimisation,” *Commun. Math. Phys.* **280**, 611 (2008) [hep-th/0603021].
- [118] J. Maldacena, D. Martelli and Y. Tachikawa, “Comments on string theory backgrounds with non-relativistic conformal symmetry,” *JHEP* **0810**, 072 (2008) [arXiv:0807.1100 [hep-th]].
- [119] I. R. Klebanov and E. Witten, “Superconformal field theory on three-branes at a Calabi-Yau singularity,” *Nucl. Phys. B* **536**, 199 (1998) [hep-th/9807080].
- [120] A. Ceresole, G. Dall’Agata, R. D’Auria and S. Ferrara, “Spectrum of type IIB supergravity on  $AdS(5) \times T^{**11}$ : Predictions on  $N=1$  SCFT’s,” *Phys. Rev. D* **61**, 066001 (2000) [hep-th/9905226].
- [121] P. Hoxha, R. R. Martinez-Acosta and C. N. Pope, “Kaluza-Klein consistency, Killing vectors, and Kahler spaces,” *Class. Quant. Grav.* **17**, 4207 (2000) [hep-th/0005172].
- [122] T. Faulkner, G. T. Horowitz and M. M. Roberts, “New stability results for Einstein scalar gravity,” *Class. Quant. Grav.* **27** (2010) 205007 [arXiv:1006.2387 [hep-th]].
- [123] N. Bobev, A. Kundu, K. Pilch and N. P. Warner, “Minimal Holographic Superconductors from Maximal Supergravity,” *JHEP* **1203**, 064 (2012) [arXiv:1110.3454 [hep-th]].
- [124] A. Donos and J. P. Gauntlett, “Superfluid black branes in  $AdS_4 \times S^7$ ,” *JHEP* **1106**, 053 (2011) [arXiv:1104.4478 [hep-th]].
- [125] S. S. Gubser, “Curvature singularities: The Good, the bad, and the naked,” *Adv. Theor. Math. Phys.* **4**, 679 (2000) [hep-th/0002160].
- [126] S. Ryu and T. Takayanagi, “Holographic derivation of entanglement entropy from AdS/CFT,” *Phys. Rev. Lett.* **96**, 181602 (2006) [hep-th/0603001].

- [127] I. R. Klebanov, “World volume approach to absorption by nondilatonic branes,” Nucl. Phys. B **496**, 231 (1997) [hep-th/9702076].
- [128] T. Albash and C. V. Johnson, “Holographic Studies of Entanglement Entropy in Superconductors,” JHEP **1205**, 079 (2012) [arXiv:1202.2605 [hep-th]].
- [129] T. Albash and C. V. Johnson, “Holographic Entanglement Entropy and Renormalization Group Flow,” JHEP **1202**, 095 (2012) [arXiv:1110.1074 [hep-th]].
- [130] R. C. Myers and A. Singh, “Comments on Holographic Entanglement Entropy and RG Flows,” JHEP **1204**, 122 (2012) [arXiv:1202.2068 [hep-th]].
- [131] N. Ogawa, T. Takayanagi and T. Ugajin, “Holographic Fermi Surfaces and Entanglement Entropy,” JHEP **1201**, 125 (2012) [arXiv:1111.1023 [hep-th]].
- [132] T. Nishioka, S. Ryu and T. Takayanagi, “Holographic Entanglement Entropy: An Overview,” J. Phys. A **42**, 504008 (2009) [arXiv:0905.0932 [hep-th]].
- [133] I. R. Klebanov, D. Kutasov and A. Murugan, “Entanglement as a probe of confinement,” Nucl. Phys. B **796**, 274 (2008) [arXiv:0709.2140 [hep-th]].
- [134] E. Witten, “Anti-de Sitter space, thermal phase transition, and confinement in gauge theories,” Adv. Theor. Math. Phys. **2**, 505 (1998) [hep-th/9803131].
- [135] I. R. Klebanov and M. J. Strassler, “Supergravity and a confining gauge theory: Duality cascades and chi SB resolution of naked singularities,” JHEP **0008** (2000) 052 [hep-th/0007191].
- [136] S. A. Hartnoll and D. Radicevic, “Holographic order parameter for charge fractionalization,” arXiv:1205.5291 [hep-th].
- [137] S. S. Gubser, “Dilaton driven confinement,” hep-th/9902155.
- [138] T. Fischbacher, K. Pilch and N. P. Warner, “New Supersymmetric and Stable, Non-Supersymmetric Phases in Supergravity and Holographic Field Theory,” arXiv:1010.4910 [hep-th].

- [139] R. G. Leigh and M. J. Strassler, “Exactly marginal operators and duality in four-dimensional  $N=1$  supersymmetric gauge theory,” Nucl. Phys. B **447**, 95 (1995) [hep-th/9503121].
- [140] Pietro Fré and Paolo Soriani, “THE  $N=2$  WONDERLAND, From Calabi–Yau Manifolds to Topological Field Theories”, World Scientific Publishing Co. (1995)
- [141] F. Benini, C. P. Herzog, R. Rahman and A. Yarom, “Gauge gravity duality for d-wave superconductors: prospects and challenges,” JHEP **1011**, 137 (2010) [arXiv:1007.1981 [hep-th]].
- [142] T. Faulkner, N. Iqbal, H. Liu, J. McGreevy and D. Vegh, “From Black Holes to Strange Metals,” arXiv:1003.1728 [hep-th].
- [143] R. Casalbuoni and G. Nardulli, “Inhomogeneous superconductivity in condensed matter and QCD,” Rev. Mod. Phys. **76**, 263 (2004) [hep-ph/0305069].
- [144] F. Bigazzi, A. L. Cotrone, D. Musso, N. P. Fokeeva and D. Seminara, “Unbalanced Holographic Superconductors and Spintronics,” JHEP **1202**, 078 (2012) [arXiv:1111.6601 [hep-th]].